

78-FM-51
Vol.V
Rev. 1

JSC-14483
MAY 29 1980

STS-1 Operational Flight Profile

Volume V
Descent - Cycle 3

Mission Planning and Analysis Division
May 1980

(NASA-TM-81077) STS-1 OPERATIONAL FLIGHT PROFILE. VOLUME 5: DESCENT, CYCLE 3 (NASA)
254 p HC A12/MF AC1 CSCL 22A N80-25371
Unclassified G3/16 23778

Supersedes T79-12405



National Aeronautics and
Space Administration

Lyndon B. Johnson Space Center
Houston, Texas

78-FM-51
Vol. V, Rev. 1

78FM51:V
JSC-14483

SHUTTLE PROGRAM

STS-1
OPERATIONAL FLIGHT PROFILE
DESCENT - CYCLE 3

By Richard Moore, Flight Analysis Branch;
Allen Baker, Richard Carter, Ralph Hite, Alan Hochstein, Jack Lyons, and
Ken Strong, McDonnell Douglas Technical Services Co.

Approved: Claude A. Graves, Jr.
Claude A. Graves, Jr., Assistant Chief
Flight Analysis Branch

Approved: Ronald L. Berry
Ronald L. Berry, Chief
Mission Planning and Analysis Division

Mission Planning and Analysis Division

National Aeronautics and Space Administration

Lyndon B. Johnson Space Center

Houston, Texas

May 1980

FOREWORD

The orbital flight test (OFT) phase of the Space Shuttle Program consists of four orbital flights beginning in March 1980 and continuing through 1981. The major purpose of the OFT program is to demonstrate and verify Shuttle systems and flight capabilities by satisfying the Space Shuttle Program Office (SSPO) OFT requirements (refs. 1 and 2).

This document (Volume V) presents the Space Transportation System (STS-1) descent (deorbit through rollout) data for the operational flight profile (OFP) trajectory phase (Cycle 3).

All STS-1 OFP documents for Cycle 3 and their scheduled distribution dates are listed in the following table.

DOCUMENT PUBLICATION SCHEDULE

Document	Scheduled distribution date
Volume I - Groundrules and Constraints, Rev. 2	September 1979 (A)
Volume II - Profile Summary, Rev. 1	April 1980 (A)
Volume III - Ascent, Rev. 1	May 1980 (P)
Volume IV - Onorbit, Rev. 1	November 1979 (A)
Volume V - Descent, Rev. 1	May 1980 (P)
Volume VI - Abort Analysis, Rev. 1	May 1980 (P)
Volume VII - OMS and RCS Consumables Analysis, Rev. 1	February 1980 (A)
Volume VIII - Nonpropulsive Consumables Analysis, Rev. 1	February 1980 (A)

PRECEDING PAGE BLANK NOT FILMED

ACKNOWLEDGMENTS

The following individuals contributed to this document:

J'Ann Hansen, Dave Heath, Oliver Hill, Dallas Ives, Moises Montez, Dan Payne, and Jim West, Flight Analysis Branch; Joe Betters, Dave Humphreys, Sam Juliano, Dave Lamar, John Manning, Patrick O'Neill, and Roger Ruda, McDonnell Douglas Technical Services Company.

CONTENTS

Section		Page
1.0	<u>INTRODUCTION</u>	1
2.0	<u>FLIGHT DESCRIPTION</u>	2
3.0	<u>DESCENT PROFILE OVERVIEW AND SUMMARY</u>	3
3.1	<u>DESCENT PROFILE OVERVIEW</u>	3
3.2	<u>DESCENT PROFILE CHANGES AND PROFILE SUMMARY FOR CYCLE 3</u>	4
3.2.1	<u>Summary of Changes for Cycle 3</u>	4
3.2.2	<u>Descent Profile Summary</u>	5
4.0	<u>STS-1 OFP FLIGHT DESIGN GROUNDRULES AND CONSTRAINTS</u>	7
4.1	<u>GENERAL</u>	7
4.8	<u>DESCENT - DEORBIT</u>	9
4.9	<u>DESCENT - ENTRY THROUGH ROLLOUT</u>	10
5.0	<u>SIMULATION DESCRIPTION</u>	12
6.0	<u>DESCENT PROFILE</u>	13
6.1	<u>DEORBIT</u>	13
6.2	<u>ENTRY</u>	15
6.2.1	<u>Entry Profile Shaping</u>	15
6.2.2	<u>Control Surface Deflection Schedules</u>	19
6.2.3	<u>Aerodynamic Crossrange Capability</u>	20
6.3	<u>TAEM</u>	20
6.4	<u>APPROACH AND LANDING</u>	22
6.4.1	<u>Trajectory Capture to Touchdown</u>	22
6.4.2	<u>Rollout</u>	23
6.5	<u>COMMUNICATIONS AND TRACKING</u>	24
7.0	<u>ASSESSMENT OF VEHICLE COMPATIBILITY</u>	26
8.0	<u>ASSESSMENT OF FLIGHT TEST OBJECTIVES</u>	27
9.0	<u>DEORBIT-THROUGH-LANDING ISSUES AND CHANGES</u>	32

Section	Page
10.0 <u>REFERENCES</u>	33
APPENDIX A - ENTRY INITIALIZATION LOAD FOR THE ONBOARD COMPUTER . . .	A-1

TABLES

Table		Page
3.2-I	STS-1 CYCLE 3 DESCENT PROFILE DESIGN CHANGES	35
3.2-II	COMPARISON OF CYCLE 2 AND CYCLE 3 OFT PROFILE SUMMARIES	37
5.0-I	STS-1 MASS PROPERTIES FOR NOMINAL END OF MISSION	38
5.0-II	OMS LOADING REQUIREMENTS	39
5.0-III	STATE VECTORS	40
5.0-IV	APRIL GLOBAL REFERENCE ATMOSPHERE DATA	41
5.0-V	APRIL GLOBAL REFERENCE ATMOSPHERE DEVIATIONS FROM 1962 STANDARD ATMOSPHERE	42
6.0-I	SEQUENCE OF EVENTS FOR STS-1 (CYCLE 3) (a) Predeorbit maneuver to entry guidance initiate (b) Entry guidance initiate to TAEM interface (c) TAEM interface to approach and landing interface (d) Approach and landing interface to main gear landing (e) Main gear touchdown through rollout	43 44 45 45 45
6.1-I	STS-1 LANDING OPPORTUNITIES AT EAFB	46
6.1-II	DEORBIT AND ENTRY INTERFACE PARAMETERS	47
6.1-III	MANEUVER PAD FOR NOMINAL EOM	49
6.1-IV	DEL PAD DEORBIT	50
6.1-V	DEORBIT MANEUVER DISPLAYS	51
6.1-VI	NOMINAL END-OF-MISSION REFSMATS	54
6.1-VII	NOMINAL END-OF-MISSION RELMATS AND RELQUATS	55
6.2-I	STS-1 DEORBIT-THROUGH-LANDING TRAJECTORY PARAMETERS	56
6.2-II	ORBITER SURFACE TEMPERATURE LIMITS	60
6.2-III	STS-1 CYCLE 3 THERMAL PROTECTION SYSTEM (TPS) SUMMARY	61
6.2-IV	SUMMARY OF CYCLE-3 ORBITER SURFACE TEMPERATURE LIMITS AND MARGINS BASED ON MONTE CARLO ANALYSIS	62
6.2-V	ELEVON AND BODY FLAP SURFACE DEFLECTION ERRORS	63

Table	Page
6.3-I ENTRY/TAEM INTERFACE CONDITIONS	64
6.4-I TAEM/A&L INTERFACE CONDITIONS	65
6.6-I STS-1 C-BAND AND S-BAND COMMUNICATION SEQUENCE OF EVENTS . . .	66
6.6-II STS-1 TACAN COMMUNICATIONS SEQUENCE OF EVENTS	67

FIGURES

Figure		Page
3.1-1	Typical entry altitude-velocity profile	68
3.1-2	Typical TAEM groundtrack and trajectory sub-phases	69
3.1-3	Typical approach and landing trajectory with sub-phases identified	70
3.2-1	Comparison of cycle 2 and 3 elevon schedules	71
3.2-2	Comparison of cycle 2 and 3 speedbrake schedules	71
3.2-3	Comparison of cycle 2 and 3 body flap deflections	72
3.2-4	TAEM guidance dynamic pressure profiles	73
3.2-5	TAEM guidance dynamic pressure limits	73
5.0-1	Mean April global reference atmosphere	74
6.0-1	STS-1 deorbit-through-landing groundtrack	75
6.1-1	Inertial velocity, inertial flightpath angle, and range target lines for Orbiter OFT-1 entry interface	76
6.1-2	OMS propellant versus T_{ig} , nominal end of mission	77
6.1-3	Geodetic altitude - deorbit	78
6.1-4	Inertial velocity magnitude - deorbit	79
6.1-5	Displayed ADI angles-reference - deorbit	80
6.1-6	Displayed ADI angles-inertial - deorbit	81
6.1-7	Displayed ADI angles-LVLH - deorbit	82
6.1-8	Current apogee and perigee altitudes - deorbit	83
6.1-9	Displayed velocity-to-go vector in body-axis coordinates - deorbit	84
6.1-10	Velocity-to-go vector in LVLH coordinates - deorbit	85
6.1-11	Velocity-to-go magnitude and time-to-go - deorbit	86
6.1-12	Velocity magnitude to be gained for no fuel wasting - deorbit	87

Figure	Page
6.1-13 Displayed ADI angles-reference - deorbit	88
6.1-14 Displayed ADI angles-inertial - deorbit	89
6.1-15 Displayed ADI angles-LVLH - deorbit	90
6.1-16 Dedicated display ADI body attitude error - deorbit	91
6.1-17 Left OMS pitch actual and commanded gimbal angles - deorbit . . .	92
6.1-18 Left OMS yaw actual and commanded gimbal angles - deorbit . . .	93
6.1-19 Right OMS pitch actual and commanded gimbal angles - deorbit	94
6.1-20 Right OMS yaw actual and commanded gimbal angles - deorbit . . .	95
6.2-1 STS-1 entry interface through landing groundtrack	96
6.2-2 Lift/drag, reference, actual and commanded angle of attack during atmospheric descent	97
6.2-3 Entry drag acceleration corridor	
(a) Nominal thermal constraints boundaries	98
(b) Two- and three-sigma thermal constraint boundaries	99
6.2-4 Surface temperature control points and panel locations	100
6.2-5 Scheduled and actual elevator deflection during atmospheric descent	101
6.2-6 Body flap and speedbrake deflection during atmospheric descent	102
6.2-7 Geodetic altitude vs. range-to-runway threshold	103
6.2-8 Delta azimuth, actual and commanded roll angles during atmospheric descent	104
6.2-9 Reference heating rate vs. relative velocity from entry interface	105
6.2-10 Control point temperatures vs. relative velocity from entry interface	106
6.2-11 Geodetic altitude during atmospheric descent	107
6.2-12 Actual and reference altitude rate during atmospheric descent	108

Figure	Page
6.2-13 Range to runway threshold during atmospheric descent	109
6.2-14 Dynamic pressure during atmospheric descent	110
6.2-15 X, Y, and Z-body axis and total load factor during atmospheric descent	111
6.2-16 Relative flightpath angle during atmospheric descent	112
6.2-17 Actual sideslip angle during atmospheric descent	113
6.2-18 Bank rate during atmospheric descent	114
6.2-19 Bank acceleration during atmospheric descent	115
6.2-20 Altitude acceleration during atmospheric descent	116
6.2-21 Body roll, pitch and yaw rates during atmospheric descent . . .	117
6.2-22 Aileron deflection during atmospheric descent	118
6.2-23 Left elevon deflection rates during atmospheric descent . . .	119
6.2-24 Right elevon deflection rates during atmospheric descent . . .	120
6.2-25 Body flap, rudder and speedbrake rates during atmospheric descent	121
6.2-26 Relative velocity vs. time from entry interface	122
6.2-27 Delta azimuth, actual and commanded roll angle vs. time from entry interface	123
6.2-28 Reference heating rate vs. time from entry interface	124
6.2-29 Control point temperatures vs. time from entry interface	125
6.2-30 Altitude vs. time from entry interface	126
6.2-31 Actual and reference altitude rate vs. time from entry interface	127
6.2-32 Range-to-runway threshold vs. time from entry interface	128
6.2-33 Lift/drag, actual and commanded angle of attack vs. time from entry interface	129
6.2-34 Dynamic pressure vs. time from entry interface	130

Figure	Page
6.2-35 X, Y, and Z-body axis components of load factor vs. time from entry interface	131
6.2-36 Relative flightpath angle vs. time from entry interface	132
6.2-37 Actual sideslip angle vs. time from entry interface	133
6.2-38 Bank rate vs. time from entry interface	134
6.2-39 Bank acceleration vs. time from entry interface	135
6.2-40 Altitude acceleration vs. time from entry interface	136
6.2-41 Body roll, pitch and yaw rates vs. time from entry interface	137
6.2-42 Aileron deflection vs. time from entry interface	138
6.2-43 Elevator, body flap, and speedbrake deflection vs. time from entry interface	139
6.2-44 Left elevon deflection rates vs. time from entry interface	140
6.2-45 Right elevon deflection rates vs. time from entry interface	141
6.2-46 Body flap, rudder and speedbrake rates vs. time from entry interface	142
6.2-47 Left elevon hinge moments vs. time from entry interface	143
6.2-48 Right elevon hinge moments vs. time from entry interface	144
6.2-49 RCS fuel usage vs. time from entry interface	145
6.2-50 RCS on-time vs. time from entry interface	146
6.3-1 TAEM through landing groundtrack	147
6.3-2 TAEM dynamic pressure corridor	148
6.3-3 TAEM angle-of-attack corridor	149
6.3-4 Actual energy over weight during TAEM	150
6.3-5 Altitude and altitude reference of gear above landing site during TAEM	151
6.3-6 Altitude rate and altitude rate reference during TAEM	152

Figure	Page
6.3-7 Relative flightpath angle during TAEM	153
6.3-8 Drag acceleration during TAEM	154
6.3-9 Actual and reference dynamic pressure during TAEM	155
6.3-10 Roll angle during TAEM	156
6.3-11 Reference altitude and gear altitude during TAEM	157
6.3-12 Topodetic altitude rate and equivalent airspeed during TAEM	158
6.3-13 Dynamic pressure and reference dynamic pressure during TAEM	159
6.3-14 Heading, roll angle, and commanded roll angle during TAEM . . .	160
6.3-15 Flightpath angle, body pitch angle, and angle of attack during TAEM	161
6.3-16 True airspeed, Earth relative velocity, and mach no. during TAEM	162
6.3-17 Body roll, pitch and yaw rates during TAEM	163
6.3-18 Normal load factor and delta NZ command at the c.g. during TAEM	164
6.3-19 Sideslip angle and Y-body load factor at the c.g. during TAEM	165
6.3-20 Aileron, elevator, and body flap deflection during TAEM . . .	166
6.3-21 Right elevon deflection during TAEM	167
6.3-22 Left elevon deflection during TAEM	168
6.3-23 Actual, commanded speedbrake deflection and rudder deflection during TAEM	169
6.4-1 Approach and landing groundtrack	170
6.4-2 Orbiter position with respect to runway in the vicinity of the runway	171
6.4-3 Altitude/gamma/load factor (NZ) during approach and landing .	172
6.4-4 Gear altitude from final flare to touchdown	173

Figure	Page
6.4-5 Gear altitude during landing gear deployment	174
6.4-6 Gear altitude AGL from preflare to touchdown X-runway position	175
6.4-7 Velocity and dynamic pressure from preflare to touchdown	176
6.4-8 Flightpath angle, body pitch angle, and angle of attack from preflare to touchdown	177
6.4-9 Normal load factor and delta NZ at the c.g. during approach and landing	178
6.4-10 Aileron, elevon, and rudder deflection from preflare to touchdown	179
6.4-11 Right inboard and outboard deflection from preflare to touchdown	180
6.4-12 Left inboard and outboard elevon deflection from preflare to touchdown	181
6.4-13 Topodetic body roll, pitch and yaw rates from preflare to touchdown	182
6.4-14 Control surface deflections during approach and landing	183
6.4-15 Altitude-altitude rate phase plane from preflare to touchdown	184
6.4-16 Altitude-altitude rate phase plane from exponential capture to touchdown	185
6.4-17 Altitude-altitude rate phase plane from final flare to touchdown	186
6.4-18 STS-1 operational flight profile perspective	187
6.4-19 View from commander eye position	
(a) 101.9 seconds prior to touchdown	188
(b) 92.3 seconds prior to touchdown	189
(c) 82.2 seconds prior to touchdown	190
(d) 72.3 seconds prior to touchdown	191
(e) 62.2 seconds prior to touchdown	192
(f) 52.3 seconds prior to touchdown	193
(g) 42.2 seconds prior to touchdown	194
(h) 32.3 seconds prior to touchdown	195
(i) 22.2 seconds prior to touchdown	196
(j) 12.3 seconds prior to touchdown	197

Figure	Page
(k) 2.2 seconds prior to touchdown	198
(l) Touchdown	199
6.5-1 Gear vertical load, EAS, pitch and elevon deflection during rollout	200
6.5-2 Time from maingear touchdown during rollout	201
6.5-3 Pitch and pitch rate during rollout	202
6.5-4 Groundspeed and acceleration during rollout	203
6.5-5 Pilot and c.g. load factors during rollout	204
6.5-6 Nose gear strut, tire deflection and loads during rollout . . .	205
6.5-7 Main gear strut, tire deflection and loads during rollout . . .	206
6.6-1 Postblackout entry groundtrack for Orbiter STS-1	207
6.6-2 STS-1 entry groundtrack and Tacan events	208
6.6-3 Elevation angle versus azimuth Buckhorn (BUC)	209
6.6-4 Elevation angle versus azimuth Goldstone (GDS)	210
6.6-5 Range and elevation versus time to touchdown	
(a) BUC	211
(b) GDS	212
(c) PTP	213
(d) VDB	214
6.6-6 MSBLS coverage sequence	215

ACRONYMS

ACIP	aerodynamic coefficients identification package
A&L	approach and landing
AOA	abort once around
AOS	acquisition of signal
ATO	abort to orbit
AVE	Avenal
BFL	Bakersfield
BUC	Buckhorn, Calif.
c.g.	center of gravity
$C_n \delta A$	yawing moment coefficient change due to aileron deflection
$C_n \delta r$	yawing moment coefficient change due to rudder deflection
CRP	configuration requirements processing
CSS	control stick steering
DFI	development flight instrumentation
DTO	detailed test objective
EAFB	Edwards Air Force Base
EAS	equivalent airspeed
EET	entry elapsed time (EET = 10:00:00 at tig)
EI	entry interface
ET	external tank
FCS	flight control system
FLW	Fellows
FSSR	functional subsystem software requirements
g	gravity acceleration
GDS	Goldstone, Calif.

GET	ground elapsed time
GMN	Gorman
GMT	Greenwich mean time
GN&C	guidance, navigation, and control
GRTLS	glide-return-to-launch site
GSTDN	ground spaceflight tracking data network
GWM	Guam
HAC	heading alignment circle
HRSI	high-temperature reusable surface insulation
IECM	induced environment contamination monitor
IFCS	integrated flight control system
IGS	inner glideslope
IMU	inertial measurement unit
KEAS	knots equivalent airspeed
KPT	Kadena Pt., Oahu, Hawaii
KSC	Kennedy Space Center
L/D	lift/drag
LOS	loss of signal
LRU	line replaceable unit
LVLH	local-vertical local-horizontal coordinate system
MCC	Mission Control Center
MSBLS	microwave scanning beam landing system
M50	mean-of-50
NZ	normal load factor
OEX	Orbiter experiments
OPP	operational flight profile

OFT	orbital flight test
OGS	outer glideslope
OMS	orbital maneuvering system
OTT	operational TAEM targeting
PEG	Powered explicit guidance
PLBD	payload bay doors
PMD	Palmdale
PRB	Paso Robles
PST	Pacific standard time
PTP	Pt. Pillar, Calif.
QMAX	TAEM phase maximum dynamic pressure limit
QMIN	TAEM phase minimum dynamic pressure limit
RCC	reinforced carbon-carbon
RCS	reaction control system
RI	Rockwell International
RSI	reuseable surface insulation
RTLS	return-to-launch site
RTV	room temperature vulcanization
SBP	San Luis Obispo
SNI	San Nicholas Is., Calif.
SSPO	Space Shuttle Program Office
STDN	Spaceflight Tracking and Data Network
STS-1	Space Transportation System flight 1
SVDS	space vehicle dynamics simulation
Tacan	tactical air navigation
TAEM	terminal area energy management

TIG	time of deorbit OMS ignition
TPS	thermal protection system
V_e	relative velocity
ΔV	velocity increment
VAFB	Vandenberg Air Force Base
WOW	weight on wheels
WONG	weight on nose gear

1.0 INTRODUCTION

This document (Volume V) supersedes the STS-1 Descent OFP, Cycle 2 (ref. 3). Volume V is one in a series that, taken together, will define the STS-1 OFP.

The descent OFP is designed to meet the requirements given in the SSPO Flight Requirements Document, STS-1 (ref. 4), and is based on the approved groundrules and constraints documented in volume I (ref. 5).

The trajectory data presented in this document should be used for Orbiter systems and subsystems evaluation, flight and Mission Control Center (MCC) software verification, flight techniques and timeline development, crew training, and evaluation of operational mission suitability.

The entry profile is very similar to Cycle 2; however, elevon and body flap temperature margins have increased, and the elevon schedule was changed. The TAEM profile was completely reshaped to conform with new angle-of-attack constraints and left-hand turn around the heading alignment cylinder. Also, the entry/TAEM interface was adjusted to minimize guidance-induced angle-of-attack transients across the interface. The approach and landing (A&L) phase was reshaped for a 20° glideslope and reduced velocity at touchdown.

The definition of the runway threshold has been standardized for all landing sites. This results in a shift at EAFB in aim points and touchdown relative to the threshold of 1000 feet. (The physical location of aim points and touchdown was not changed.) The rollout remains essentially unchanged with the exception of the speedbrake, which is now deployed to 50 percent at touchdown.

2.0 FLIGHT DESCRIPTION

The STS-1 will be a 54.5-hour flight launched from Kennedy Space Center (KSC) on March 31, 1980 at 11:30 Greenwich mean time (GMT). The flight test will be achieved in a 150-n. mi. circular orbit with a 40.3-degree inclination. This orbit will be achieved by two orbital maneuvering system (OMS) maneuvers, OMS-1 (ground elapsed time (GET) = 00:10:34) and OMS-2 (GET = 00:45:50). The OMS-1 maneuver will occur shortly after external tank (ET) separation with the OMS-2 maneuver occurring at the apogee of the orbit resulting from OMS-1. The payload bay doors will be opened as early as possible on day 1. The Orbiter will be placed in a Z-axis (payload bay down) local vertical (Z-LV) attitude for most of the STS-1 flight. This attitude will be maintained unless other requirements (flight test requirements, inertial measurement unit alignment, etc.) preclude Z-LV attitude. Two orbital OMS maneuvers will be performed during the flight to satisfy flight test objectives. The OMS-3 maneuver ($\Delta V = 30$ fps) will be performed following the deorbit rehearsal on day 2 at GET = 30:59:44. The OMS-4 maneuver ($\Delta V = 30$ fps) will be performed approximately 30 minutes after the OMS-3 maneuver at GET = 31:29:44. Both of these OMS maneuvers will be performed out of plane with the Orbiter remaining in a 150-n. mi. circular orbit. Deorbit (GET = 53:31:04) will occur on April 2, 1980. Nominal landing will occur on runway 23 during a descending pass (orbit 37) to Edwards Air Force Base (EAFB). The GET for the nominal landing will be 54:30:44 (10:01 a.m. Pacific standard time (PST)).

3.0 DESCENT PROFILE OVERVIEW AND SUMMARY

3.1 DESCENT PROFILE OVERVIEW

The Orbiter descent profile is divided into four phases as follows:

a. The deorbit phase, which extends from attitude hold prior to the deorbit maneuver to entry interface (EI) at 400 000 feet altitude.

b. The entry phase, which extends from EI to the initiation of the terminal area energy management (TAEM) phase at an Earth-relative velocity (V_e) of 2500 fps. The entry phase is divided into four subphases as follows:

(1) Temperature control -

The temperature control phase defines an entry profile shape consistent with the thermal protection system (TPS) constraints during the high-heating part of entry.

(2) Equilibrium glide -

The equilibrium glide phase provides an entry profile that has the fundamental shape of equilibrium flight. It is used during the intermediate velocity region of entry.

(3) Constant drag -

The constant drag phase provides a profile shape consistent with control system limits.

(4) Transition -

The transition phase provides a profile shape consistent with the control system limits and guides the vehicle to the proper TAEM interface conditions..

A typical entry altitude-velocity profile showing the flight regime of the four subphases is shown in figure 3.1-1.

c. The TAEM phase extends to the A&L interface at a nominal altitude of 10 000 feet above the runway. The TAEM phase is divided into four subphases as follows:

(1) S-turn -

This mode is used only when A&L interface constraints cannot otherwise be met. The vehicle turns away from the target until sufficient energy is dissipated to allow a normal approach.

(2) Acquisition -

The vehicle turns until it is tangent to the nearest heading alignment cylinder and continues until it reaches the cylinder.

(3) Heading alignment -

The heading alignment cylinder is followed until the Orbiter is near the runway entry point.

(4) Prefinal -

The vehicle leaves the heading alignment circle and rolls to acquire the runway centerline.

Figure 3.1-2 presents a typical TAEM groundtrack with subphases identified.

- d. The A&L phase extends through rollout and is comprised of five subphases as follows:

- | | |
|------------------------------------|--|
| (1) Trajectory capture - | Trajectory capture starts at the TAEM/A&L interface and steers the vehicle to the steep glideslope. Normally, the software cycles through this phase only one time because the vehicle will be on the glideslope well within specified tolerances. |
| (2) Steep glideslope - | The steep glideslope is tracked in elevation and azimuth. |
| (3) Flare and shallow glideslope - | The glideslope angle is reduced in preparation for landing. |
| (4) Final flare - | Final flare reduces the sink rate to near zero for touchdown. |
| (5) Touchdown and rollout - | The vehicle is directed along the runway centerline from weight on wheels (flat turn) until it comes to a complete stop. |

The A&L occurs essentially in the vertical plane containing the runway centerline. Figure 3.1-3 shows a typical A&L trajectory and trajectory subphases.

For additional information see references 6, 7, and 8.

3.2 DESCENT PROFILE CHANGES AND PROFILE SUMMARY FOR CYCLE 3

3.2.1 Summary of Changes for Cycle 3

Table 3.2-I presents a summary of the cycle 3 descent profile design changes. Figure 3.2-1 through 3.2-3 present a comparison of elevon and speedbrake schedules and body flap deflections between cycles 2 and 3.

- a. Entry - The entry profiles are very similar with the exception of elevon and body flap maximum temperatures and maximum temperature limits. The maximum temperature limits were increased because the three-sigma dispersion allowance was reduced by 101° F on the body flap and 34° F on the elevon, and maximum temperatures between the two surfaces were rebalanced by positioning the elevon 1° up as compared to 0° in cycle 2.

Table 3.2-II presents a comparison between cycles 2 and 3 thermal data, EI state vectors, and minimum margin above equilibrium glide.

- b. Terminal Area Energy Management (TAEM) - The TAEM profile for cycle 3 was reshaped to conform with new angle-of-attack constraints that resulted in a

new dynamic pressure reference and new dynamic pressure upper limits. (figs. 3.2-4 and 3.2-5).

The nominal altitude at TAEM interface was biased approximately 5000 feet below the TAEM reference altitude in order to force guidance to generate a pitch-up command to minimize the pitch-down transient that normally occurs at entry/TEAM interface. Also, TAEM was reshaped to fly a left-hand turn around the heading alignment cylinder (HAC) and to conform with a 20° outer glideslope in A&L.

- c. Approach and Landing - The A&L outer glideslope was changed from 22° to 20° as a result of Orbiter weight growth. The other changes enumerated in table 3.2-I were motivated by a desire to reduce touchdown speed due to more restrictive tire and wheel constraints and a desire to provide satisfactory landing conditions with this profile should the launch slip into the summer months.

3.2.2 Descent Profile Summary

- a. Deorbit - The deorbit maneuver is normally performed using two OMS engines; however, deorbit targeting and OMS propellant loading provide the capability to deorbit with either one OMS engine or the RCS engines using OMS propellant to achieve the nominal entry conditions.

This OMS loading makes it necessary to use 225 pounds of excess OMS propellant for nominal deorbit to achieve the desired entry longitudinal center-of-gravity (c.g.) position of 66.7 percent at EI. This propellant wasting is accomplished by an out-of-plane deorbit maneuver component resulting in a total deorbit velocity increment (ΔV) of 292.9 fps with a thrust duration of 2 minutes 28 seconds and with a 25-minute 47-second free-fall time between thrust termination and EI.

- b. Entry - Nominal conditions at the EI of 400 000 feet altitude are 4358 n. mi. range-to-go, 25 752 fps inertial velocity, and -1.21 degrees inertial flightpath angle with an Orbiter weight of 191 902 pounds.

A 40-degree angle of attack is maintained during the early part of atmospheric descent to minimize the aerodynamic heating environment. This angle of attack is maintained until the aerodynamic heating is reduced to a relatively low level with pitchover to a lower angle of attack beginning at an Earth-relative speed of 14 500 fps. This pitchover continues until an angle of attack of 14.0 degrees is reached at the entry/TAEM interface at 2500 fps Earth-relative speed.

The entry profile is shaped in the temperature control region to conform with surface temperature limits at five control points on the vehicle (fig. 6.2-3). When 30° dispersions are considered (fig. 6.2-4), the surface temperature on the wing leading edge becomes most constraining. This profile was shaped to a wing leading-edge temperature limit of 2663°F (table 6.2-II). The heat load and maximum reference heating rate for this trajectory is 53 731 Btu/ft² and 61.4 Btu/ft²/sec, respectively.

The entry angle-of-attack profile for STS-1 results in a crossrange capability of 700 n. mi.

- c. TAFM - The TAFM trajectory is shaped within the TAFM flight corridor to minimize trajectory transients and provide adequate maneuver margins for entry trajectory dispersions, winds, and aerodynamic uncertainties while maintaining dynamic pressure, descent rates, and turning rates that are acceptable for compartment venting and sonic boom overpressures. At entry/TAFM interface, 2500 fps relative velocity, the dynamic pressure is 209 psf, which is near the center of the flight corridor. The dynamic pressure is reduced to 160 psf at Mach 0.9 and is then ramped to the 265 psf required for the A&L phase outer glideslope (OGS).
- d. Approach and Landing - The A&L phase is initialized when the altitude decreases through 10 000 feet. The basic geometry consists of a 20-degree OGS followed by a preflare (first flare) maneuver to a 1.5-degree inner glideslope (IGS). The criteria used for the design of these constants were to provide as shallow an OGS as possible while maintaining adequate performance margins, to provide as much time as possible on the IGS, and to provide an energy reserve at nominal touchdown corresponding to 4 seconds of flight time under stressed conditions. Two OGS intercept points and two speedbrake retraction altitudes can be used to accommodate from 20-percent tailwinds to 100-percent headwinds.

At A&L interface, the body flap is commanded to retract to the trail position (0 degrees). The speedbrake is modulated to maintain a constant 473 rps equivalent airspeed (280 knots equivalent airspeed (KEAS) or 265 psf dynamic pressure) on the OGS. Nominal speedbrake retraction occurs at 2500 feet altitude. The preflare maneuver starts at 2000 feet altitude and is designed to result in a normal acceleration of 1.3 g's or less. The transition from the pullup circle to the exponential capture mode is commanded at a range of 3784 feet from the runway threshold. When the velocity decreases through 270 KEAS, the landing gear is deployed. A nominal gear deployment time of 7.5 seconds was used and resulted in the gear being down and locked 11.8 seconds prior to touchdown. This 270 KEAS is the minimum velocity to start gear deployment and still have the gear down and locked 5 seconds prior to touchdown for a three-sigma deployment time of 9.4 seconds. Touchdown occurs at a range of 2942 feet past the runway threshold with a 2.4-fps sink rate. The velocity at touchdown is 185 KEAS, which equates to a 8.1-second energy reserve; the ground relative velocity is 191 knots.

- e. Touchdown and Rollout - Immediately after main-gear touchdown, the speedbrake is commanded to 50 percent, and a 6- to 8-degree vehicle pitch attitude is maintained until the equivalent airspeed decelerates to 165 knots. Derotation at a pitch rate of -3 deg/sec is then commanded with weight on nose gear occurring at a range of 5538 feet from the runway threshold. The range at the end of rollout is 9510 feet, which occurs 36 seconds after main-gear touchdown.

4.0 STS-1 OFP FLIGHT DESIGN GROUNDRULES AND CONSTRAINTS

The following groundrules and constraints (ref. 5) were used in the generation of the OFP for STS-1.

4.1 GENERAL

- 4.1.1 Trajectory techniques will provide maximum vehicle subsystem margins from design specifications when possible. Priorities and trade analyses will determine the best compromise when conflicts exist.
- 4.1.2 The launch date is March 31, 1980 at 11:30:00 GMT (6:30 a.m. EST).
- 4.1.3 The nominal orbit is 150/150 n. mi.
- 4.1.4 The nominal inclination is 40.3 degrees. This inclination will provide an ET groundtrack that, for excessive MECO overspeeds, passes to the south of King Island and north of the Furneaux Group off the southern coast of Australia.
- 4.1.5 Nominal and abort to orbit (ATO) landings will be on Rogers Lakebed runway 23 at EAFB. Abort-once-around (AOA) landing will be on runway 17 at Northrup strip. Landing for glide return to launch site (GRTLS) will be on runway 15 at KSC. Because of the high probability of landing on either runway 15 or 33 for RTLS, OFT performance assessment will be based on the capability to achieve either runway for RTLS. Nominal and abort landing site locations are given in appendix A.
- 4.1.6 Standard GSTDN contact data will be provided for selected stations depending on the mission phase. Table II of appendix A establishes the AOS/LOS computational requirements for each phase. Minimum elevation may be computed assuming zero degree or 3 degrees maximum elevation with no masking. However, normally all AOS/LOS is computed assuming zero degree elevation with masking and keyholes considered. Exclusion of a site from table II, appendix A does not preclude it from being used in the tracking network.
- 4.1.7 All landings (nominal, abort, and contingency) except AOA will be no earlier than 30 minutes after sunrise and no later than 30 minutes before sunset. AOA landings may be as early as sunrise. It is desirable that nominal landing at EAFB occur prior to 10:00 a.m. local time.
- 4.1.8 A 1-hour launch window (as a minimum) will be provided.

- 4.1.9 There is no ontime launch requirement.
- 4.1.10 There are to be two crewmen. Crew provisions will be loaded for 5 days.
- 4.1.11 The planned flight duration will be approximately 5^{1/2} hours.
- 4.1.12 There will be landing opportunities at EAFB on at least four orbits each day.
- 4.1.13 The payload will include the development flight instrumentation (DFI), the induced environment contamination monitor (IECM), the aerodynamic coefficients identification package (ACIP), and the Orbiter experiments (OEX) tape recorder. Mass properties for total payload weight are given in appendix A.
- 4.1.14 The payload bay doors (PLBD) are to be opened as soon as operationally practicable after OMS-2. However, the contingency capability will exist to leave the PLBD closed for up to 8 hours following OMS-2.
- 4.1.15 (Deleted)
- 4.1.16 All nominal deorbit opportunities will be planned such that the entry crossrange is <550 n. mi.; however, a crossrange of <690 n. mi. is acceptable for AOA and contingency cases.
- 4.1.17 (Deleted)
- 4.1.18 Reaction control system (RCS) backup deorbit capability is required. For this contingency, propellant from both OMS pods is assumed to be available.
- 4.1.19 The deorbit targeting will be biased to accommodate the designated backup deorbit propulsion mode.
- 4.1.20 Aerodynamic data, atmosphere and wind models, I-load values, software baseline (including implemented CR's), engine data, assumed constants, geodetic locations for TACAN/MSBLS/launch and landing sites and mass properties data for the nominal, RTLS, ATO, and AOA analysis are specified in appendix A. The limitations and constraints defined in

volume I and volume II of the SODB (JSC-08934) will be adhered to in the design of the nominal and abort OFF profile except as defined in appendix B. (See 4.1.21.)

- 4.1.21 Appendix B summarizes the groundrules and constraints that deviate either from reference 2 or from reference 3 of this document.

4.8 DESCENT - DEORBIT

- 4.8.1 The IMU alignment will be designed to minimize the IMU misalignment at the entry interface. To maintain system performance margins, the maximum platform misalignment at entry interface will be 950 arc-seconds. For a contingency where degraded system performance margins are necessary during entry, the maximum IMU misalignment at entry interface will be 1900 arc-seconds.
- 4.8.2 The deorbit maneuver will nominally be performed using two OMS engines, but due to targeting and guidance flexibility, the capability will exist to downmode to other thruster configurations during the burn. Specifically, the TIG and targets will be selected so that if one OMS engine fails at TIG, or any time later in the burn, the deorbit maneuver can be successfully completed using the remaining OMS engine. Furthermore, if the other OMS engine should also fail at the same time or at any time after the first failure, the deorbit maneuver could still be successfully completed using the +X RCS engines.
- 4.8.3 Propellant-critical contingency deorbit will be based on a shallower-than-nominal targeting criteria to provide the best compromise between deorbit capability, RCS propellant availability for attitude control during atmospheric descent, and entry thermal environment.
- 4.8.4 Between the termination of the deorbit maneuver (except ATO) and entry interface for two OMS, one OMS, and RCS modes that result from the triple downmoding operation, a minimum free-fall time of 15 minutes is required for entry preparation.
- 4.8.5 In addition to satisfying the entry velocity, flightpath angle, and range requirements, the deorbit maneuver will include an out-of-plane component to achieve an acceptable Orbiter entry interface center of gravity and weight.
- 4.8.6 The Orbiter entry weight will be minimized by reducing remaining content with reasonable operations techniques.

- 4.8.7 When selecting the nominal deorbit revolution, it is highly desirable to have communication with and tracking of the spacecraft postdeorbit.
- 4.8.8 During descent, the Orbiter shall operate within the limits established in Structural Flight Restrictions for Orbital Flight Test Program (SD78-SH-0121).
- 4.9 DESCENT - ENTRY THROUGH ROLLOUT
- 4.9.1 The environment model used for computing the nominal OFP will be a mean monthly atmospheric model for the planned entry date as defined by the Four-D Global Reference Atmospheric Model. The environment model for the nominal profile simulation will not include winds.
- 4.9.2 The entry profile will be shaped to achieve a balance between the TPS surface and bondline temperatures and Orbiter structural temperatures such that the TPS performance during entry is optimized. This balance will include allowances for aerodynamic heating and trajectory dispersions.
- 4.9.3 (Deleted)
- 4.9.4 Entry-through-landing profiles will conform to control surface hinge moment limits, aerodynamic load limits, actuator rate limits, and structural load limits. For actual Orbiter weights for nominal end of mission, the structural load limits are +0.3 to 2g normal load factor between a Mach no. of 5.0 and an Earth relative speed of 24 000 fps and -0.3 to 2.0g normal load factor for a Mach no. ≤ 5
- 4.9.5 Optimization of the entry profiles will include consideration of sonic boom ground-level overpressures.
- 4.9.6 Nominal entry profiles will be targeted so that post-blackout target changes are not required. However, the profiles will be shaped to maximize post-blackout redesignation capability.
- 4.9.7 At entry interface, the nominal Orbiter longitudinal c.g. will be 66.70 percent and the lateral c.g. displacement will be 0.0. The nominal vertical c.g. will be 375 \pm 3 inches.

- 4.9.8 The terminal area energy management (TAEM) guidance reference dynamic pressure will be based on the concept of flying directly to the heading alignment circle without employing an S-turn in tailwind conditions.
- Additionally, this dynamic pressure will allow the TAEM/approach and landing interface constraints to be met in the presence of severe headwinds. The energy control will provide conditions suitable for the initiation of a manual approach.
- 4.9.9 The TAEM profile will be compatible with manual and automatic modes of operation.
- 4.9.10 The max q will be limited to 300 psf for a Mach number >5 and to 342 psf for a Mach number <5. The dynamic pressure on the nominal profile will be less than 240 psf for a Mach number >5 and less than 300 psf for a Mach number <5. During the terminal area maneuvers for a Mach number <2.5, the minimum dynamic pressure will be restricted to a value that keeps the vehicle's lift/drag (L/D) on the front side of the L/D curve. Therefore, the minimum dynamic pressure is a function of Orbiter weight and varies from 133 to 161 psf as the Orbiter weight varies from 181 000 to 218 000 pounds.
- 4.9.11 To conform to compartment venting constraints, the maximum descent rate and dynamic pressure will be 400 fps and 300 psf, respectively, in the transonic region. In addition, the minimum dynamic pressure on the nominal profile will be 150 psf in this flight region.

5.0 SIMULATION DESCRIPTION

The Orbiter mass properties and c.g. locations (ref. 9) used to design the STS-1 deorbit-through-landing flight profile are presented in table 5.0-I. The OMS loading requirement is summarized in table 5.0-II. The state vectors at deorbit ignition minus 35 minutes, deorbit ignition, and EI minus 5 minutes (descent simulation initiation), and EI are presented in table 5.0-III.

The STS-1 deorbit trajectory presented in this document was generated using the space vehicle dynamics simulation (SVDS) program (ref. 10). All phases were simulated with the SVDS 6-degree-of-freedom option, except the initial coast period prior to deorbit, which was simulated with the 3-degree-of-freedom option. The STS-1 entry trajectory was generated using the 6-degree-of-freedom SVDS program documented in reference 11. The flight profile is generated using zero winds and the aerodynamics data defined in the April 1979 Aerodynamic Design Data Book (ref. 12). The atmospheric model used for this profile is the mean monthly atmospheric model for the month of April, as defined by the Four-D Global Reference Atmospheric Model (ref. 13) and is presented in table 5.0-IV. Table 5.0-V presents pressure density and temperature deviations from the 1962 Standard Atmosphere. The density deviation data are presented graphically in fig. 5.0-1. The 6-degree-of-freedom integrated flight control system (IFCS), as described in reference 14 and supported in reference 15, was used during the descent phase. Guidance commands and control surface deflections were implemented using the automode logic for all channels. Longitudinal control is maintained by the moments resulting from the modulation of the elevons and body flap and from RCS jet firings. Lateral-directional control is maintained via moments resulting from aileron and rudder deflections and from RCS jet firings. A preset speedbrake schedule is maintained until $M = 0.9$. Flight control sensor and controller models (ref. 16) were utilized. Thermal models used to define TPS surface and backface temperatures are the simplified models described in reference 17. The entry, TAEM, and autoland guidance (with modifications from reference 18) used in simulating the STS-1 profile are defined in reference 16. The navigation simulation used in this reference trajectory is defined in references 19 and 20. Coordinate system definitions are contained in reference 21.

6.0 DESCENT PROFILE

The cycle 3 descent profile is initiated with a deorbit maneuver at 53:31:04 GET. The deorbit maneuver is followed by a coast period of 25 minutes 42 seconds prior to the EI, which occurs at 400 000 feet altitude. The entry phase of the profile begins at EI and is terminated at the entry/TAEM interface, which occurs at a relative velocity of 2500 fps. The TAEM phase of the profile is terminated at the TAEM/A&L interface, which occurs at approximately Mach 0.6 and at an altitude of 10 000 feet. Modified autoland guidance, which simulates a manually flown trajectory, is used to guide the Orbiter to touchdown.

The prime landing site for STS-1 is runway 23 on Rogers Lakebed at EAFB. The runway azimuth and the coordinate systems origin, with respect to the Fischer 1960 ellipsoid for runway 23, are 244.41 degrees east of north, 34.96 degrees north geodetic latitude, and 117.820 degrees west longitude, and 208.0 feet altitude (ref. 5).

The design of the STS-1 OFP has resulted in a change in postdeorbit tracking by the Guam station as reflected in a decrease in maximum elevation angle from 23.5 degrees for the previous profile to 16.7 degrees for this profile. Approximately 5.5 minutes of tracking coverage is provided based on being clear of masking.

A detailed discussion of the deorbit, entry, TAEM, and A&L phases is presented in sections 6.1 through 6.4. The descent groundtrack is presented in figure 6.0-1. An overall sequence of events is presented in table 6.0-I.

6.1 DEORBIT

STS-1 will be launched from KSC into an approximate 150-n. mi. altitude circular orbit with a 40.3-degree inclination. The nominal deorbit maneuver is thrust-initiated at 53:31:04 GET during the 36th orbit, with subsequent landing on Rogers Lakebed runway 23 at EAFB at 10:01 a.m. PST. The 36th orbit was selected for deorbit because it provides the best combination of predeorbit and postdeorbit tracking and communication. A backup deorbit opportunity occurs during the 37th orbit with degraded postdeorbit tracking and communication and with no coverage during the last orbit through the Ascension tracking station. The STS-1 orbits that provide deorbit opportunities with subsequent landings at EAFB are presented in table 6.1-I. The deorbit maneuver will be nominally performed using two OMS engines, with a capability to downmod to either a one-OMS engine or RCS thruster configuration if required. The time of ignition (TIG) is biased to provide the capability to achieve the same desired EI state vector with a two-OMS maneuver, a one-OMS maneuver, or a +X RCS maneuver. The range-inertial velocity-inertial flightpath angle target lines for these conditions are presented in figure 6.1-1.

The deorbit guidance maneuvers the Orbiter to the desired EI conditions assuming a conic coast. The deorbit targets represent the actual desired EI conditions, so biased targets must be used onboard to achieve these conditions. The Cycle 3 targets have been biased by reducing the first coefficient of the velocity-flightpath angle target line (C_1) by 1.0 fps and by reducing the targeted

central angle between ignition and EI (Θ_I) by 0.003 degree to account for Earth oblateness effects.

The inplane two-OMS deorbit delta V for the biased TIG and targeting is 282 fps. It is necessary to use 225 pounds of excess OMS propellant to achieve the desired entry longitudinal c.g. position of 66.70 percent with a resulting Orbiter entry weight of 191 902 pounds. This propellant wasting for the two-OMS deorbit is accomplished by an out-of-plane deorbit maneuver with a total delta V of 292.9 fps. The burn duration is 2 minutes 28 seconds followed by a 25-minute 42-second free-fall time from thrust termination to EI. For the one-OMS backup deorbit, the biased TIG and targeted total delta V is 292.9 fps, and the resulting out-of-plane propellant wasting is 375 pounds to achieve the entry c.g. and weight. The one-OMS deorbit burn maneuver lasts 4 minutes 56 seconds with a free-fall time of 23 minutes 15 seconds. For the +X RCS deorbit, the total delta V is 270 fps with a resulting weight and c.g. of 191 827 pounds and 66.78 percent, respectively. The +X RCS deorbit burn lasts 7 minutes 32 seconds with a free-fall time of 20 minutes 36 seconds. Significant deorbit parameters are summarized in table 6.1-II. The OMS propellant usage is depicted graphically in figure 6.1-2.

The ideal maneuver pads (MNVR PADS) for the two-OMS, the one-OMS, and the +X RCS deorbit modes are shown in tables 6.1-III, IV, and V, respectively. Similar computer-generated displays at selected events from the 6-DOF two-OMS nominal EOM simulation are presented in table 6.1-VI. The differences between the actual and ideal attitudes are due to deadbands in the attitude control systems. The Deorbit-Entry-Landing Pad (DEL PAD) for the nominal EOM is presented in table 6.1-VII. The time history plots of trajectory, attitude, and burn-related parameters from the 6-DOF deorbit simulation are presented in figures 6.1-3 through 6.1-20.

The APU's are started 5 minutes before the deorbit maneuver and remain operating until landing. Aerosurface cycling is not required for this flight because of the benign thermal environment. Nominal conditions at EI are 4358 n. mi. range to go, 25 752 fps inertial velocity, and -1.21 degrees inertial flightpath angle. These nominal conditions at EI have changed slightly from the cycle 2 values of 4399 n. mi., 25 753 fps, and -1.18 degrees, respectively. The nominal end-of-mission reference to stable member matrix (REFSMATS) for stable members 1, 2, and 3 are presented in table 6.1-VIII. The RELMATS and RELQUATS for the deorbit maneuver are presented in table 6.1-IX.

A RELMAT is a mean-of-50-to-attitude display indicator (ADI) reference frame transformation matrix. For the deorbit/entry flight phase, two RELMATS are used called the REF RELMAT and the INRTL RELMAT (RELMAT's, nine-element matrices, are converted to RELQUATS, four element quaternions, for onboard use).

The REF RELMAT is computed so that when the vehicle is in the nominal deorbit attitude (includes out-of-plane wasting), the ADI attitudes (REF setting) will read pitch = 80° , yaw = 0° , roll = 0° . The INRTL is computed so that if wasting is terminated at ignition and the vehicle is maneuvered back inplane, the ADI attitudes (INRTL setting) will read pitch = 180° , yaw = 0° , roll = 0° .

The ADI attitudes are assumed to be computed in a pitch/yaw/roll sequence with the ADI in a +X sense direction.

6.2 ENTRY

The STS-1 EI-through-landing groundtrack is presented in figure 6.2-1. Entry profile shaping, control surface deflection schedules, nominal trajectory data, and the aerodynamic crossrange capability are discussed in sections 6.2.1, 6.2.2, 6.2.3, and 6.2.4, respectively. Significant trajectory parameters for the entry are presented in figures 6.2-2 through 6.2-50. Table 6.2-I presents a comparison of the trajectory and aerosurface parameters used in designing the STS-1 profile to the actual values achieved by the profile. The entry-through-landing guidance constants (I-loads) are given in appendix A.

6.2.1 Entry Profile Shaping

The objective of the entry profile shaping for STS-1 is to minimize the effects of the TPS thermal environment, maximize the FCS performance margins, and minimize structural loads while providing sufficient maneuver margins to compensate for trajectory, navigation, aerodynamic, and environment dispersions. In some cases, these objectives result in conflicting requirements for the entry profile. For example, shortening the entry range reduces the TPS backface temperatures but increases the TPS surface temperatures for a particular angle-of-attack profile.

The entry profile developed for STS-1 is a compromise between the conflicting requirements for profile shaping. The angle-of-attack profile for STS-1 (fig. 6.2-2) is designed to provide improved thermal conditions at high speeds at the expense of crossrange capability and differs from the design entry profile developed to achieve a high crossrange by maintaining the initial entry angle of attack at lower speeds, thus eliminating the intermediate ramp to the lower angle-of-attack levels required for high crossrange. Minor deviations from the reference angle-of-attack profile occur as a result of the incorporation of angle-of-attack modulation logic in the entry guidance. This involves modulation of the angle of attack to prevent major deviations from the drag acceleration profile during the pullout maneuver and during roll reversals. The reference angle-of-attack profile and the drag-velocity profile are very similar to those of reference 3.

With this reference angle-of-attack profile, the entry corridor, as limited by TPS surface temperatures, structural loads, flight control considerations, and the equilibrium glide capability, can be defined. This latter constraint must be met to ensure that the flight conditions can be sustained (i.e., no subsequent trajectory transients will necessarily occur) and that crossrange maneuvering is possible. The corridor, as limited by these considerations, is presented in figure 6.2-3(a) in the drag acceleration relative velocity plane. The TPS backface temperature is minimized by dissipating the Orbiter kinetic and potential energy as quickly as possible within the limits defined by systems and by flight dynamic constraints as illustrated in figure 6.2-3. This is achieved by maintaining the drag acceleration as high as possible throughout entry

consistent with surface temperature, systems, and flight dynamics constraints. The backface is more sensitive to the drag acceleration level at the higher speed during entry and is relatively insensitive to the drag acceleration level at speeds below 10 000 to 12 000 fps.

The basic policy in shaping for the thermal criteria is to first achieve the surface temperature margin and then the backface temperature margin. In the event both criteria cannot be met, the backface temperature criterion is exceeded while the surface temperature criterion is met. However, this OFP marginally meets both the surface and backface temperature requirements with onorbit cooldown prior to deorbit.

The design-drag-acceleration/velocity profile for this update is very similar to the previous operational flight profile (ref. 3). The drag-velocity corridor is restricted between the surface temperature constraint boundaries and the equilibrium glide boundary in the high-velocity region of entry. The drag profile in this region reflects a slight increase in vehicle structural temperatures when compared to the previous profile as a result of the small increase in Orbiter weight. This drag-acceleration profile intercepts the same constant drag level as in the previous operational profile at 33 fps². From this point, the design-drag-acceleration profile is essentially unchanged from the previous OFP down to 3564 fps. Between 3564 fps and 2500 fps, a slight change in the angle-of-attack schedule resulted in a small change in the drag-acceleration profile. At entry/TAEM interface the design drag acceleration was reduced slightly from 21.0 fps² for cycle 2 to 20.8 fps² for the current profile.

An entry weight of 191 902 pounds was used for the current entry profile compared to 189 844 pounds for the previous cycle 2 design profile of reference 3; the longitudinal center-of-gravity position remains unchanged at 66.7 percent. The increased Orbiter pitchdown moment reflected in the April 1979 aerodynamic data of reference 12 requires smaller down control surface deflections. The ± 12.5 -degree azimuth deadband is replaced by a ± 10.5 -degree deadband until the first roll reversal is completed, after which the magnitude of the deadband is expanded to ± 17.5 degrees. The change in the deadband limit is made to keep the first roll reversal from occurring at the guidance phase change from the temperature control phase to the equilibrium glide phase. This reduces the probability of a transient occurring in the drag acceleration profile during a guidance phase change.

There have been no changes in the TPS surface temperatures model since reference 3 was published. In shaping the STS-1 entry profile, the TPS surface temperatures were evaluated at five locations as illustrated in figure 6.2-4. The single-mission maximum surface temperatures are 2600° F for high-temperature reusable surface insulation (HRSI) material, (LI-1100), 2700° F for HRSI material on the chine (LI-2200), and 2800° F for the RCC material on the nose and wing leading edge. Because the TPS surface temperatures are computed using a simplified TPS model, the limiting temperatures on the nose and wing leading edge must be adjusted to 2950° F to account for a bias in the temperature prediction. The most critical surface temperature location is on the wing leading edge, which is slightly more restrictive than the forward chine region.

The surface temperature limits and margins used for aerodynamic heating uncertainties and trajectory dispersions in designing the STS-1 OFP are presented in table 6.2-II. Because the aerodynamic heating uncertainties and effects of trajectory dispersions on the TPS temperatures are independent, the effects of these two sources of temperature dispersions are combined statistically by the root-sum-square technique. In addition, the elevon temperature can be further dispersed because of steady-state deflections required to compensate for lateral c.g. offset and airframe asymmetries and by transient deflections required for high-frequency attitude control. Table 6.2-V lists the source of these elevon and body flap surface deflection errors. The temperature dispersions resulting from these elevon deflections were added to the combined aerodynamic, heating uncertainty and trajectory dispersion effects. The material limits on the nominal surface temperatures are translated into constraints on the entry corridor in figure 6.2-3(a). The limiting surface temperatures are on the forward chine (control point 6) at velocities greater than 19 500 fps and on the outer elevon underside (control point 4) at velocities less than 19 500 fps. When translated into constraints on the entry corridor, the two-sigma and three-sigma thermal boundaries give limiting surface temperatures on the wing leading edge (control point 3) at velocities greater than 17 500 fps and on the outer elevon underside at velocities less than 17 500 fps as illustrated in figure 6.2-3(b). Also shown in figure 6.2-3(a) are the effects of additional constraints and the guidelines on the entry corridor. On the first flight, it is desirable to limit the structural loads to a 2.0g normal load factor, which is 80 percent of the design value of 2.5g's. Also shown for information purposes is the 1.5g normal load factor line.

The Orbiter elevon and body flap surface temperature limits during entry for this profile have increased from those of the previous profile. The elevon and body flap control surface temperature limits have increased 34 degrees and 101 degrees, respectively. These increases are primarily due to the technique in which the trajectory dispersion effects were evaluated. The present profile provides an improvement in the temperature control margin for the body flap and elevon because of the increased aerodynamic pitchdown moment characteristics reflected in the aerodynamic update. The increased pitchdown moment requires decreased control surface down deflections. Additionally, the elevon deflection schedule has been changed from the cycle 2 zero-deflection schedule to a 1-degree up deflection schedule in the high-heating region. This results in a more favorable balance of temperature margins on the body flap and elevon.

The heat load and maximum reference heating rate on this trajectory is 53 731 Btu/ft² and 61.4 Btu/ft²/sec, respectively, compared to the respective cycle 2 values of 53 147 Btu/ft² and 59.7 Btu/ft²/sec.

The equilibrium glide boundary defines the minimum drag level that the time rate of change of flightpath angle can be maintained equal to zero. Thus, this line defines the limit for sustaining equilibrium flight. Although flight conditions with lower values of drag acceleration can be achieved, this condition is temporary, and a subsequent trajectory transient to higher drag acceleration will occur. This equilibrium glide boundary is a function of bank angle as well as angle of attack and relative velocity. Therefore, the boundaries were defined for the minimum bank angles required to ensure a turning capability for

crossrange maneuvering. This minimum bank angle is a function of entry speed with higher values required to overcome the higher inertia at high speeds.

Thus, the entry guidance uses two discrete levels of minimum bank angle to achieve turning; 37 degrees at high speeds and 20 degrees at low speeds. These bank angle limits result in significant turning capability with little loss in entry corridor because turning capability and entry corridor are functions of the sine and cosine of the bank angle, respectively.

The entry profile was shaped to satisfy the surface temperature constraints while keeping the drag level as high as possible to minimize the backface temperature. The resulting nominal entry profile is presented in figure 6.2-3 along with the entry corridor. The summary of the resulting thermal environment for several surface panels is presented in table 6.2-III. Orbiter surface temperature limits and margins for the five temperature control points of interest are presented in table 6.2-IV. Data in this table are based on a 50-case Monte Carlo analysis, Appendix C. Table 6.2-V presents the elevon and body flap bias and random errors used to compute corresponding TPS temperature dispersions. When the three-sigma trajectory and deflection dispersions from this analysis are combined with the aerothermal heating dispersion and added to the maximum mean temperature, the actual OFP temperature margins can be determined. Table 6.2-V shows that the OFP is designed with sufficient temperature margins to maintain acceptable surface temperatures. The Monte Carlo analysis results demonstrate that the backface temperature margin is the same as that anticipated by the design of the OFP. The negative back-face temperature margin shown on panel 2 is representative of an AOA case where high initial vehicle temperatures (summer launch) are encountered. Acceptable back-face temperature margin for EOM will be achieved by onorbit cool down, if required.

A 40-degree angle of attack is maintained during the early part of atmospheric descent to minimize the aerodynamic heating environment. This angle of attack is maintained until the aerodynamic heating is reduced to a relatively low level with pitchover to a lower angle of attack beginning at an Earth-relative speed of 14 500 fps. This pitchover continues until an angle of attack of 14.0 degrees is reached at the entry/TAEM interface at 2500 fps Earth-relative speed.

The low-speed part of the entry profile, during transition to the low-angle-of-attack and trajectory conditions at the TAEM interface, was shaped to achieve the desired TAEM initial flight conditions and to maintain the entry profile at the location in the entry corridor that maximizes the capability to compensate for navigation, aerodynamic, and environmental dispersions while providing a capability for postblackout runway redesignation. The target flight conditions at this interface were selected to provide proper positioning within the TAEM flight corridor and the entry profile was designed to achieve these conditions. The lateral guidance requirement of a roll reversal at 2900 fps resulted in a lower dynamic pressure and a shallower flightpath angle than desired at the entry/TAEM interface. Although the roll reversal results in transient trajectory conditions being present at entry/TAEM interface, these flight conditions are sufficiently close to the target interface conditions to allow for rapid convergence of conditions within the TAEM flight corridor by the selected TAEM profile.

The transition phase angle-of-attack schedule remained the same as that of the previous profile with the exception of a slight change in the profile between 3564 fps and 2500 fps. This change incorporates a linear angle-of-attack ramp and provides a design angle of attack of 14.0 degrees at the entry/TAEM interface compared with 13.5 degrees for the cycle 2 profile.

6.2.2 Control Surface Deflection Schedules

The nominal elevator and speedbrake deflection schedules and the corresponding body flap deflections are designed to aerodynamically trim the Orbiter to maximize the effectiveness of the control surfaces, to provide Orbiter attitude control while maintaining aerodynamic heating on the control surfaces within limits, and to minimize the attitude control moments required from the RCS. The elevator deflection schedule (ref. 14) and actual elevator deflection, the speedbrake schedule, and the actual body-flap deflection to accomplish this are presented in figures 6.2-5 and 6.2-6. During the period of high aerodynamic heating, the speedbrake is fully retracted to minimize the aerodynamic heating on these surfaces, and elevator and body-flap deflection schedules are balanced to control the surface temperatures of these two control surfaces. At speeds above 13 600 fps, the elevator is maintained at 1 degree up, and the body flap is deflected approximately 7.0 degrees down during most of this region. A linear ramp is introduced in the elevator schedule at 13 600 fps to move the elevator to a 5.0-degree down deflection at 4000 fps. This down deflection is necessary to ensure that the rolling moment due to aileron deflection is not nulled by the rolling moment from the yaw angle induced by the aileron deflection. This provides favorable aileron yawing moment characteristics ($C_{n\delta A}$) required when using the aileron to compensate for the aerodynamic moments caused by lateral c.g. offset and aerodynamic asymmetries.

Use of the rudder is initiated at Mach 3.5, but rudder effectiveness is initially low. Aileron control for lateral-directional trim is gradually reduced from this point as the rudder effectiveness increases. For this reason, the 5.0-degree down elevator deflection is maintained between 4000 fps and 3000 fps. At 3000 fps, the elevator is moved to a position favorable to switching to a traditional airplane-type flight control system (FCS). The FCS is blended from the early-to-late configuration in the Mach range from 3.0 to 0.9, where traditional airplane-type control surface functioning is introduced. In the Mach range from 2 to 1.5, the elevator is at 3 degrees up deflection to minimize the effect of elevator deflection on lateral dynamics and to aid in the reduction of elevon hinge moments. In the transonic speed range, the elevator is deflected to a down position to reduce the elevon hinge moment.

The speedbrake is deflected to a full-out position at a speed of 9000 fps to induce a pitchup moment so that the elevator can normally be deflected down in this region. Conversely, at a speed of 2500 fps, the speedbrake is retracted to 65 degrees to improve rudder effectiveness ($C_{n\delta r}$) and reduce the nose-up pitching moment. At subsonic speeds, the nominal speedbrake deflection is the midvalue to allow for modulation for speed control. The body flap is used to balance the pitching moment to trim the Orbiter.

6.2.3 Aerodynamic Crossrange Capability

The crossrange capability is a function of energy and targeting conditions at EI. For this reason the early AOA with an apogee altitude of 105 n. mi. is most restrictive for STS-1. This profile has a nominal crossrange capability of 792 n. mi., with a 99.86 percent probability of achieving a 700-n. mi. crossrange with the first roll reversal occurring at a relative velocity of 3500 fps. However, for normal operations, the Orbiter should limit the maximum entry crossrange to 550 n. mi.

6.3 TAEM

The primary factors that influence trajectory shaping during the TAEM phase are aerodynamic maneuver capability, adequate margins to compensate for winds and dispersions, compartment venting requirements, flight control constraints, and sonic boom overpressure considerations. The best profile for providing flight control and aerodynamic maneuver margins, reducing transonic hinge moments, minimizing sonic boom overpressures and optimizing compartment venting is a profile with low dynamic pressure and high angle of attack in the transonic region. The TAEM altitude reference has been shaped to provide a smooth dynamic pressure and angle-of-attack transition from TAEM guidance initiation at 2500 fps Earth-relative velocity to Mach 0.9, which avoids flight control lateral directional constraints and provides adequate maneuver margins without excessive sonic boom over-pressures. The TAEM dynamic pressure is then ramped to achieve the A&L OGS requirements. Since reference 3 was published, a left-hand turn onto the OGS has been incorporated into the TAEM phases.

Significant STS-1 trajectory parameters for the TAEM phase are presented in figures 6.3-1 through 6.3-23. The TAEM-through-landing groundtrack is given in figure 6.3-1. The entry/TAEM interface conditions are summarized in table 6.3-I. Appendix A lists the TAEM guidance constants required for this profile.

The guidelines and constraints used in defining the flight corridor during the TAEM region are presented in figures 6.3-2 and 6.3-3 in the dynamic pressure-relative velocity plane and in the angle-of-attack-Mach number plane, respectively. Figure 6.3-2 presents the flight limits for the structural and flight control systems, the ground-level sonic boom overpressure, the minimum dynamic pressure that constrains operation to the front side of the L/D curve as required by the TAEM guidance altitude and energy controllers, and the dynamic pressure limit to accommodate vehicle pressure differentials due to compartment venting limitations. The sonic boom guideline corresponds to a 2.0 lb/ft² ground-level overpressure and is based on the data and analysis given in reference 4.

The TAEM dynamic pressure profile in figure 6.3-2 is shaped to achieve an angle-of-attack profile that will avoid the new lateral/directional dynamic stability (β dynamic) boundary resulting from the April 1979 aeroelastic updates (ref. 10). At entry/TAEM interface the dynamic pressure at initiation of TAEM guidance is 209 psf (233 psf for the previous profile design) and is near the center of the flight corridor. The dynamic pressure is then gradually reduced to 160 psf at Mach 0.9 to achieve angle-of-attack flight that will avoid

the $C_{n\beta}$ dynamic stability boundary. The dynamic pressure is then ramped to 265 psf to achieve conditions for the A&L OGS of 20 degrees.

This dynamic pressure profile biases the trajectory toward the toe of the maneuver footprint and accomplishes six desirable objectives as follows:

- a. Provides a maneuver margin to compensate for winds that, on the average, present a tailwind component during the planned mission date.
- b. Provides a margin adequate to allow subsonic acceleration to the dynamic pressure of 265 psf required at initiation of the A&L phase without undue penalization of the capability for excess energy dissipation.
- c. Provides a smooth angle-of-attack profile with minimum pitch transients around Mach 1.
- d. Provides sufficient margin from compartment venting constraints to avoid structural integrity problems under dispersed conditions.
- e. Minimizes transonic hinge moments. The high-hinge moment coefficients encountered in this region are compensated for by lower dynamic pressure.
- f. Minimizes sonic boom overpressures. The reduction in dynamic pressure from the value at entry/TAEM interface maintains dynamic pressure below the 2 psf overpressure guideline to the extent that maneuverability and flight constraints will not be compromised.

The angle-of-attack corridor presented in figure 6.3-3 defines the angle-of-attack limit for the flight control system (FCS) as defined in reference 14. Below Mach 3.0, in the low-supersonic transonic Mach 2.0 to 1.0 flight regime, the April 1979 aeroelastic update has resulted in a significant reduction in lateral stability ($C_{l\beta}$) and directional stability ($C_{n\beta}$). Because the aeroelastic effect is proportional to the dynamic pressure, the reduction in lateral/directional stability is more pronounced at the lower angles of attack. Consequently, the lower angle-of-attack limit in the Mach 1.0 to 2.0 region is defined by the ability of two RCS yaw jets to successfully augment the unstable $C_{n\beta}$ dynamic as presented in figure 6.3-3. Also shown in this figure are the regions where the Orbiter has a tendency for rolloff, noselike, and buffet onset. Although the effect of these characteristics on the FCS performance are acceptable due to their transient nature, these regions are avoided to the extent possible for STS-1.

The TAEM altitude and altitude reference have been adjusted at the entry/TAEM interface to minimize the angle-of-attack transients produced by guidance logic changes. As indicated in figure 6.3-5, the altitude reference is approximately 4700 feet higher than the actual altitude thus requiring the Orbiter to maintain nose-up flight to recapture the altitude reference. This minimizes the pitchdown transient at entry/TAEM interface. Equilibrium conditions on the TAEM reference profile are reestablished just prior to aligning the vehicle with the HAC tangency point. After the heading toward the HAC is attained, the turn compensation logic causes a second pitchdown to occur.

6.4 APPROACH AND LANDING

6.4.1 Trajectory Capture to Touchdown

The objective of the A&L profile shaping for STS-1 is to minimize the descent rate to the extent possible while providing benign maneuvers and sufficient energy to achieve the desired touchdown conditions. Based on these considerations, the A&L profile consists of an OGS followed by a preflare maneuver to an IGS and a final flare maneuver prior to touchdown.

The OGS is designed to be as shallow as possible to minimize the descent rate. The dynamic pressure on the OGS is selected to provide sufficient speedbrake reserve to cope with winds and dispersions and to provide the energy required at initiation of the preflare maneuver. The energy at initiation of the preflare maneuver must be sufficient to accommodate the subsequent deceleration during the preflare maneuver and the deceleration on the IGS and to provide the targeted touchdown airspeed. For the STS-1 profile, the OGS angle is -20 degrees and the dynamic pressure on the OGS is 265 psf, which corresponds to a reference velocity of 280 KEAS.

The preflare phase of the A&L trajectory transitions the Orbiter from the OGS to the IGS. Profile shaping criteria for the preflare phase are to provide a normal acceleration of 1.3 g's or less during the maneuver and to minimize oscillations in the normal acceleration during the maneuver.

The criteria used to shape the A&L profile for the IGS are to provide a minimum of 5 seconds on the IGS and an energy reserve at touchdown corresponding to at least 4 seconds of flight time. Time on the IGS is crucial because it allows time for the Orbiter to stabilize after completion of the preflare maneuver prior to the final flare maneuver and allows time for the pilot to assess the approach and make corrections, if needed, to establish a controlled approach to the runway. The IGS for STS-1 is -1.5 degrees.

The final flare maneuver is designed to reduce the sink rate at touchdown to less than 2 to 3 fpm, to provide a smooth increase in the pitch attitude at an altitude high enough to allow the pilot to effect a safe landing and to provide the desired touchdown conditions. Touchdown conditions must satisfy the tirespeed limit of 218 knots groundspeed, avoid tailscrape, and provide at least 4 seconds of energy reserve time in all wind conditions.

The A&L profile was shaped with a modified autoland guidance to simulate a manually flown flightpath, as specified in the STS-1 Groundrules and Constraints document (ref. 5). These modifications include compensation for transport lag time and open-loop guidance command filters during the flare and shallow glideslope mode. The modifications were verified in the Ames IV simulations (ref. 6) and result in better tracking of the reference altitude profile.

Since reference 3 was published, the A&L OGS has been changed from 22 degrees to 20 degrees, and the reference velocity on the OGS has been lowered from 290 KEAS to 280 KEAS for this profile. The speedbrake retraction altitude has been lowered from 3000 feet to 2500 feet, and the gear deployment speed has been

reduced from 280 KEAS to 270 KEAS. These changes have resulted in a decreased velocity at touchdown of 185 KEAS compared to 194 KEAS for the previous profile.

TAEM/A&L interface conditions are presented in table 6.4-1. The STS-1 final approach conditions and the design values used as guidelines to shape the profile are presented in table 6.2-1. The groundtrack for A&L is presented in figure 6.4-1. Figures 6.4-2 through 6.4-17 present detailed plots from the 6-degree-of-freedom simulation for some specific parameters describing A&L conditions.

The A&L phase starts at an altitude of 9825 feet and a flightpath angle of -20.07 degrees. The initial altitude error (from the OGS reference path) is -26 feet. The body flap is retracted to the trail position (0 degrees) at the beginning of the A&L phase. The Orbiter stays on the OGS and maintains the 280 KEAS reference velocity (265 psf dynamic pressure) until the altitude decreases to 2000 feet. The descent rate on the OGS varies from approximately 196 to 175 fps. The ground intercept point of the OGS is 6500 feet from the runway threshold. The speedbrake is modulated on the OGS to maintain the reference velocity, and is retracted when the altitude has decreased to 2500 feet.

At 2000 feet altitude, the preflare maneuver begins. The normal acceleration during the preflare maneuver is less than 1.5g's. During the preflare maneuver, the gear deployment is commanded when the velocity decreases to 270 KEAS. The altitude at this time is 238 feet. A nominal gear deployment time of 7.5 seconds was used and resulted in the gear being down-and-locked 11.8 seconds prior to touchdown. This 270 KEAS is the minimum velocity to start gear deployment and still have the gear down and locked 5 seconds prior to touchdown for a three-sigma deployment time and trajectory dispersions. The transition from the preflare to the exponential capture mode is commanded at a range of 3700 feet from the runway threshold.

The time on the IGS is approximately 5.1 seconds, and the ground intercept point for the IGS is 2500 feet past the runway threshold. At initiation of the final flare maneuver, the sink rate is 11 fps, the wheel altitude is 59 feet, and the range is 945 feet from the runway threshold.

Touchdown occurs 2942 feet past the runway threshold at an airspeed of 185 KEAS with a sink rate of 2.4 fps. The energy reserve time for the zero wind case is 8.1 seconds; the ground-relative velocity is 191 knots. A perspective of the flight profile with actual Orbiter attitudes displayed at 1-minute intervals from touchdown is given in fig. 6.4-15. Out-the-window views as seen from the commander's eye position are presented at 10-second intervals from touchdown minus 100 seconds to touchdown in fig. 6.4-7.

6.4.2 Rollout

The objective of the rollout technique developed for STS-1 was to find the best compromise between maximum main-gear and nose-gear loads, braking, and rollout distance. The technique is a compromise because what alleviates one concern is usually detrimental to another area. Maximum main-gear loads occur very near nose-wheel contact due to the aerodynamic loading. Therefore, derotation is not started until the velocity has been reduced to a value that will not result in

excessive aerodynamic loading. Starting derotation at too slow a velocity can result in loss of elevon control, and the rollout range is increased significantly. Losing elevon control will result in high nose-gear slapdown loads. Longer rollout distances before nose-gear contact will require more braking.

The technique developed first commands the speedbrake to open to 50 percent after main-gear touchdown. Opening the speedbrake increases deceleration and relieves elevon deflection requirements. A pitch attitude of 6 to 8 degrees is maintained until the velocity decreases to 165 KEAS. The range at this point is 5054 feet past the runway threshold. Derotation at -3 deg/sec is then commanded with nose-wheel contact occurring at 5538 feet. The maximum main-gear load is 132 379 pounds, which is under the 166 667-pound limit. The elevons are lowered to 10 degrees down deflection after nose-gear contact to help alleviate main-gear loads. The maximum nose-gear load is 48 777 pounds; the steady-state load on the nose gear is 36 294 pounds. Moderate braking is initiated when the velocity is below 140 knots, which corresponds to the brake reuse limit. This occurs approximately 6 seconds after nosewheel contact. Nose-wheel steering is engaged when the groundspeed decreases to 110 knots. The vehicle comes to a halt after a rollout of 6568 feet, or 9510 feet past the runway threshold and 36.5 seconds after main-gear touchdown. Significant rollout parameters are presented in table 6.0-I(e), and figures 6.5-1 through 6.5-7.

6.5 COMMUNICATIONS AND TRACKING

Significant communications and tracking events relative to the OFT-1 groundtrack are presented in figures 6.6-1 and 6.6-2.

A summary of STS-1 S-band and C-band data is presented in table 6.6-I. Tacan data are presented in table 6.6-II and station locations are presented in table 6.6-III. The data for the Buckhorn and Goldstone S-band communications stations are based on detailed analyses of terrain masking with 30 seconds allowed for lockup after clearing masking. The Pt. Pillar and Vandenberg C-band tracking stations AOS is based on a zero-degree elevation angle with 60 seconds for firm lockup using skin tracking.

Approximately 18 minutes after the deorbit maneuver, communications and tracking by the Guam station are established with AOS based on clearing terrain masking at 53 hours 52 minutes 8 seconds GET. Coverage lasts for 5 minutes 25 seconds with LOS occurring 1 minute 41 seconds prior to EI.

The Orbiter enters S-band blackout approximately 5 minutes 9 seconds after EI when the Orbiter is at an altitude of 262 157 feet and a relative velocity of 24 481 fps. There are no S-band stations available for communications after Guam until Buckhorn acquisition.

The theoretical S-band blackout exit occurs 18 minutes 23 seconds after EI at an altitude of 177 266 feet and a relative velocity of 12 330 fps. The theoretical blackout exit for L-band communication used by the Tacan stations occurs about 18 minutes 57 seconds after EI at an altitude of 170 299 feet and a relative velocity of 11 284 fps. Communications blackout entry and exit computations are based on the criteria presented in reference 18 and are presented in the

altitude/range plane, altitude/relative velocity plane and altitude/time plane in figures 6.2-7, 6.2-11 and 6.2-30, respectively.

Figures 6.6-3 and 6.6-4 present the OFT-1 trajectory profile in the elevation azimuth plane for the Buckhorn and Goldstone stations, respectively.

C-band tracking by the Pt. Pillar station is established at about 183 956 feet altitude and a relative velocity of 13 716 fps and by the Vandenberg station at about 176 167 feet altitude and a relative velocity of 12 192 fps. These data from these two C-band stations are available to provide an estimate of the state vector by the MCC before establishing the S-band communications lockup with the Buckhorn station. Fifteen seconds later, after communication is established through the Buckhorn S-band station, the crew could initiate a runway redesignation, if given a ground command, at an altitude of 158 307 feet and a relative velocity of 9212 fps. The first MCC state vector update (ref. 9) could occur about 67 seconds after the Buckhorn S-band AOS at an altitude of 145 806 feet and a relative velocity of 7763 fps. Range and elevation data from C-and S-band sites are presented in figure 6.6-5.

The Tacan acquisition logic is based on the three-tier concept. A total of 10 Tacan stations is used for navigation with acquisition and switching of these stations based on the arrangement within three tiers or regions: the acquisition region, the navigation region, and the landing region. The acquisition region includes the San Luis Obispo, Paso Robles, and Gaviota stations and is used for ranges greater than 120 n. mi. The navigation region includes the Fellows, Gorman, Bakersfield, and Avenal stations and a mobile Tacan station and is used for ranges between 10 and 120 n. mi. The landing region includes the Palmdale and EAFB stations and is used for ranges less than 10 n. mi. Table 6.0-I presents the Tacan switching times. Based on favorable acquisition and data comparison, the MCC will confirm the Tacan information 30 seconds after acquisition by the Buckhorn station. This allows incorporation of Tacan data as early as 150 000 feet altitude.

Lock-on by two Tacan line replacement units (LRU) will occur at approximately 149 345 feet. If the navigation state residuals are acceptable and the navigation filter is in the AUTO mode, incorporation of Tacan will then occur with no verification required from the MCC (ref. 21). Otherwise, crew action and MCC verification is required to incorporate the Tacan data into the navigation state.

The microwave scanning beam landing system (MSBLS) coverage sequence during TAEM and A&L is presented in figure 6.6-6. The MSBLS coverage data is first processed at a groundtrack range of 52 252 feet. All three channels (azimuth, elevation and distance) of the MSBLS data can be used until the range reduces to 2248 feet past the runway threshold on the nominal trajectory. At this point, the Orbiter flies past the elevation antenna beam. The azimuth and distance data are continually used through rollout.

7.0 ASSESSMENT OF VEHICLE COMPATIBILITY

A comparison of the parameters used in designing the STS-1 OFP to the actual values achieved by the profile was presented in table 6.2-I. A brief summary of the Monte Carlo results is as follows:

- a. With onorbit thermal conditioning, the entry profile meets all groundrules and constraints.
- b. The TAEM profile meets all groundrules and constraints except the rolloff, nose slice, and buffet onset guidelines. The short time period flown in this region prevents this from being a serious problem, however.
- c. The A&L profile meets all groundrules and constraints.

A more detailed assessment of the Orbiter and trajectory compatibility will be presented in appendix C of this document.

8.0 ASSESSMENT OF FLIGHT TEST OBJECTIVES

The descent OFP meets all of the STS-1 flight test requirements with the following exceptions:

- a. The elevon schedule during peak heating (relative velocities greater than 13 600 fps) will be 1 degree up. (See paragraph 3.1.u below.)
- b. The entry profile was shaped to achieve a maximum nominal RCC surface temperature of 2663° F on the wing leading edge and a maximum nominal surface temperature of 2504° F on the elevon. These are currently the most constraining control points using the simplified TPS mode. A panel 2 bondline/structural temperature of 325° F results from this profile. (See paragraph 3.2.h. below.)

The flight test requirements are contained in reference 4. Those requirements applicable to the development of the OFP are presented below: (original section and paragraph numbers have been retained).

1.3 FLIGHT PURPOSE

The primary purpose of STS-1, the first manned orbital flight of the Space Shuttle vehicle, is to demonstrate a safe ascent and return of the Orbiter and crew. Additionally, STS-1 is to provide data to support verification of the following:

- b. Combined Shuttle vehicle aerodynamic, structural and systems characteristics and predicted loads.
- c. Orbiter entry characteristics and performance including crossrange capabilities, TPS performance, control performance, and predicted structural loads.
- d. Orbiter vehicle and systems thermal response.
- e. Inflight vehicle hardware and software systems checkout and performance.
- f. Attitude and translational control capabilities, and guidance and navigation performance.

3.1 OPERATIONAL REQUIREMENTS

For STS-1, the following operational/test requirements and limitations will be observed during flight profile and crew activity planning.

- p. Orbital altitude will be between 90 and 150 n.m.
- q. This flight will have a deorbit plan which will allow a nominal and next orbit backup landing opportunity with less than 550 n.m. crossrange.

- r. Deorbit burn will be planned for a two engine OMS burn but deorbit must be achievable with one OMS engine.
- s. Nominal Orbiter c.g. for entry (at time of entry interface) will be as follows: X = STA 1098.63 (X/L= 66.7%), Y = STA 0, Z = STA 375.
- t. The entry profile shall provide the least demanding thermal environment possible by minimizing heat loads (40° angle-of-attack schedule).
- u. Elevon position during entry peak heating (from 24 760 fps to approximately 10 000 fps) should be targeted for 3°.
- v. Nominal approach to the landing site will be such as to minimize sonic boom and overpressures near heavily populated areas.
- w. The final approach and landing profile must be compatible with both a manual and an automatic mode; however, a pilot-controlled approach and landing will be the planned mode.
- x. Landing will be on the lake bed at EAFB. Runway 23 will be the primary runway, 17 the backup, and 04 the alternated.

3.2 SUBSYSTEM REQUIREMENTS

For STS-1, certain subsystems requirements more conservative than design limitations must be imposed. The subsystem requirements will be observed as follows:

- f. Orbiter normal load factors will not exceed -0.3g to +2.0g for entry.
- g. Orbiter shall be configured and entry profile established to maximize the probability of a successful entry, approach, and landing with a single functioning APU within other system operational and flight safety considerations.
- h. The bondline temperature will be maintained below 312 °F for nominal entry. (Note that the RSI surface temperatures of reference 4 resulted from the Cycle 2 entry profile shaping. Updates to these temperatures are given in table 6.2-1.)
- i. No later than 12 hours prior to schedule entry time, the ground will evaluate real-time telemetry of Orbiter bondline temperatures and assure the bondline temperatures are within acceptable limits. The ground will continue to monitor the bondline temperatures, provide attitude change instructions as required and provide go/no-go instructions to the crew for deorbit and entry. (Ref: DTO111 Preentry Thermal Conditioning).

3.3 CARGO REQUIREMENTS

For STS-1 the following limitations must be imposed on items of cargo being carried:

a. Item	<u>Weight/lb</u>
ACIP	164
IECM	985
DFI	<u>9 015</u>
Total	<u>10 164</u>

- b. The DFI (including IECM) will be located at station 1069.
- c. Ballast will be carried to optimize the c.g. location as specified in paragraph 3.1.s. Primary ballasting will be provided by addition of OMS propellant. Additional ballast will be added as required.

4.1.4 DTO 10⁴ Entry/Approach and Landing Phase Tests

4.1.4.1 Purpose

The purpose is to allow verification of structural, thermal, dynamic and systems performance of the Orbiter vehicle, during the entry, approach and landing phase of the flight. This test partially accomplishes the following flight test objectives defined in the Master Flight Test Assignment Document (ref. 17):

- (1) Safe return of the Orbiter and crew; verify capability for the expected range of operational flight profiles, c.g. and payload weights
- (2) Orbiter alone aerodynamics
- (3) Verify the Orbiter is free of flutter and adverse aeroelastic effects
- (4) Normal operation of all vehicle systems/subsystems including propulsion, electrical power, avionics, guidance, navigation and control (GN&C) mechanical systems, and flight control
- (5) Predicted payload environment
- (6) Entry and crossrange control capabilities for a range of payload weight and vehicle c.g. conditions to verify maximum crossrange entry performance
- (7) Verify Orbiter heat rate and heat load predictions and entry aerothermodynamic environment
- (8) Predicted structural loads and load paths
- (9) Approach and landing capability

- (10) TPS performance over a range of entry conditions as required to verify nominal TPS capability

The following functional test objective requires evaluation:

- a. FTO 104-01 SYSTEMS PERFORMANCE DATA. Assure that the proper data is obtained during the entry and approach and landing phase of the flight to allow proper evaluation and postflight analysis of the Orbiter systems.

4.2.1 DTO 111 Preentry Thermal Conditioning

4.2.1.1 Purpose

The purpose is to thermally precondition the Orbiter structure to obtain desired initial bondline temperatures prior to entry. This preconditioning is in support of verification activities associated with the following flight test objectives defined in the Master Flight Test Assignment Document:

- (1) Demonstrate thermal response to selected attitudes which support predictions of Orbiter thermal performance in operational situations.
(2) Verify Orbiter entry heat rate and heat load predictions.

The following functional test objective requires evaluation:

- a. FTO 111-1. STRUCTURAL CONDITIONING. Prior to deorbit for entry, the structural thermal condition must be determined and/or adjusted to assure that predetermined initial bondline temperatures are proper to allow a safe entry and to enable a thermal stress and TPS analysis postflight.

4.2.1.2 Test Conditions/Activity Required

- a. FTO 111-01. No later than 12 hours prior to the scheduled deorbit burn, the ground will evaluate real-time telemetry of Orbiter bondline temperatures to assure that temperatures are at or below the limits specified in the Shuttle Operational Data Book. If bondline temperatures are within acceptable limits, they will continue to be monitored.

If the bondline temperatures are not within acceptable limits, the ground will evaluate the data and provide attitude control instructions to the crew to obtain the desired temperatures prior to the scheduled deorbit time. The ground will continue to monitor the bondline temperatures and provide go/no-go instructions to the crew for deorbit and entry.

4.2.1.3 Verification/Evaluation

- a. FTO 111-01. Successful accomplishment of this FTO requires that real-time telemetry be provided to allow determination of bondline temperatures for

go/no-go evaluation and that the proper bondline temperatures be achieved prior to entry.

4.2.1.4 Data Requirements

a. Flight data requirements

1. OI telemetry formats: 161, 162 or 129 (M)

Real-time OI data are required during the test whenever station coverage is available.

2. DFI PCM telemetry format 140 (M)

DFI PCM is required during the test period at 10 seconds every 10 minutes.

b. Preflight data requirements - none

c. Postflight data requirements

1. OI data continuously from touchdown until touchdown plus 30 minutes (M)

2. DFI PCM telemetry to be recorded by ground facilities continuously from touchdown until touchdown plus 30 minutes (M)

4.2.1.5 Background and Justification

The Orbiter structure must be thermally preconditioned prior to entry to allow postflight verification of the structural system operational capability and to verify the stress/temperature response of critical structural components. This preconditioning is also required to allow an analysis to verify the thermal performance, structural integrity, and reusability of the thermal protection system for OFT and operations.

9.0 DEORBIT-THROUGH-LANDING ISSUES AND CHANGES

No significant issues have been identified prior to going to publication of the document.

Subsequent to the generation of this profile, the following changes/updates are being considered:

- a. Launch date (atmosphere)
- b. Flight control system
- c. Center of gravity
- d. Deorbit maneuver (no fuel wasting)

10.0 REFERENCES

1. Space Shuttle Program Office: Shuttle Master Verification Plan, Master Flight Test Assignments Document. JSC-07700-10-MVP-10, rev. C, June 1979.
2. Space Shuttle Program Office: Shuttle Master Verification Plan, Flight Test Requirements Document. JSC-07700-10-MVP-11, rev. A, August 1979.
3. Mission Planning and Analysis Division: STS-1 Operational Flight Profile, Descent-Cycle 2. JSC IN 78-FM-51, vol. V, February 1979.
4. Space Shuttle Program Office: Flight Requirements Document, STS-1. Basic rev. C, change 1, JSC 10780, November 1979.
5. Mission Planning and Analysis Division: STS-1 Operational Flight Profile, Groundrules and Constraints, Cycle 3. JSC 14483, vol. I, rev. 2, September 1979.
6. Space Shuttle Orbital Flight Test Level C Functional Subsystem Software Requirements Document, Guidance, Navigation and Control, Part A, Guidance, Entry Through Landing.^a SD-76-SH-0001-C, 15 December 1978.
7. Analytic Drag Control Entry Guidance System, rev. 1, JSC IN 08974, January 21, 1975.
8. Shuttle Entry Guidance. The Journal of the Astronautical Sciences, vol. XXVII, no. 3, pp. 239 to 268, July-September 1979.
9. Entry Flight Procedures Handbook. JSC-11542, June 30, 1978.
10. Software Development Branch: Space Vehicle Dynamics Simulation (SVDS) Program Description. JSC IN 76-FM-26, vol. I, rev. 2, change 2, May 1978.
11. Software Development Branch: Space Vehicle Dynamics Simulation (SVDS) Program Description. JSC IN 76-FM-26, vol. I, rev. 1, Nov. 1976.
12. Aerodynamic Design Data Book - Vol. I, Orbiter Vehicle 102, Rockwell Document Rev. K. SD72-SH-0050-1L, October 1978 with April 1979 update.
13. Four-D Global Reference Atmosphere Technical Description. NASA TMX-64871, September 1974.

^a Plus CR's 19256A, 19549A. Functionally simulates April 1, 1979 IBM software delivery.

14. Space Shuttle Orbital Flight Test Level C Functional Subsystem Software Requirements Document, Guidance, Navigation and Control, Part C, Flight Control, Entry Through Landing.^b SD-76-SH-0007B, 1 May 1979.
15. Data to Support Entry FCS FSSR Usage^c, Memorandum FR-94-79, 18 July 1979.
16. Space Shuttle Orbital Flight Test Level C Functional Subsystem Software Requirements Document, Guidance, Navigation and Control, Part E, Flight Control Sensors/Controllers, Entry Through Landing.^c SD-76-SH-0015, November 26, 1976.
17. Rockwell International: RI/Houston Simplified Weight Synthesis Program, rev. 3, SEH-ITA-75-192, May 1978.
18. Sperry Flight Systems: Sperry Autoland Memo No. 31. March 9, 1978.
19. Space Shuttle Orbital Flight Test Level C Functional Subsystem Software Requirements Document, Guidance, Navigation and Control, Part B, Entry Through Landing Navigation.^d SD76-SH-0004D, December 15, 1978.
20. Subsystem Operating Programs, Navigation Aids, Part E^e, SD-76-CH-0014, November 26, 1976 through PCN update no. 5, December 15, 1978.
21. Coordinate Systems for the Space Shuttle Program, NASA TMX-58153, October, 1974.

^fPlus CR's 29094D, 19570A, 19564, 19054, 19182, 19394C, 19415A, 19442, 19564. Functionally simulates auto flight control mode in April 1979 IBM software delivery.

^cPlus CR12416A updated air-data sensor model. Functionally simulates April 1, 1979 IEM software delivery.

^dPlus CR's 12924A, 19031C, 19045A, 19292, 19390, 19563. Functionally simulates April 1, 1979 IBM software delivery.

^ePlus CR's 19611A, 19391. Functionally simulates April 1, 1979 IBM software delivery.

78FM51:V

TABLE 3.2-I.- STS-1 CYCLE 3 DESCENT PROFILE DESIGN CHANGES

General

April 13, 1979 aerodynamics

Mean April atmosphere

Orbiter weight

Nominal: Increased from 189 844 to 191 902 lb

AOA: Decreased from 194 325 to 192 202 lb

AOA landing site changed from EAFB to Northrup strip

Revised elevon schedule from entry interface to Mach 2.0

Revised speedbrake schedule between Mach 10.0 and 2.5

Entry

Changed elevon schedule from 0 to 1° up to better balance elevon/body flap surface temperatures for Mach > 13.6

Changed heading error deadband for initial bank maneuver in entry from 12.5° to 10.5°

Adjusted entry/TAEM interface to minimize angle-of-attack transients

Adjusted the altitude/altitude reference at entry/TAEM interface

Changed the angle-of-attack reference at entry/TAEM interface from 13.5° to 14.0°

TAEM

Redesigned TAEM for new alpha-Mach constraint boundary

Incorporated left-hand turn onto final approach

Adjusted the TAEM profile to be compatible with revised approach and landing profile

TABLE 3.2-I.- Concluded

Approach and landing	
	Reduced outer glideslope from 22° to 20°
	Reduced dynamic pressure on outer glideslope from 285 psf to 265 psf
	Reduced nominal landing speed from 197 KEAS to 186 KEAS
	Standardized inner glideslope location relative to the runway threshold
	Reduced landing gear deployment speed from 280 KEAS to 270 KEAS
	Speedbrake retraction altitude lowered from 3000 ft to 2500 ft
	Speedbrake deployment during rollout decreased from 70 percent to 50 percent

TABLE 3.2-II.- COMPARISON OF CYCLE 2 AND CYCLE 3 OFT PROFILE SUMMARIES

	Cycle 2		Cycle 3	
	Nominal	Margin °F	Nominal	Margin °F
Orbiter wt, lb	189 844		191 902	
Max surf temp., °F				
CP1 - nose	2 517	241	2 524	241
CP2 - body flap	2 134	128	2 103	171
CP3 - wing (leading edge)	12 669!	0	12 675!	-5
CP4 - elevon	2 319	77	2 302	127
CP6 - forward chine	2 477	25	2 485	22
Panel 2 struct temp, °F	325.	a-13	25.3	a-13
Max heating rate, Btu/ft ² -sec . . .	59.7		61.4	
Heat load, Btu/ft ²	53 147		53 731	
Traj margin wrt eq glide, ft/sec ² .	2.38		2.26	
Entry state				
V, ft/sec	25 753		25 752	
γ, deg	-1.18		-1.21	
Range, n. mi.	4 399		4 358	

! ! Exceed temperature limits.

a Preentry thermal conditioning used to achieve positive margin

TABLE 5.0-I.- STS-1 MASS PROPERTIES FOR NOMINAL END OF MISSION

ORBITER PRIOR TO DEORBIT BURN

MASS PROPERTIES		
WEIGHT AND C. G.	MOMENT OF INERTIA (SF2)	PRODUCT OF INERTIA (SF2)
WEIGHT 197961.0(LB) X 1128.4(IN) Y -0.2(IN) Z 377.0(IN) X CG IN PERCENT BODY LENGTH = 67.5	IXX 873658.4 IYY 8902741.8 IZZ 7172723.6	IXY -267.4 IXZ 210266.4 IYZ 1177.0

ORBITER POST DEORBIT BURN

MASS PROPERTIES		
WEIGHT AND C. G.	MOMENT OF INERTIA (SF2)	PRODUCT OF INERTIA (SF2)
WEIGHT 192288.7(LB) X 1098.7(IN) Y -0.0(IN) Z 374.1(IN) X CG IN PERCENT BODY LENGTH = 66.7	IXX 848740.5 IYY 6749156.6 IZZ 7220396.1	IXY -37.5 IXZ 168113.9 IYZ 1187.1

ORBITER AT ENTRY INTERFACE

MASS PROPERTIES		
WEIGHT AND C. G.	MOMENT OF INERTIA (SF2)	PRODUCT OF INERTIA (SF2)
WEIGHT 191901.6(LB) X 1098.6(IN) Y -0.0(IN) Z 374.0(IN) X CG IN PERCENT BODY LENGTH = 66.7	IXX 847901.1 IYY 6736480.4 IZZ 72207833.1	IXY 267.2 IXZ 166406.1 IYZ 1177.4

ORBITER AT TADM INTERFACE

MASS PROPERTIES		
WEIGHT AND C. G.	MOMENT OF INERTIA (SF2)	PRODUCT OF INERTIA (SF2)
WEIGHT 191113.4(LB) X 1097.8(IN) Y -0.0(IN) Z 373.7(IN) X CG IN PERCENT BODY LENGTH = 66.6	IXX 845592.4 IYY 6721526.2 IZZ 6993233.6	IXY 494.0 IXZ 162740.5 IYZ 1168.4

ORBITER AT LANDING GEAR DOWN

MASS PROPERTIES		
WEIGHT AND C. G.	MOMENT OF INERTIA (SF2)	PRODUCT OF INERTIA (SF2)
WEIGHT 191029.4(LB) X 1098.8(IN) Y -0.0(IN) Z 371.5(IN) X CG IN PERCENT BODY LENGTH = 66.7	IXX 869228.0 IYY 6733524.0 IZZ 6986244.0	IXY 1503.1 IXZ 162660.1 IYZ 1167.9

TABLE 5.0-II.- OMS LOADING REQUIREMENTS

Requirement	ΔV , fps
Insertion	204
Circularization	167
OMS-3	30
OMS-4	30
Deorbit	293
Total ΔV	724

TABLE 5.0-III.- STATE VECTORS

Parameter	Deorbit ignition minus 35 minutes	Deorbit ignition	Entry interface -5min	Entry interface
GET, hr:min:sec	52:56:00	53:31: 4.32	53:54:15.24	53:59:14.28
Inertial velocity, fps	25 400.0	25 389.0	25 562.0	25 752.0
Inertial flightpath angle, deg	0.0262	-0.0066	-1.1930	-1.2045
Inertial heading from north, deg	122.5014	82.4006	50.2812	54.4072
Longitude, deg	62.9785W	63.6885E	144.9013E	160.3836E
Geodetic latitude, deg	25.3757N	39.8340S	7.7782N	20.4924N
Geocentric latitude, deg . . .	25.2332N	39.6529S	7.7269N	20.3666N
Altitude of c.g. above the Flischer ellipsoid, ft	919 885.0	937 220.0	554 962.0	399 965.0
Orbital inclination, deg . . .	40.3	40.3	40.3	40.3
Entry range, n. mi.				4 358.0
Entry weight, lb				191 902.0

TABLE 5.0-IV-APRIL GLOBAL REFERENCE ATMOSPHERE DATA

NO. OF ATMOSPHERIC ELEMENTS	ALTITUDE ABOVE 1960 FISCHER ELLIPSOID, FT	PRESSURE, PSF	DENSITY SLUGS/FT ³	TEMPERATURE DEG RANKINE
1	.39736987+06	.53328117-04	.40615683-10	.69597837+03
2	.39081040+06	.62662069-04	.51532454-10	.64827484+03
3	.38426937+06	.74550837-04	.66332719-10	.60277415+03
4	.37774648+06	.89916127-04	.86639381-10	.56000337+03
5	.37032273+06	.11629991-03	.12199375-09	.51793913+03
6	.36385046+06	.14499297-03	.16465228-09	.48140059+03
7	.35740391+06	.18630682-03	.22703018-09	.44974556+03
8	.35098518+06	.24559865-03	.32180145-09	.42221984+03
9	.3459723+06	.32174869-03	.45373947-09	.39473502+03
10	.33824320+06	.44472125-03	.65856908-09	.37866176+03
11	.33102835+06	.64102716-03	.10056372-08	.35951508+03
12	.32476291+06	.89135778-03	.14458049-08	.34966802+03
13	.31854983+06	.12471247-02	.20644166-08	.34494904+03
14	.31152618+06	.18215383-02	.30855946-08	.33977265+03
15	.30546384+06	.25360267-02	.42953829-08	.31113279+03
16	.29865877+06	.36804175-02	.62370153-08	.31243058+03
17	.29202714+06	.52469712-02	.88393691-08	.31509737+03
18	.28562784+06	.72934476-02	.12153754-07	.31936086+03
19	.27880412+06	.10361143-01	.1706388C-07	.31404478+03
20	.27252371+06	.14270612-01	.23284728-07	.35763-80+03
21	.26586755+06	.20043662-01	.32337740-07	.31191272+03
22	.25929588+06	.27814818-01	.44204618-07	.30712656+03
23	.25260108+06	.38456105-01	.59910273-07	.37443107+03
24	.24603352+06	.52709006-01	.80292385-07	.31243455+03
25	.23949223+06	.71373107-01	.10640155-06	.31058584+03
26	.23286649+06	.97172506-01	.14185165-06	.31427204+03
27	.22635619+06	.13060263+00	.18669764-06	.40711227+03
28	.21992056+06	.17352931+00	.24283215-06	.41947320+03
29	.21323262+06	.23317931+00	.31922484-06	.42566733+03
30	.20659753+06	.30924516+00	.41438679-06	.43445130+03
31	.20022302+06	.40521456+00	.53251439-06	.41-440394+03
32	.19376217+06	.52832058+00	.679180-7-06	.45337857+03
33	.18716679+06	.6801371C+00	.80015619-06	.41145288+03
34	.18043773+06	.89543696+00	.10958337-05	.47818104+03
35	.17377569+06	.11578637+01	.13973096-05	.44239662+03
36	.16730218+06	.14870722+01	.17773364-05	.48745-03
37	.16065391+06	.19204148+01	.22956091-05	.48703926+03
38	.15417348+06	.24541315+01	.29569240-05	.44413332+03
39	.14790715+06	.31158781+01	.37770094-05	.41005323+03
40	.14113922+06	.40576962+01	.50061896-05	.47212756+03
41	.13451527+06	.52740240+01	.66554-92-05	.41-48257+03
42	.12820703+06	.67970527+01	.87414232-05	.45230104+03
43	.12122139+06	.90453405+01	.11676685-04	.44317112+03
44	.11469924+06	.11102543-02	.15600761-04	.41-07259+03
45	.10836202+06	.15550135+02	.21171399-04	.42629000+03
46	.10184533+06	.20525722+02	.28501752-04	.42662012+03
47	.95242335+05	.27837514+02	.39260141-04	.4121301+03
48	.88714803+05	.37860612+02	.54479862-04	.40465227+03
49	.82057295+05	.51840077+02	.76084101-04	.39084654+03
50	.75490973+05	.70902573-C2	.10577378-03	.24600727+03
51	.68899793+05	.97416029+02	.14702566-02	.31564245+03
52	.65629219+05	.11403226+03	.17307192-03	.39771990+03
53	.62269766+05	.13464464+03	.20425720-03	.39194600+03
54	.59074073+05	.15733625+03	.23914002-03	.30328187+03
55	.55836322+05	.18441088+03	.28078113-03	.31257801+03
56	.52509586+05	.21712500+03	.33454116-03	.37819541+03
57	.49224850+05	.26553160+03	.39177556-03	.37742054+03
58	.45890337+05	.30608405+03	.45968428-03	.31148420+03
59	.42672789+05	.35243286+03	.5557869-03	.31-1752+03
60	.39401906+05	.41317454+03	.62591679-03	.34960247+03
61	.36135761+05	.484308043+03	.71464432-03	.31437450+03
62	.32810819+05	.56589625+03	.81270164-03	.41-65117-03
63	.29564866+05	.65674505+03	.91744-61-03	.41701314+03
64	.26290148+05	.75881775+03	.10265765-02	.43061497+03
65	.22996521+05	.87355456+03	.11453744-02	.44336851+03
66	.19606257+05	.10011055+04	.12742153-02	.45803557+03
67	.16358336+05	.11459767+04	.14184039-02	.47017001+03
68	.13095232+05	.13027514+04	.15720906-02	.41256676+03
69	.106401593+04	.14755646+04	.17397369-02	.41411194+03
70	.85589745+04	.16676215+04	.19321864-02	.50264875+03
71	.62796303+04	.18811144+04	.21593788-02	.50769786+03
72	.22895908+04	.19507994+04	.22330733-02	.50692911+03

ORIGINAL PAGE IS
OF POOR QUALITY

TABLE 5.0-V.- APRIL

GLOBAL REFERENCE ATMOSPHERE DEVIATIONS FROM
1962 STANDARD ATMOSPHERE

NO. OF ATMOSPHERIC ELEMENTS	ALTITUDE ABOVE ELLIPSOID, FT	PRESSURE	DENSITY	TEMPERATURE
		1960 FISCHER DEVIATIONS FROM 1962 STANDARD, PERCENT	1962 STANDARD DEVIATIONS FROM 1962 STANDARD, PERCENT	1962 STANDARD DEVIATIONS FROM 1962 STANDARD, PERCENT
1	.39736987+06	.11811280+02	.77516052+00	.43860234+01
2	.39031040+06	.96720902+01	.19539317+01	.54561640+01
3	.38426937+06	.76806728+01	.17490175+01	.35700770+01
4	.37774848+06	.5966270+01	.15644951+01	.19850843+01
5	.37032273+06	.69180265+01	.20837721+00	.13055925+01
6	.36385046+06	.56129125+01	.70092223-01	.72546817+00
7	.35740391+06	.58535098+01	.21194105+01	.91033269+00
8	.35098518+06	.77800642+01	.71051739+01	.35277283+01
9	.34459723+06	.80937092+01	.11064795+02	.63069314+01
10	.33024320+06	.13221234+02	.17143378+02	.66104054+01
11	.33102835+06	.17449037+02	.2235902+02	.68283094+01
12	.32476291+06	.20889778+02	.25707894+02	.62407475+01
13	.31854983+06	.24500751+02	.20501100+02	.48151902+01
14	.31152618+06	.27226191+02	.30184016+02	.33021941+01
15	.30546384+06	.28871630+02	.28113237+02	.13593290+00
16	.29865877+06	.29376913+02	.24469032+02	.35534614+01
17	.29202714+06	.27392489+02	.19788546+02	.61202960+01
18	.28562784+06	.23087954+02	.15041781+02	.74345284+01
19	.27880412+06	.19015430+02	.10137059+02	.88799061+01
20	.27252371+06	.15985462+02	.56288742+01	.90055056+01
21	.26586755+06	.12080960+02	.92079065+00	.11299545+02
22	.25929588+06	.76093517+01	.24931707+01	.10618018+02
23	.25260108+06	.37521405+01	.3933297+01	.81544032+01
24	.24603552+06	.11726473+01	.46624746+01	.61344346+01
25	.23949223+06	.11145423+01	.52649022+01	.43350963+01
26	.23286849+06	.20627560+01	.46490994+01	.26149500+01
27	.22635619+06	.26784621+01	.38703054+01	.11329912+01
28	.21992056+06	.30686430+01	.30754201+01	.12112043+00
29	.21323212+06	.25500614+01	.13506597+01	.13.02658+01
30	.20659753+06	.21672247+01	.14139364+00	.23763055+01
31	.20022362+06	.10927132+01	.18936708+01	.21156502+01
32	.19376217+06	.40032094+00	.19087876+01	.2.292233+01
33	.18716679+06	.24081209+00	.10605646+01	.13422315+01
34	.18043773+06	.36514908+00	.68081358+00	.46012580+00
35	.17377669+06	.47019319+00	.99286914+00	.5.090365+00
36	.16730218+06	.97647011+00	.92039160+00	.10232633+00
37	.16065391+06	.13734327+01	.13325285+01	.13057468+00
38	.15417348+06	.14092952+01	.17183021+01	.25.08257+00
39	.14790715+06	.11112130+01	.12360431+00	.97266241+00
40	.14113922+06	.94302172+00	.46068430+00	.13911967+01
41	.13.51527+06	.55639458+00	.76198290+00	.12896192+01
42	.12820703+06	.24202575+01	.14235375+01	.14402000+01
43	.12122139+06	.75456638+00	.26037123+01	.19162190+01
44	.11499924+06	.20950447+01	.43074952+01	.23687508+01
45	.10836262+06	.24760540+01	.52919394+01	.20604727+01
46	.10184533+06	.35054395+01	.60832848+01	.26910796+01
47	.95242335+05	.37088155+01	.53489035+01	.16.675594+01
48	.88714803+05	.29331096+01	.35665769+01	.61027184+00
49	.82057295+05	.24675285+01	.20087139+01	.49319367+00
50	.75549037+05	.19316630+01	.74649768+00	.11716250+01
51	.68819793+05	.13506610+01	.84075951+01	.14209441+01
52	.65620219+05	.96310730+00	.37936705+00	.13.62819+01
53	.6226976+05	.63456715+00	.90086329+00	.15.47171+01
54	.59074073+05	.31527729+00	.14198998+01	.17150350+01
55	.55836322+05	.64952163+01	.19890672+01	.18955261+01
56	.52500586+05	.49448027+00	.36461737+01	.30193431+01
57	.49224050+05	.10232715+01	.37313423+01	.25832897+01
58	.45898337+05	.14983385+01	.37636245+01	.21730120+01
59	.42672789+05	.18046219+01	.36799765+01	.17443586+01
60	.39401906+05	.22063587+01	.36659717+01	.12994651+01
61	.36135761+05	.23760847+01	.1396648+01	.12426845+01
62	.32810019+05	.22577149+01	.12996731+01	.94912348+00
63	.29564866+05	.22042937+01	.13708334+01	.80482244+00
64	.26290140+05	.21039291+01	.77649520+00	.13144112+01
65	.22998521+05	.18953551+01	.15643381+00	.17457034+01
66	.19696257+05	.16437648+01	.48334390+00	.21217924+01
67	.16358936+05	.13127553+01	.88762803+00	.22051491+01
68	.13095232+05	.10475235+01	.11510581+01	.22216561+01
69	.98401593+04	.74531294+00	.14010932+01	.21747496+01
70	.65580874+04	.42272757+00	.10007238+01	.15266688+01
71	.32700083+04	.2680225+00	.10313650+00	.10291214+00
72	.22095908+04	.19977476+00	.50736464+00	.30865706+00

TABLE 6.0-1.- SEQUENCE OF EVENTS FOR STS-1 (CYCLE 3)

(a) Pre-deorbit maneuver to entry guidance initiate.

EVENT	EVENT TIME SEC	EVENT TIME SEC	EVENT TIME SEC	EVENT TIME SEC	ALT ENTRY INTERFACE	GEODETIC ALTITUDE FT	REL VEL FPS	REL AZIMUTH DEG	RELATIVE FLT PATH ANGLE DEG	LONGITUDE DEG	GEODETIC LATITUDE DEG	ORBITER WEIGHT LB	ANGLE OF ATTACK DEG	DYNAMIC PRESSURE LB/FT ²
INITIATE MANEUVER TO ENTRY ATTITUDE	53 24 54 24	64 54 54 24	8 52 49 92	- 0 36 18 68	927297. 24175	103 810	+ .013	33 35 E	26 57 S	190064.	119 87	.00		
APU ACTIVATION	53 26 4 32	64 54 4 32	8 55 00	- 0 32 9 67	928059. 24174	99 803	+ .011	38 35 E	29 56 S	198027.	152 14	.00		
TERMINATE MANEUVER TO ENTRY ATTITUDE	53 26 19 20	64 54 19 20	8 55 14 88	- 0 32 54 73	928164. 24174	98 796	+ .011	40 15 E	30 71 S	197983.	151 43	.00		
PROGRAM TO EJECT SECA 303	53 29 54 24	64 59 54 24	8 58 49 92	- 0 28 19 68	927997. 24174	86 106	+ .008	37 93 E	40 20 S	197979.	169 50	.00		
GUIDANCE INITIALIZATION MM303	53 30 49 92	65 00 49 92	8 59 45 60	- 0 28 24 01	927400. 24175	82 348	+ .007	62 51 E	39 59 S	197978.	173 67	.00		
ESCAPE ENABLE	53 30 59 04	65 00 59 04	8 59 54 72	- 0 28 14 69	927281. 24175	82 321	+ .007	63 24 E	39 59 S	197977.	174 24	.00		
DEBUT EVAH INITIATION MM31	53 31 4 32	65 01 4 32	10 00 00	- 0 28 9 61	927220. 24175	82 016	+ .007	63 69 E	39 53 S	197977.	174 52	.00		
DECOIT BURN TERMINATION	53 33 32 16	65 03 32 16	10 02 27 84	- 0 29 41 77	928925. 23910	73 607	- 121	73 37 E	37 04 S	192320.	-178 78	.00		
PROGRAM TO EJECT SECA 303	53 41 11 04	65 11 11 04	10 10 47 72	- 0 18 2 23	925150. 23978	55 331	- 1340	105 04 E	25 05 S	192314.	-149 44	.00		
INITIATE POSTDEORBIT ATTITUDE MANEUVER	53 42 10 08	65 12 10 08	10 11 5 76	- 0 17 3 05	928873. 23998	52 766	- 1310	109 15 E	22 00 S	192313.	-142 24	.00		
TERMINATE POSTDEORBIT ATTITUDE MANEUVER	53 48 24 00	65 18 24 00	10 17 19 69	- 0 10 49 63	927844. 24174	47 004	- 1304	120 16 E	2 62 S	192146.	-17 11	.00		
CLEAR STABIL AGO (CLEAR BASE)	53 52 7 68	65 22 7 68	10 21 3 26	- 0 07 6 25	920317. 24307	47 310	- 13100	130 77 E	3 18 N	192143.	30 08	.00		

TABLE 6.0-I.- Continued

(b) Entry guidance initiate to TACM Interface

EVENT	EVENT TIME (SEC) HR MN SEC	EVENT TIME (SEC) HR MN SEC	EVENT TIME (SEC) HR MN SEC	EVENT TIME NET ENTRY INTERFACE HR MN SEC	GEODETIC ALTITUDE FT	RANGE TO DEST THRESHOLD NM	REL VEL IPS	REL AZIMUTH DEG	REL FLAT PATH ANGLE DEG	LONGITUDE DEG	GEODETIC LATITUDE DEG	BARTH NUMBERS	ANGLE OF ATTACK DEG	DYNAMIC PRESSURE LB/SEC ²
INITIATE ENTRY GUIDANCE DATA FOR 304	63 54 16.24	63 24 19.24	10 23 11.24	- 0 04 00.00	934042.	8811.0	44204.	-47.950	-1.250	144.90 E	9.78 N	10.65	61.95	.05
GAIN S-BAND LOS (ENTER AREA)	63 57 23.00	63 27 23.00	10 20 29.00	- 0 01 41.26	932053.	4750.0	24517.	50.415	-1.276	154.86 E	10.21 N	12.93	46.67	.00
ENTRY INTERFACE	63 59 14.20	63 29 14.20	10 20 47.20	0 00 00.00	399945.	4317.5	24582.	52.426	-1.263	160.30 E	20.49 N	18.48	29.54	.01
ACTIVATE ELEVON TRIM	64 01 51.24	63 31 51.24	10 30 47.24	0 02 29.94	323148.	3734.0	24670.	56.849	-1.191	168.57 E	26.87 N	26.06	30.70	.01
ENTER COMMUNICATION BLACKOUT	64 01 54.04	63 31 54.04	10 30 52.04	0 02 41.75	219982.	3711.0	24672.	56.821	-1.187	168.92 E	26.78 N	27.04	30.88	.00
RESURFACE CONTROL ACTIVATED	64 02 44.52	63 32 44.52	10 31 40.52	0 03 30.36	297448.	2820.0	24877.	50.420	-1.110	172.90 E	20.49 N	27.39	30.88	.01
DEACTIVATE RCS ROLL THRUSTERS	64 04 11.60	63 34 11.60	10 33 7.60	0 04 57.12	265082.	3177.1	24531.	51.590	-1.065	176.77 E	31.38 N	36.30	39.90	.00
INITIATE TEMPERATURE CONTROL PHASE	64 04 19.28	63 34 19.28	10 33 10.28	0 05 00.00	344322.	3161.0	24521.	51.506	-1.050	176.56 E	31.49 N	36.27	40.32	.00
FIRST NON-ZERO ROLL COMMAND	64 04 22.64	63 34 22.64	10 33 19.64	0 06 00.00	362157.	3122.0	24687.	52.184	-1.090	178.02 E	31.70 N	36.17	40.12	.01
DEACTIVATE RCS PITCH THRUSTERS, INITIATE ANGLE OF ATTACK MODULATION	64 07 26.28	63 37 26.28	10 36 22.28	0 08 12.00	247926.	2416.0	23336.	73.036	-1.192	167.21 E	36.35 N	34.43	40.13	.00
INITIATE DRG UPDATING IN NAVIGATION FILTER	64 10 42.12	63 40 42.12	10 39 36.12	0 11 27.84	238109.	1699.0	21970.	87.170	-1.232	182.43 E	36.45 N	32.12	39.52	.01
INITIATE EQUIPMENT CLOICE PHASE	64 13 50.76	63 42 50.76	10 41 44.76	0 12 26.40	227933.	1266.1	19910.	97.357	-1.294	143.72 E	36.18 N	20.01	39.36	.01
FIRST ROLL REVERSAL	64 13 47.88	63 42 47.88	10 42 42.88	0 14 23.00	314097.	1080.0	18909.	102.804	-1.440	170.47 E	27.88 N	16.74	39.37	.01
INITIATE CONSTANT CLOC PHASE	64 16 .84	63 44 .84	10 44 55.84	0 16 43.54	192102.	715.0	15524.	99.213	-1.672	131.64 E	36.20 N	14.92	39.33	.01
INITIATE ANGLE OF ATTACK TRANSITION	64 16 32.52	63 44 32.52	10 45 30.52	0 17 18.34	186633.	840.0	14494.	98.830	-1.450	130.28 E	36.12 N	13.71	39.00	.01
PT. PILLAR C-BAND AOS TO RCS ELEV (40 SEC)	64 18 54.92	63 46 54.92	10 45 52.92	0 17 42.24	189994.	822.0	13718.	94.737	-1.491	129.19 E	36.08 N	12.91	39.92	.01
EXIT S-BAND COMMUNICATIONS BLACKOUT	64 17 27.80	63 47 27.80	10 46 33.80	0 18 33.82	177264.	497.0	12380.	90.983	-1.669	137.32 E	35.98 N	11.94	38.86	.01
TRANSIENT C-BAND AOS TO RCS ELEV (40 SEC)	64 17 43.84	63 47 43.84	10 46 29.84	0 18 29.25	178187.	498.0	12182.	99.952	-1.611	127.00 E	35.98 N	11.93	38.42	.01
EXIT L-BAND COMMUNICATIONS BLACKOUT	64 18 31.40	63 48 31.40	10 47 7.40	0 18 57.12	170209.	421.0	11284.	96.637	-1.128	125.98 E	35.98 N	10.48	37.43	.00
INITIATE TRANSITION PHASE	64 18 38.28	63 48 38.28	10 47 34.28	0 19 24.00	144115.	394.0	10407.	92.872	-1.267	121.02 E	34.08 N	9.64	39.90	.01
INITIATE SPEEDBRAKE DEPLOYMENT TO 100%	64 18 51.34	63 48 51.34	10 47 57.34	0 19 36.94	181026.	398.0	9997.	81.110	-1.100	124.50 E	36.10 N	9.28	34.82	.01
EXIT L-BAND COMMUNICATIONS BLACKOUT	64 19 .36	63 49 .36	10 47 54.36	0 19 46.00	159731.	251.0	8708.	81.257	-1.624	126.28 E	36.14 N	8.97	33.81	.01
SOUTHERN S-BAND AOS (CLEAR MASSIVE SEC)	64 19 3.28	63 49 3.28	10 47 58.28	0 19 48.00	159877.	249.0	8617.	81.501	-1.423	134.32 E	36.18 N	8.61	33.83	.01
EARLIEST OPPORTUNITY FOR RCS STATE UPDATE (CLEAR 45-67 SEC)	64 19 17.16	63 49 17.16	10 48 13.16	0 20 0 0.00	158301.	236.0	9212.	84.948	-1.010	132.75 E	36.20 N	8.52	33.70	.01
INITIATE TACAN ACQUISITION REGION UPDATING ANY SELECTED	64 19 53.04	63 49 53.04	10 48 51.04	0 20 40.80	149345.	274.0	8147.	93.930	-1.227	132.65 E	35.28 N	7.98	31.20	.01
AMMONIA BOILER ACTIVATED	64 21 40.84	63 51 40.84	10 50 36.84	0 22 26.40	121020.	197.0	9562.	120.493	-1.567	129.26 E	35.21 N	9.30	33.70	.01
GO/COME C-BAND AOS (CLEAR MASSIVE SEC)	64 21 46.80	63 51 46.80	10 50 36.80	0 22 26.40	121020.	197.0	9562.	120.483	-1.567	129.24 E	35.21 N	9.30	33.70	.01
INITIATE TACAN ACQUISITION REGION UPDATING ANY SELECTED	64 21 56.52	63 51 56.52	10 50 52.52	0 23 42.24	117020.	194.0	8216.	129.832	-1.744	120.19 E	35.88 N	9.67	31.60	.00
AVG TACAN ELEVATION GREATER THAN 45 DEG	64 21 57.96	63 51 57.96	10 50 53.96	0 23 43.60	117946.	142.0	8104.	126.000	-1.750	120.00 E	35.50 N	9.08	21.61	.00
TACAN SELECTED	64 22 20.32	63 52 20.32	10 51 16.32	0 23 0 24	113220.	127.0	4405.	129.150	-1.375	119.78 E	35.38 N	4.66	20.31	.00
Avg TACAN Elevation GREATER THAN 45 DEG	64 22 20.52	63 52 20.52	10 51 16.52	0 23 0 24	113220.	127.0	4400.	129.170	-1.375	119.78 E	35.38 N	4.66	20.31	.00
TACAN SELECTED	64 22 49.32	63 52 49.32	10 51 45.32	0 23 26.04	107382.	107.0	4118.	119.341	-0.200	110.42 E	35.22 N	4.66	19.36	.00
INITIATE SPEEDBRAKE DEPLOYMENT TO 45%	64 22 55.64	63 52 55.64	10 51 51.64	0 23 41.20	106300.	162.0	3997.	112.164	-1.599	110.34 E	35.10 N	3.95	18.90	.00
PT. PILLAR C-BAND LOS (30 DEG ELEVATION)	64 22 58.44	63 52 58.44	10 51 54.44	0 23 44.10	103063.	101.0	3941.	112.183	-1.655	110.31 E	35.17 N	3.90	18.70	.00
INITIATE AIR DATA SYSTEM PROBE DEPLOYMENT	64 23 8.12	63 53 8.12	10 53 2.12	0 23 51.04	103090.	99.0	3704.	106.493	-3.010	110.31 E	35.18 N	3.77	18.36	.01
CIR TACAN SELECTED	64 23 19.24	63 53 19.24	10 53 11.24	0 24 0 0.00	100739.	90.4	3621.	106.131	-0.067	110.44 E	35.12 N	3.61	17.80	.00
CREW EJECTION CAPA L1/T	64 23 18.12	63 52 18.12	10 52 14.12	0 24 3.01	99544.	93.0	2647.	106.010	-1.193	110.07 E	35.11 N	3.56	17.71	.00
INITIATE RADAR TRIM	64 23 21.94	63 52 21.94	10 52 17.94	0 24 7.00	99464.	97.0	2498.	103.507	-0.317	110.03 E	35.10 N	3.49	17.62	.00
IRL TACAN SELECTED	64 24 12.64	63 54 12.64	10 53 8.64	0 24 56.04	85206.	81.0	3570.	97.481	-0.316	110.02 E	35.08 N	3.43	14.32	.00

TABLE 8.0-2.- Concluded
(c) TADN Interface to approach and landing interface

EVENT	EVENT TIME (TGT) MM DD SEC	GEODETIC ALTITUDE FT	RANGE TO RUNWAY THRESHOLD FT	REL VEL IPS	REL AZIMUTH DEG	RELATIVE FLT PATH ANGLE DEG	LONGITUDE DEG	GEODETIC LATITUDE DEG	BACH NUMBER	TIME STAMPED MM/DD/YY	EQUIVALENT ALTITUDE FEET	ANGLE OF ATTACK DEG	DYNAMIC PRESSURE PSF/PSI			
INITIATE INTERFACE INITIATE AIR DATA SYSTEM UPDATING	04-24 17:04	04-24 17:04	04-24 17:04	04-24 17:04	00.0	0000.	00.0	000.	00.0	110.000	30.00	3.00	1970.	340.	10.30	200.00
INITIATE PAYLOAD DAY VENTING	04-24 23:46	04-24 23:46	04-24 23:46	04-24 23:46	00.0	0112.	0200.	00.0	00.0	110.000	30.00	3.00	1971.	340.	10.30	200.01
WATER RELEASED	04-24 23:44	04-24 23:44	04-24 23:44	04-24 23:44	00.0	0202.	0200.	00.0	00.0	110.000	30.00	3.00	1970.	340.	10.30	200.00
DEACTIVATE ALL CIRCUITS	04-24 44:52	04-24 44:52	04-24 44:52	04-24 44:52	00.0	0200.	0200.	00.0	00.0	110.000	30.00	3.00	1970.	320.	10.30	200.02
TRANSITION TO LAND SITE INITIATE	04-25 01:06	04-25 01:06	04-25 01:06	04-25 01:06	00.0	0200.	0200.	00.0	00.0	110.000	30.00	3.00	1970.	320.	7.40	200.01
DEACTIVATE RCS FOR THRUSTERS	04-26 20:57:32	04-26 20:57:32	04-26 20:57:32	04-26 20:57:32	00.0	0200.	0200.	00.0	00.0	110.000	30.00	3.00	1970.	320.	7.40	200.02
INITIATE SPEEDBRAKE DEPLOYMENT	04-26 01:04	04-26 01:04	04-26 01:04	04-26 01:04	00.0	0200.	0200.	00.0	00.0	110.000	30.00	3.00	1970.	310.	8.17	200.00
INITIATE HEADING ALIGNMENT PHASE	04-27 00:00	04-27 00:00	04-27 00:00	04-27 00:00	00.0	0200.	0200.	00.0	00.0	110.000	30.00	3.00	1970.	320.	8.01	200.02
CHECK IN FLIGHT CAS MODE	04-27 20:15	04-27 20:15	04-27 20:15	04-27 20:15	00.0	0200.	0200.	00.0	00.0	110.000	30.00	3.00	1970.	320.	8.07	200.01
INITIATE FLIGHT LANDING SITE SEQUENCE	04-28 40:26	04-28 40:26	04-28 40:26	04-28 40:26	00.0	0200.	0200.	00.0	00.0	110.000	30.00	3.00	1970.	320.	8.09	200.04
INITIATE WHEEL UPDATING	04-28 51:34	04-28 51:34	04-28 51:34	04-28 51:34	00.0	0200.	0200.	00.0	00.0	110.000	30.00	3.00	1970.	320.	8.09	200.03
INITIATE LANDING GEAR DEPLOYMENT	04-29 04:00	04-29 04:00	04-29 04:00	04-29 04:00	00.0	0200.	0200.	00.0	00.0	110.000	30.00	3.00	1970.	320.	8.07	200.04
INITIATE FINAL PHASE	04-29 09:00	04-29 09:00	04-29 09:00	04-29 09:00	00.0	0200.	0200.	00.0	00.0	110.000	30.00	3.00	1970.	320.	8.09	200.00

(d) Approach and landing interface to main gear landing

EVENT	EVENT TIME (TGT) MM DD SEC	GEODETIC ALTITUDE FT	RANGE TO RUNWAY THRESHOLD FT	REL VEL IPS	REL AZIMUTH DEG	RELATIVE FLT PATH ANGLE DEG	LONGITUDE DEG	GEODETIC LATITUDE DEG	BACH NUMBER	TIME STAMPED MM/DD/YY	EQUIVALENT ALTITUDE FEET	ANGLE OF ATTITUDE DEG	ANGLE OF ALTITUDE DEG			
INITIATE APPROACH AND LANDING INTERFACE INITIATE BODY FLAT POSITIONING TO 0 DEG.	04-29 27:34	04-29 27:34	04-29 27:34	04-29 27:34	00.0	0200.	-32370.	070.	-110.000	117.700	30.00	1970.	320.	3000.	-100.0	-100.0
INITIATE LANDING GEAR	04-29 53:53	04-29 53:53	04-29 53:53	04-29 53:53	00.0	0200.	-30000.	02011.	-110.000	117.700	30.00	1970.	320.	3000.	-100.0	-100.0
INITIATE SPEEDBRAKE RETRACTION	04-30 0:00	04-30 0:00	04-30 0:00	04-30 0:00	00.0	0200.	-32370.	010.	-110.000	117.700	30.00	1970.	320.	3000.	-100.0	-100.0
INITIATE APPROX CRZ	04-30 3:43	04-30 3:43	04-30 3:43	04-30 3:43	00.0	0200.	-30000.	02011.	-110.000	117.700	30.00	1970.	320.	3000.	-100.0	-100.0
INITIATE LANDING GEAR DEPLOYMENT	04-30 10:36	04-30 10:36	04-30 10:36	04-30 10:36	00.0	0200.	-2500.	-473.	-110.000	117.700	30.00	1970.	320.	3000.	-100.0	-100.0
INITIATE E ROLLER ATTITUDE UPDATING	04-30 19:12	04-30 19:12	04-30 19:12	04-30 19:12	00.0	0200.	-25170.	-469.	-110.000	117.700	30.00	1970.	320.	3000.	-100.0	-100.0
COMPLETION OF FREELINE	04-30 20:00	04-30 20:00	04-30 20:00	04-30 20:00	00.0	0200.	-25170.	-469.	-110.000	117.700	30.00	1970.	320.	3000.	-100.0	-100.0
GEAR DOWN AND LOCKED	04-30 21:00	04-30 21:00	04-30 21:00	04-30 21:00	00.0	0200.	-25170.	-469.	-110.000	117.700	30.00	1970.	320.	3000.	-100.0	-100.0
INITIATE FINAL PHASE	04-30 22:00	04-30 22:00	04-30 22:00	04-30 22:00	00.0	0200.	-25170.	-469.	-110.000	117.700	30.00	1970.	320.	3000.	-100.0	-100.0
ROLL-OFF	04-30 23:01	04-30 23:01	04-30 23:01	04-30 23:01	00.0	0200.	-25170.	-469.	-110.000	117.700	30.00	1970.	320.	3000.	-100.0	-100.0
DEPLOYMENT OF MAIN GEAR SPEEDBRAKE TO ROLL-OFF	04-30 42:22	04-30 42:22	04-30 42:22	04-30 42:22	00.0	0200.	-25170.	-469.	-110.000	117.700	30.00	1970.	320.	3000.	-100.0	-100.0

(e) Main gear touchdown through rollout

EVENT	EVENT TIME (TGT) MM DD SEC	TIME FROM MAIN GEAR TOUCHDOWN SEC	RELATIVE DISTANCE METERS	EQUVALENT ALTITUDE FEET	RANGE FROM MAIN GEAR THRESHOLD FEET	ROLL-OFF DISTANCE FEET	ANGLE OF ATTACH. DEG			
01. G. ON MAIN GEAR DEPLOYMENT TO 0 DEG. DEPLOYMENT	04-30 43:12	04-30 43:12	04-30 43:12	04-30 43:12	0	000.	000.	2941.0	0	0.00
01. G. DEPLOYED	04-30 43:33	04-30 43:33	04-30 43:33	04-30 43:33	0.0	172.	172.	2941.0	0	0.35
02. GEAR CRASH DET	04-30 52:52	04-30 52:52	04-30 52:52	04-30 52:52	0.0	172.	172.	2941.0	0	0.35
INITIATE BRAKING	04-30 55:53	04-30 55:53	04-30 55:53	04-30 55:53	14.0	100.	100.	2941.0	6123.1	-2.18
INITIATE HOLE WHEEL CROWNING	04-31 0:00	04-31 0:00	04-31 0:00	04-31 0:00	0.0	576.	2990.0	2990.0	6123.1	-10.18
INITIATE STOP	04-31 20:04	04-31 20:04	04-31 20:04	04-31 20:04	0.0	576.	6510.0	6510.0	6510.0	-10.18

78FM51:V

TABLE 6.1-I.- STS-1 LANDING OPPORTUNITIES AT EAFB

Crossrange \leq 700 n. mi.

Deorbit orbit	Crossrange, n. mi. ^a	GET deorbit, hr:min	GET entry interface, hr:min	GET landing, hr:min ^b	Time since sunrise, hr:min ^b
2	129 N	2:17	2:47	3:17	1:18
3	248 S	3:52	4:22	4:52	2:52
4	317 S	5:27	5:57	6:27	4:27
5	66 S	7:02	7:32	8:02	6:02
6	459 N	8:37	9:07	9:37	7:37
17	515 N	24:46	25:16	25:46	-0:14
18	30 S	26:26	26:50	27:20	1:20
19	308 S	27:55	28:25	28:55	2:55
20	266 S	29:30	30:00	30:30	4:30
21	86 N	31:05	31:35	32:05	6:05
22	687 N	32:40	33:10	33:40	7:39
33	305 N	48:48	49:18	49:48	-0:12
34	158 S	50:23	50:53	51:23	1:23
35	330 S	51:58	52:28	52:58	2:58
36	179 S	53:33	54:03	54:33	4:33
37	266 N	55:07	55:37	56:07	6:08
49	119 N	72:51	73:21	73:51	-0:09
50	252 S	74:25	74:55	75:25	1:26
51	315 S	76:00	76:30	77:00	3:01
52	58 S	77:35	78:05	78:35	4:36
53	472 N	79:10	79:40	80:10	6:10

^aNOTE: "N" means Orbiter must fly north of groundtrack to reach landing site and "S" means Orbiter must fly south of groundtrack to reach landing site.

^bNOTE: Touchdown assumed to occur 1 hour after deorbit.

(-) = Before sunrise
(+) = After sunrise

TABLE 6.1-II.- DEORBIT AND ENTRY INTERFACE PARAMETERS

Parameter	2 OMS	1 OMS	RCS	Contingency 1 OMS
<u>Deorbit</u>				
GMT of ignition, day:hr:min:sec	93:17:01:04	93:17:01:04	93:17:01:04	93:16:58:36
GET of ignition, hr:min:sec	53:31:04	53:31:04	53:31:04	53:28:36
Vehicle weight at ignition, lb	197 961.0	197 961.0	197 961.0	197 961.0
Propellant, lb	5672.0	5672.0	6134.0	4229.0
ΔV total, including c.g. control, fps	292.9	292.9	270.0	217.6
ΔV min for in-plane solutions, fps	282.0	273.2	270.0	217.6
Wasting angle, deg	15.9	21.4	0	0
Burn time, min:sec	2:28	4:56	7:32	3:41
Coast-to-entry interface from burn cutoff, min:sec.	25:42	23:15	20:36	25:44
<u>Entry interface</u>				
Longitudinal c.g., in . .	1098.6 (66.7%)	1098.6 (66.7%)	1099.6 (66.78%)	--
Weight, lb	191 902	191 902	191 827	--
H_a (burnout), n. mi. . . .	150.7	149.9	149.5	149.6
H_p (burnout), n. mi. . . .	1.8	1.5	1.3	27.9
Range-to-runway threshold, EAFB, n. mi.	4358.0	4358.0	4358.0	4603.0
Crossrange to EAFB, n. mi.	196.0	196.0	196.0	197.0
Inertial velocity, fps . .	25 752.2	25 750.0	25 749.0	25 796.5

78FM51:V

TABLE 6.1-II.- Concluded

Parameter	2 OMS	1 OMS	RCS	Contingency 1 OMS
Inertial flightpath angle, deg	-1.206	-1.203	-1.202	-0.911
Thrust vector roll, deg. .	180	180	180	180
Ignition attitude, deg				
Pitch } LVLH	171	175	173	191
Yaw }	343	326	0	348
Roll }	357	358	0	0
Pitch } ADI	180	184	181	209
Yaw } REF	0	343	17	4
Roll }	0	0	2	354
Pitch } ADI	181	185	183	210
Yaw } INRTL	343	326	0	348
Roll }	357	358	0	0

TABLE 6.1-III.- MANEUVER PAD FOR NOMINAL EOM

49

M N V R P A D

BURN ATT 8 R	3	5	7
9 P	1	8	1
10 Y	3	4	3

HA	HP
TGT	1 5 1 (+) 0 0 2

TXX	2	5	:	4	2
REI	4	3	5	2	

AV TOT	0	2	9	2	.	9
--------	---	---	---	---	---	---

TGO	0	2	:	2	8
X (+)	0	2	8	2	.
VGO Y (-)	0	0	0	.	5
Z (+)	0	7	9	.	1

TRIM L	R
P	1 2 (+) 0 . 1
Y 1 3 (-) 6 . 5	1 4 (+) 6 . 5
ENG SEL	
OHS BOTH	1 5 *
L	1 6
R	1 7
RCS + X ACC	1 8
21 WT	1 9 7 9 6 1

27 TIG 0 0 0 / 1 0 : 0 0 : 0 0 . 0

31 C1	1	5	3	1	0	3 6 Δ V X	(-) 0	2	5	4	.	7
32 C2	(-)	.	6	1	5	7	3 7 Δ YY	(-)	0	7	9	.
33 HT	0	6	5	.	8	3	2	3 8 Δ V Z	(-)	1	2	1
34 QT	1	1	3	.	2	0	6					
35 PRPLT	(+)	0	5	6	7	2						

TABLE 6.1-IV.-

DEL PAD		
DEORBIT		
BURN ATT	R 3	5 7
	P 1	8 1
	Y 3	4 2
TGT IIA	1 5 1	HP (+) 0 0 2
ΔV TOT	2 9 2	9
TGO	2	2 8
ENTRY/LANDING		
UNDERBURN PREDANK DIRECTION (3-10)	L/R	
EI-5 INRTL ATT (3-10)	R 0	0 1
	P 3	1 6
	Y 3	5 8
GWM AOS (3-11)	EI -	0 8
GWM LOS (4-2)	EI -	2
ALTM SET (2-20 PDP)		
D=4 (4-3)	1 0	3 3 0 9
VREL 1ST REVERSAL (4-5)	1 8 9	0 2
L HAND TURN	RWY	2 3
WINDS: (4-12)		
7K		
SURFACE		
REMARKS:		

TABLE 6.1-V.- DEORBIT MANEUVER DISPLAYS

3011/ /		DEORB MNVR COAST	1 000/09:53:20		3021/ /		DEORB MNVR EXEC	1 000/09:59:46	
GMBL CK 1			000/00:06:40		GMBL CK 1		000/00:00:14		
L	R	TRIM	L	R	L	TRIM	L	R	
P.		P	12	.1	P.	P	12	.1	
Y		Y	13	-6.5	Y	Y	13	-6.5	
SEL			14	6.5	SEL				
PRI 2*	5*	ENG SEL		OMS	PRI 2*	5*	ENG SEL	OMS	
SEC 3	6	OMS BOTH	15*	PURGE ENA 19*	SEC 3	6	OMS BOTH	15*	PURGE ENA 19*
OFF 4	7		L	16	OFF 4	7	L	16	
BURN ATT 8 R357			R	17	SURF DRIVE	BURN ATT 8 R357		SURF DRIVE	
9 P180		RCS +X ACC 18		ON 22	9 P180	RCS +X ACC 18		ON 22	
10 Y344		21 WT 197961		OFF 23*	10 Y344	21 WT 197961		OFF 23*	
HA	HP		F RCS	ARM 24	HA	HP		F RCS	ARM 24
TGT 151	2			DUMP 25	TGT 151	2			DUMP 25
CUR 150	148	TARGET		OFF 26*	CUR 150	148	TARGET		OFF 26*
TFF	25:42	27 TIG 000/10:00:00.0			TFF	25:42	27 TIG 000/10:00:00.0		
REI	4327	31 C1	15310	36 DVX	REI	4327	31 C1	15310	36 DVX
	EXEC	32 C2	-.6157	37 DVY		EXEC	32 C2	-.6157	37 DVY
DVTOT	292.9	33 HT	65.832	38 DVZ	DVTOT	292.9	33 HT	65.832	38 DVZ
TGO	2:28	34 BT	113.206		TGO	2:28	34 BT	113.206	
VGO X	276.16	35 PRPLT	5672		VGO X	276.16	35 PRPLT	5672	
Y	8.43				Y	8.43			
Z	97.36	LOAD 39		ST CRT TMR 40	Z	97.36	LOAD 39		ST CRT TMR 40

LOAD COMMAND

GUIDANCE INITIATE

TABLE 6.1-V.- Continued

3021/	/	DEORB MNVR EXEC	1 000/10:00:00
GMBL CK 1			000/00:00:00
L	R	TRIM	L R
P .1	.1	P	12 .1
Y -6.5	6.5	Y	13 -6.5 14 6.5
SEL			
PRI 2*	5*	ENG SEL	OMS
SEC 3	6	OMS BOTH	15* PURGE ENA 19*
OFF 4	7	L	16
BURN ATT 8 R357		R	17 SURF DRIVE
9 P180		RCS +X ACC 18	ON 22
10 Y344		21 WT 197961	OFF 23*
HA HP		F RCS	ARM 24
TGT 151	2		DUMP 25
CUR 150	148	TARGET	OFF 26*
TFF 25:42		27 TIG 000/10:00:00.0	
REI 4327		31 C1	15310 36 DVX
	EXEC	32 C2	-.6157 37 DVY
DVTOT 292.9		33 HT	65.832 38 DVZ
TGO 2:28		34 BT	113.206
VGO X 276.75		35 PRPLT	5672
Y 8.60		Z	.04
Z 95.66		LOAD 39	ST CRT TMR 40

OMS IGNITION

3021/	/	DEORB MNVR EXEC	1 000/10:02:28
GMBL CK 1			000/00:02:28
L	R	TRIM	L R
P .4	-.2	P	12 .1
Y -6.0	6.9	Y	13 -6.5 14 6.5
SEL			
PRI 2*	5*	ENG SEL	OMS
SEC 3	6	OMS BOTH	15* PURGE ENA 19*
OFF 4	7	L	16
BURN ATT 8 R357		R	17 SURF DRIVE
9 P180		RCS +X ACC 18	ON 22
10 Y344		21 WT 197961	OFF 23*
HA HP		F RCS	ARM 24
TGT 151	2		DUMP 25
CUR 151	4	TARGET	OFF 26*
TFF 25:42		27 TIG 000/10:00:00.0	
REI 4327		31 C1	15310 36 DVX
	EXEC	32 C2	-.6157 37 DVY
DVTOT 2.6		33 HT	65.832 38 DVZ
TGO 0:00		34 BT	113.206
VGO X 2.54		35 PRPLT	5672
Y .04		Z .73	LOAD 39
Z			ST CRT TMR 40

OMS CUTOFF

TABLE 6.1-V.- Concluded

3021/	/	DEORB MNVR EXEC	1 000/10:02:33
GMBL CK 1			000/00:02:33
L	R	TRIM L	R
P .4	-.2	? 12	.1
Y -6.0	6.9	Y 13 -6.5	14 6.5
SEL			
PRI 2*	5*	ENG SEL	OMS
SEC 3	6	OMS BOTH	15* PURGE ENA 19*
OFF 4	7	L	16
BURN ATT 8 R357		R	17 SURF DRIVE
9 P180		RCS +X ACC 18	ON 22
10 Y344		21 WT 197961	OFF 23*
HA	HP	F RCS	ARM 24
TGT 151	2		DUMP 25
CUR 151	2	TARGET	OFF 26*
TFF 25:42		27 TIG 000/10:00:00.0	
REI 4327		31 C1 15310 36 DVX	
EXEC		32 C2 -.6157 37 DVY	
DVTOT	.0	33 HT 65.832 38 DVZ	
TGO	0:00	34 BT 113.205	
VGO X	.00	35 PRPLT 5672	
Y	.01		
Z	.00	LOAD 39	ST CRT TMR 40

AFTER TAILOFF

3031/	/	DEORB MNVR COAST	1 000/10:10:06
GMBL CK 1			000/00:10:06
L	R	TRIM L	R
P 6.0	6.0	P 12	.1
Y 7.0	-7.0	Y 13 -6.0	14 6.9
SEL			
PRI 2*	5*	ENG SEL	OMS
SEC 3	6	OMS BOTH	15* PURGE ENA 19*
OFF 4	7	L	16
BURN ATT 8 R 0		R	17 SURF DRIVE
9 P317		RCS +X ACC 18	ON 22
10 Y 0		21 WT 197961	OFF 23*
HA	HP	F RCS	ARM 24
TGT			DUMP 25
CUR 151	2	TARGET	OFF 26*
TFF 18:05		27 TIG	
REI 4327		31 C1	36 DVX
EXEC		32 C2	37 DVY
DVTOT		33 HT	38 DVZ
TGO		34 BT	
VGO X		35 PRPLT	
Y		LOAD 39	ST CRT TMR 40
Z			

PRO TO MM303

TABLE 6.1-VI.- NOMINAL END-OF-MISSION REFSMATS

REFSMAT FOR STABLE MEMBER #1		
-.74224394+00	-.26936383+00	.61360984+00
-.66760481-01	-.88138038+00	-.46766616+00
.66679603+00	-.38808727+00	.63621639+00
REFSMAT FOR STABLE MEMBER #2		
.27283688+00	.35604039+00	.89375345+00
.94832034+00	-.25597617+00	-.18752255+00
.16201399+00	.89872766+00	-.40748008+00
REFSMAT FOR STABLE MEMBER #3		
-.54381812+00	.83134827+00	.11455071+00
.13166533+00	.21933172+00	-.96672529+00
-.82881001+00	-.51064040+00	-.22873631+00

TABLE 6.1-VII.- NOMINAL END-OF-MISSION RELMATS AND RELQUATS

REFERENCE RELMAT (M50 to ADI)		
-.29909217+00	-.95376793+00	-.29505944-01
.62551605+00	-.17261702+00	-.76087648+00
.72060636+00	-.24602864+00	.64822555+00
INRTL RELMAT (M50 to ADI)		
-.44939156-00	-.86814561+00	.21064281+00
.47763892+00	-.43276111+00	-.76457757+00
.75492268+00	-.24298351+00	.69913932+00
REFERENCE RELQUAT		
(M50 to ADI)		(ADI to M50)
.54233669+00		.54233669
.23732852+00		-.23732852
-.34577797+00		.34577797
.72799978+00		-.72799978
INRTL RELQUAT		
(M50 to ADI)		(ADI to M50)
.42631756+00		.42631756
.30587180+00		-.30587180
-.31917516+00		.31917516
.78919136+00		-.78919136

TABLE 6.2-I.- STS-1 DEORBIT-THROUGH-LANDING TRAJECTORY PARAMETERS

Parameter		Design value	Actual value
Deorbit			
Minimum coast time prior to entry interface, min			
2 OMS		15	26
1 OMS		15	23
+X-RCS		15	21
Center of gravity at entry interface			
Longitudinal, percent		^a 66.70	66.70
Lateral, in		^a 0.00	0.00
Vertical, in		^a 375 ± 3	373.5
Entry			
Maximum normal load factor, g		^a 2.0	1.63
Maximum dynamic pressure, psf			
Mach >5		^a 300	190
Mach ≤5		^a 342	218
Maximum hinge moments, in-lb × 10 ⁶			
Left Inboard elevon		^a ±0.93	-0.397
Right Inboard elevon		^a ±0.93	-0.395
Left Outboard elevon		^a ±0.43	-0.179
Right Outboard elevon		^a ±0.43	-0.188
Body flap		^a -1.4	-0.507

^aDenotes hardware/systems constraint.

TABLE 6.2-I.- Continued

Parameter	Design value	Actual value
Entry (concluded)		
Maximum hinge moments, in-lb $\times 10^6$ (concluded)		
Speedbrake	^a +2.5	0.535
Maximum heating rate, Btu/ft ² /sec	--	61.4
Heat load, Btu/ft ²	--	53 731
Target (runway threshold)		
Longitude, deg W	117.820	
Geodetic latitude, deg N	34.966	
Height above Fischer ellipsoid, ft	2086.0	
True heading, deg	244.41	
TAEM		
Maximum hinge moments, in-lb $\times 10^6$		
Left inboard elevon	^a -0.78	-0.257
Right inboard elevon	^a -0.78	-0.298
Left outboard elevon	^a -0.35	-0.156
Right outboard elevon	^a -0.35	-0.175
Body flap	^a -0.74	-0.275
Speedbrake	^a 2.1	0.839
Maximum normal load factor, g	^a 2.0	1.38

^aDenotes hardware/systems constraint.

TABLE 6.2-I.- Continued

Parameter	Design value	Actual value
TAEM (concluded)		
Maximum dynamic pressure, psf		
Mach > 0.9	a,b 250-220	209
Mach ≤ 0.9	a 340	267
Approach and landing		
Maximum normal load factor, g	a 2.0	1.33
Maximum dynamic pressure, psf	a 340	278
Maximum hinge moments, in-lb x 10 ⁶		
Left inboard elevon	a ± 0.955	0.169
Right inboard elevon	a ± 0.955	0.167
Left outboard elevon	a ± 0.46	0.042
Right outboard elevon	a ± 0.46	0.041
Body flap	a ± 1.4	0.276
Speedbrake	a ± 2.5	0.803
Time on the IGS, sec	≥ 5	5.1
Speedbrake deflection at 5000 ft, deg	55-60	64.8
Preflare velocity, KEAS	281	282
Normal acceleration during preflare maneuver, g	1.3	1.33

^aDenotes hardware/systems constraint.^bSee figure 6.3-2.

TABLE 6.2-I.- Concluded

Parameter		Design value	Actual value
Approach and landing (concluded)			
Final flare altitude, ft (c.g.)	50-60	59
Conditions at main gear touchdown			
Groundspeed, knots	a218	191
Velocity, KEAS	185	185
Range from threshold, ft	3000	2942
Descent rate, fps	a9.6	+2.4
Angle of attack, deg	<11	9.8
Energy reserve, sec	≥ 4	8.1

^aDenotes hardware/system constraint.

TABLE 6.2-II.-- ORBITER SURFACE TEMPERATURE LIMITS

Control point	Control point location	Single mission temp limit, °F		Temperature dispersion, °F				Combined effect	Temp limit, °F
		Material limit	Equiv simp model	Aero heat uncert	Traj disp	Control surface deflection			
						Bias	Random		
1	Nose	2800	2950	180	65	--	--	191	2759
2	Body flap	2600	2600	247	146	0	33	289	2311
3	Wing leading edge	2600	2950	272	92	--	--	287	2663
4	Elevon	2600	2600	135	75	4	34	158	2442
5	Forward chine	2700	2700	187	58	--	--	196	2504

TABLE 6.2-III.- STS-1 CYCLE 3 THERMAL PROTECTION SYSTEM (TPS) SUMMARY

PANEL NO.	PANFL AREA (FT) ²	MAXIMUM HEATING RATE, BTU/(FT) ² /SEC	MAXIMUM SURFACE TEMPERATURE DEG F	SURFACE INSULATION TYPE	TOTAL HEAT LOAD BTU/(FT) ²	STRUCTURAL TEMPERATURE MARGIN, DEG F
1	24.00	22.07	2257.62	RCC	19329.16	*****
2	362.00	11.00	1854.08	FRSI	10177.72	25.05
3	113.00	9.77	1756.57	FRSI	8568.10	17.03
4	446.00	9.02	1713.10	FRSI	7903.21	14.41
5	559.00	6.58	1548.16	FRSI	5892.93	15.73
6	403.00	4.79	1394.03	FRSI	4450.71	14.92
7	158.00	11.14	1330.42	RCC	10678.34	*****
8	435.00	13.15	1924.17	FRSI	13127.39	22.54
9	412.00	10.99	1817.78	FRSI	10206.76	21.66
10	641.00	21.03	2226.35	FRSI	8915.16	-14.27
11	165.00	21.08	2194.15	FRSI	9115.07	10.50
12	360.00	10.92	1819.29	FRSI	4756.06	4.00
13	275.00	2.93	1179.95	FRSI	2562.36	30.50
14	472.00	2.02	1034.32	FRSI	1794.30	25.82
15	1631.00	.21	390.67	FRSI	190.75	*****
16	764.00	.17	253.07	FRSI	78.31	*****
17	114.00	.49	538.37	FRSI	284.21	*****
18	631.00	.37	520.39	FRSI	267.46	*****
19	155.00	7.23	1613.07	FRSI	4434.55	68.49
20	673.00	1.72	974.93	FRSI	1635.07	28.23
21	242.00	1.11	827.81	FRSI	690.99	32.64
22	610.00	.76	709.42	FRSI	662.73	24.24
23	1132.00	.41	545.54	FRSI	364.10	*****
24	372.00	.44	563.45	FRSI	390.00	24.84
25	32.00	33.74	2561.74	FRSI	14105.19	9.30

TABLE 6.2-IV.- SUMMARY OF CYCLE-3 ORBITER SURFACE TEMPERATURE LIMITS
AND MARGINS BASED ON MONTE CARLO ANALYSIS

Control point	Control point location (velocity fps) ^a	Maximum TPS temperatures, °F							Simplified model limit, °F	Margin, °F	
		Dispersion, 3σ									
		Nominal	Mean	Traj	Bias	Surf. defl.	Aero heating	Combined	Mean + 3σ dispersion		
1	Nose (22 800)	2524	2515	72	--	--	180	194	2709	2950	241
4	Body flap (18 000)	2103	2132	161	0	33	247	297	2429	2600	171
5	Wing leading edge (21 600)	2675	2670	54	--	--	272	285	2955	2950	-5
4	Elevon (18 000)	2302	2323	44	4	34	135	150	2473	2600	127
6	Forward chine (22 800)	2485	2478	70	--	--	187	200	2678	2700	22
Panel 2	Forward lower	325	325	10	--	--	37	38	363	350	-13

^aVelocity of maximum dispersed temperature

TABLE 6.2-V.- ELEVON AND BODY FLAP SURFACE DEFLECTION ERRORS

Error source	Deflection errors, deg			
	Elevon		Body flap	
	Bias	Random	Bias	Random
y_{CG} (± 0.5 IN)	--	± 0.40	--	--
Maneuver capability	± 1.0	--	--	--
Asymmetric airframe thermal (orbital) manufacturing	--	± 1.2	--	--
Bending under load	N/A	--	N/A	--
Deadband	± 1.0	-----> ± 2.0		--
Aero variations	--	(Varies along -----> (Varies along trajectory) trajectory)		
Elevon position accuracy corrections	$\pm .16$	$\pm .46$	$-.32$	$\pm .93$
Sum bias errors	$+2.16$		$+1.68$	
RSS random errors		± 1.34		$\pm .93$
^a Sum bias errors without deadband	$+1.16$		$-.32^{\circ}$	
^b Errors used in Monte Carlo analysis (table 6.2-IV)				
Bias	$\pm .16$		0	
Random		$+1.34$		$\pm .93$

^aDeadband modeled in simulation.^bOnly positive errors (down deflections produce increased heating).^c 1° subtracted from elevon bias as elevon schedule is -1° (1° up).

TABLE 6.3-I.- ENTRY/TAEM INTERFACE CONDITIONS

PARAMETER	VALUE
GET.HR:MN:SEC	54:24:17.64
TIME FROM ENTRY INTERFACE,MIN:SEC	0:25:3.36
TAEM WEIGHT,LB	191901.6
RELATIVE VELOCITY,FPS	2494.9
RELATIVE FLIGHT PATH ANGLE,DEG	-4.4470
RELATIVE HEADING FROM NORTH,DEG	90.0537
LONGITUDE,DEG W	118.4817
GEODETIC LATITUDE,DEG NORTH	35.0765
GEOCENTRIC LATITUDE,DEG NORTH	34.8958
ALTITUDE OF C.G. ABOVE FISCHER ELLIPSOID,FT	84393.4
ALTITUDE OF C.G. ABOVE RUNWAY,FT	82531.8
MACH NUMBER	2.55
ANGLE OF ATTACK,DEG	14.26
DYNAMIC PRESSURE,PSF	208.7
DOWNRANGE TO RUNWAY THRESHOLD,NM	60.1
DELTA AZIMUTH TO MAC,DEG	-14.03

TABLE 6.4-1- TAEM/ASL INTERFACE CONDITIONS

PARAMETER	VALUE
GET.HR:MN:SEC	54:29:27.24
TIME FROM ENTRY ENTERFACE.MIN:SEC	0:30:12.96
RELATIVE VELOCITY.FPS	573.6
RELATIVE FLIGHT PATH ANGLE.DEG	-19.9889
RELATIVE HEADING FROM NORTH.DEG	-115.1516
LONGITUDE.DEG W	117.7191
GEODETIC LATITUDE.DEG N	35.0058
GEOCENTRIC LATITUDE.DEG N	34.8232
ALTITUDE OF C.G. ABOVE FISCHER ELLIPSOID.FT	11928.0
ALTITUDE OF C.G. ABOVE RUNWAY.FT	9824.6
DOWNRANGE TO RUNWAY THRESHOLD.FT	-33371.7

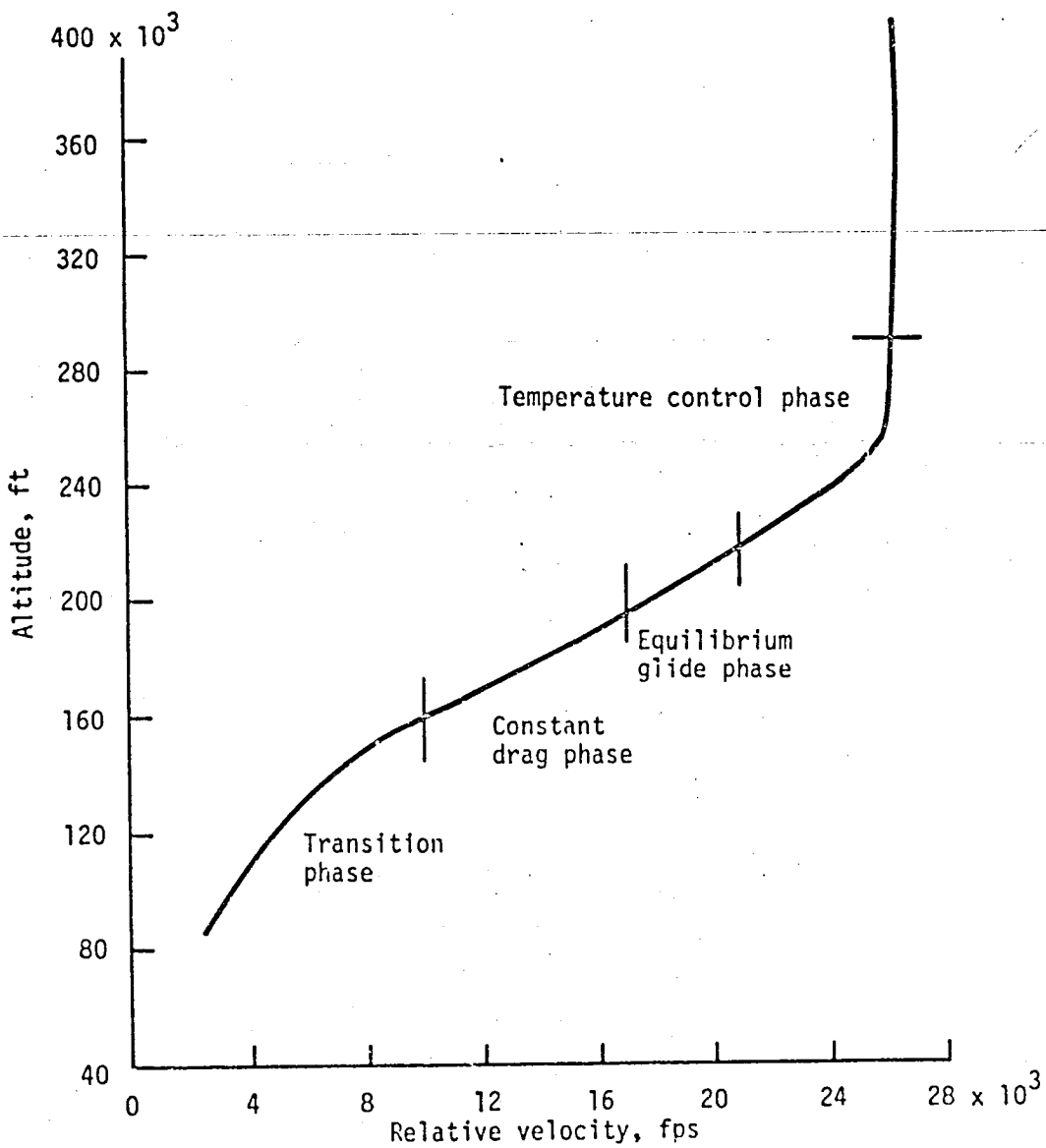


Figure 3.1.1. - Typical entry altitude-velocity profile.

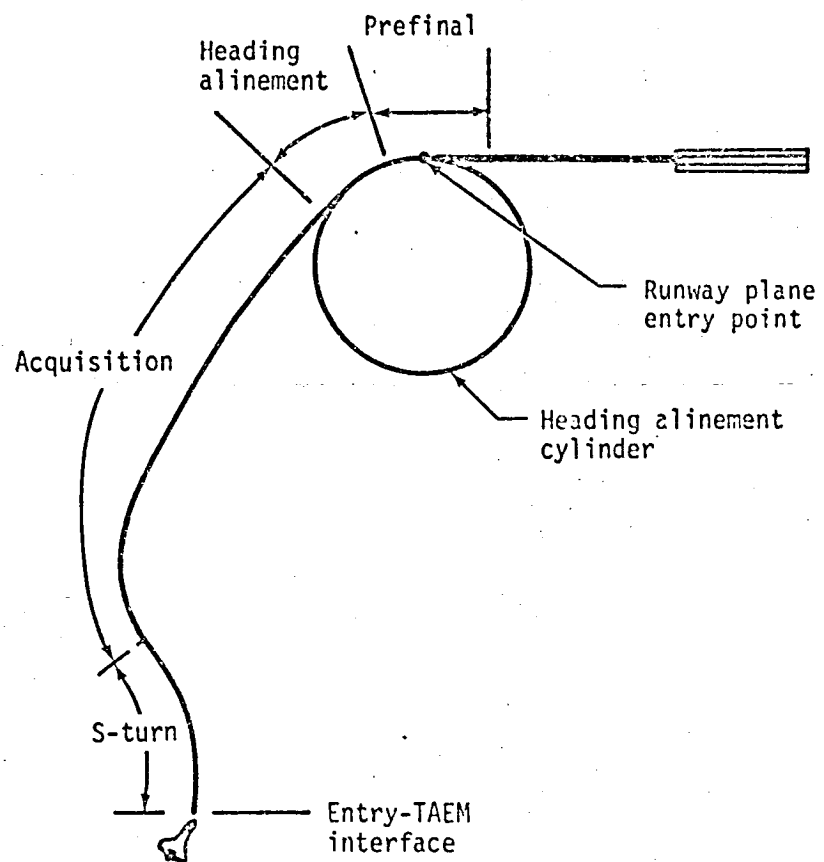


Figure 3.1.2.- Typical TAEM groundtrack and trajectory sub-phases.

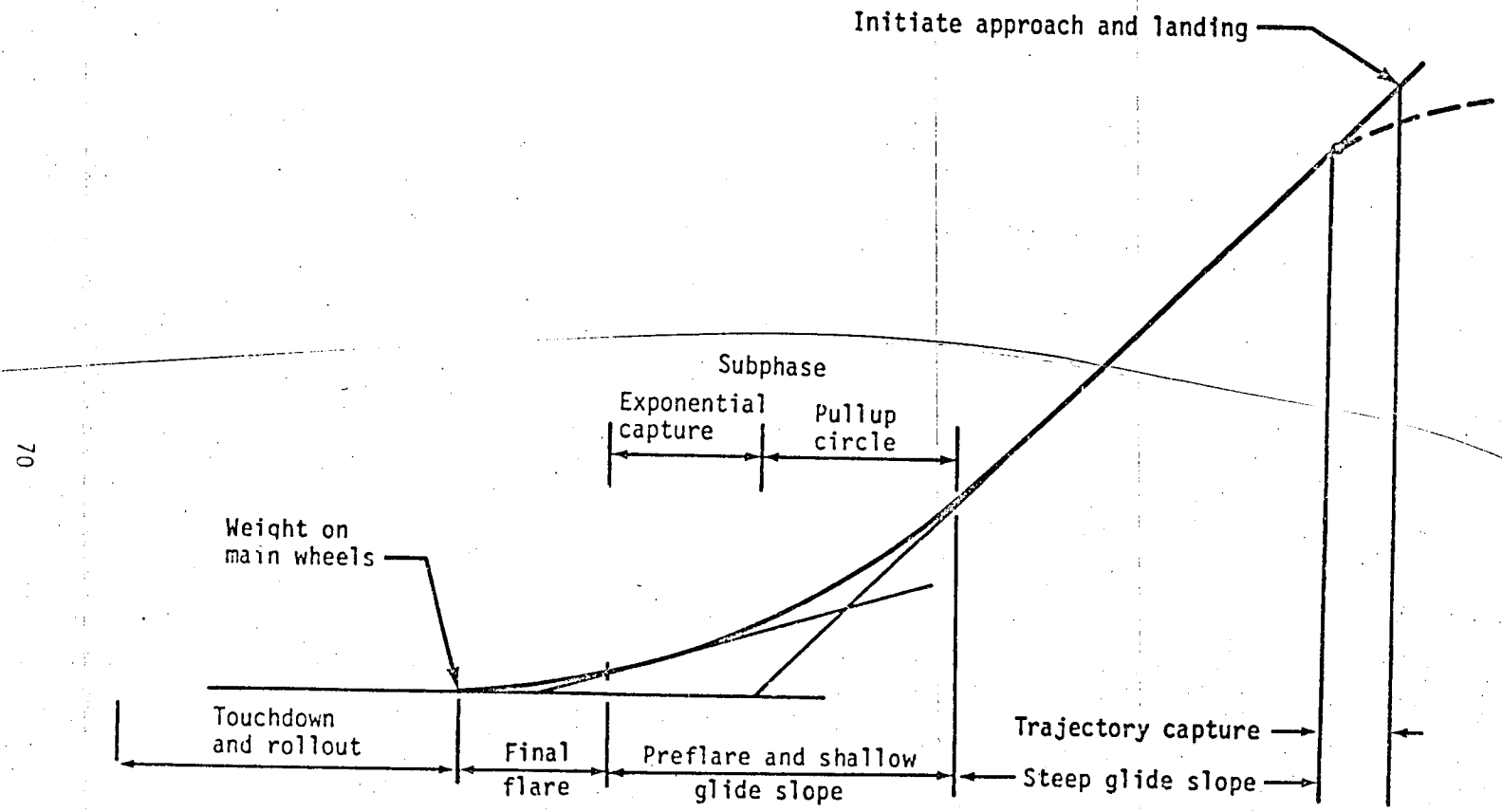


Figure 3.1-3.- Typical approach and landing trajectory with sub-phases identified.

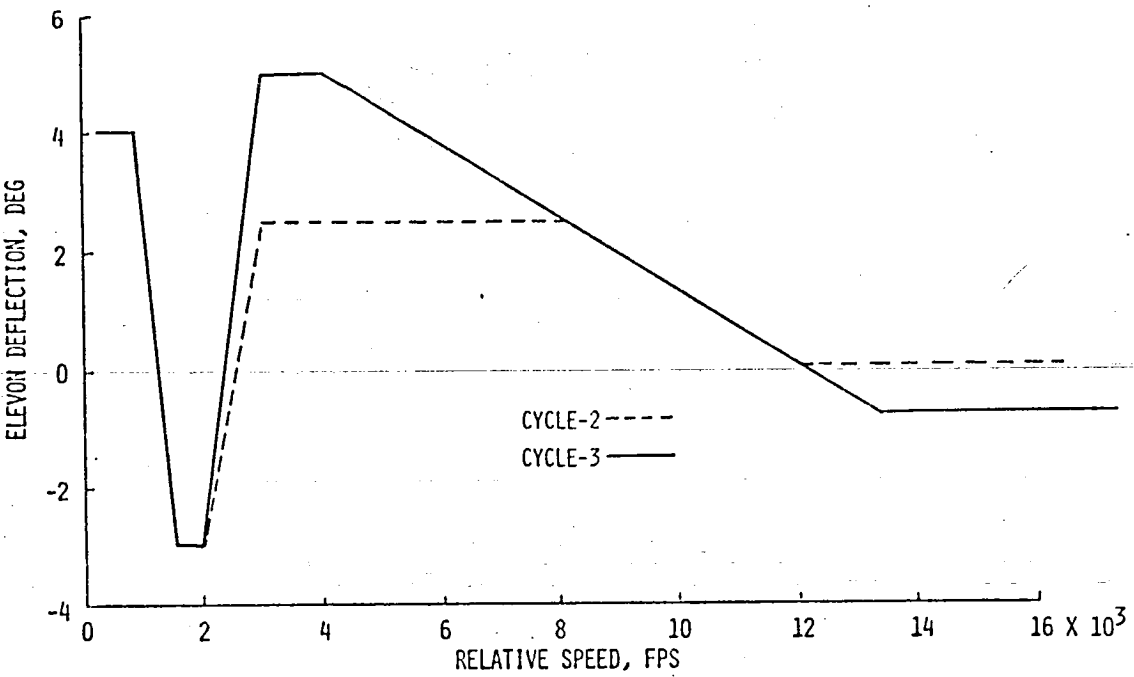


Figure 3.2-1.- Comparison of cycle 2 and 3 elevon schedules.

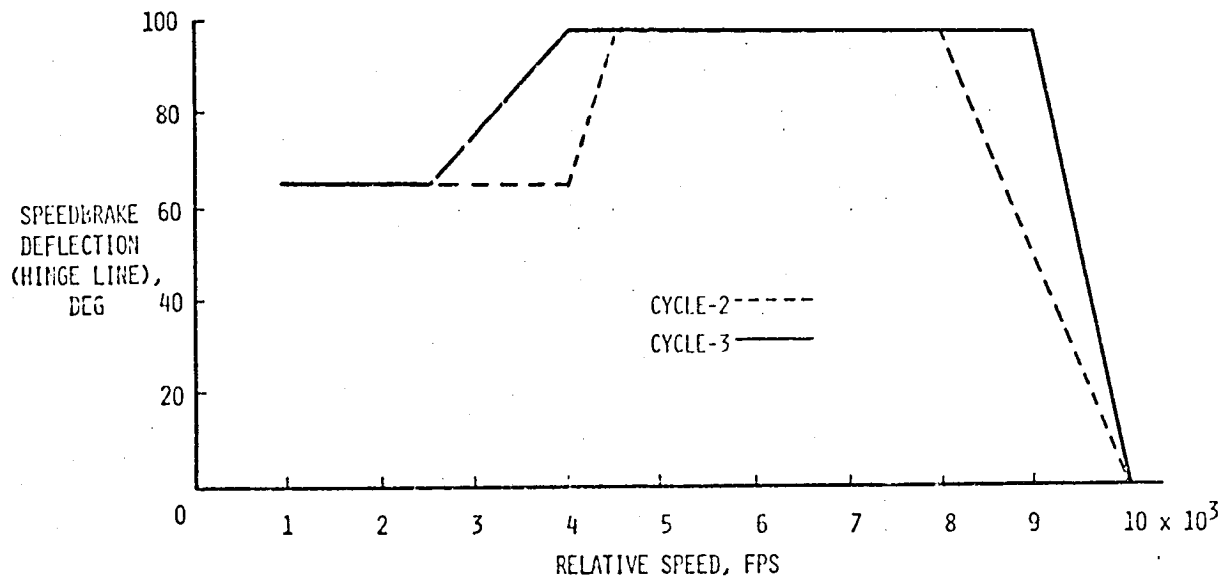


Figure 3.2-2.- Comparison of cycle 2 and 3 speedbrake schedules.

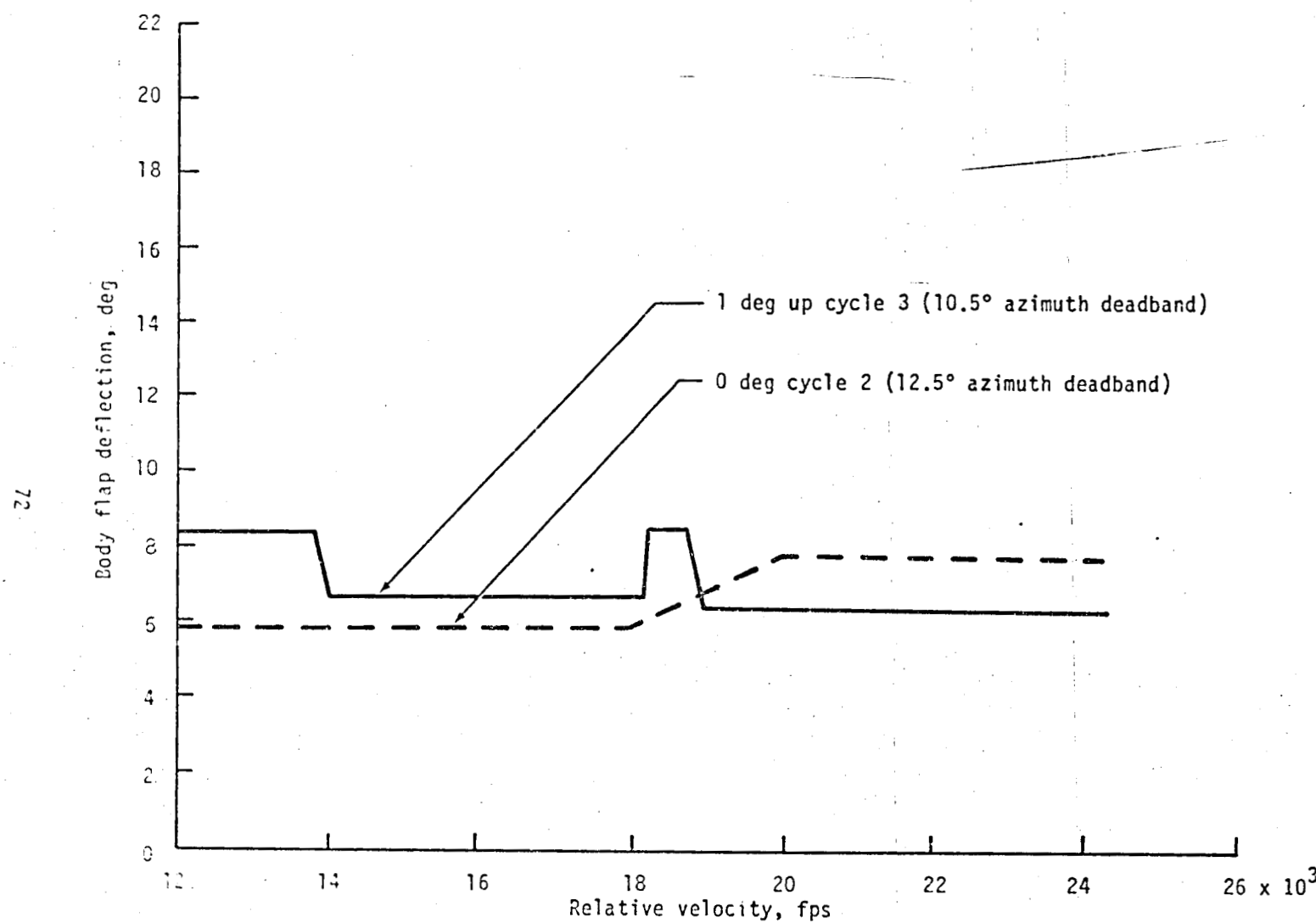


Figure 3.2-3.- Comparison of cycle 2 and 3 body flap deflections.

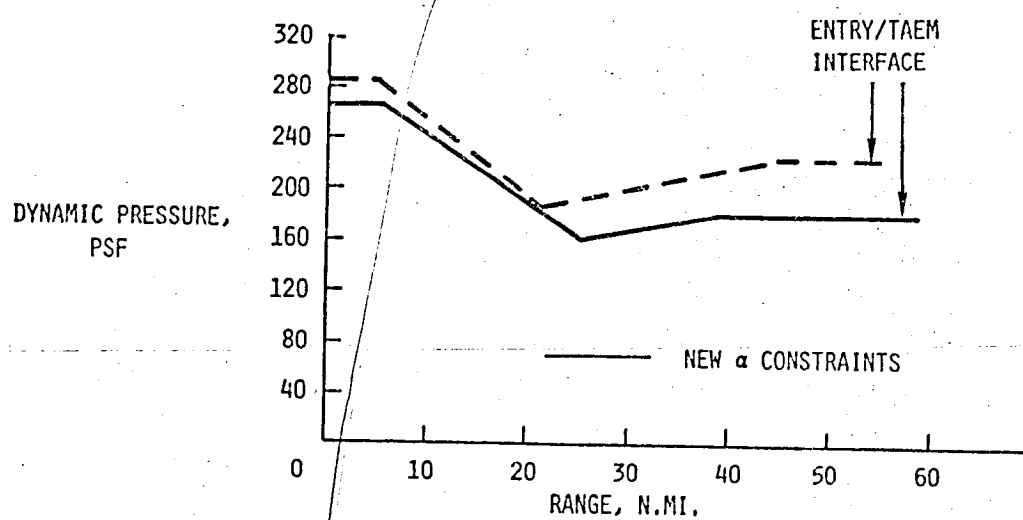


Figure 3.2-4. Taem reference dynamic pressure profiles.

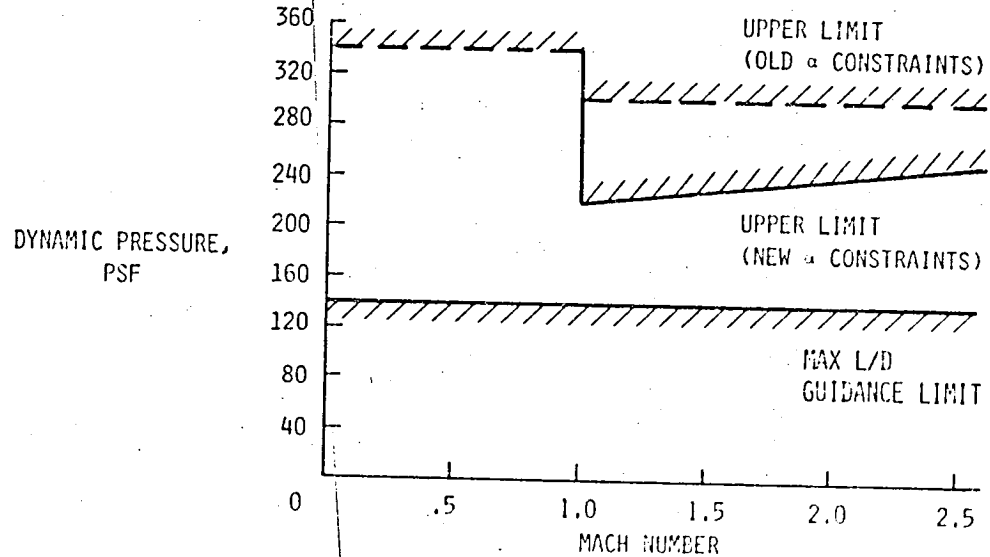


Figure 3.2-5. Taem guidance dynamic pressure limits.

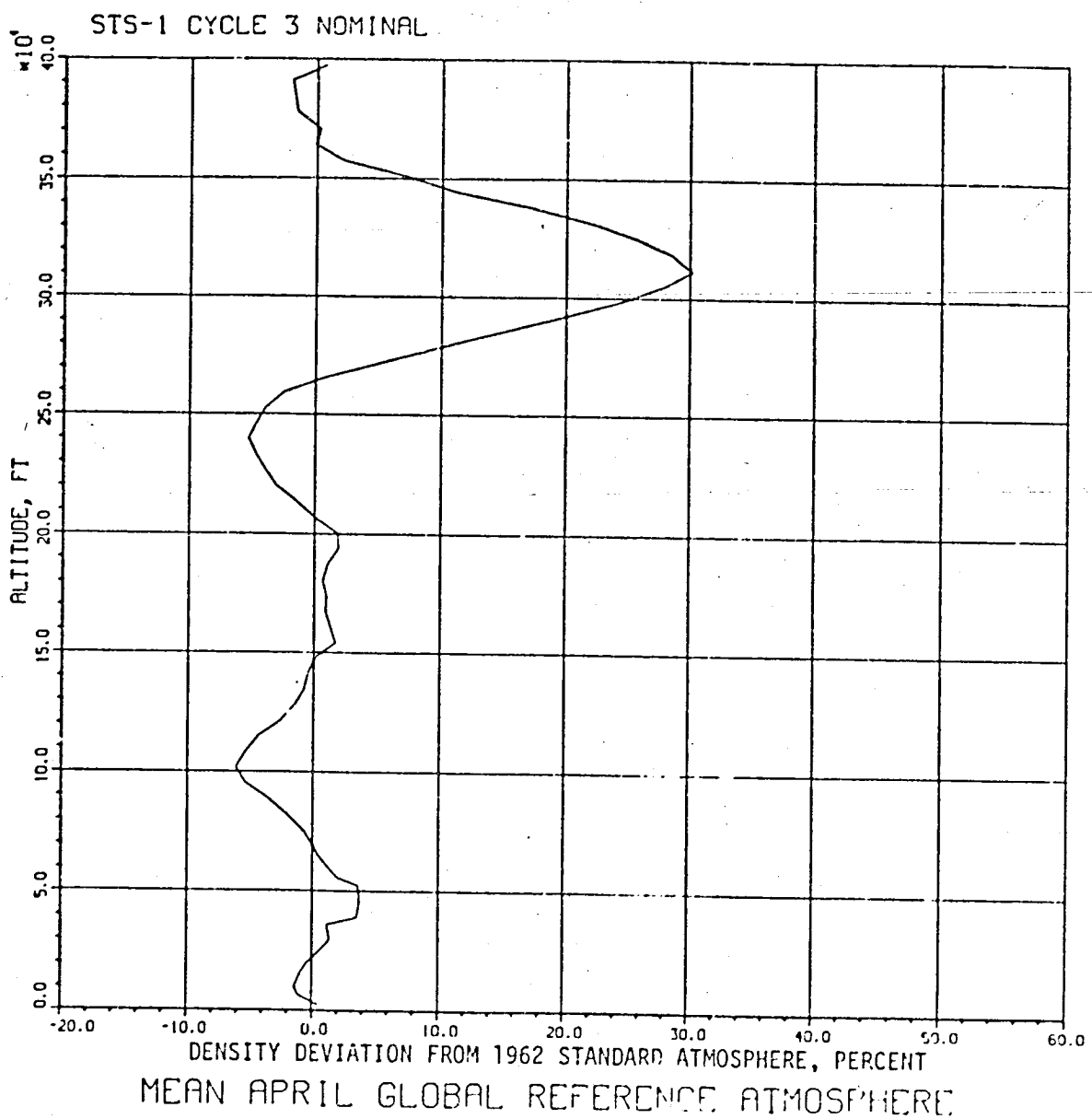


Figure 5.0-1

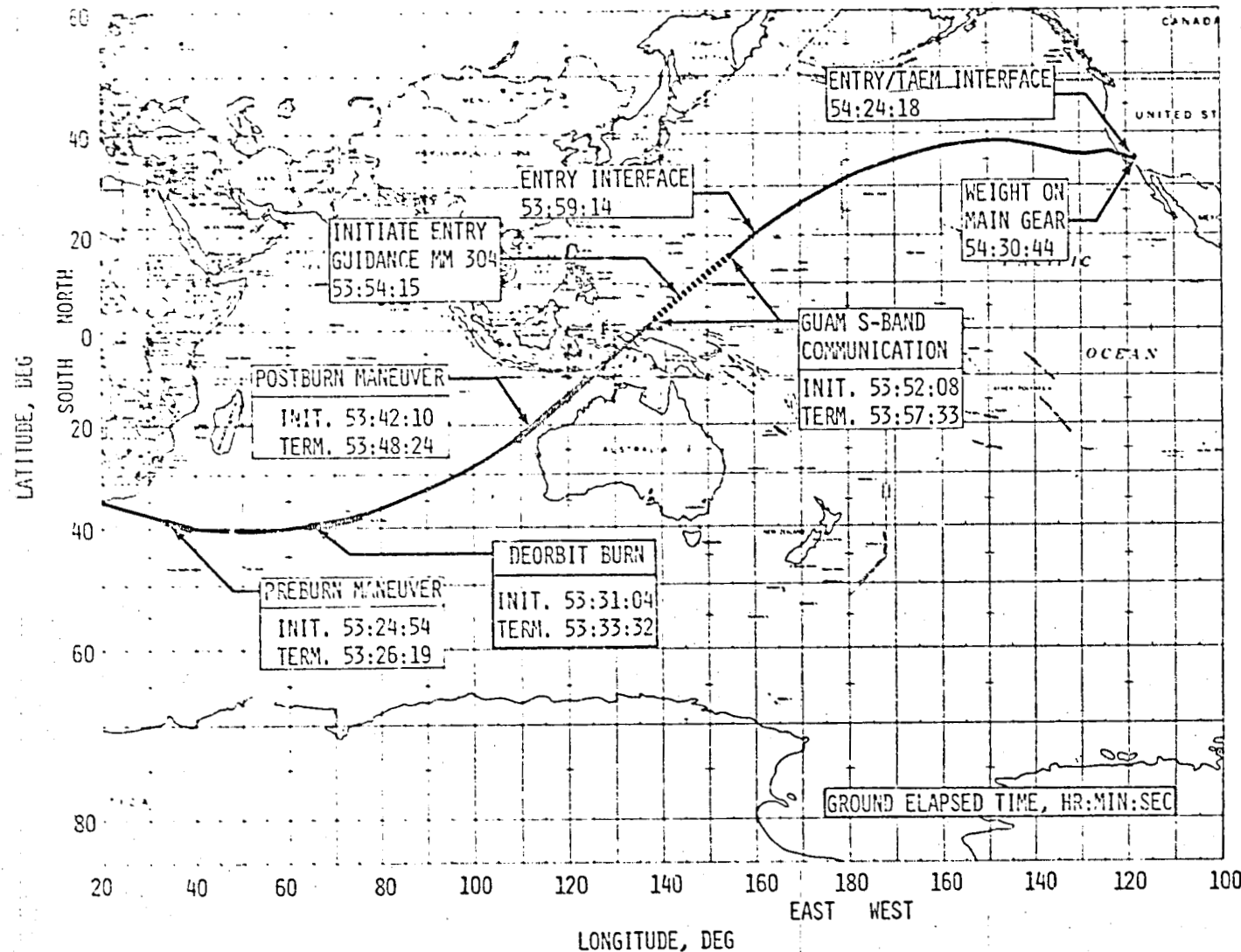


Figure 6.0-1.- STS-1 decorbit-through-landing groundtrack.

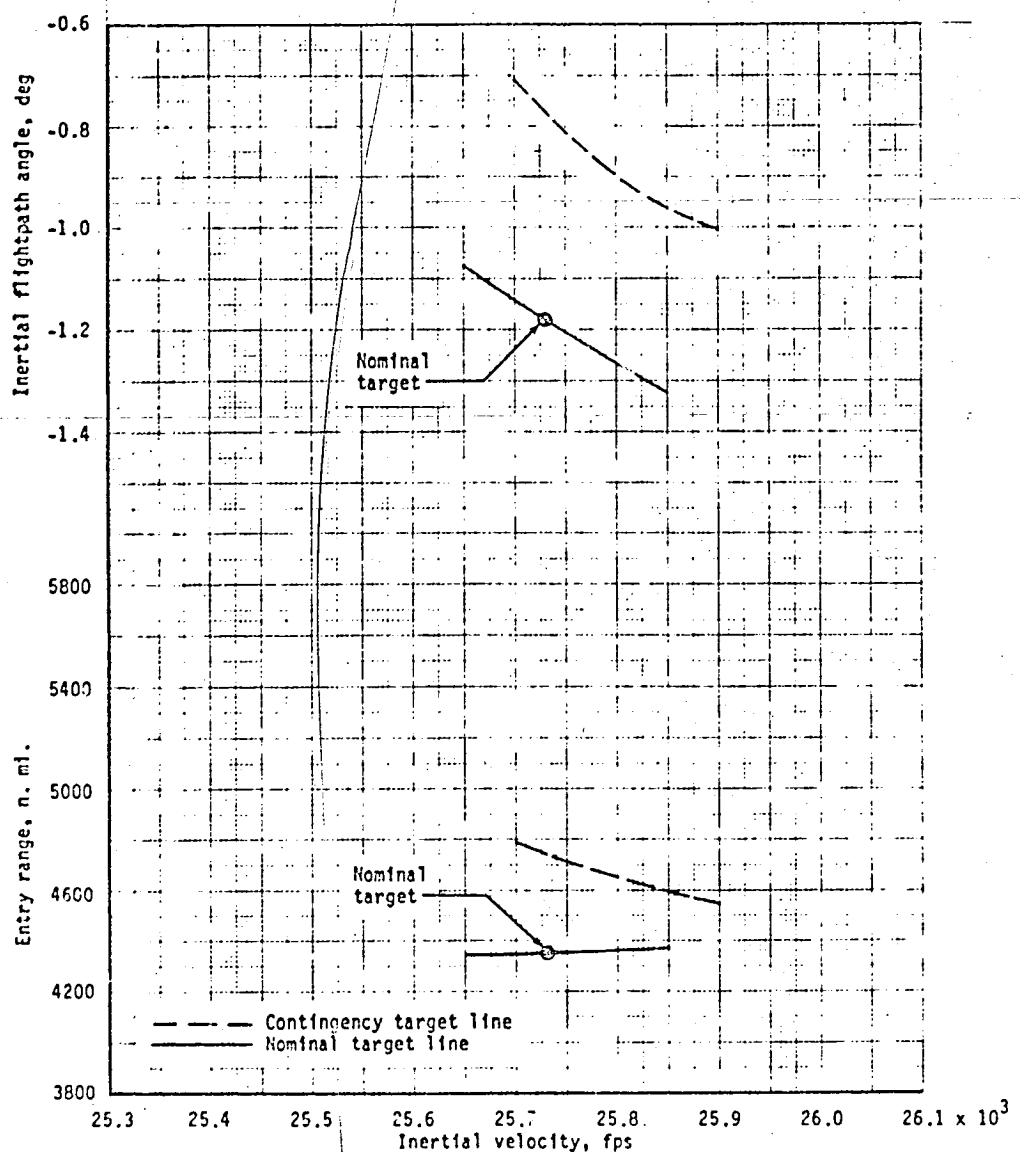


Figure 6.1-1.-- Inertial velocity, inertial flightpath angle, and range target lines for Orbiter OFT-1 entry interface.

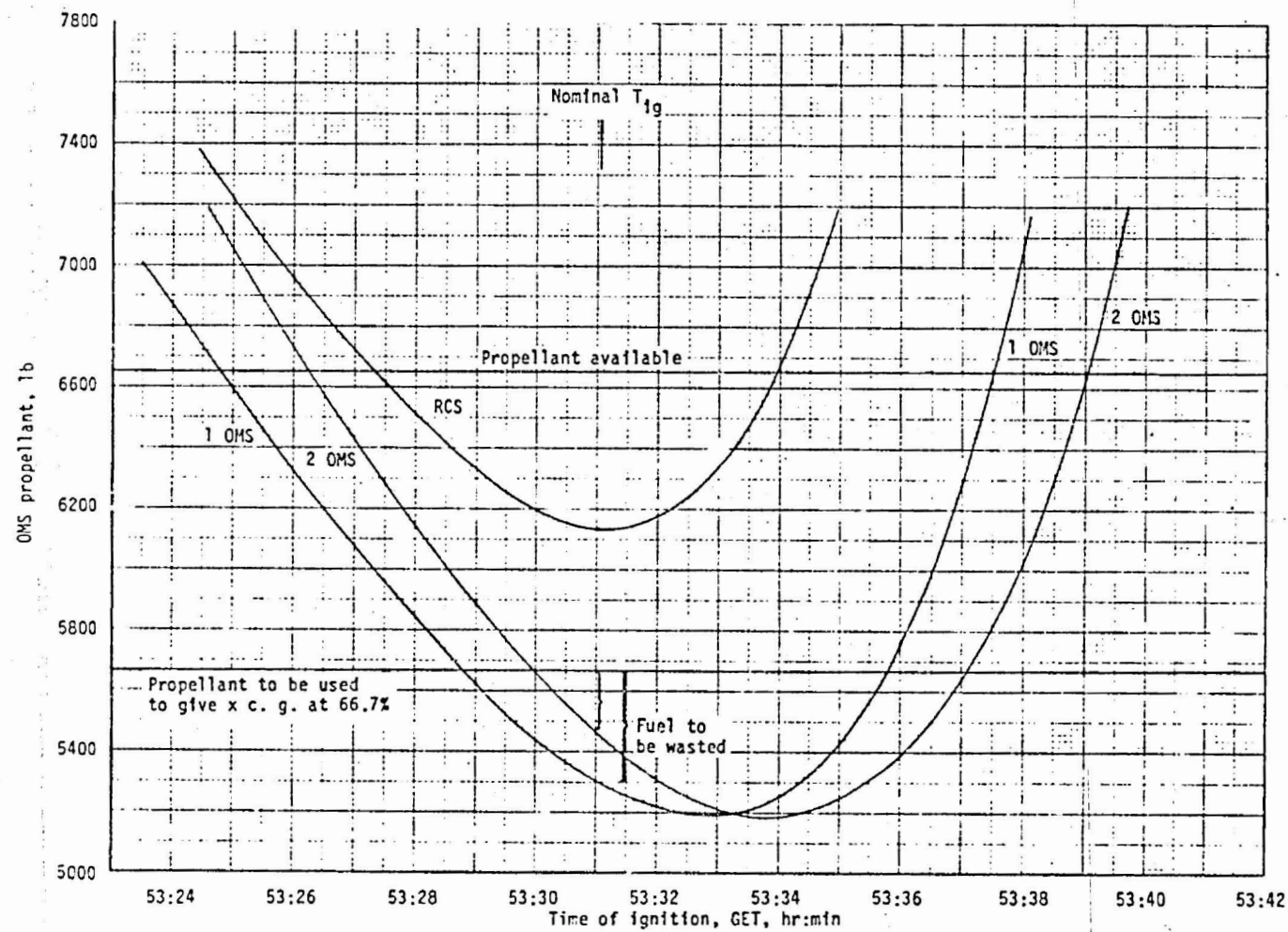


Figure 6.1-2.- OMS propellant versus T_{ig} , nominal end of mission.

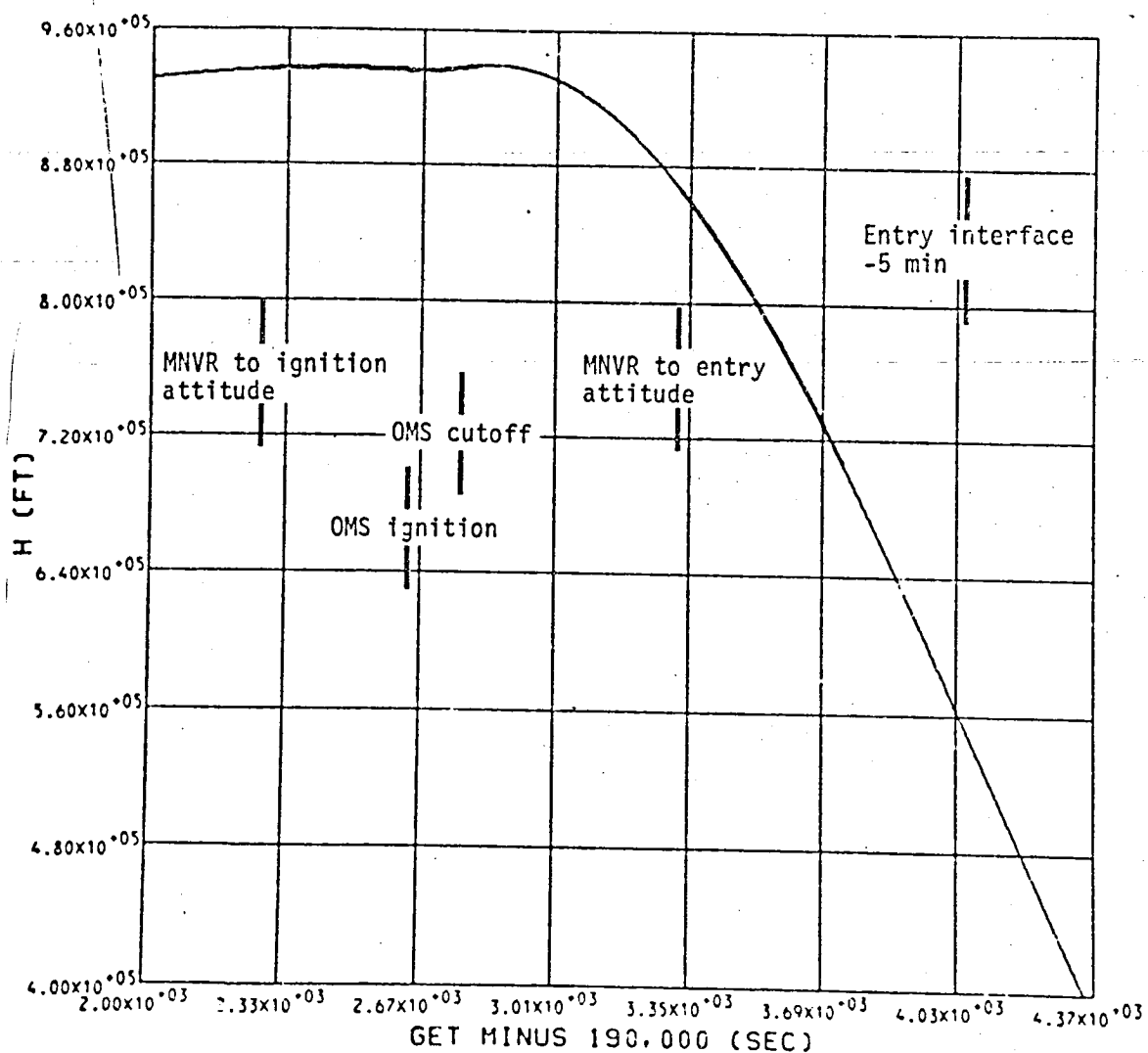


Figure 6.1-3.- Geodetic altitude - deorbit.

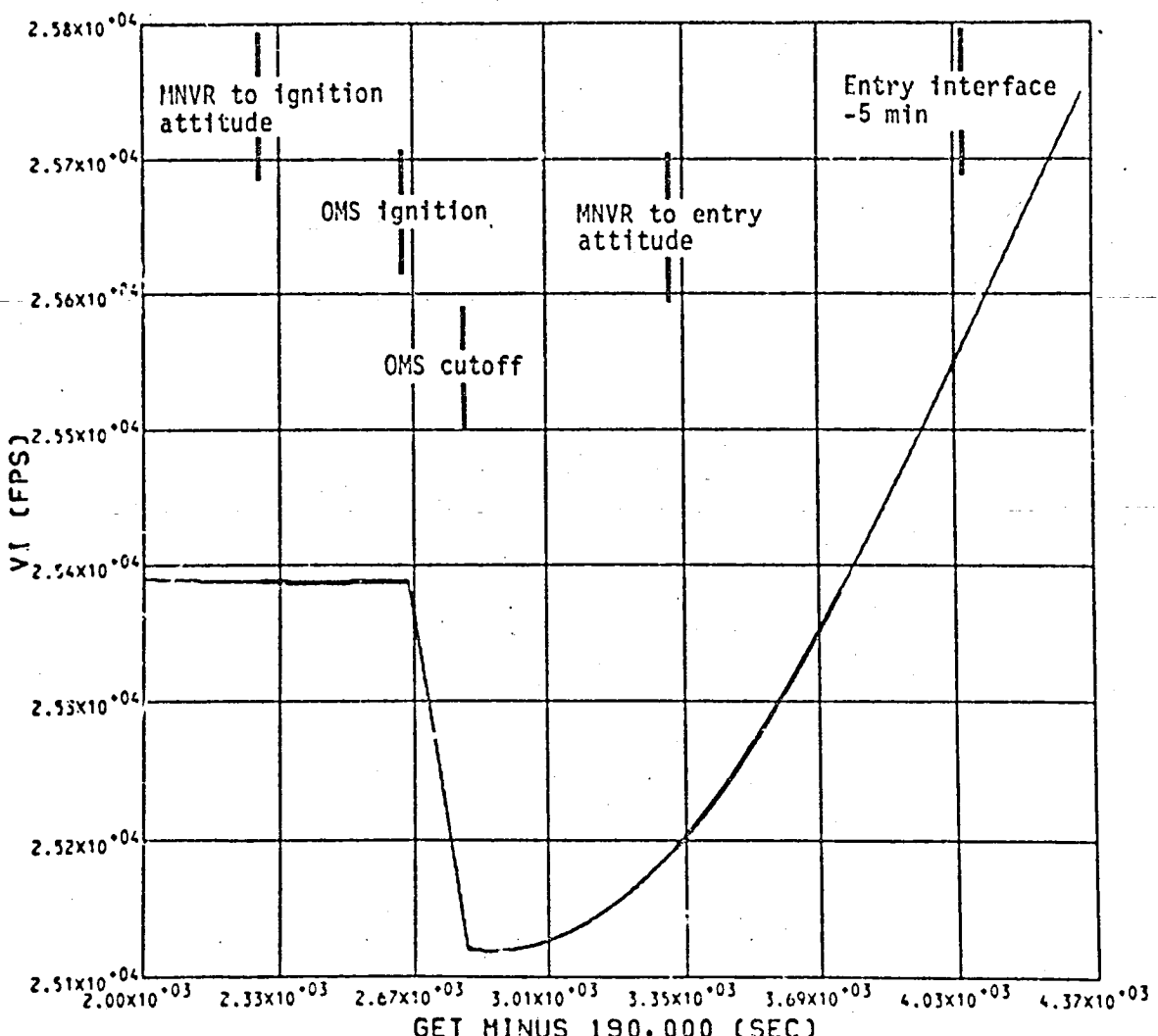


Figure 6.1-4.- Inertial velocity magnitude - deorbit..

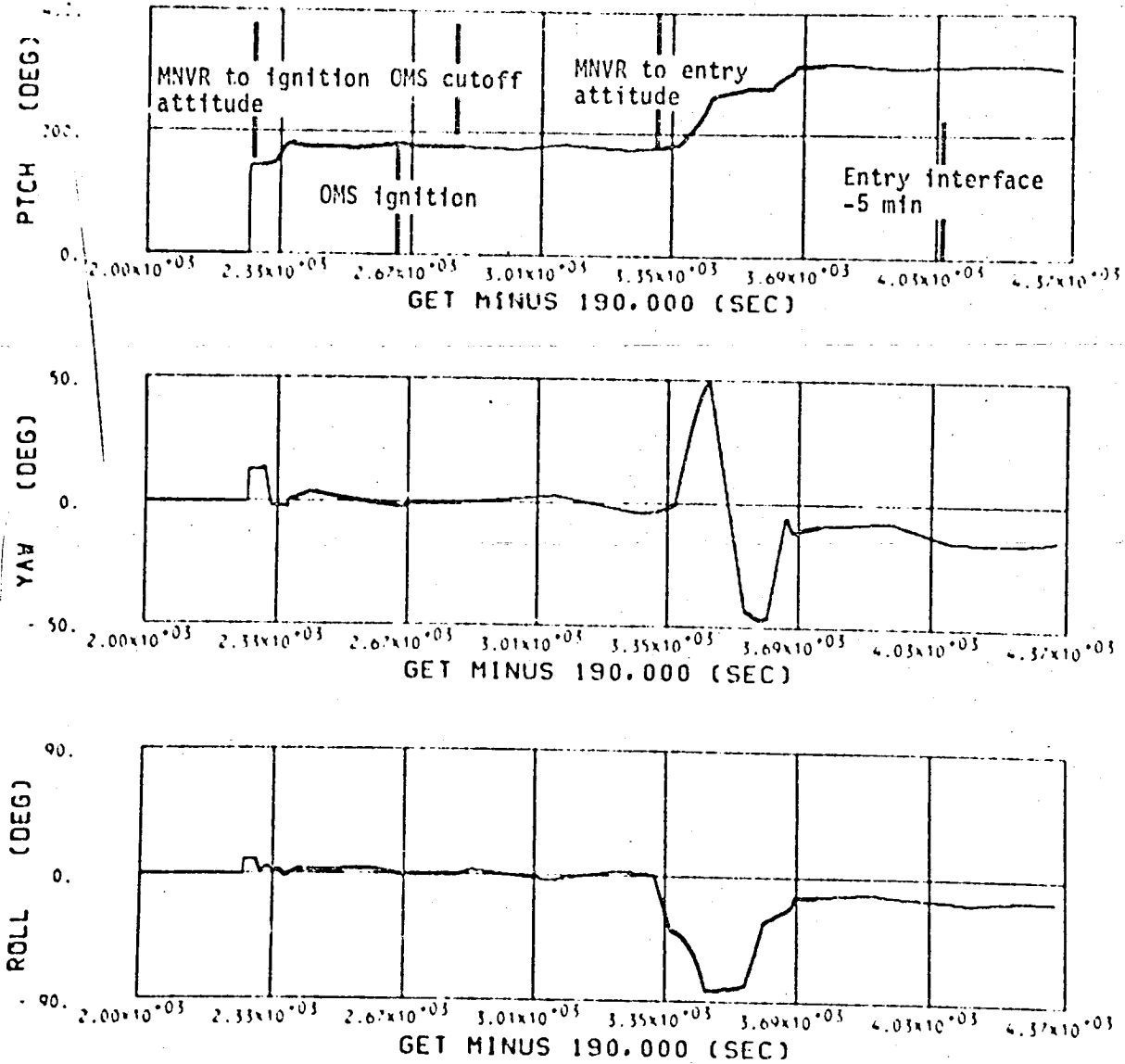


Figure 6.1-5.- Displayed ADI angles-reference - deorbit.

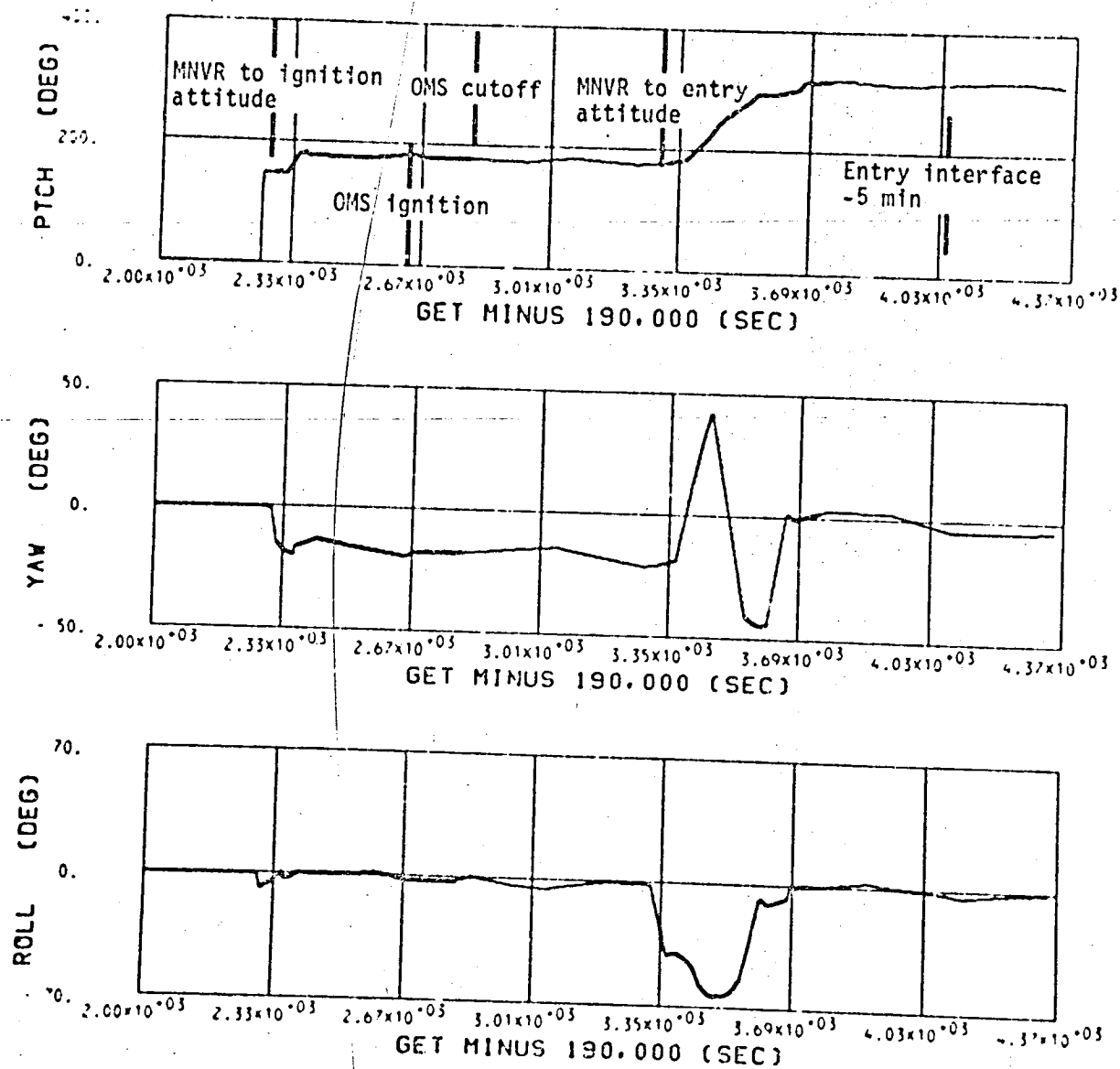


Figure 6.1-6.- Displayed ADI angles-intertial - deorbit.

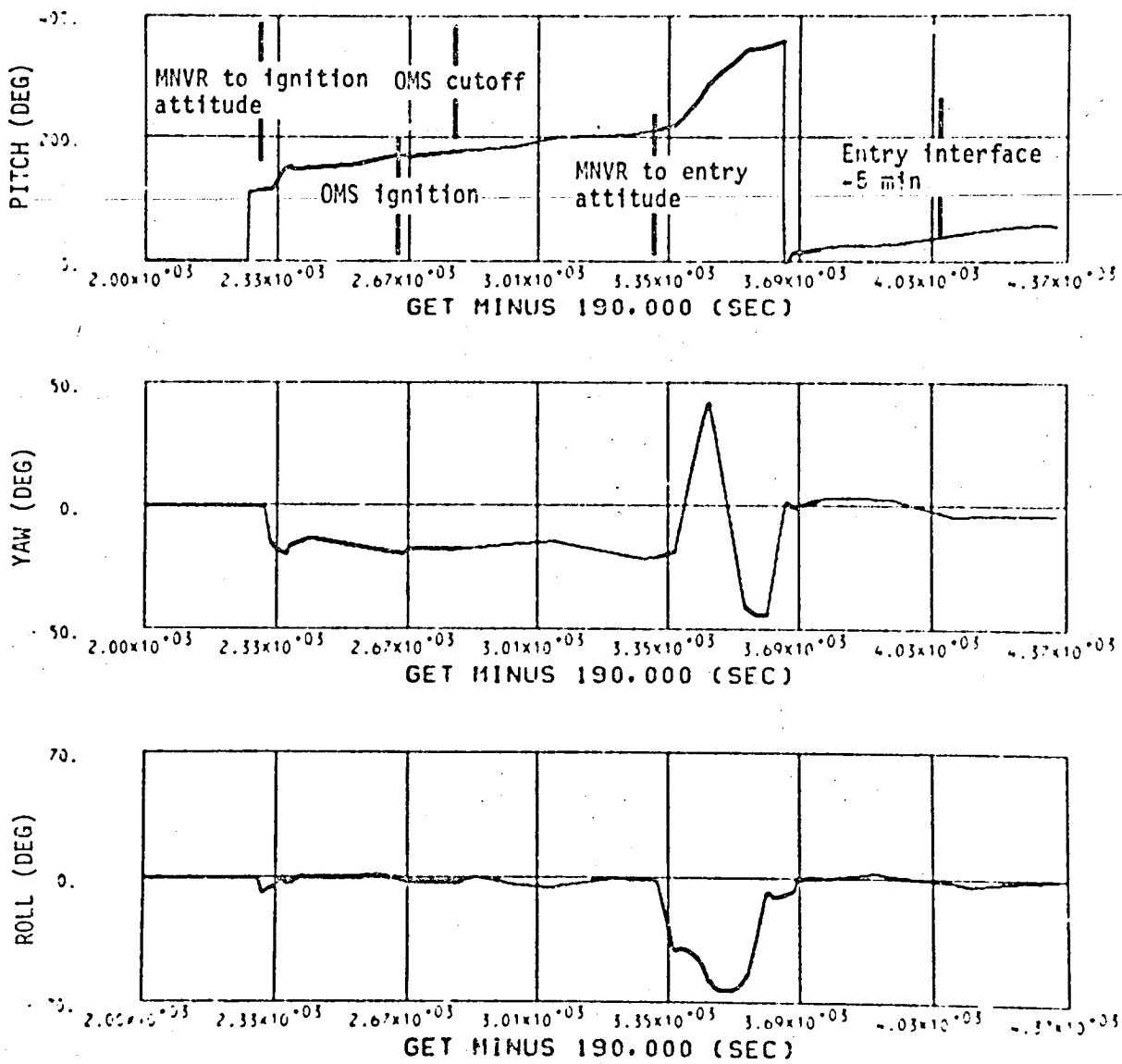


Figure 6.1-7.- Displayed AOI angles-LVLH - deorbit.

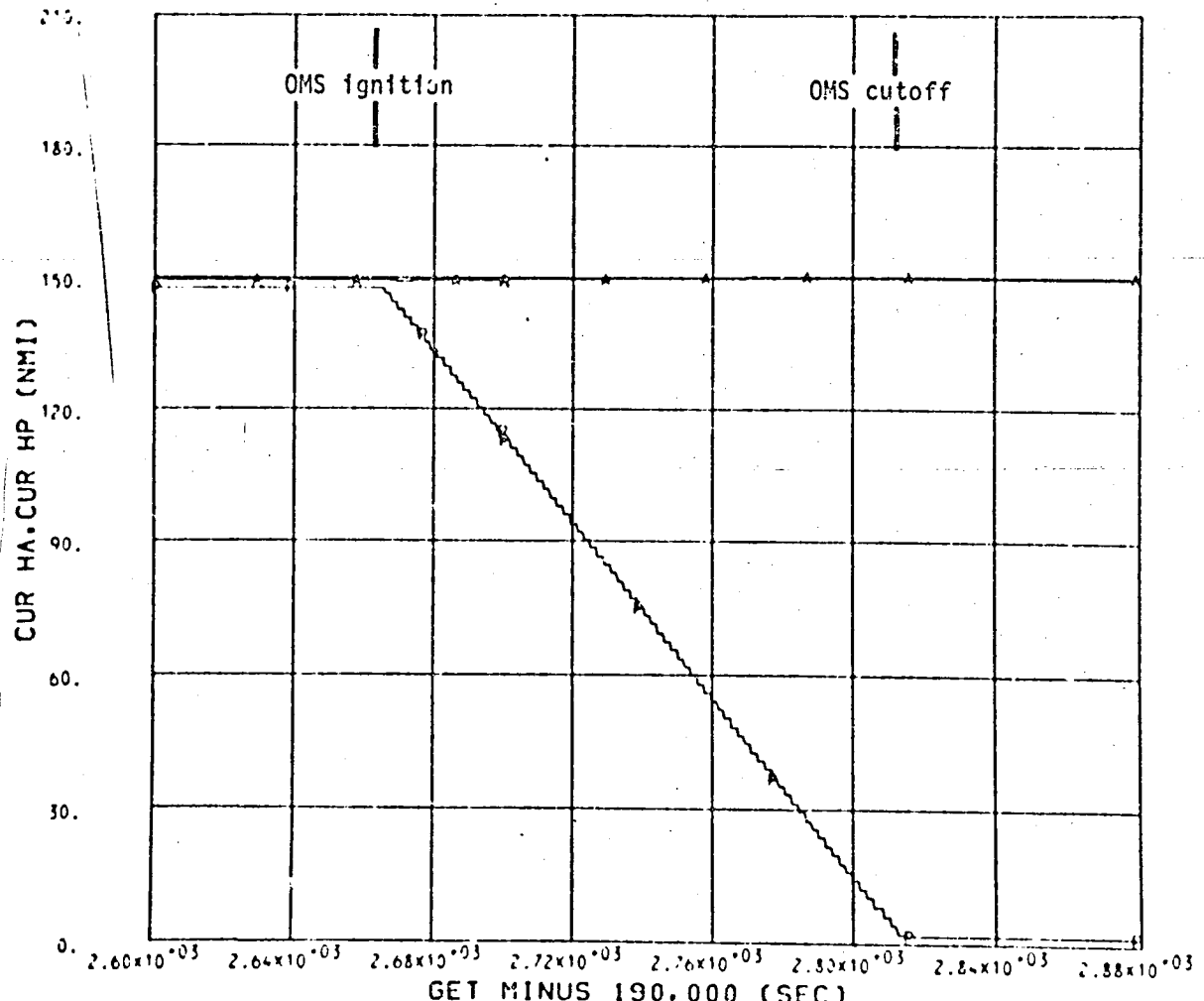


Figure 6.1-8.- Current apogee and perigee altitudes - deorbit.

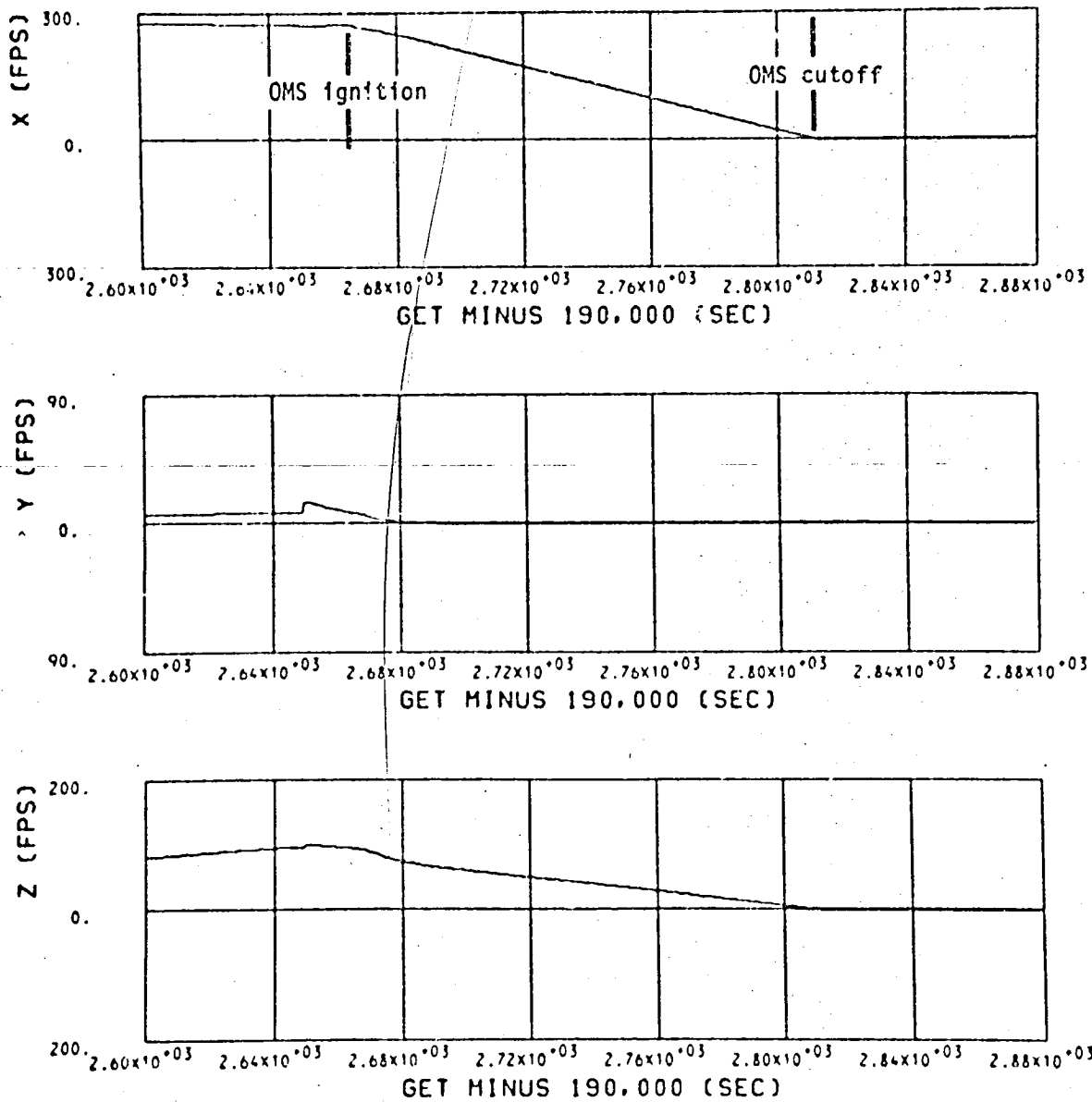


Figure 6.1-9.- Displayed velocity-to-go vector in body-axis coordinates - deorbit.

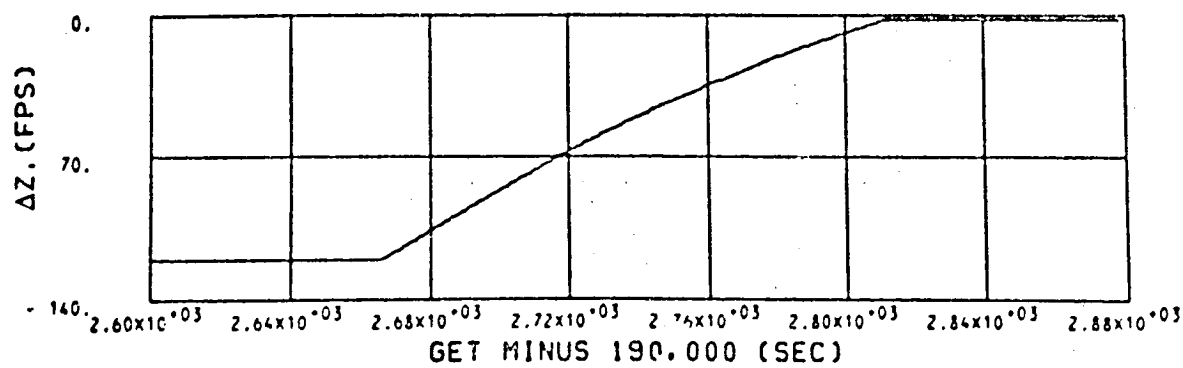
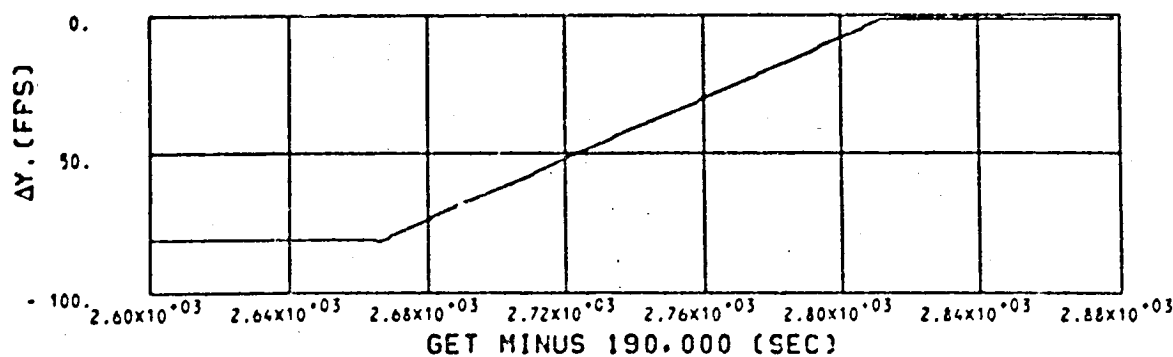
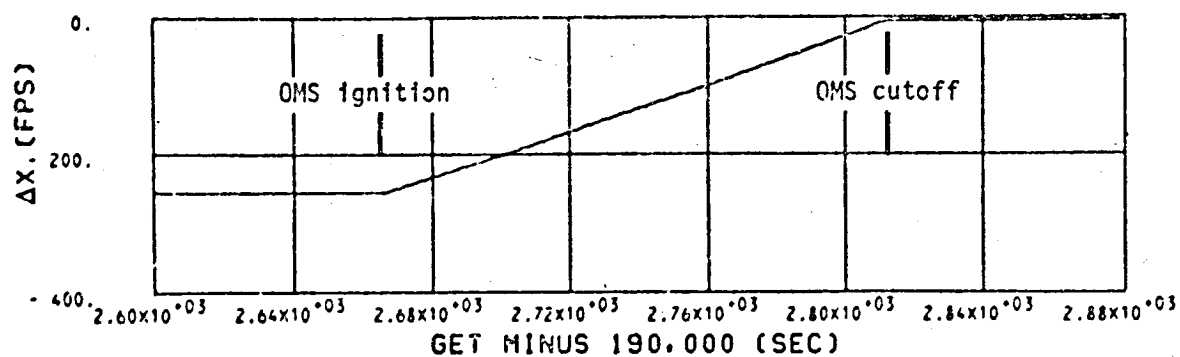


Figure 6.1-10.- Velocity-to-go vector in LVLH coordinates - deorbit.

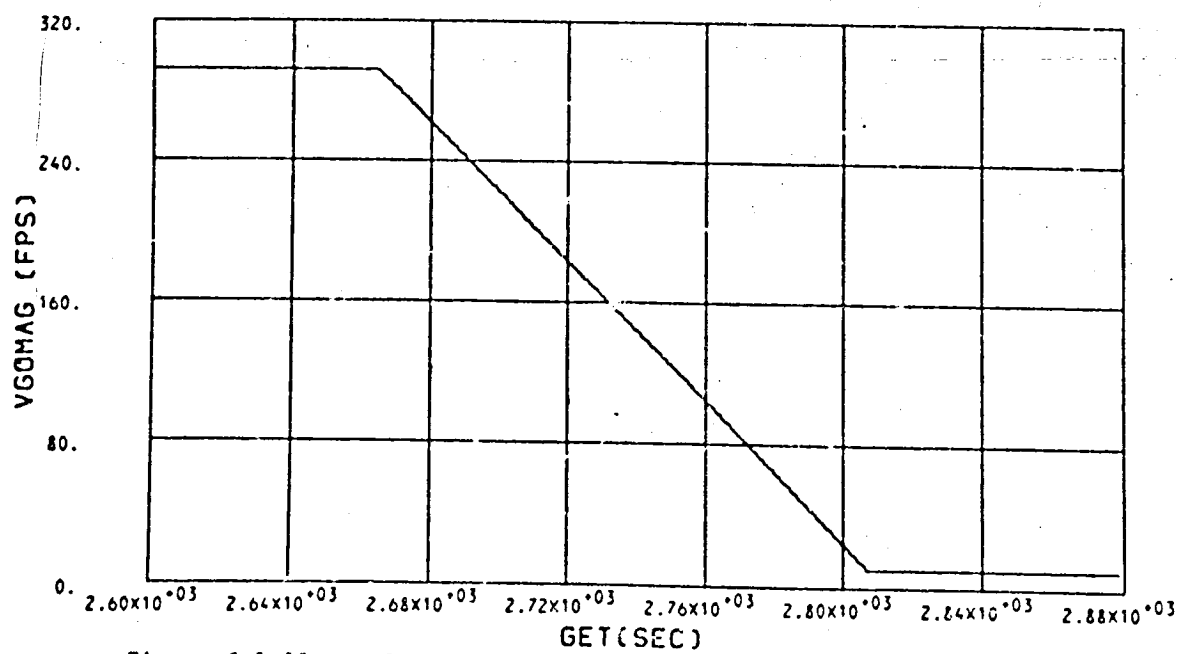
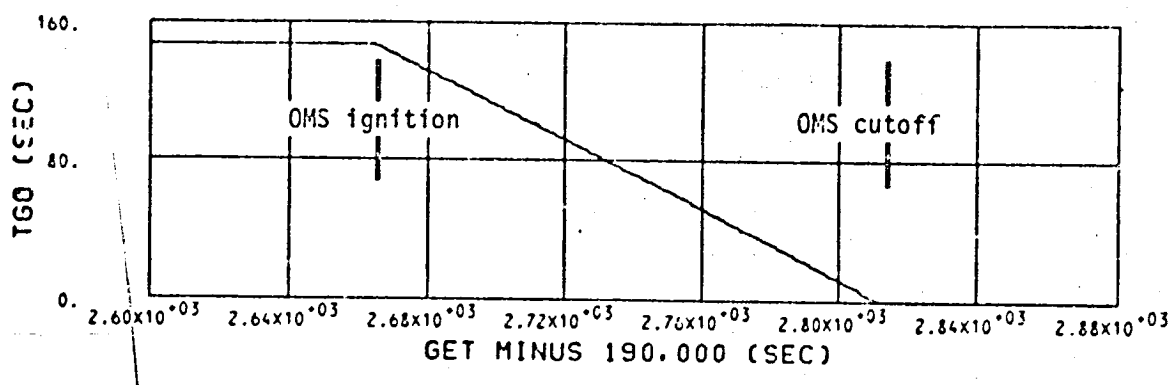


Figure 6.1-11.- Velocity-to-go magnitude and time-to-go - deorbit.

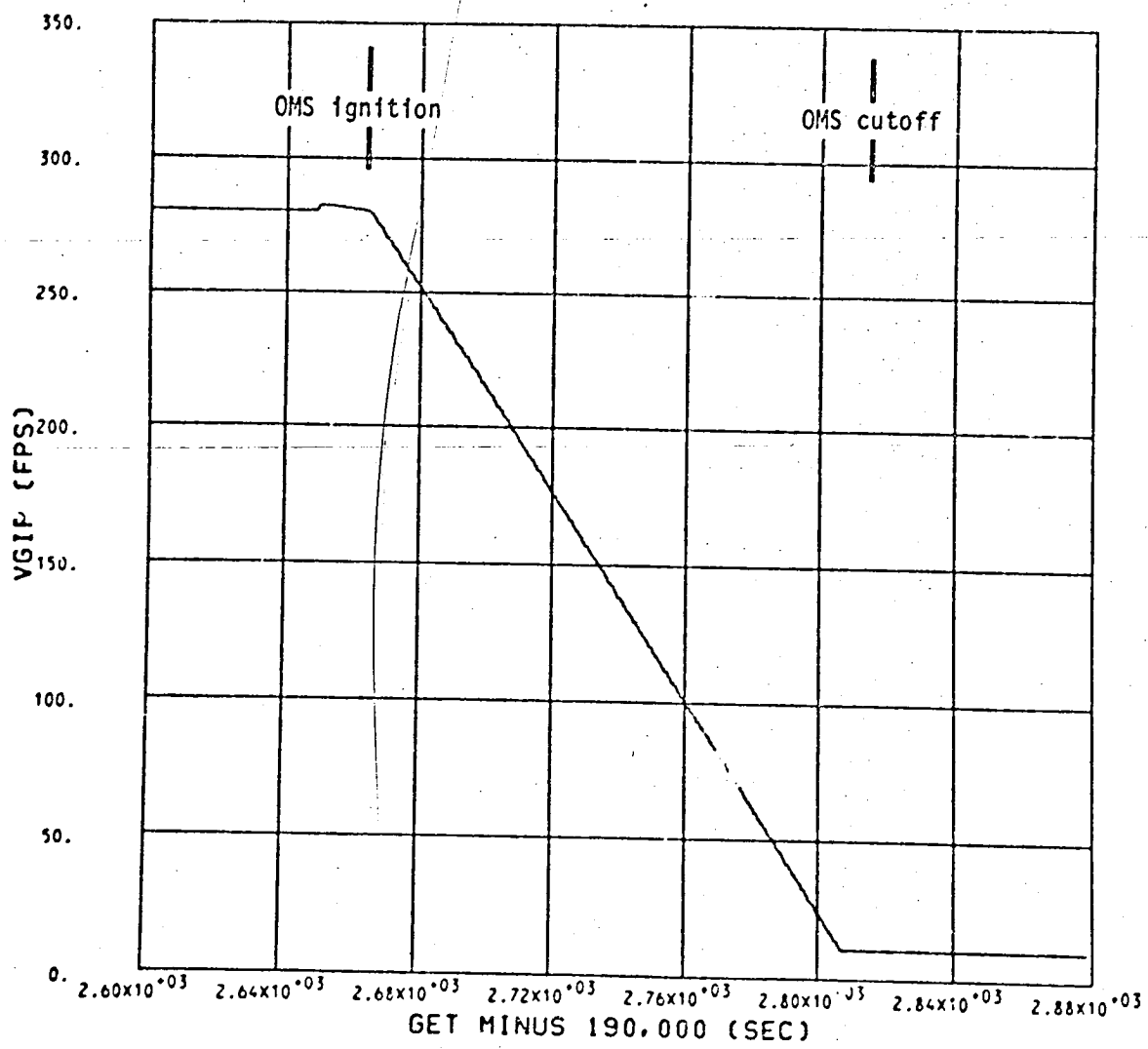


Figure 6.1-12.- Velocity magnitude to be gained for no fuel wasting - deorbit.

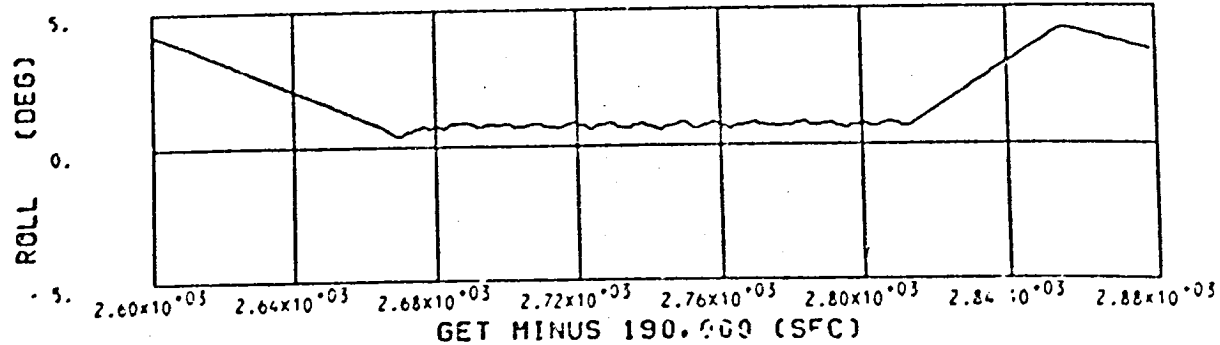
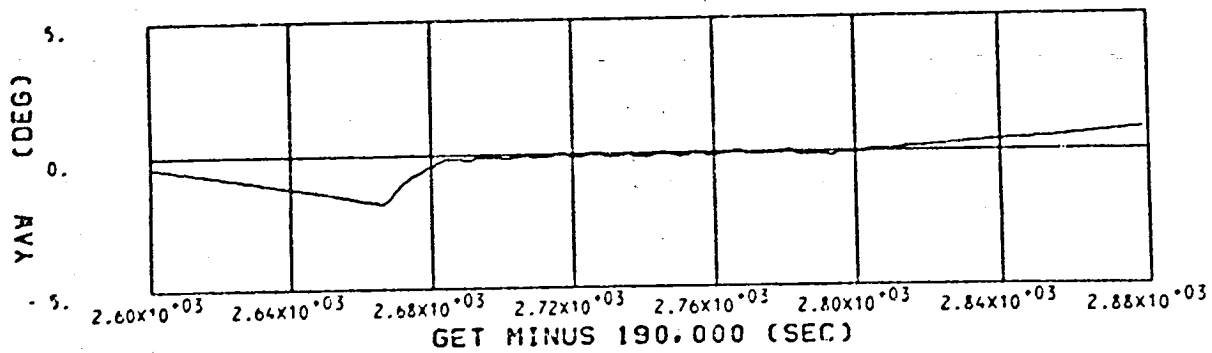
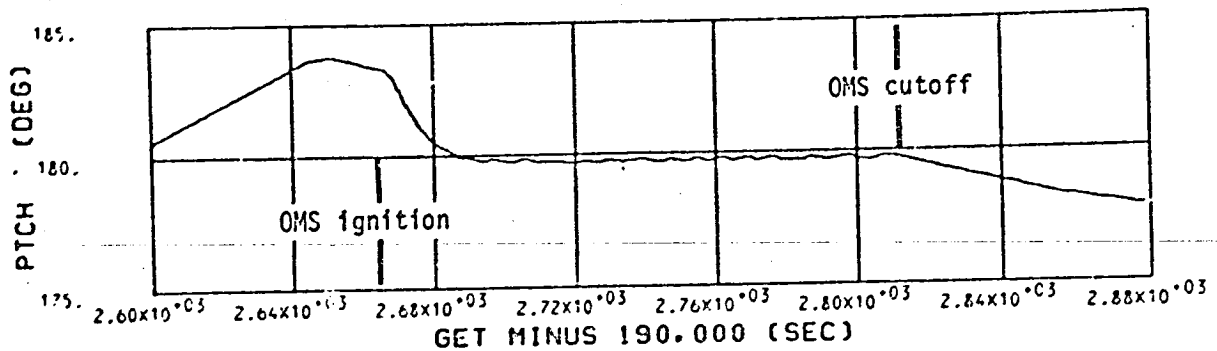


Figure 6.1-13.- Displayed ADI angles-reference - deorbit.

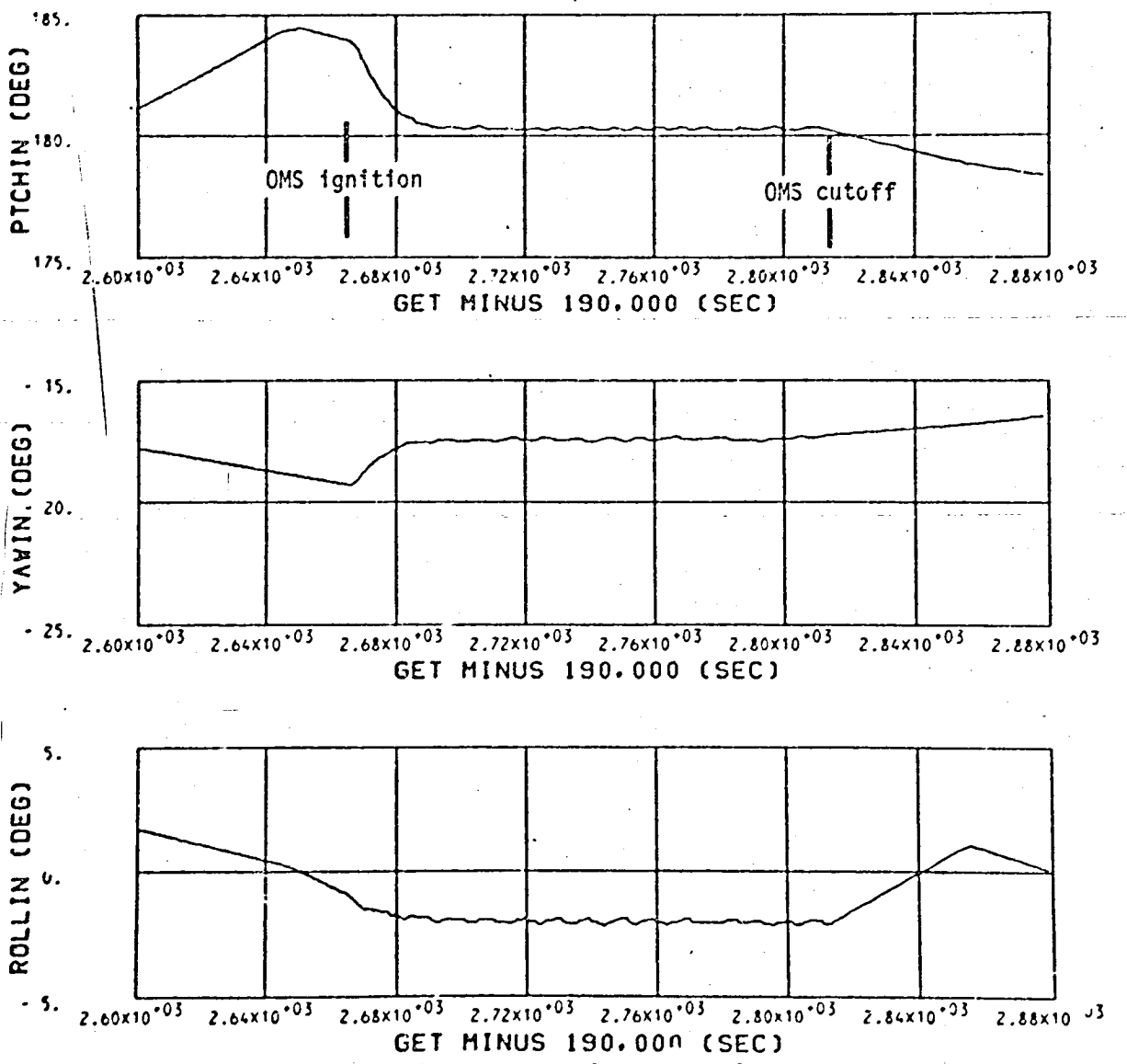


Figure 6.1-14.- Displayed ADI angles-inertial - deorbit.

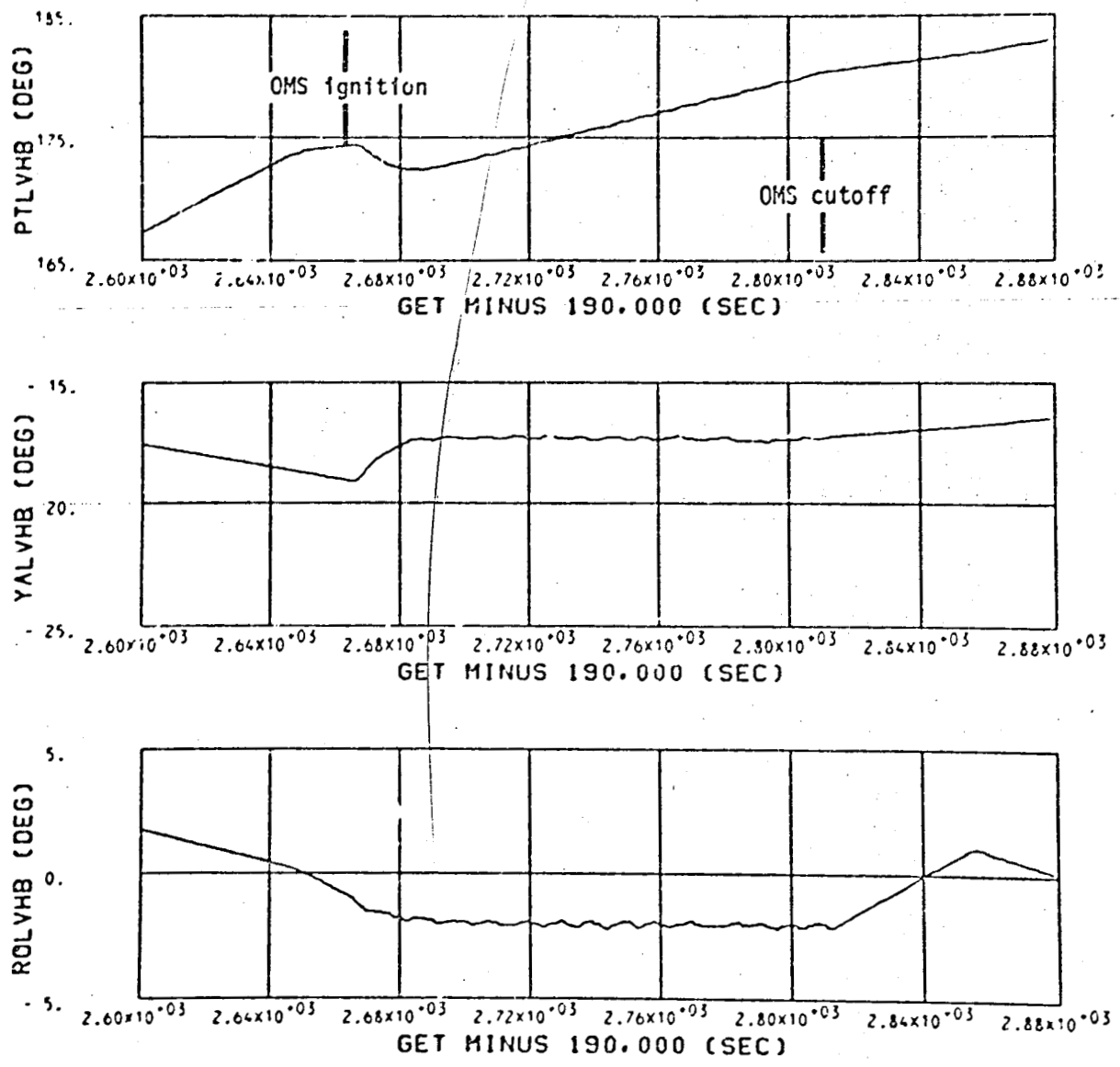


Figure 6.1-15.- Displayed ADI angles-LVLH - deorbit.

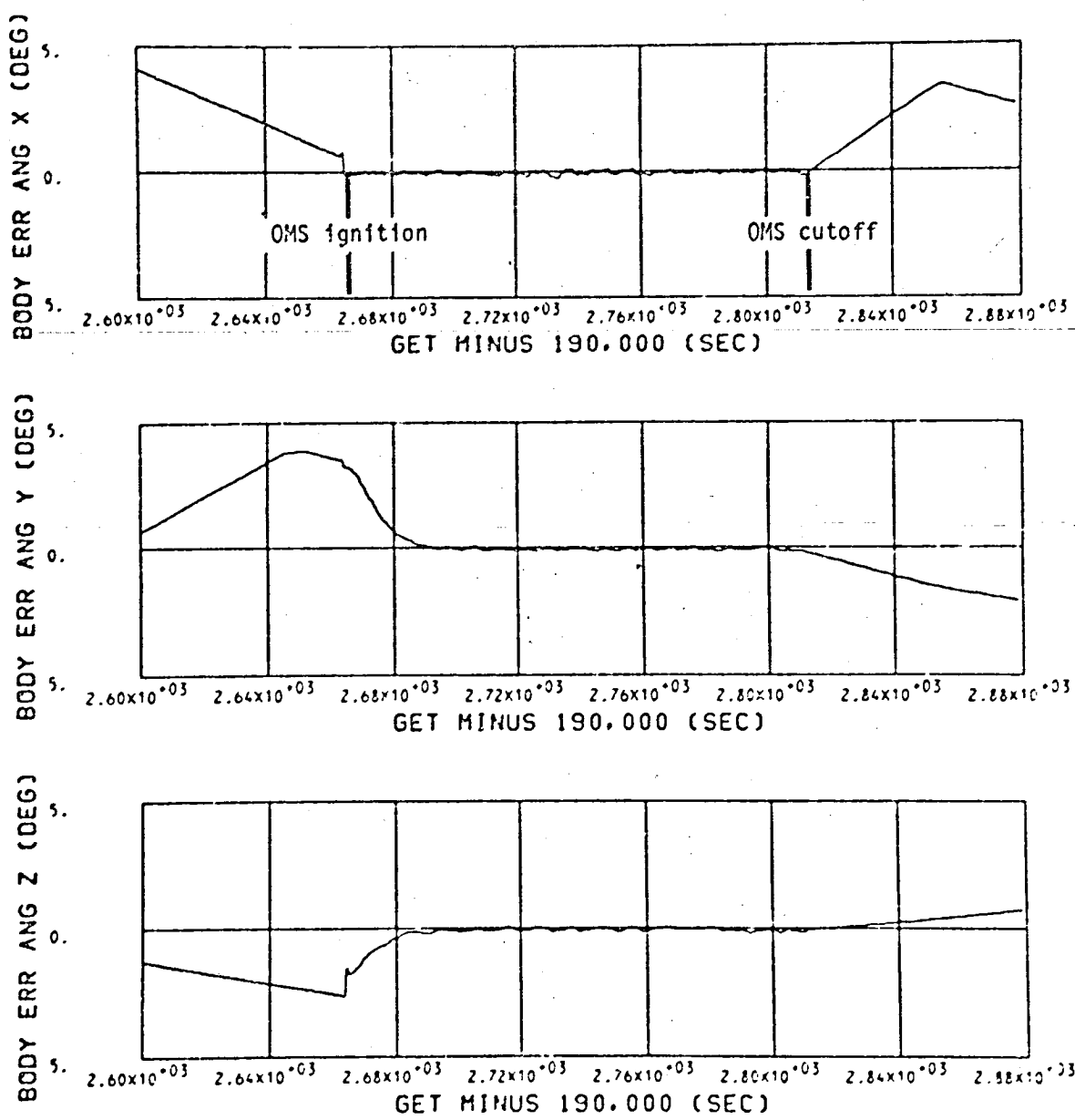


Figure 6.1-16.- Dedicated display ADI body attitude error - deorbit.

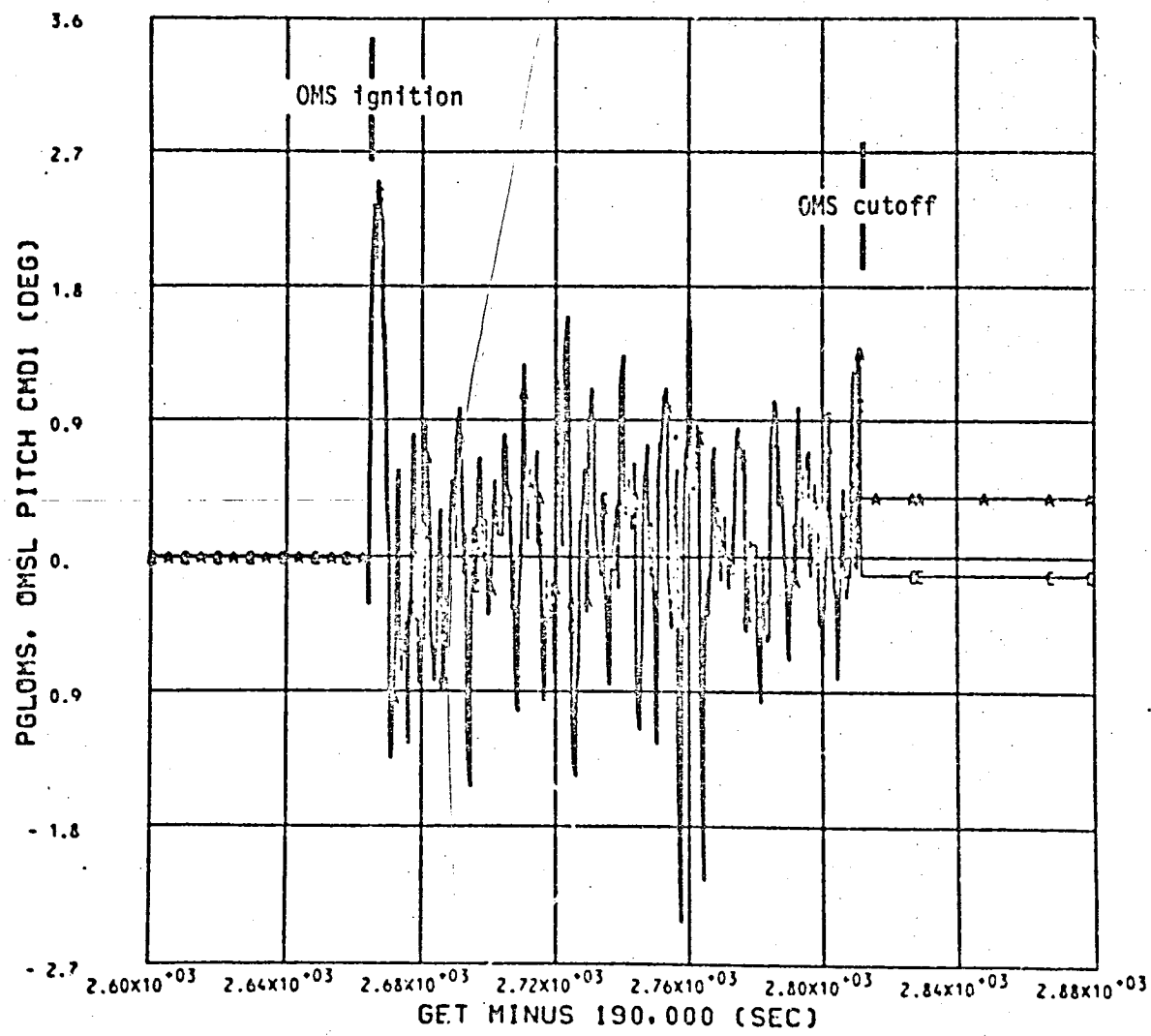


Figure 6.1-17.- Left OMS pitch actual and commanded gimbal angles - deorbit.

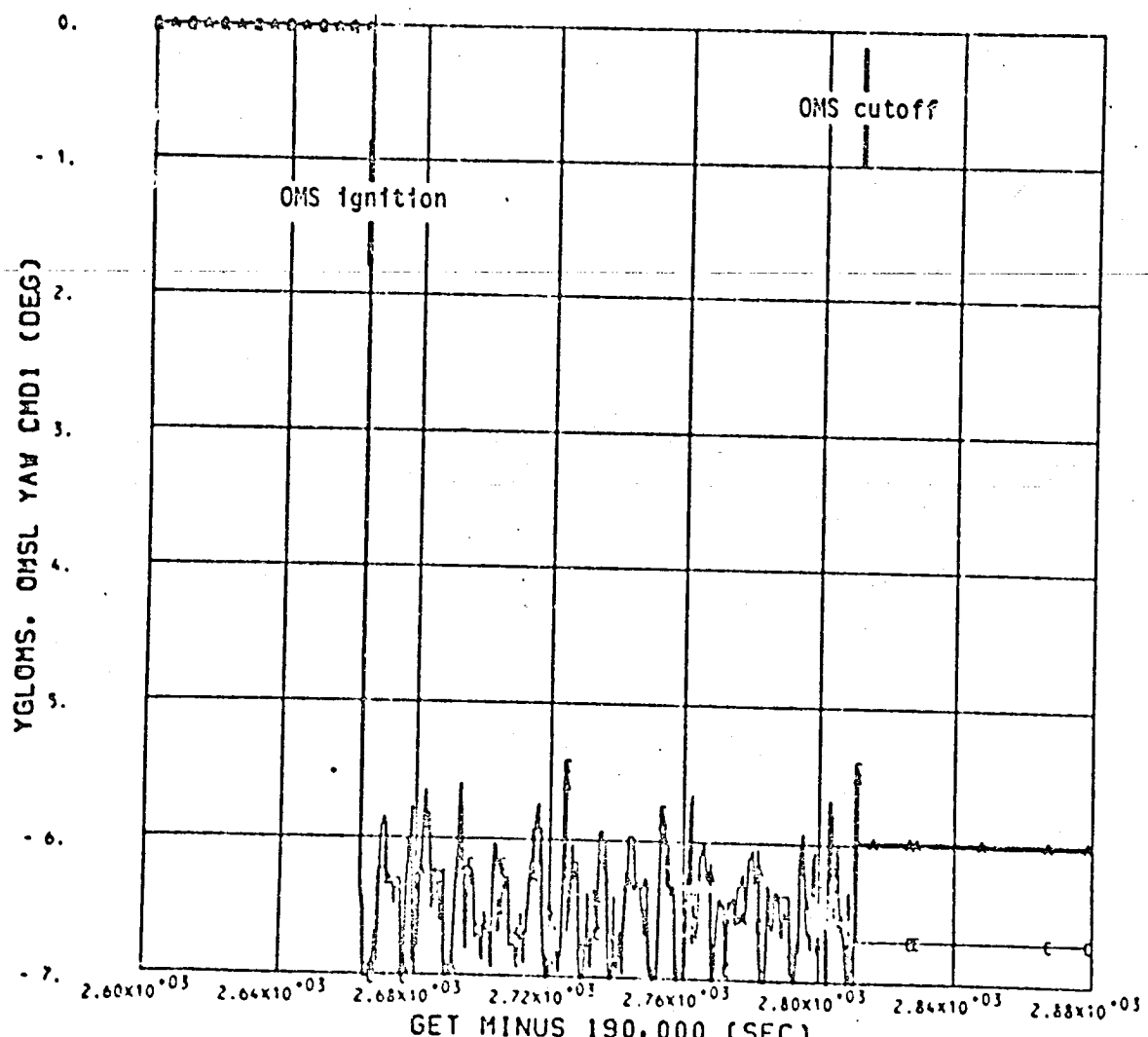


Figure 6.1-18.- Left OMS yaw actual and commanded gimbal angles - deorbit.

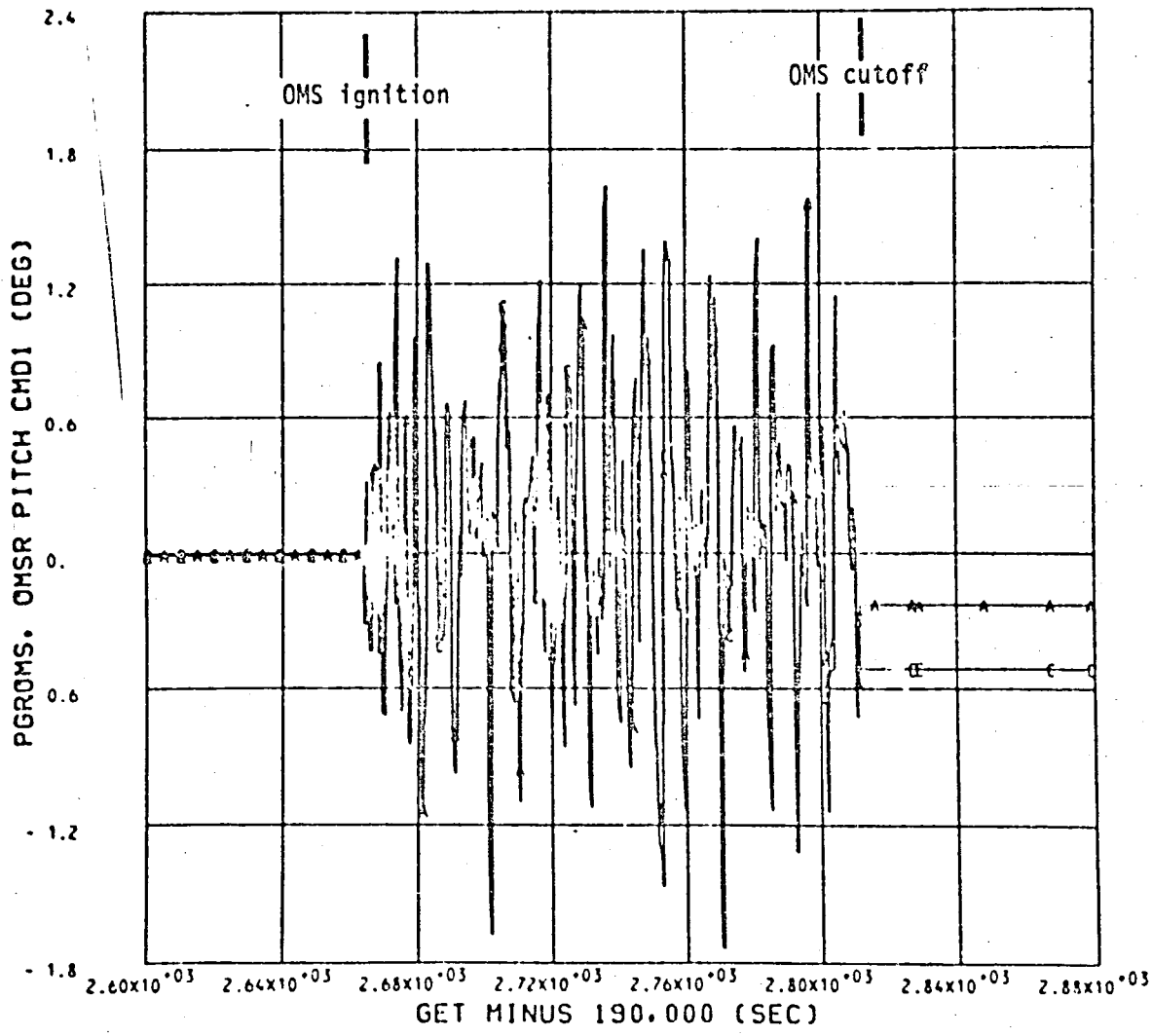


Figure 6.1-19.- Right OMS pitch actual and commanded gimbal angles - deorbit.

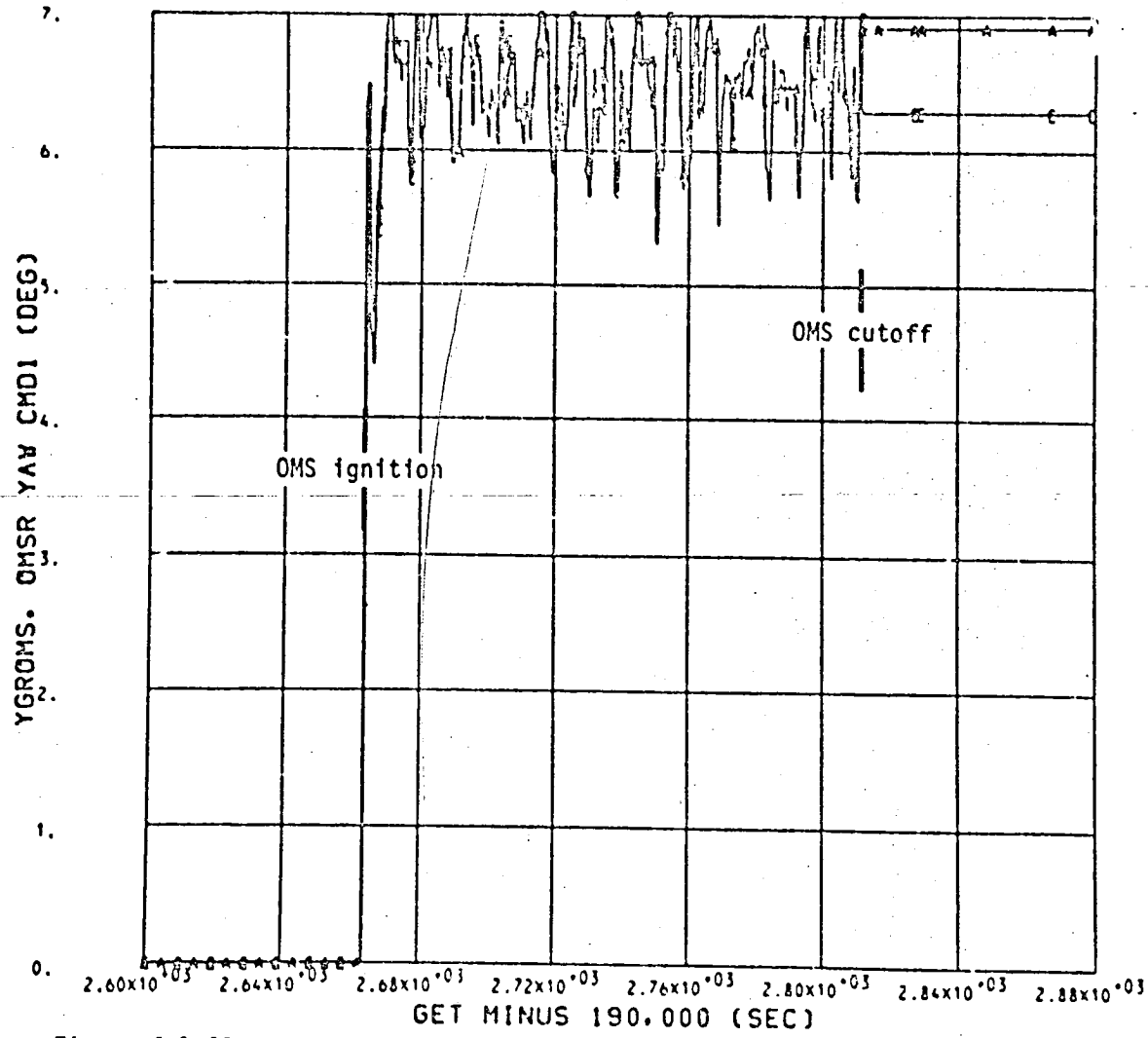


Figure 6.1-20.- Right OMSR yaw actual and commanded gimbal angles - deorbit.

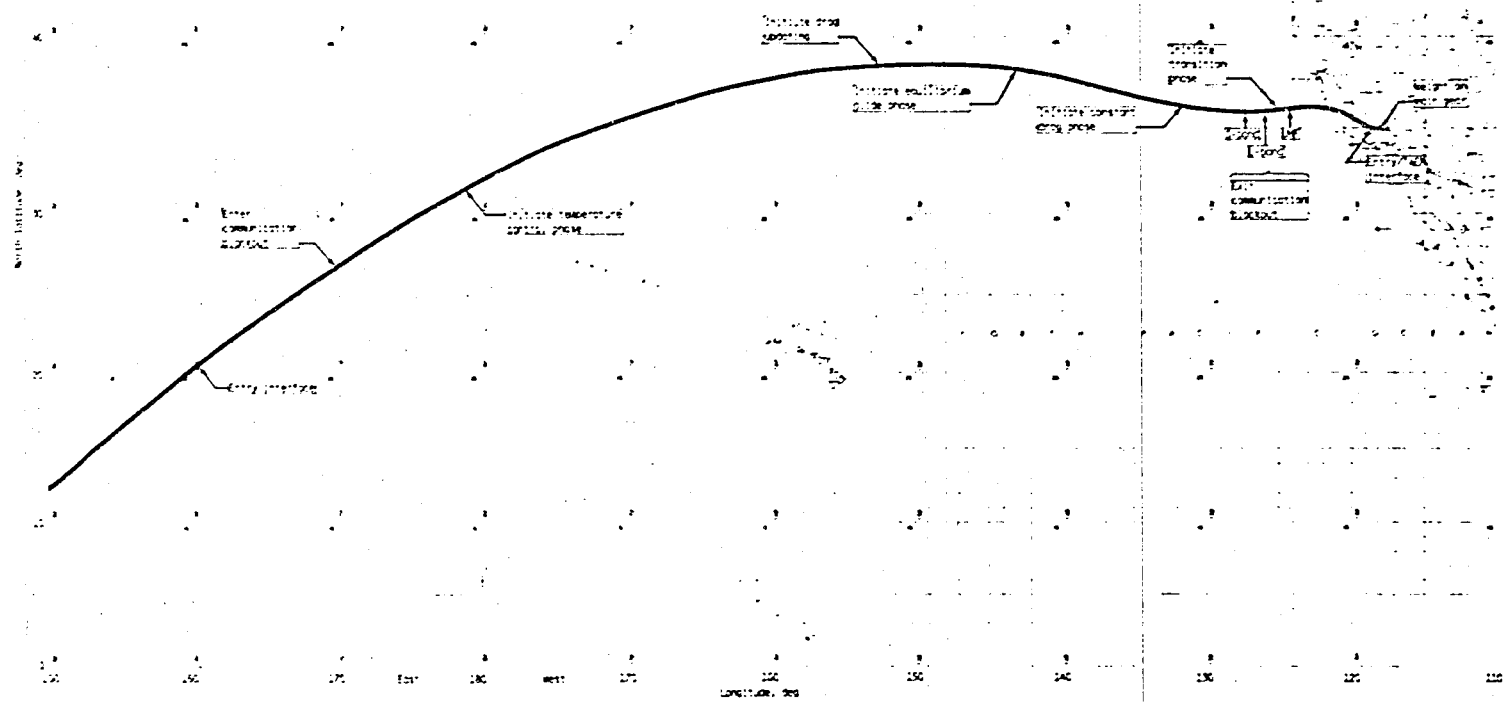
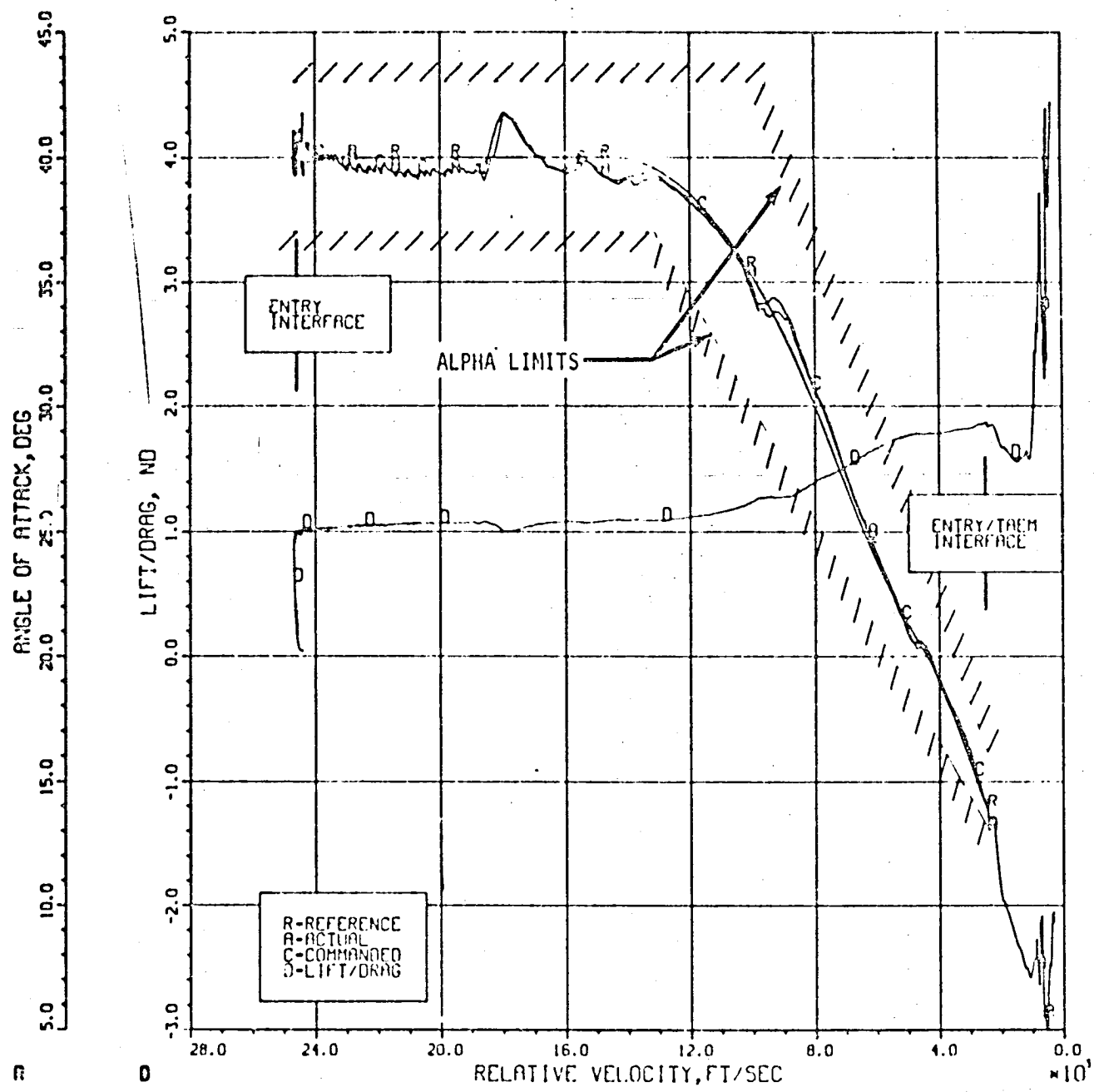


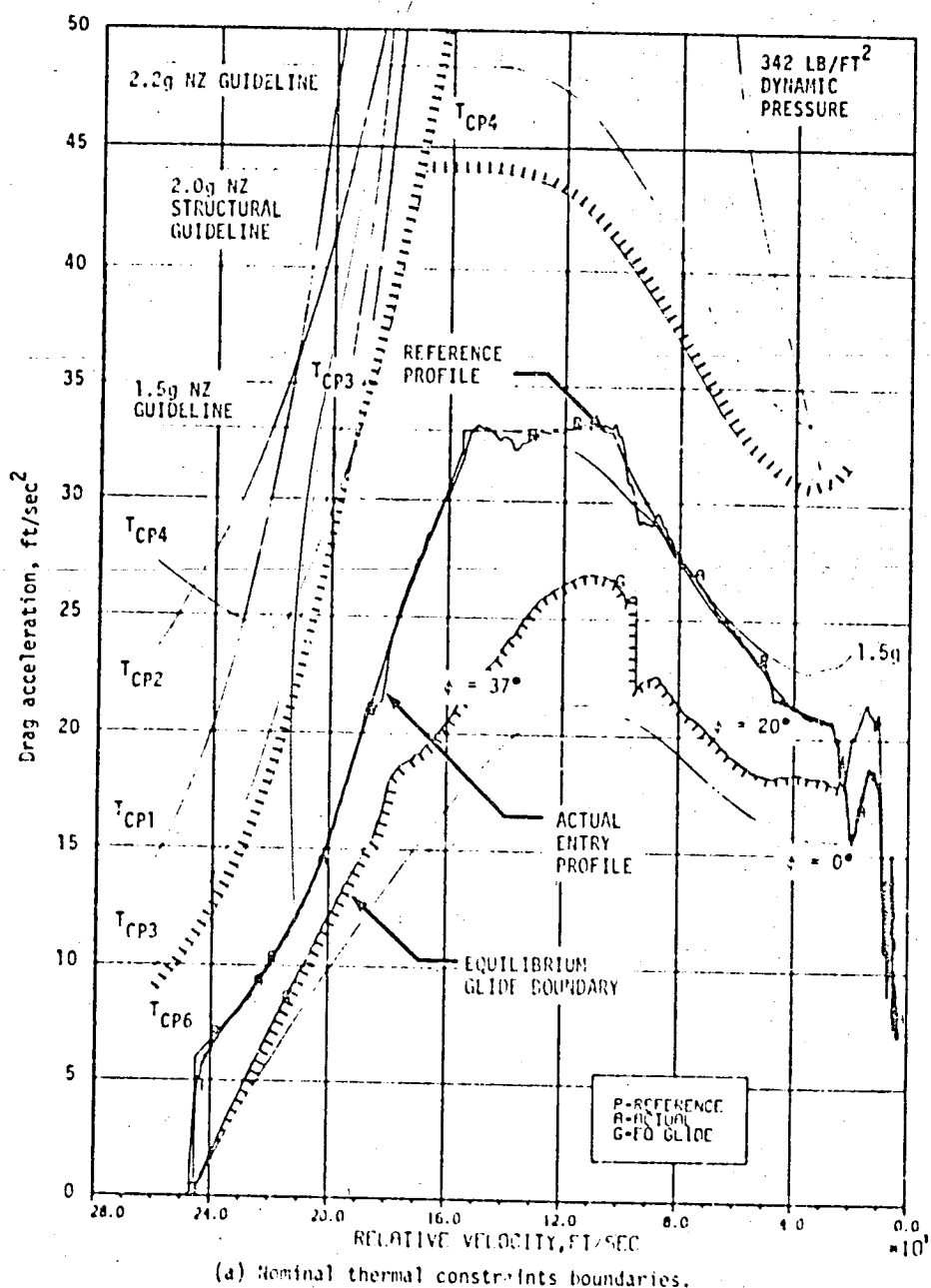
Figure 6.2.1 - Cyclic energy interaction through heating processes.

ORIGINAL PAGE IS
OF POOR QUALITY



LIFT/DRAG, REFERENCE, ACTUAL AND COMMANDED ANGLE OF ATTACK DURING ATMOSPHERIC DESCENT

Figure 6.2-2



(a) Nominal thermal constraints boundaries.

Figure 6.2-3 - Entry drag acceleration corridor.

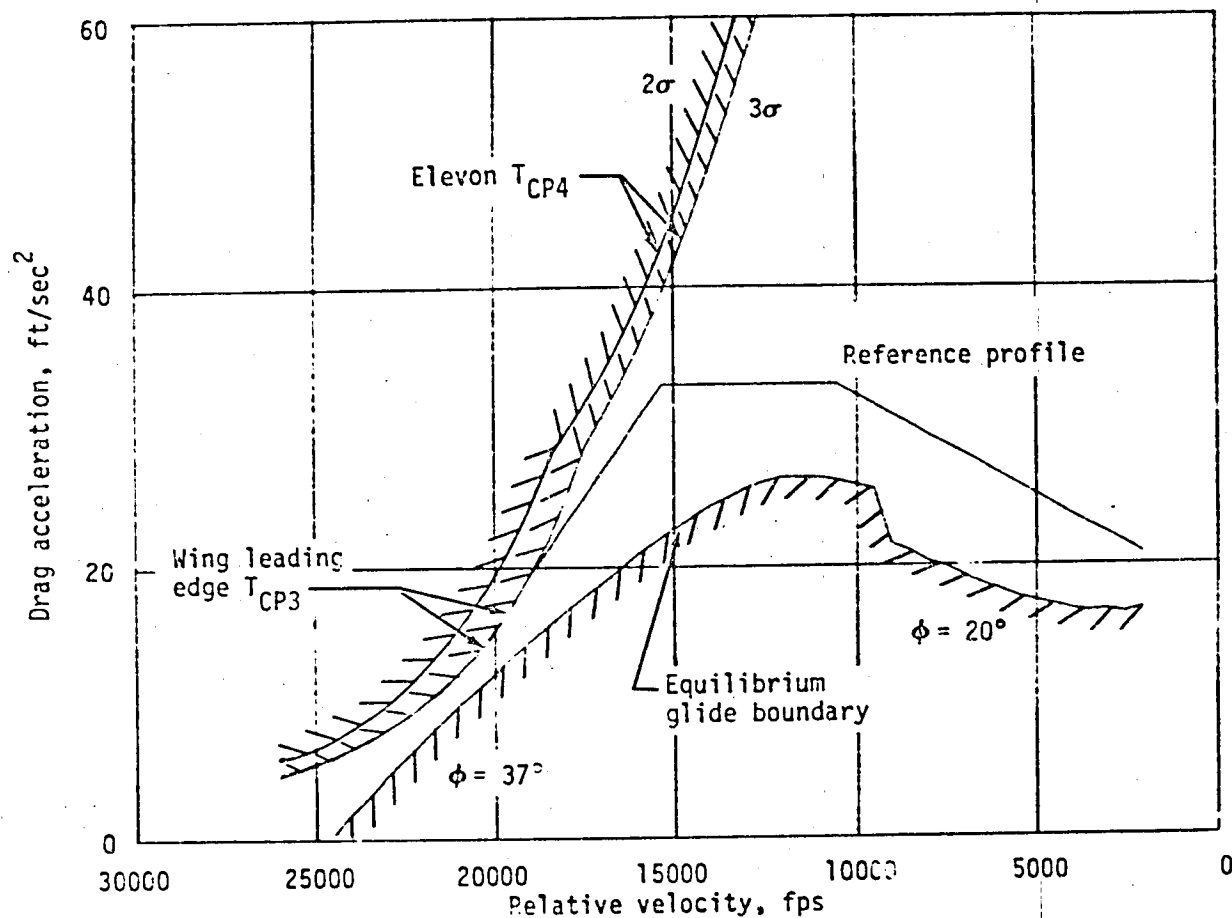
(b) Two- and three- σ thermal constraint boundaries.

Figure 6.2-3.- Concluded.

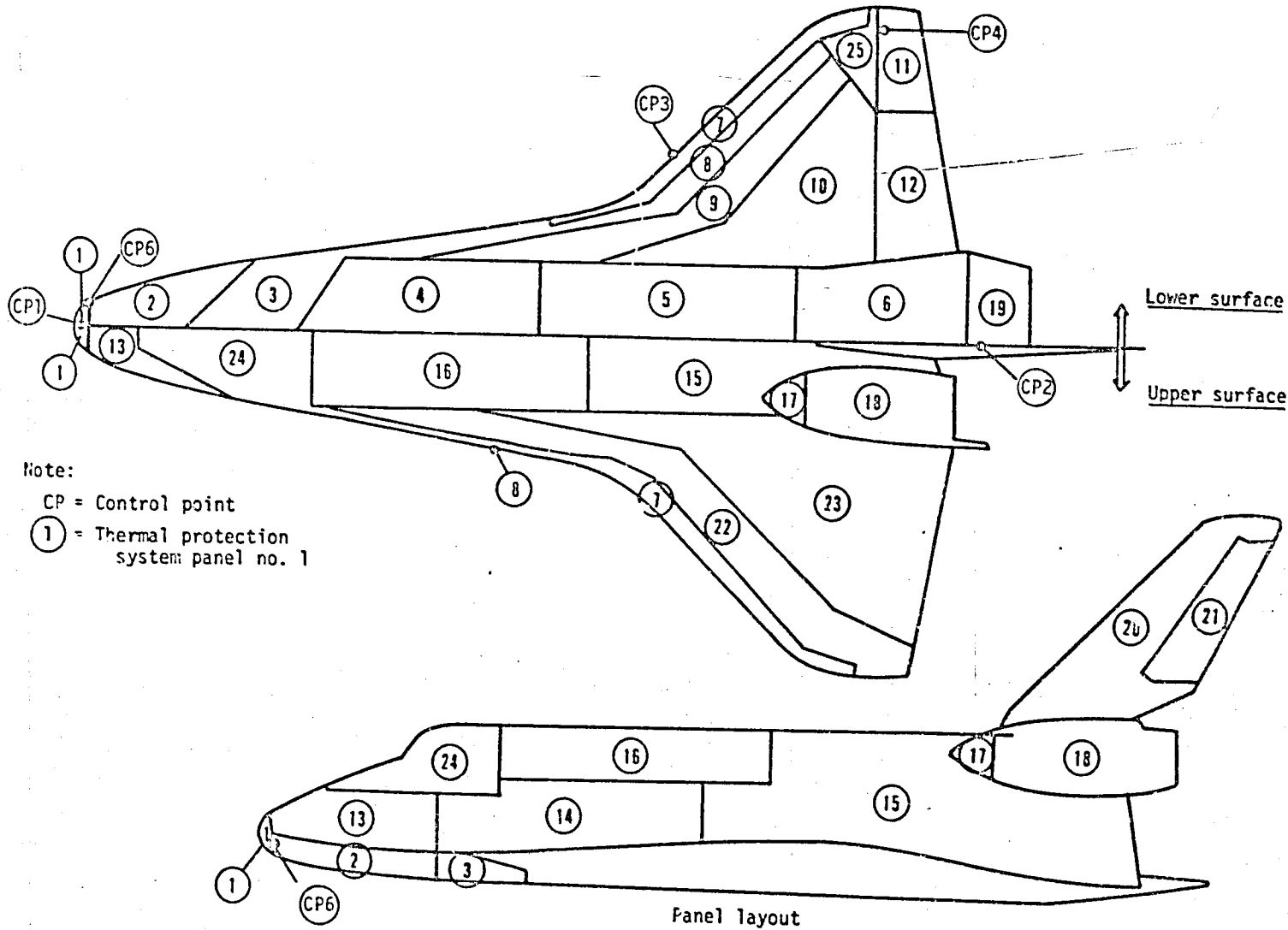
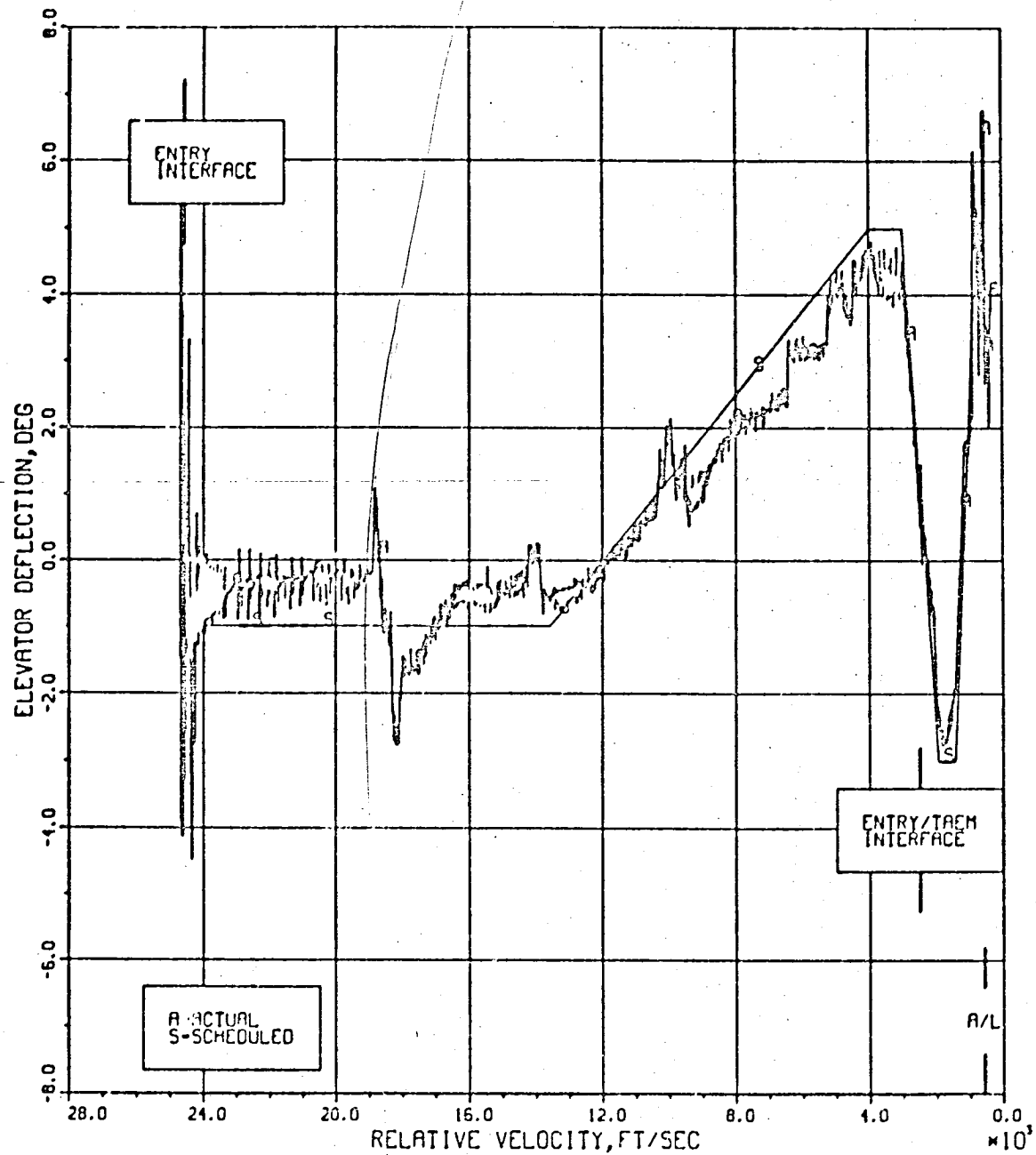


Figure 6.2-4.- Surface-temperature control points and panel locations.



SCHEDULED AND ACTUAL ELEVATOR DEFLECTION
DURING ATMOSPHERIC DESCENT

Figure 6.2-6

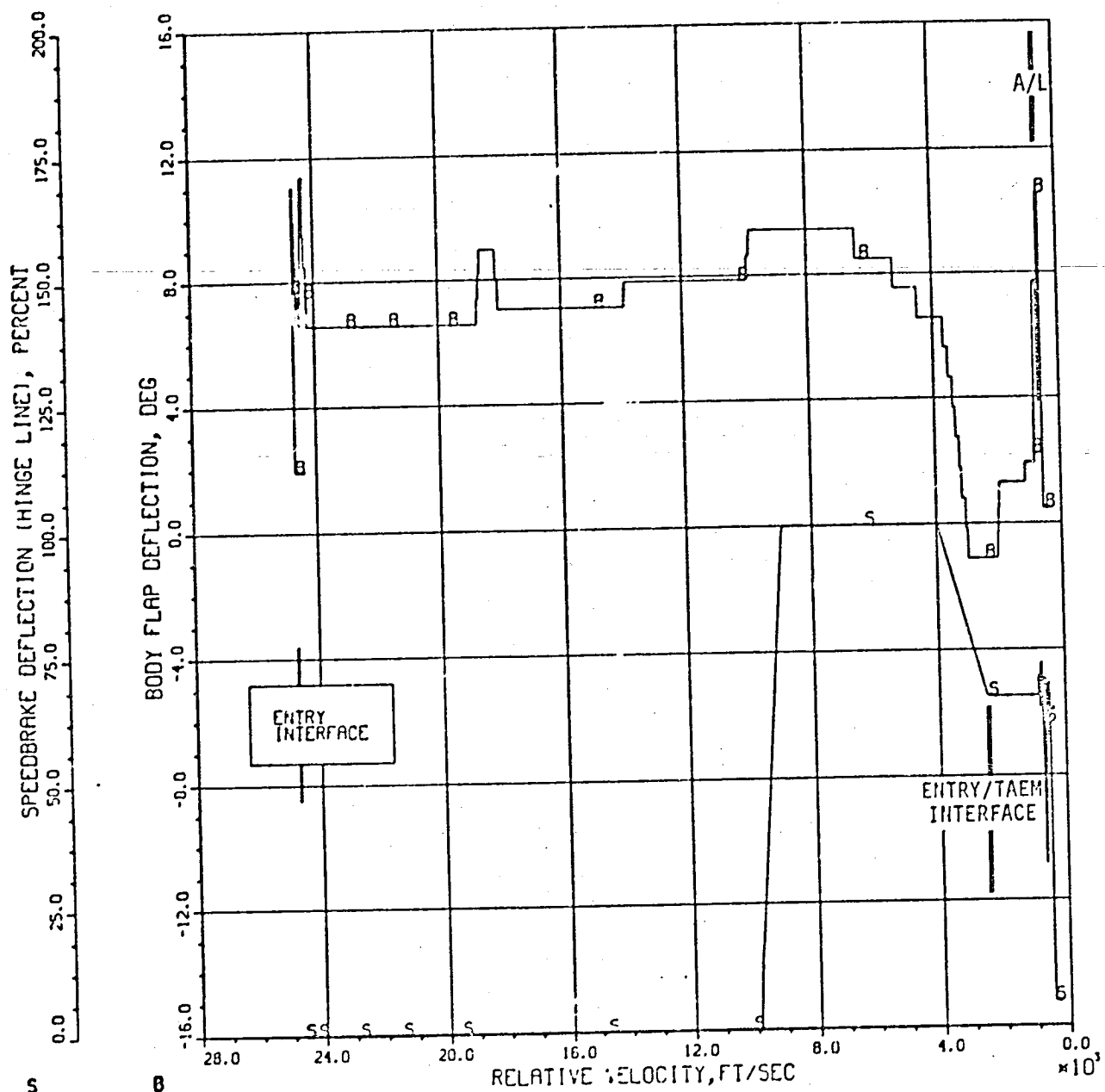
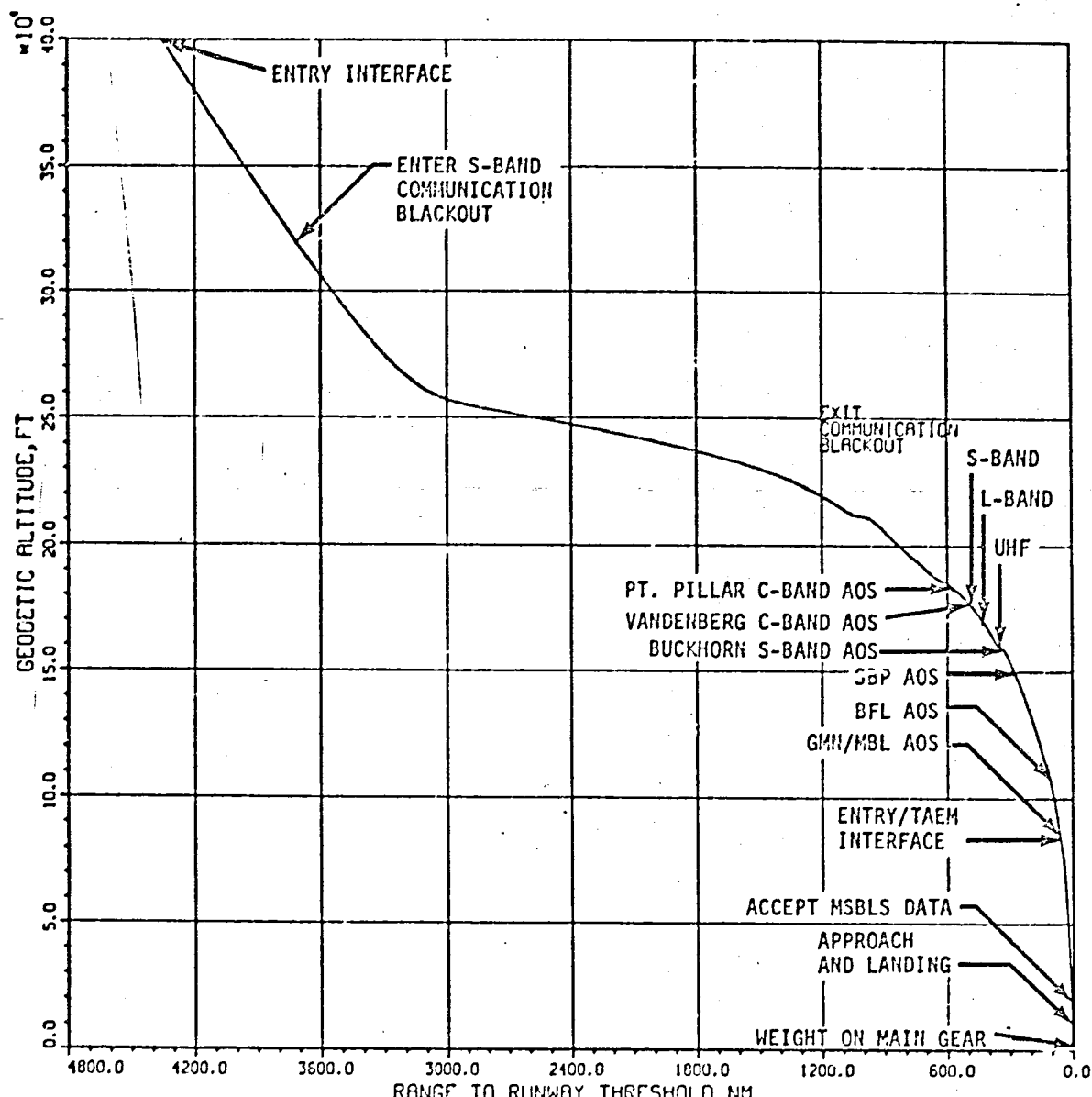
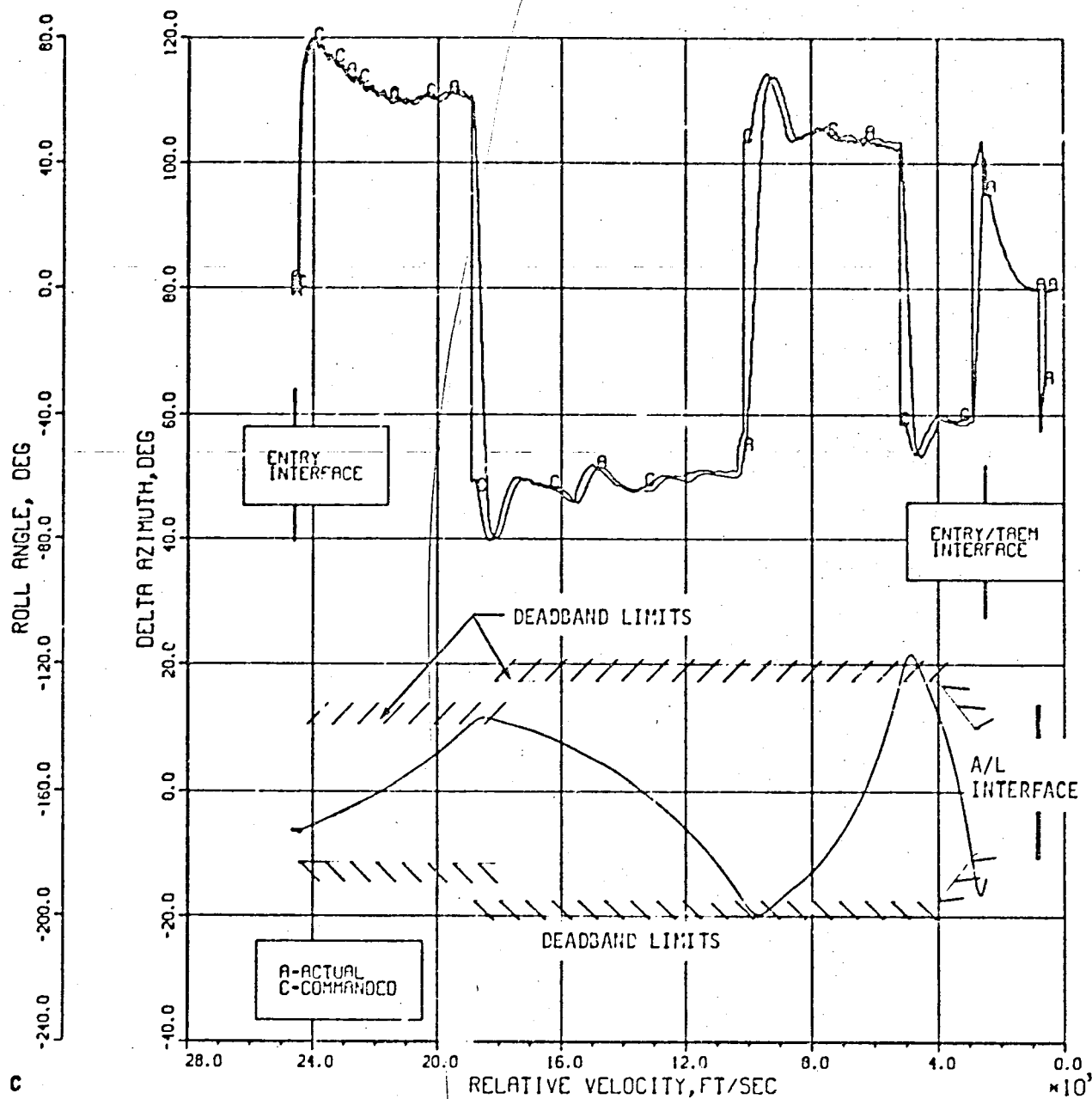


Figure 6.2-6



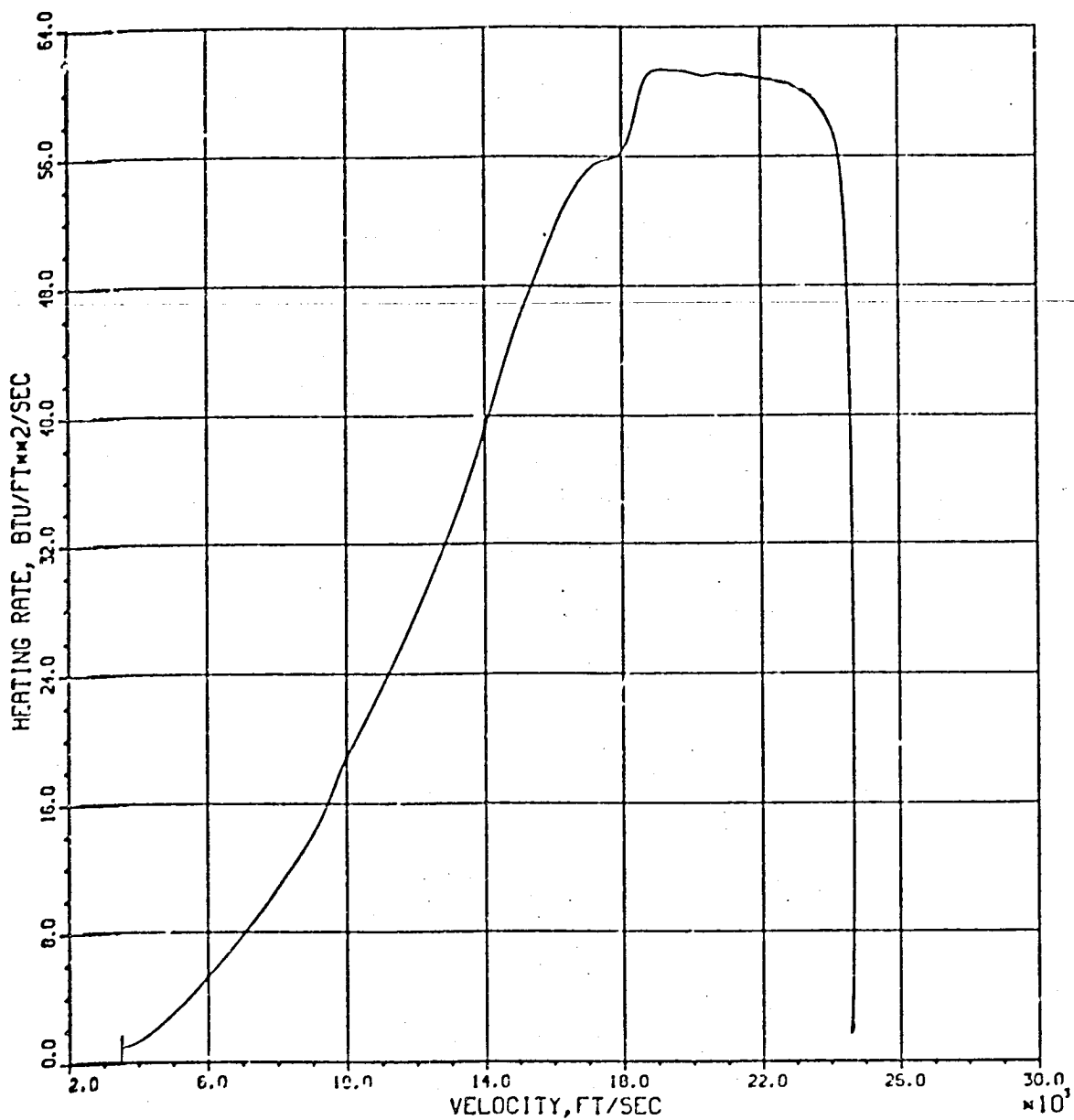
GEODETIC ALTITUDE VS. RANGE TO RUNWAY THRESHOLD

Figure 6.2-7



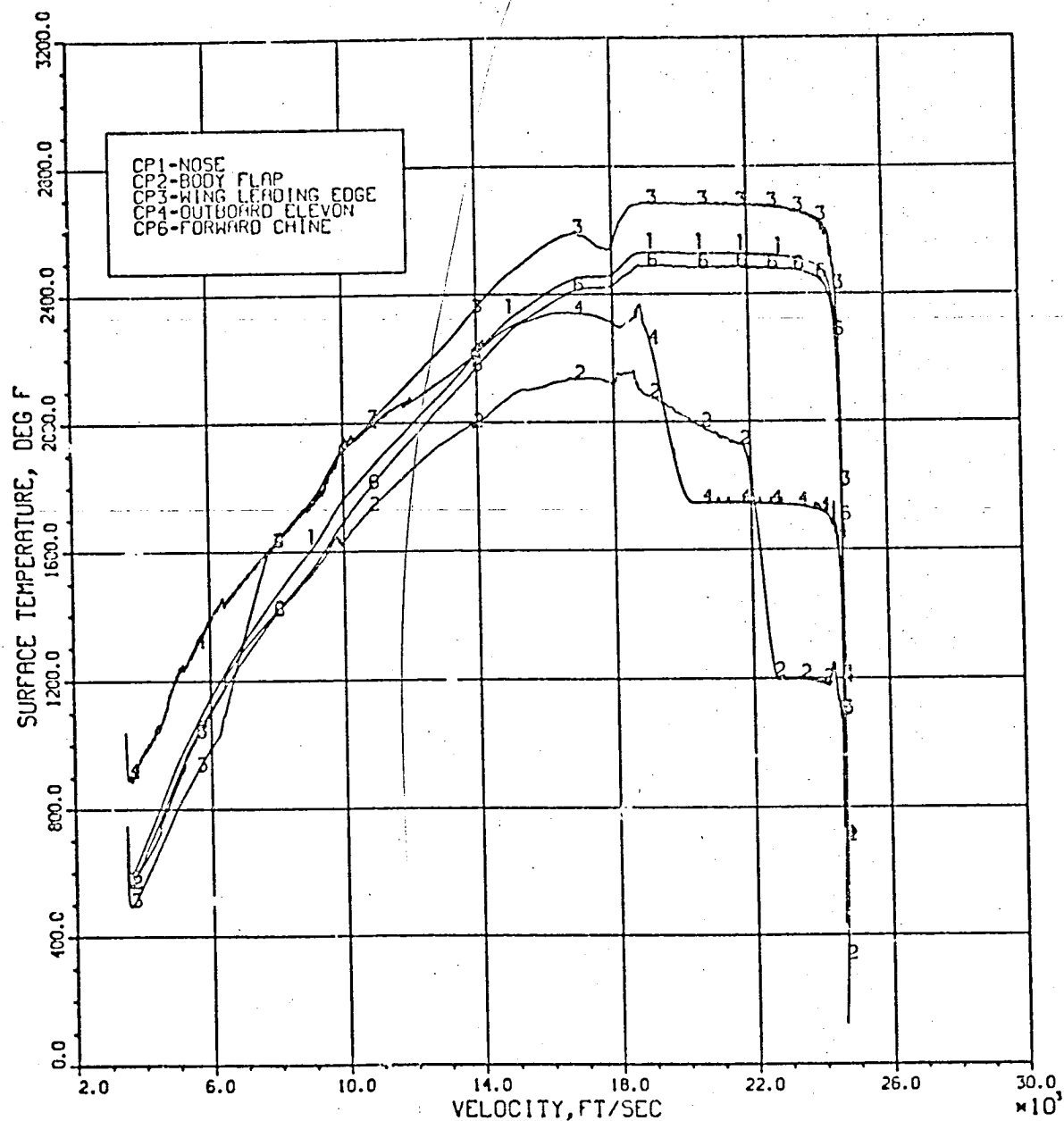
DELTA AZIMUTH, ACTUAL AND COMMANDED
ROLL ANGLES DURING ATMOSPHERIC DESCENT

Figure 6.2-8



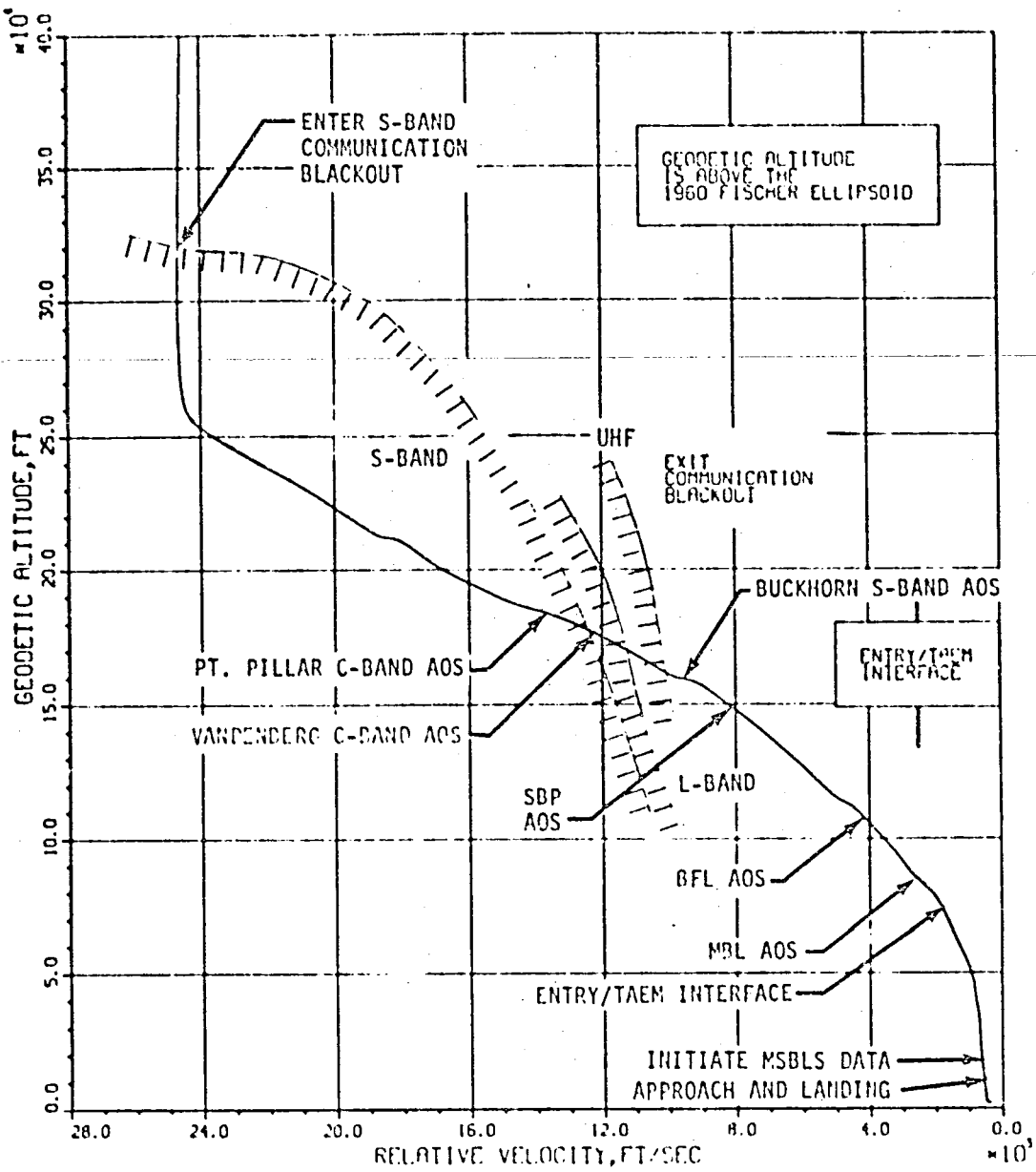
REFERENCE HEATING RATE VS. RELATIVE
VELOCITY FROM ENTRY INTERFACE

Figure 6.2-9



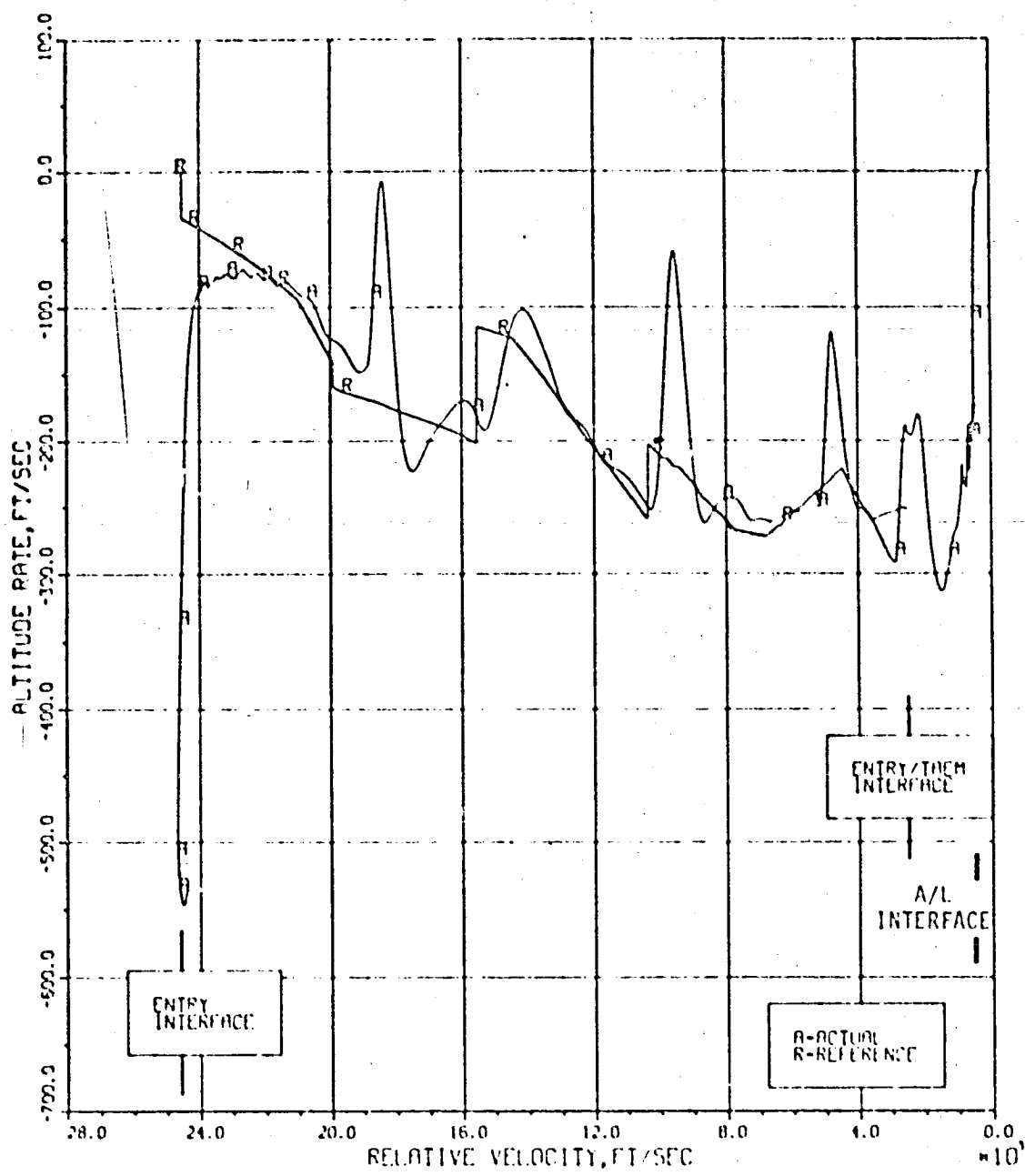
CONTROL POINT TEMPERATURES VS. RELATIVE VELOCITY FROM ENTRY INTERFACE

Figure 6.2-10



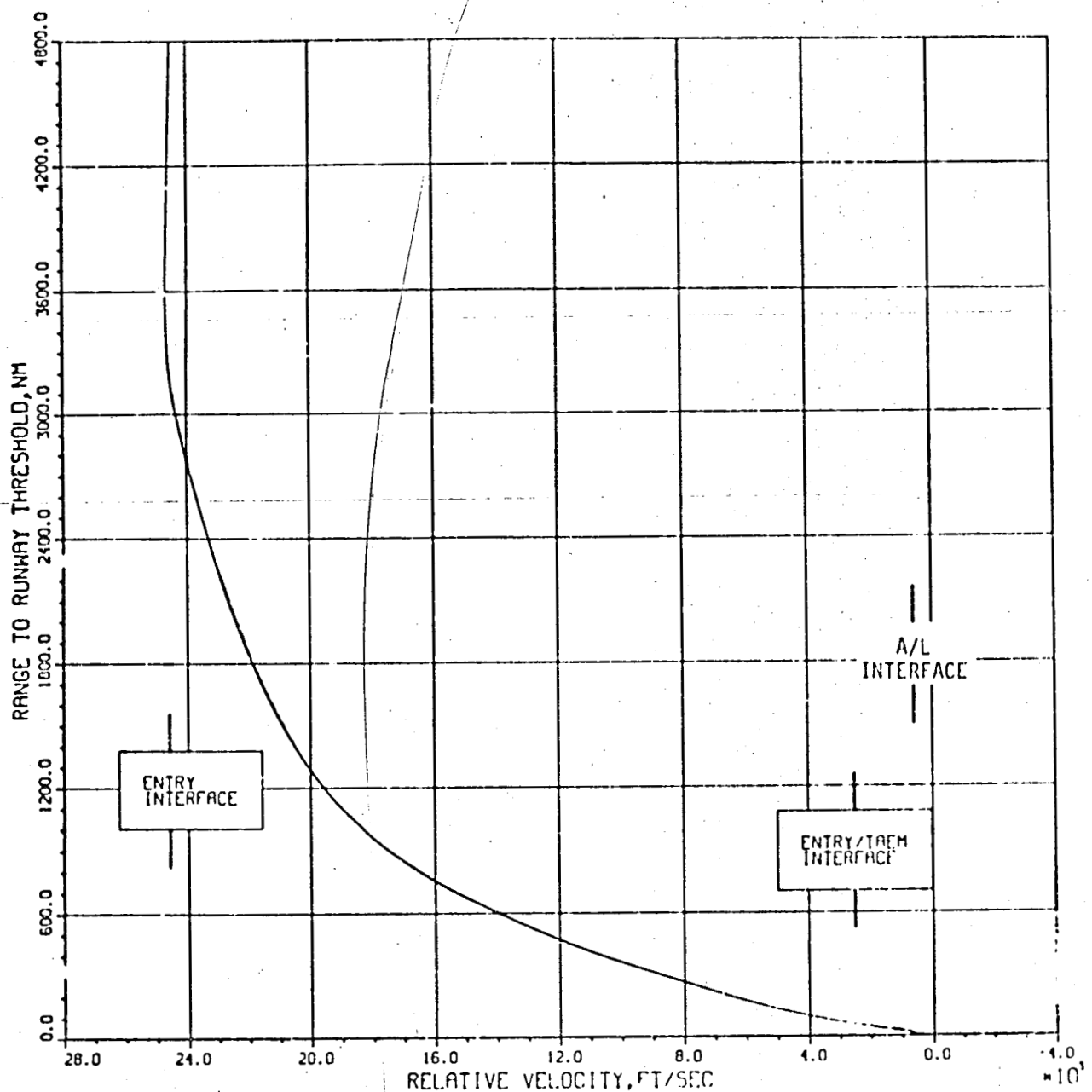
GEODETIC ALTITUDE DURING ATMOSPHERIC DESCENT

Figure 6.2-11



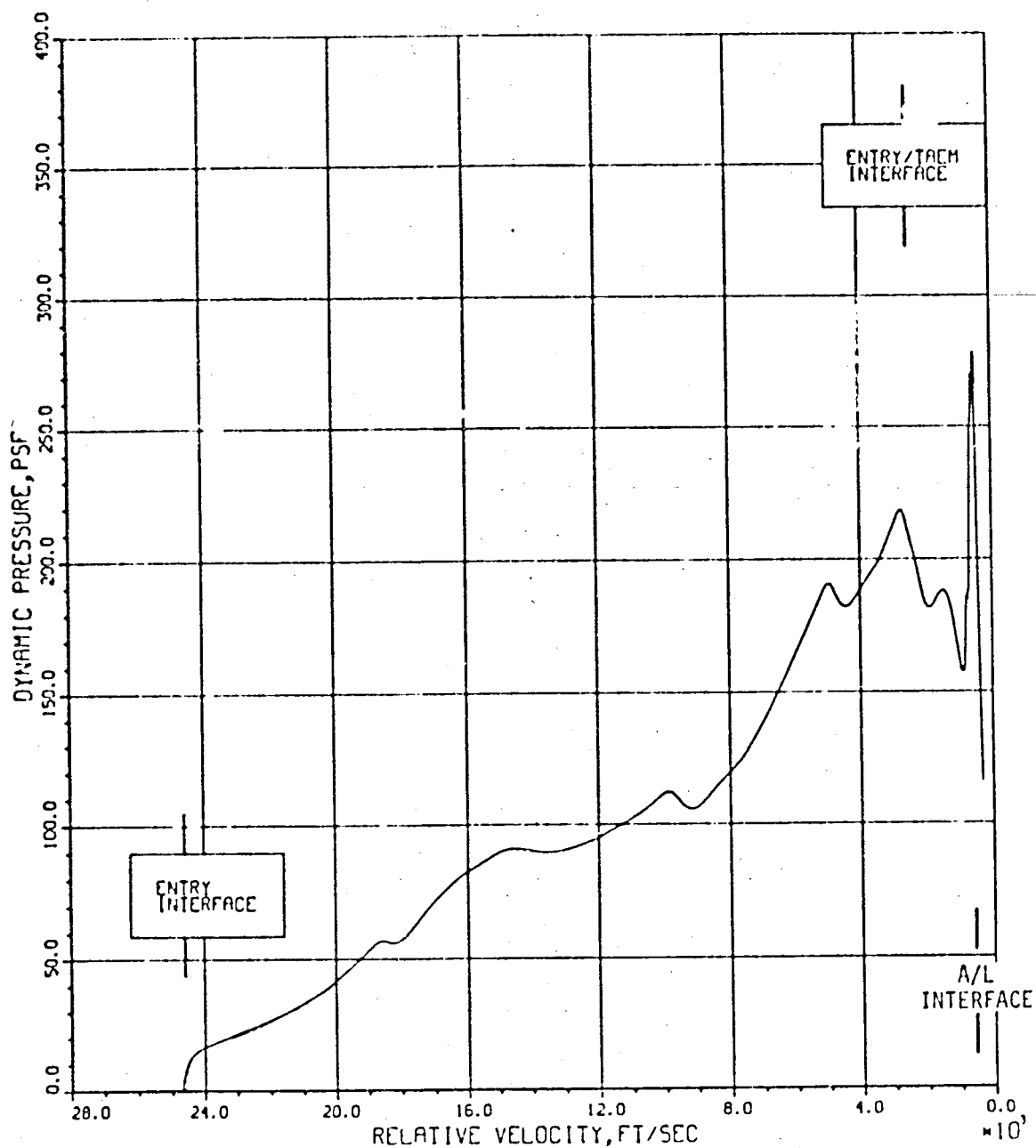
ACTUAL AND REFERENCE ALTITUDE RATE DURING ATMOSPHERIC DESCENT

Figure 6.2-12



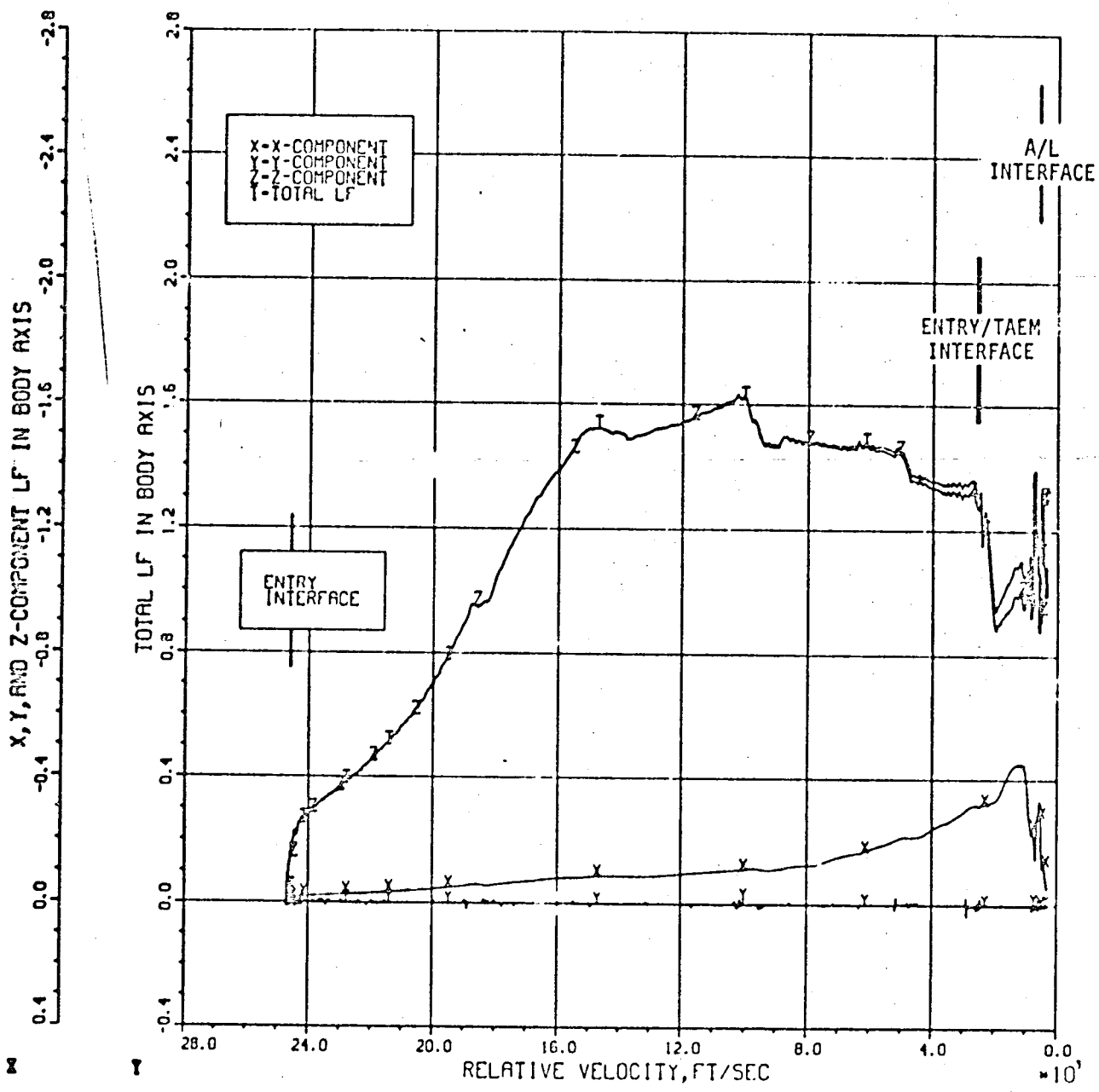
RANGE TO RUNWAY THRESHOLD
DURING ATMOSPHERIC DESCENT

Figure 6.2-13



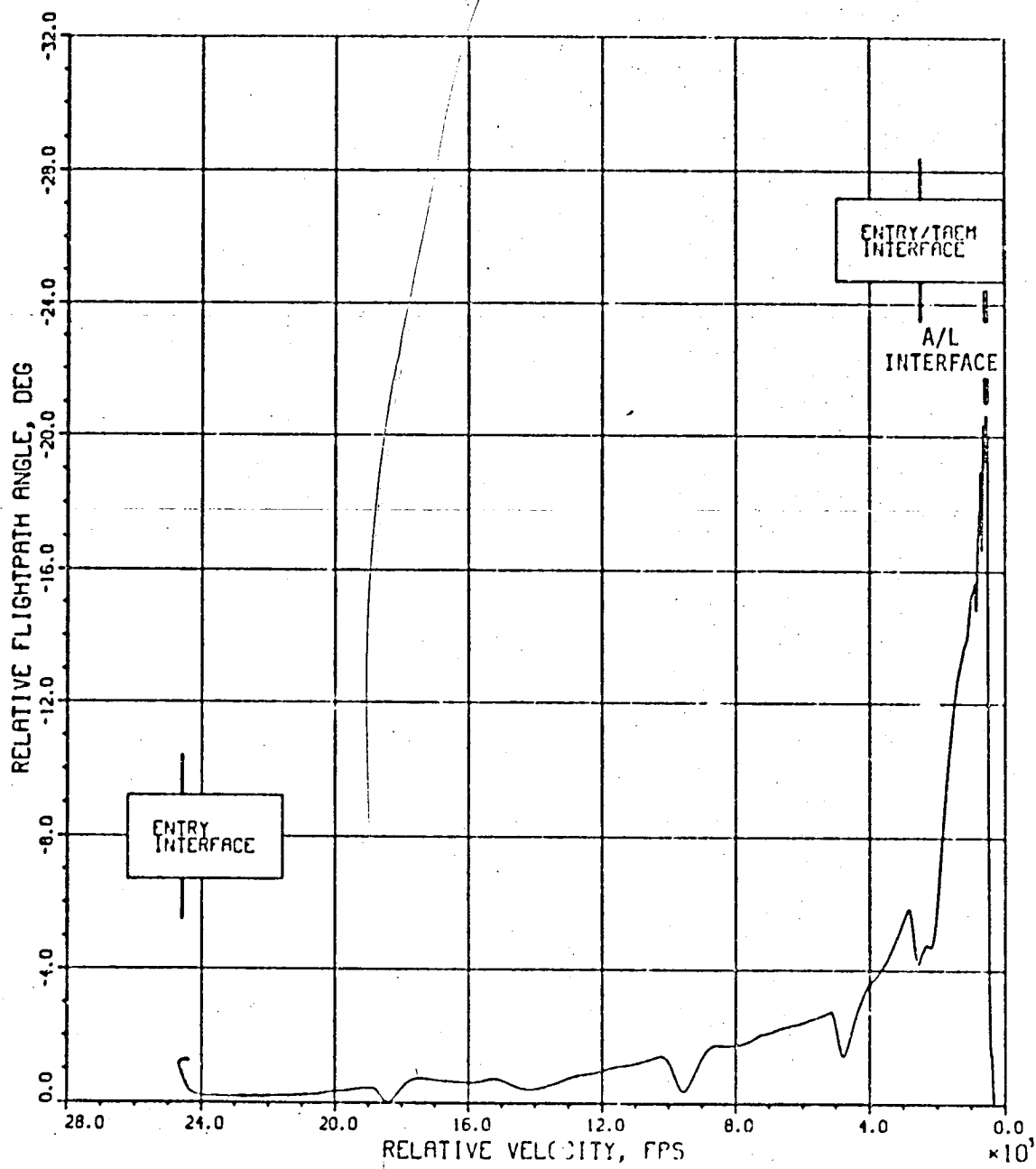
DYNAMIC PRESSURE DURING ATMOSPHERIC DESCENT

Figure 6.2-14



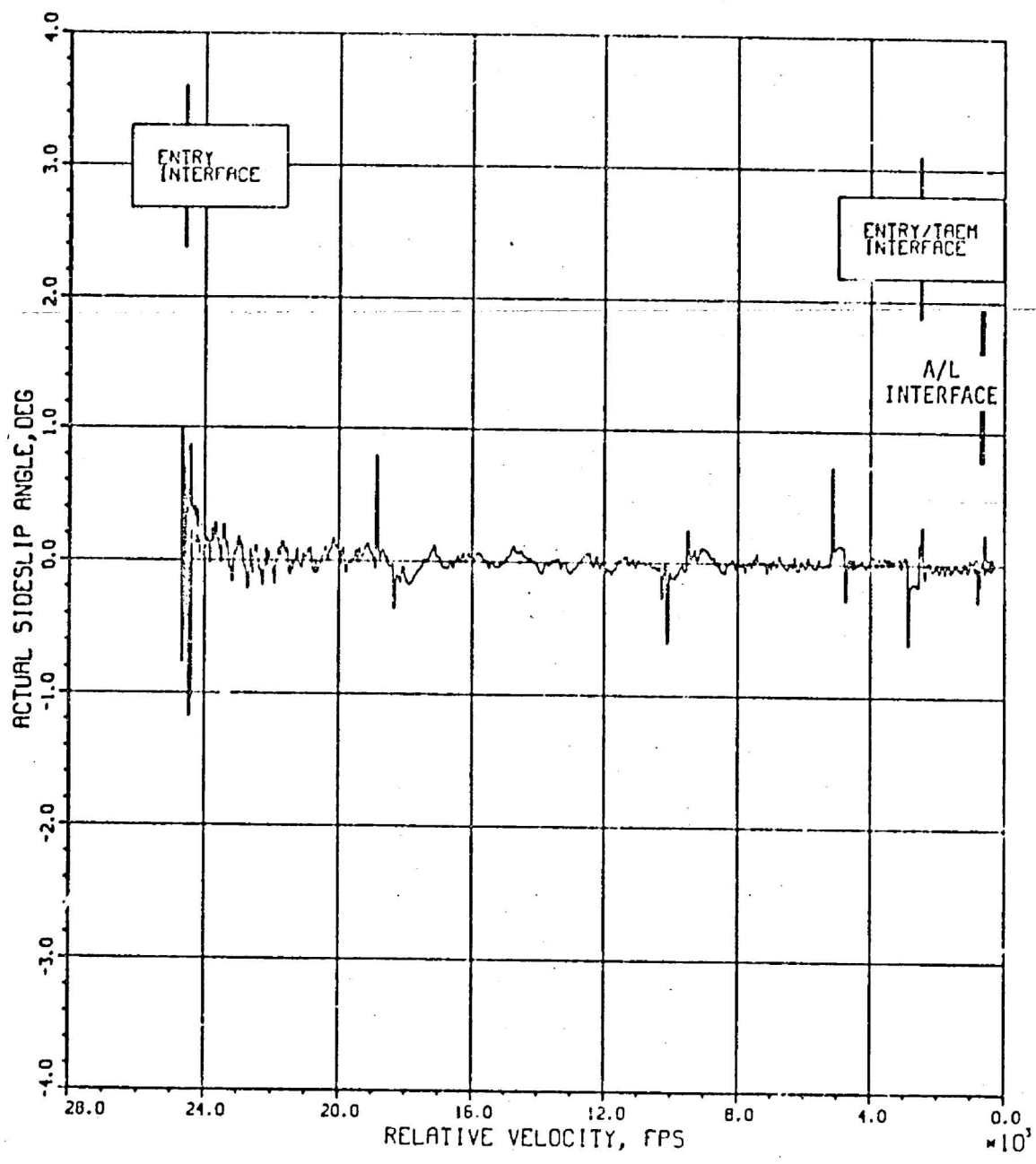
X, Y, AND Z-BODY AXIS AND TOTAL LOAD FACTOR DURING ATMOSPHERIC DESCENT

Figure 6.2-15



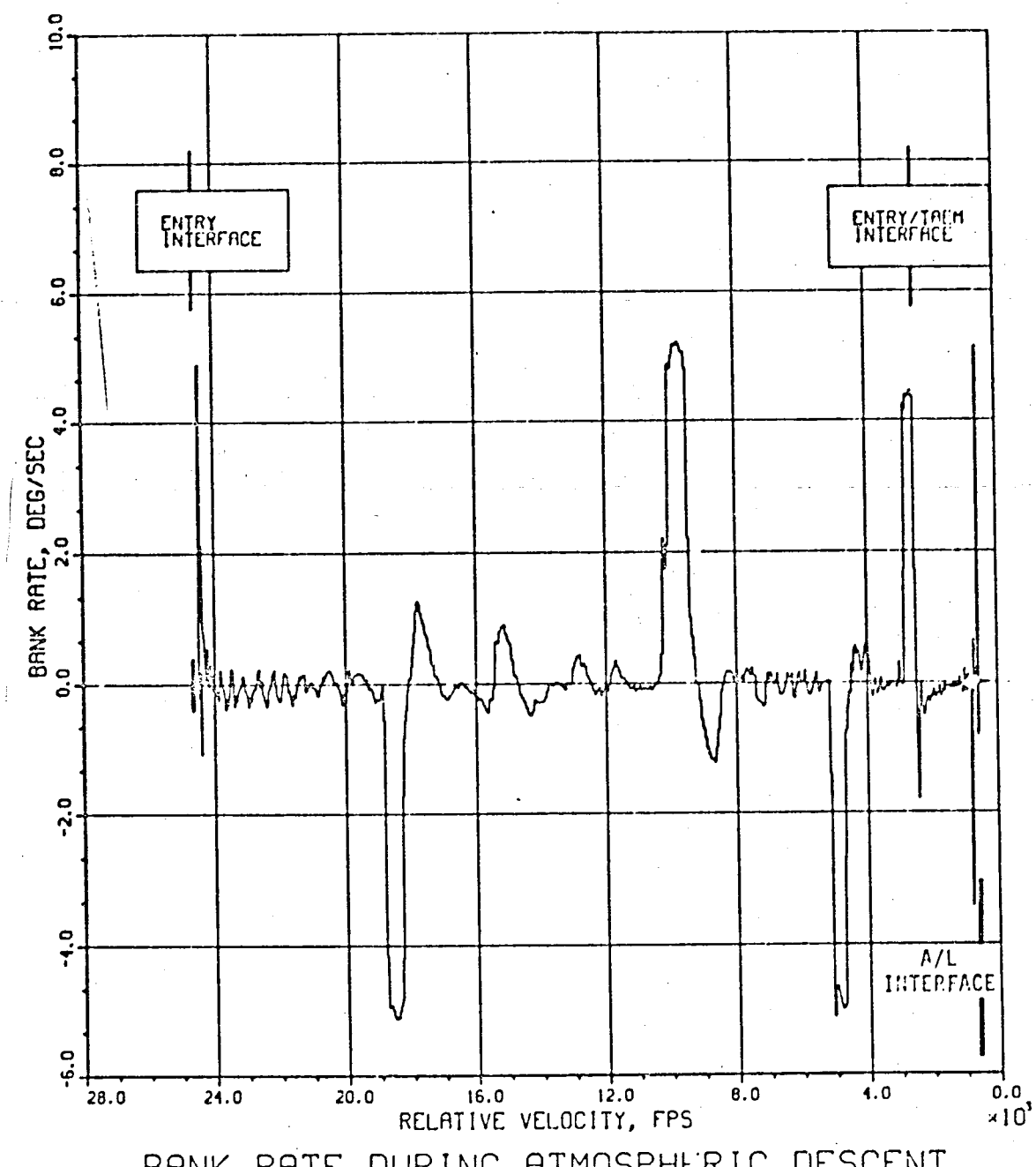
RELATIVE FLIGHTPATH ANGLE
DURING ATMOSPHERIC DESCENT

Figure 6.2-16



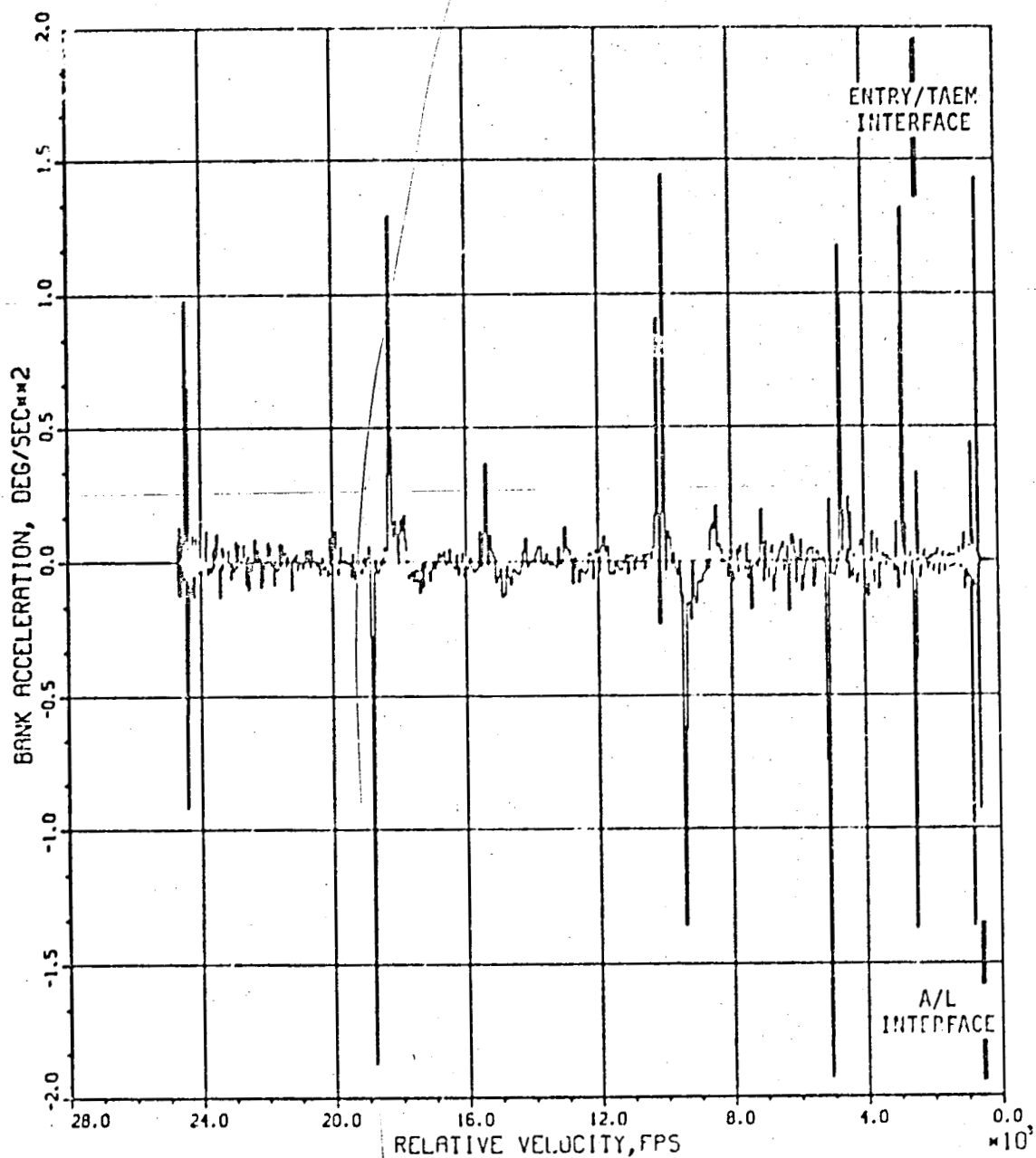
ACTUAL SIDESLIP ANGLE
DURING ATMOSPHERIC DESCENT

Figure 6.2-17



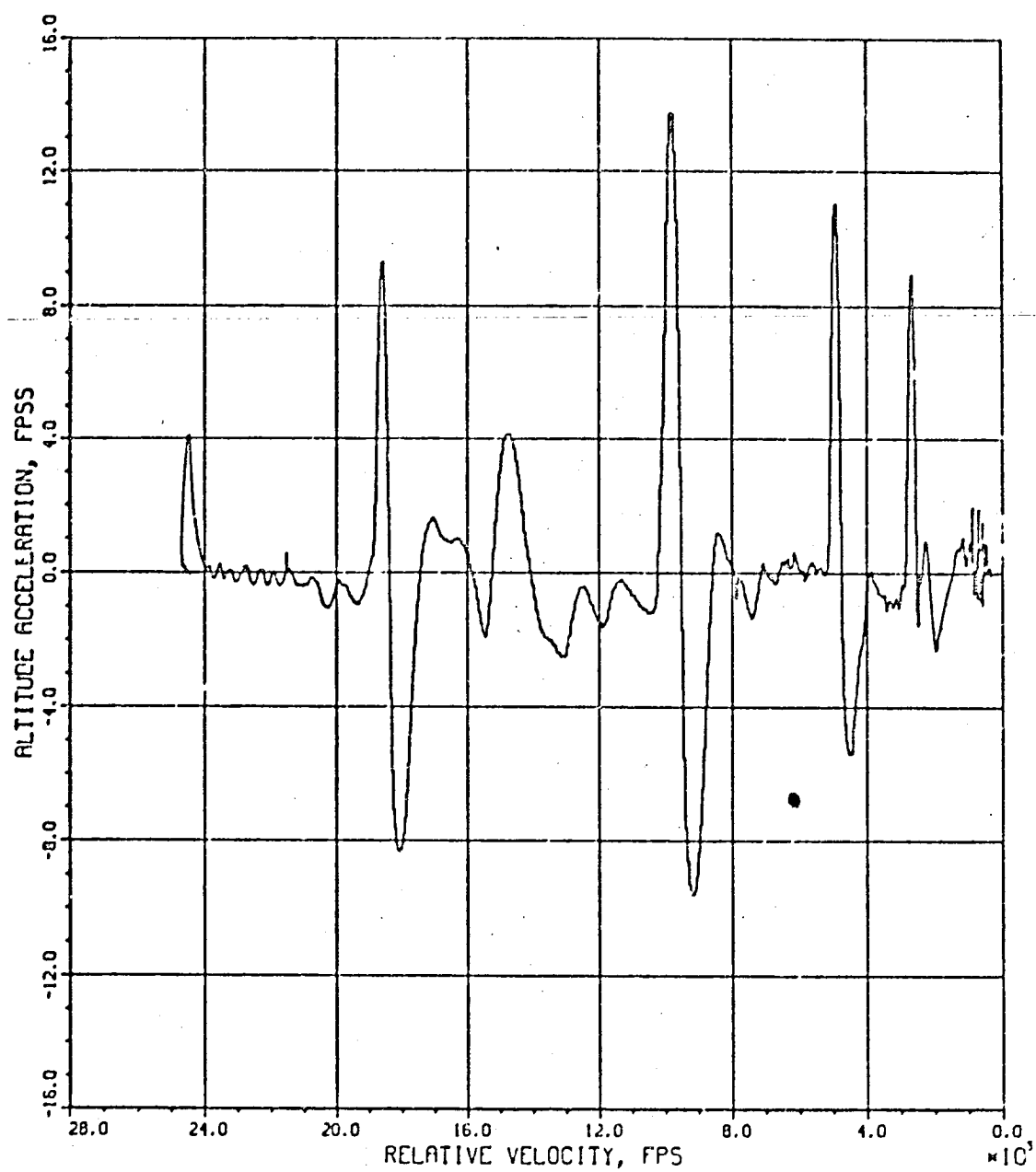
BANK RATE DURING ATMOSPHERIC DESCENT

Figure 6.2-18



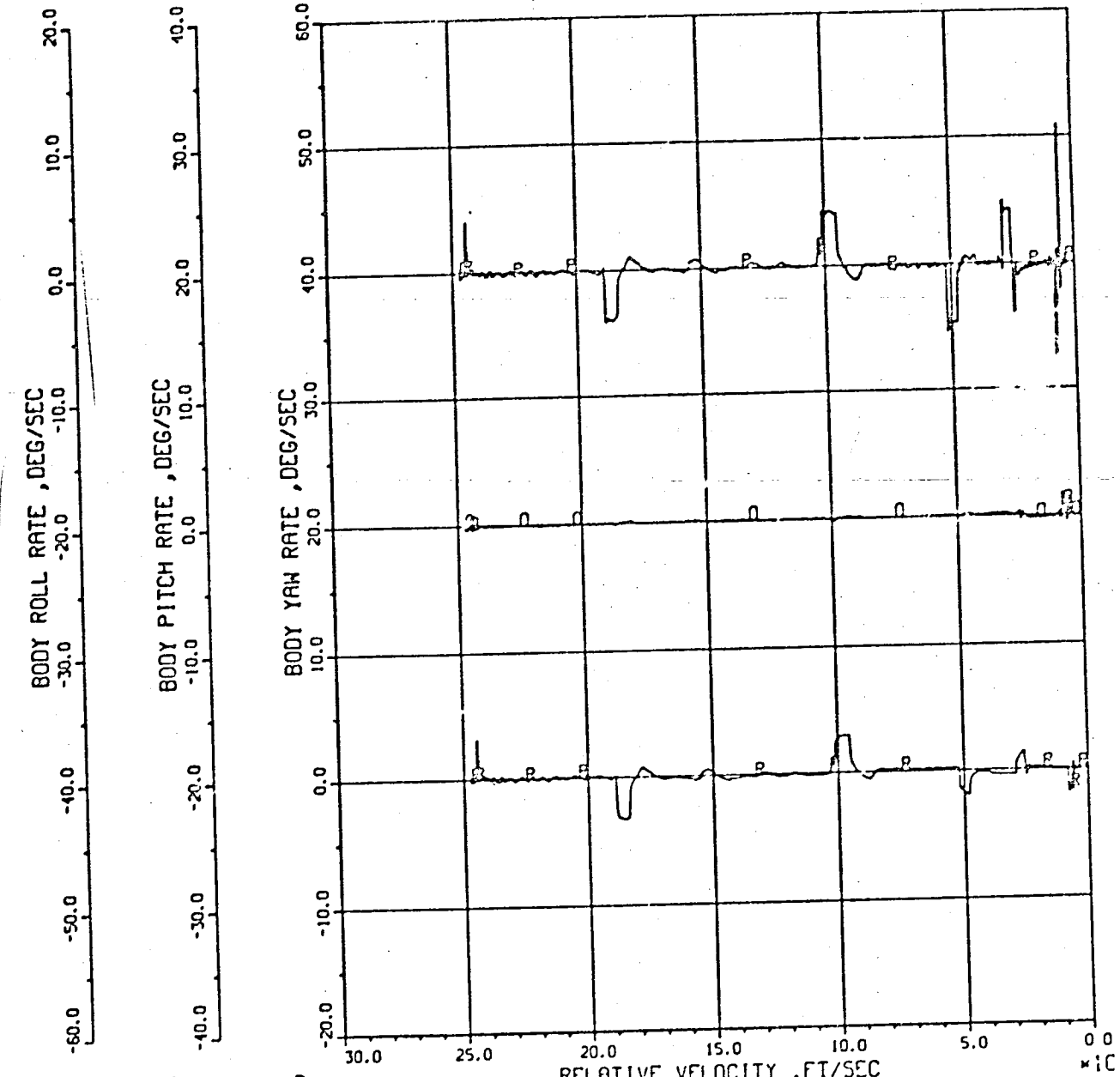
BANK ACCELERATION DURING ATMOSPHERIC DESCENT

Figure 6.2-19



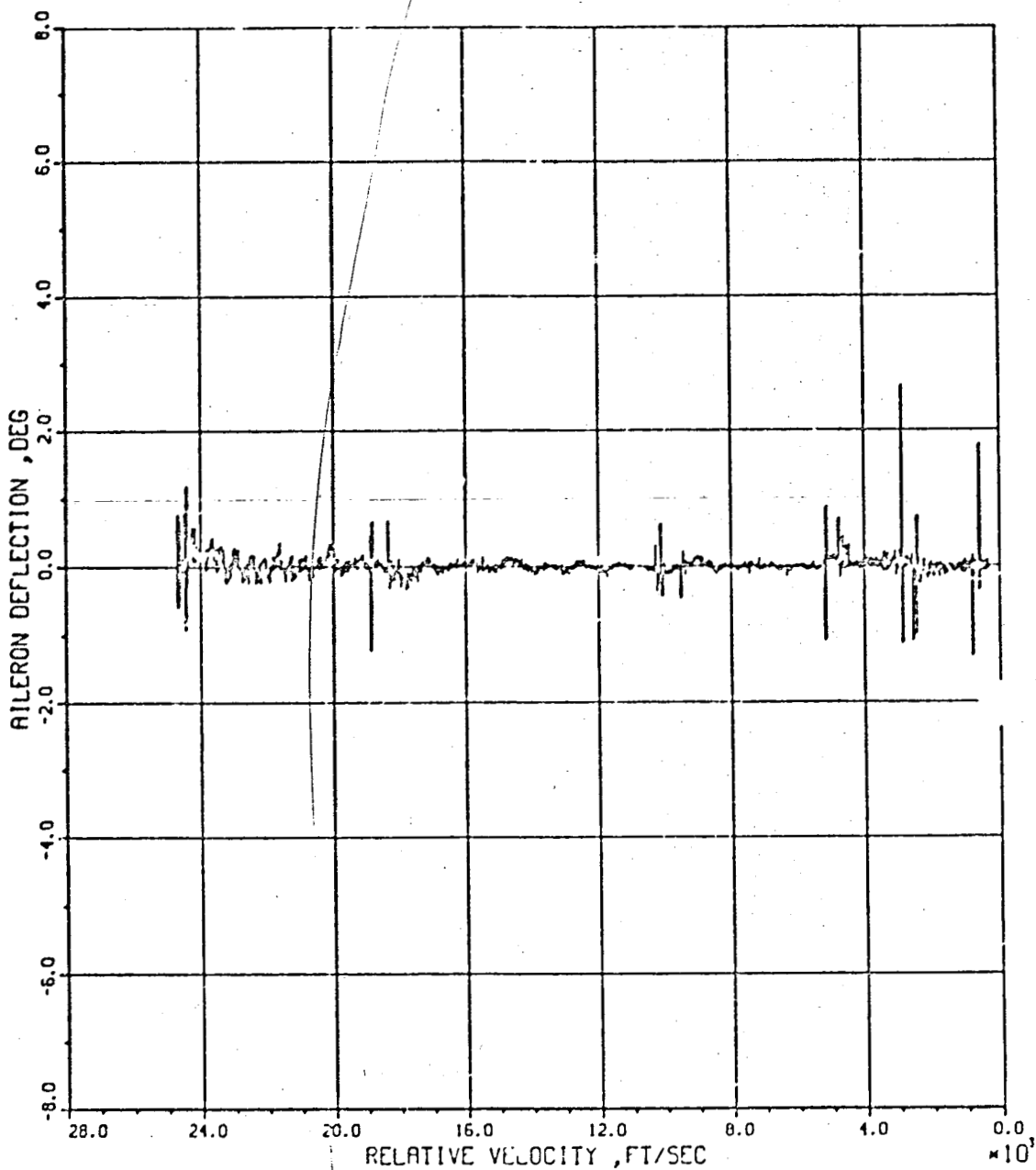
ALTITUDE ACCELERATION
DURING ATMOSPHERIC DESCENT

Figure 6.2-20



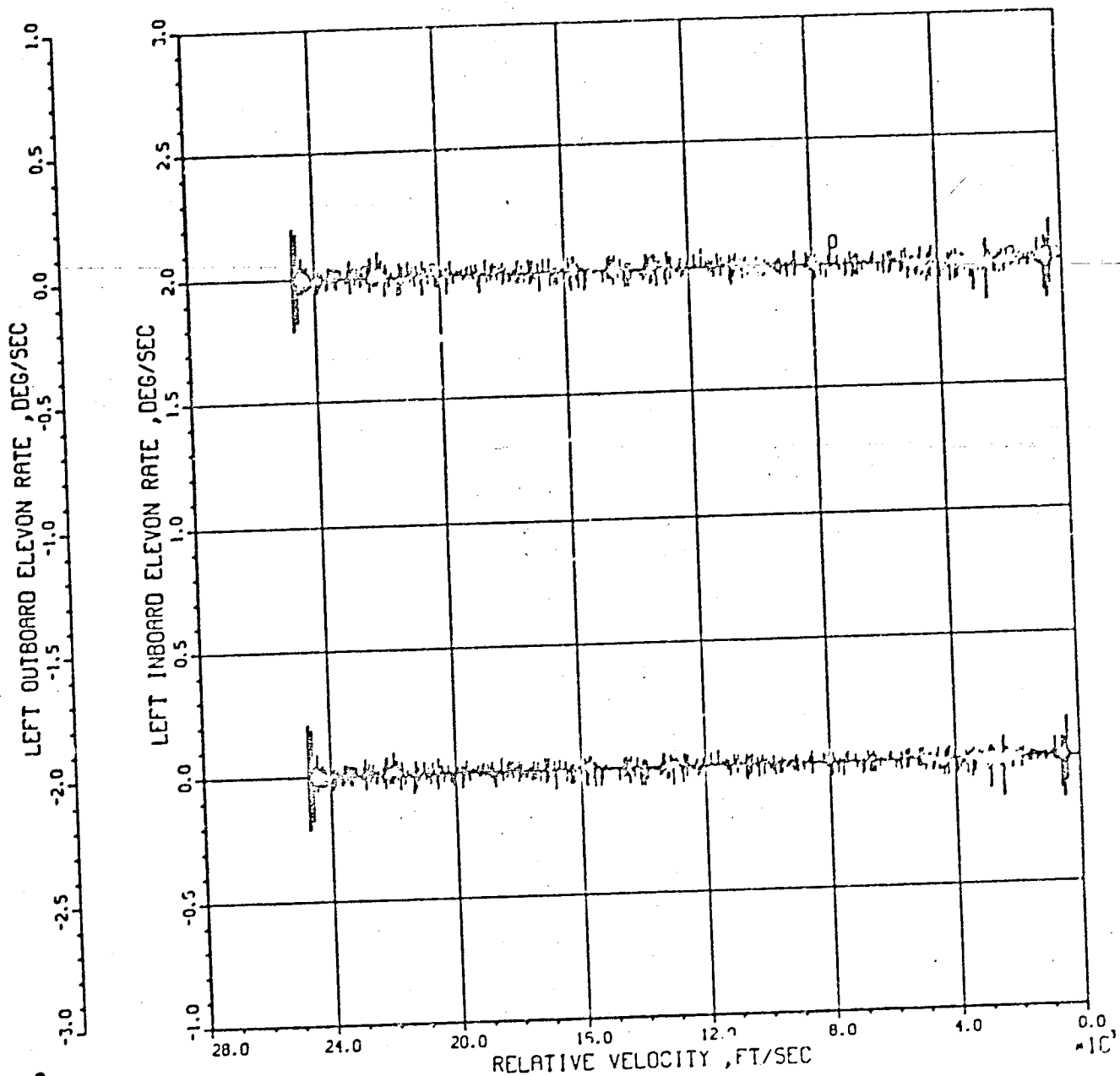
BODY ROLL , PITCH AND YAW RATES
DURING ATMOSPHERIC DESCENT

Figure 6.2-21



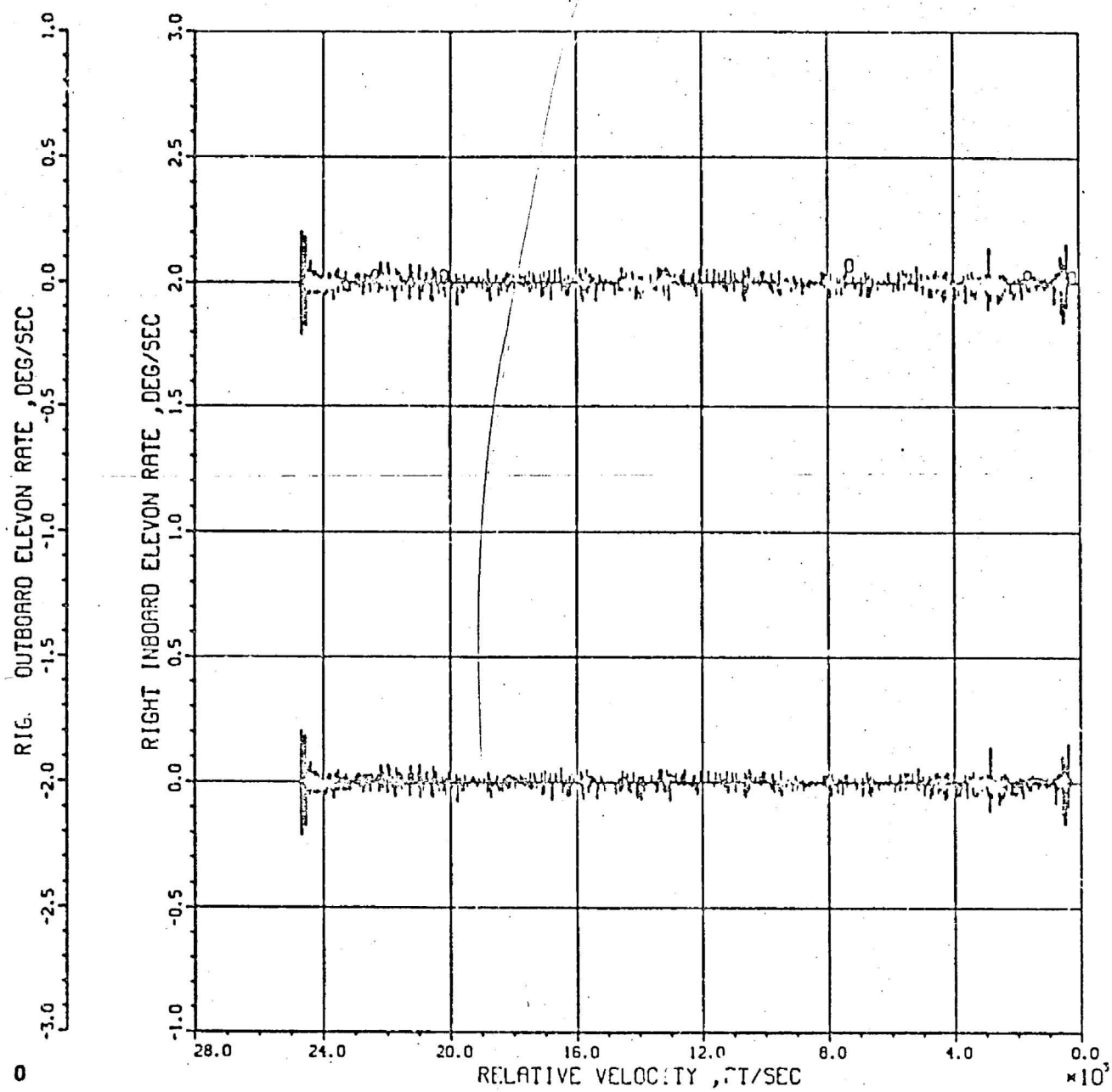
AILERON DEFLECTION
DURING ATMOSPHERIC DESCENT

Figure 6.2-22



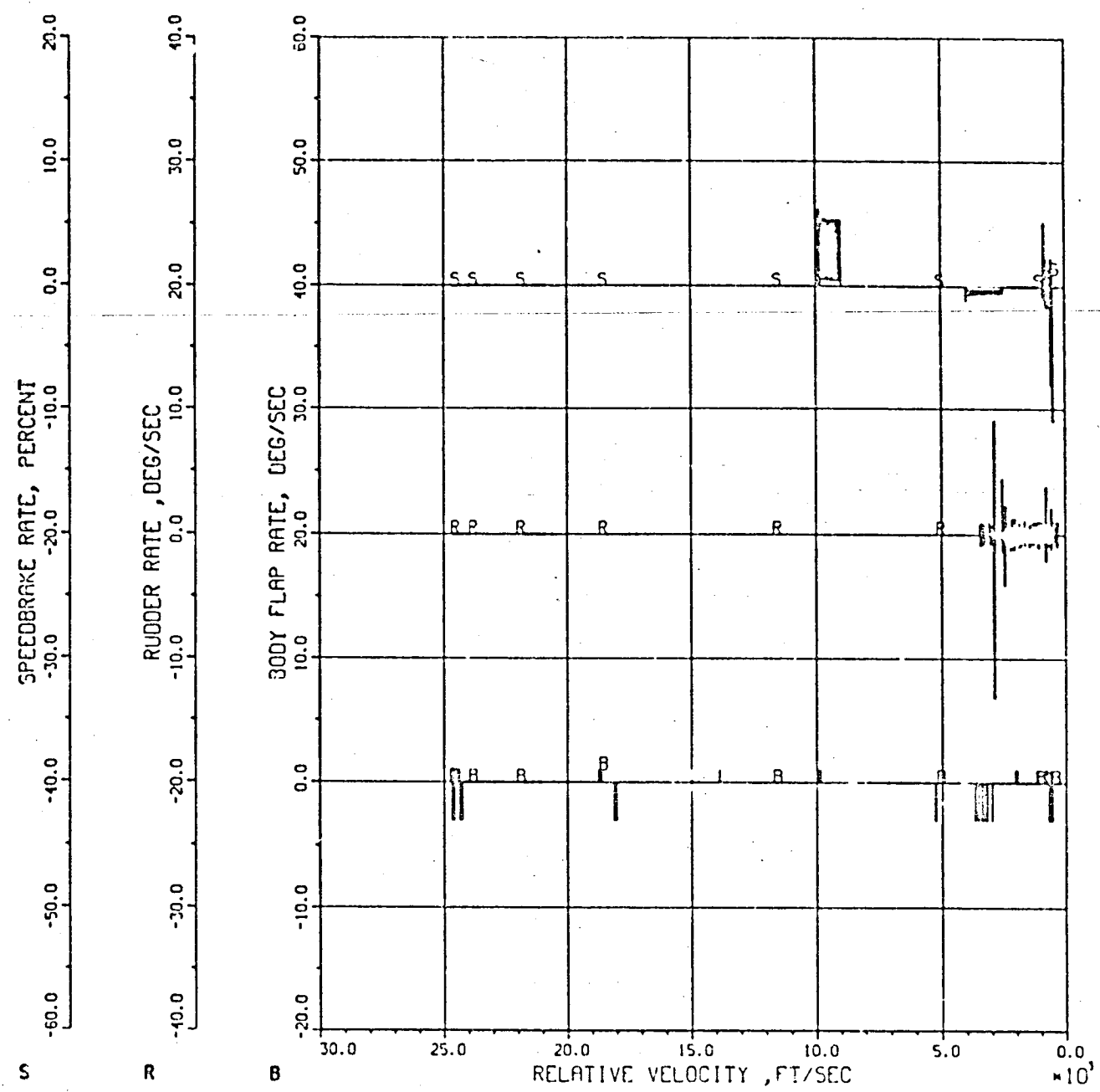
LEFT ELEVON DEFLECTION RATES
DURING ATMOSPHERIC DESCENT

Figure 6.2-23



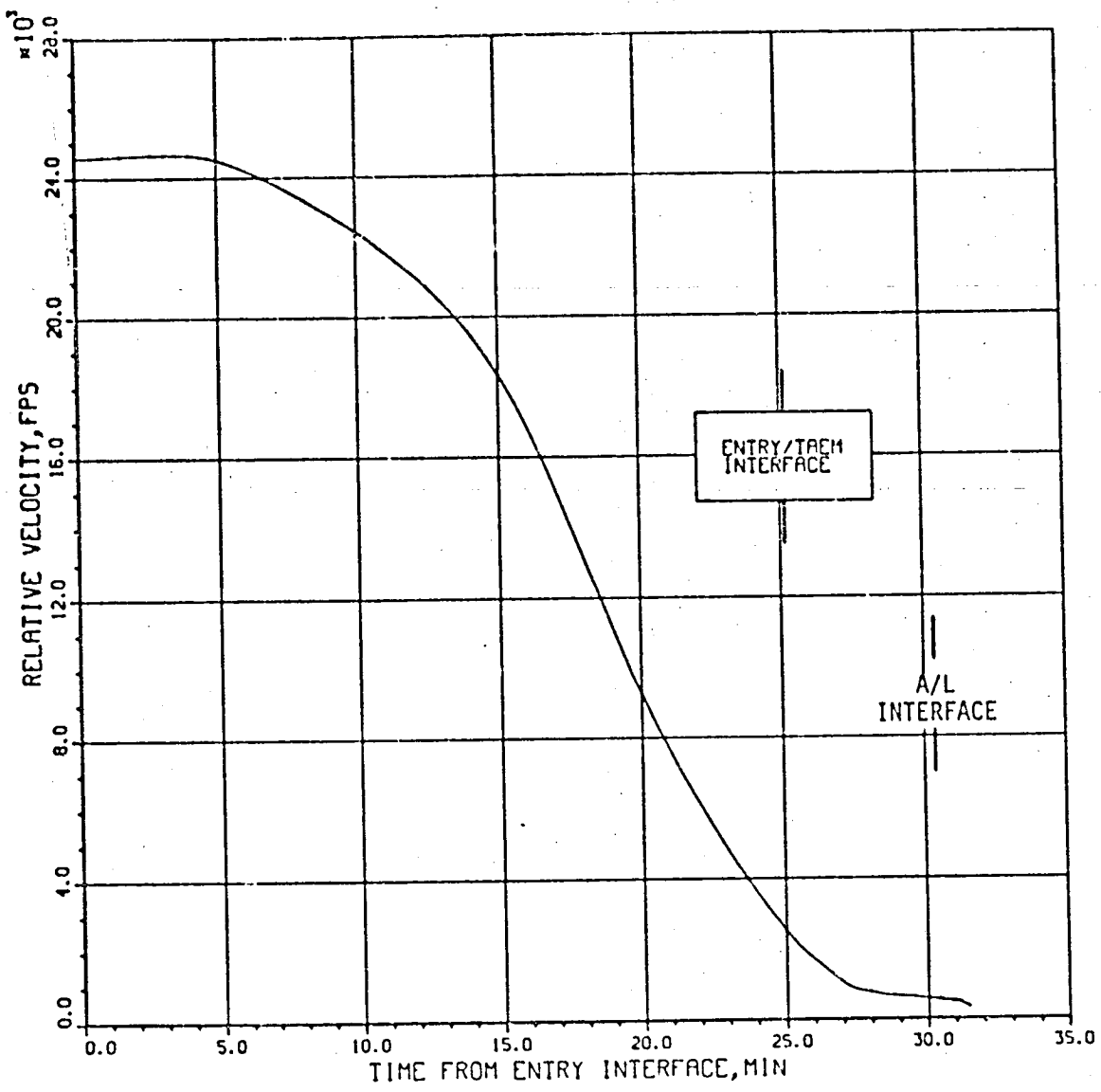
RIGHT ELEVON DEFLECTION RATES
DURING ATMOSPHERIC DESCENT

Figure 6.2-24



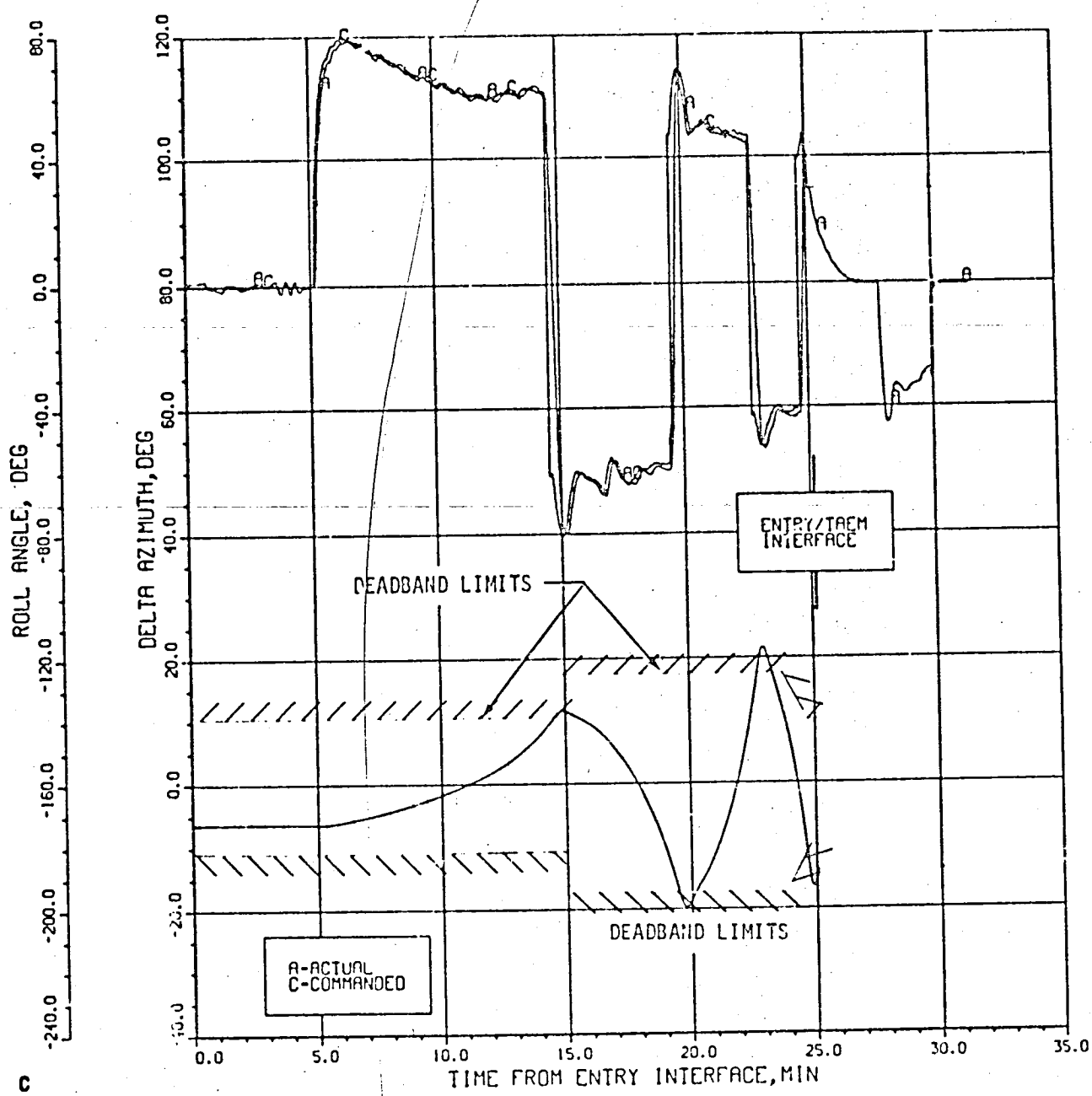
BODY FLAP , RUDDER AND SPEEDBRAKE
RATES DURING ATMOSPHERIC DESCENT

Figure 6.2-25



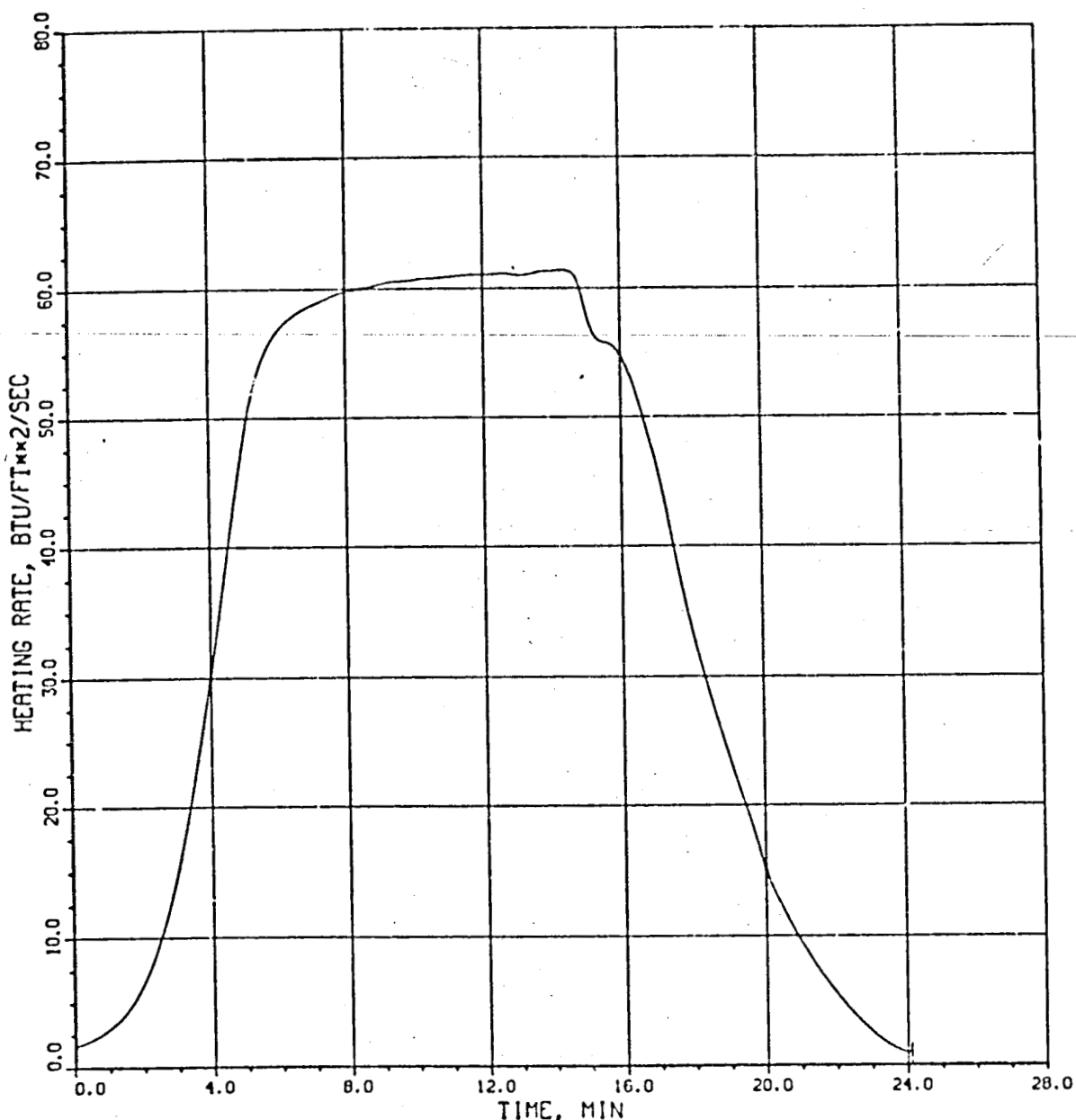
RELATIVE VELOCITY VS. TIME
FROM ENTRY INTERFACE.

Figure 6.2-26



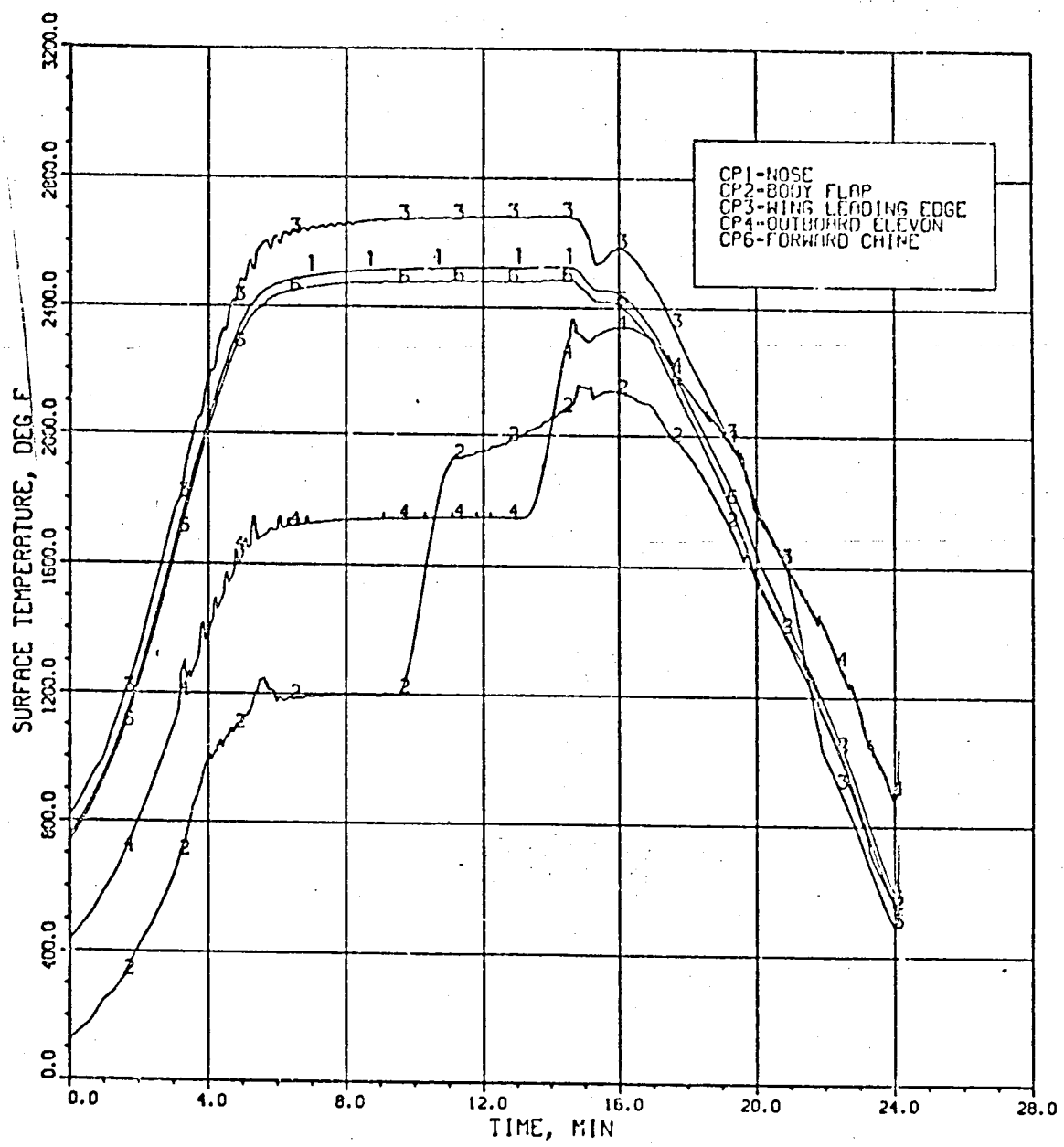
DELTA AZIMUTH, ACTUAL AND COMMANDED
ROLL ANGLE VS. TIME FROM ENTRY INTERFACE

Figure 6.2-27



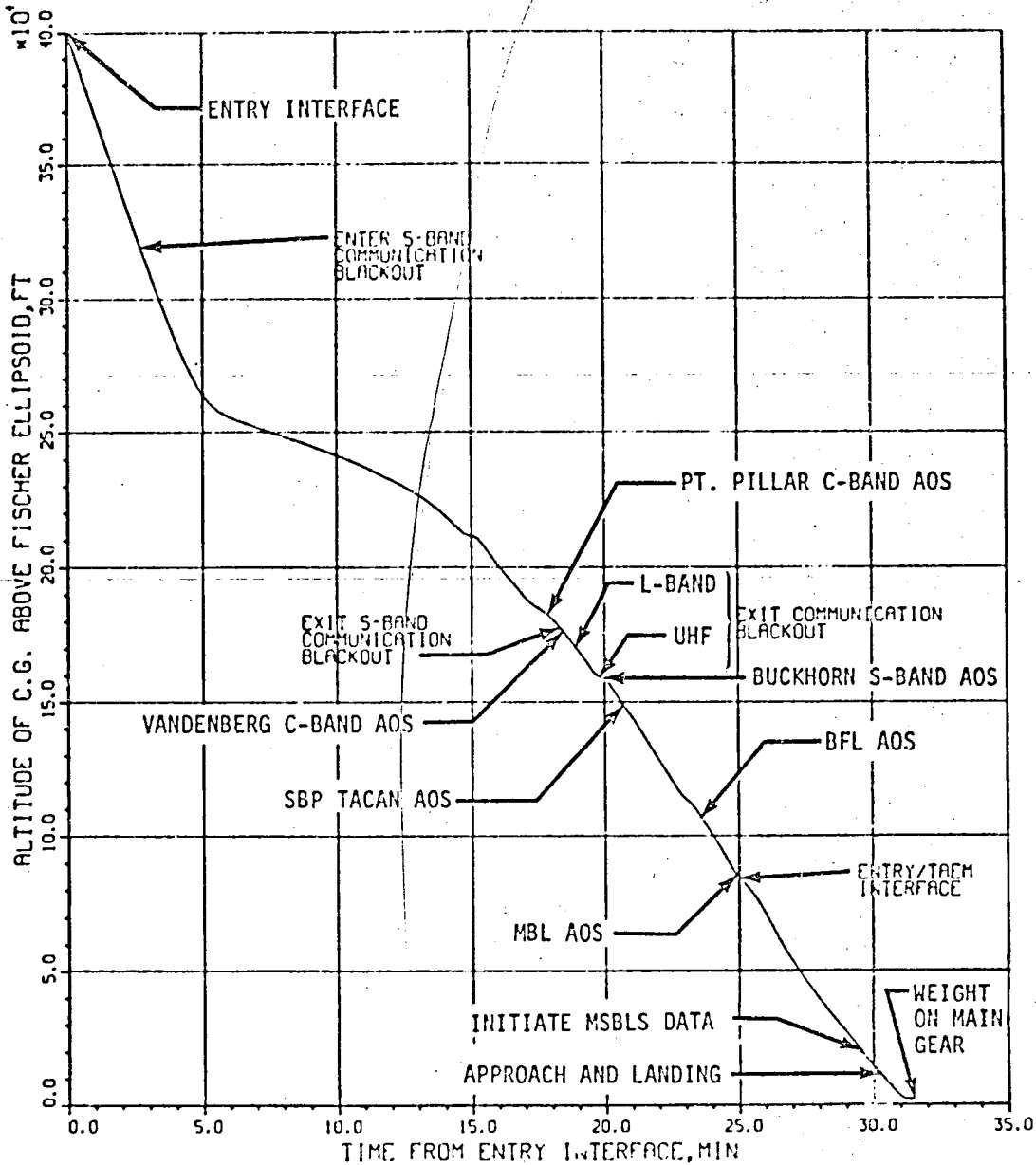
REFERENCE HEATING RATE VS.
TIME FROM ENTRY INTERFACE

Figure 6.2-28



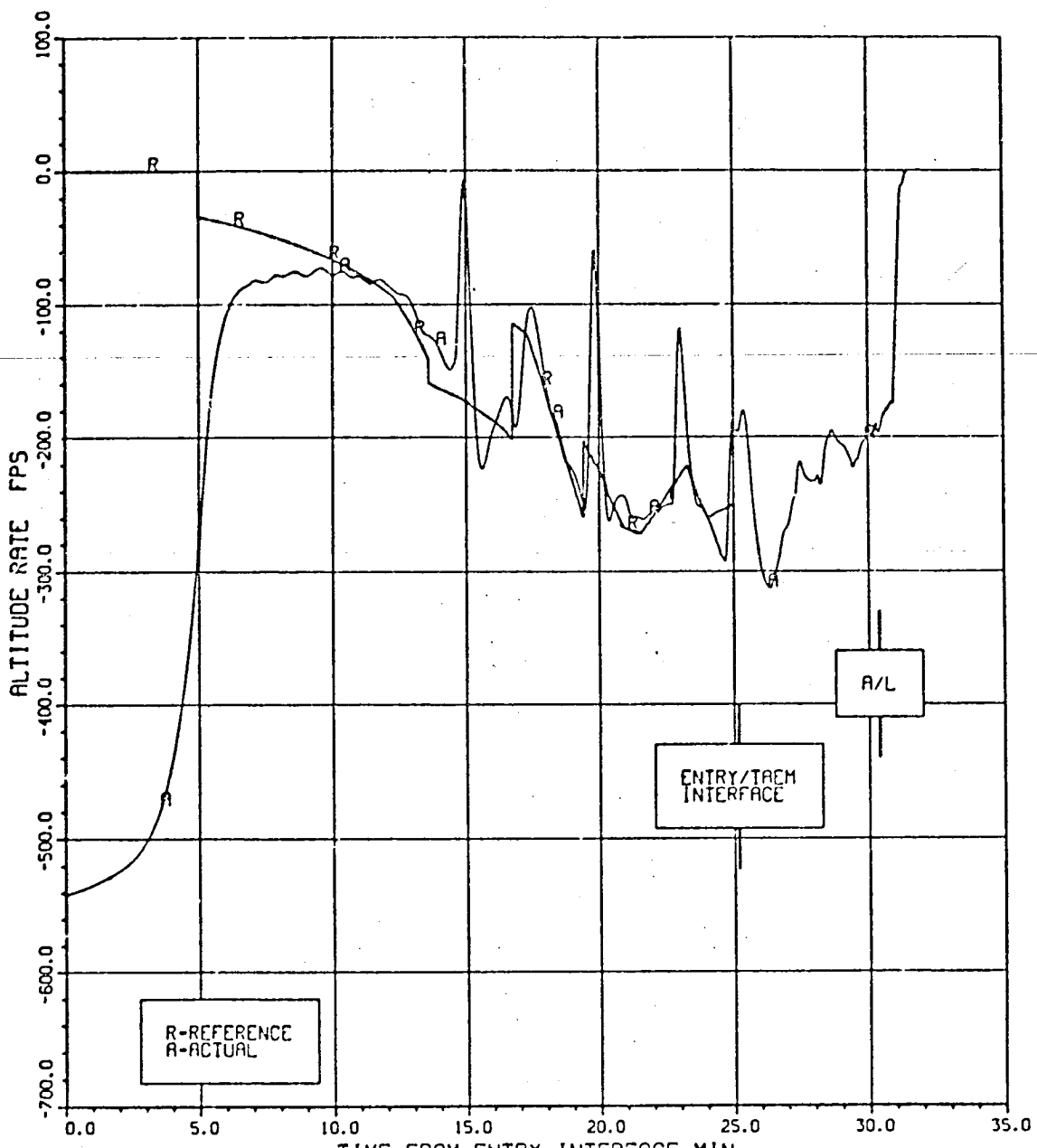
CONTROL POINT TEMPERATURES
VS. TIME FROM ENTRY INTERFACE

Figure 6.2-29



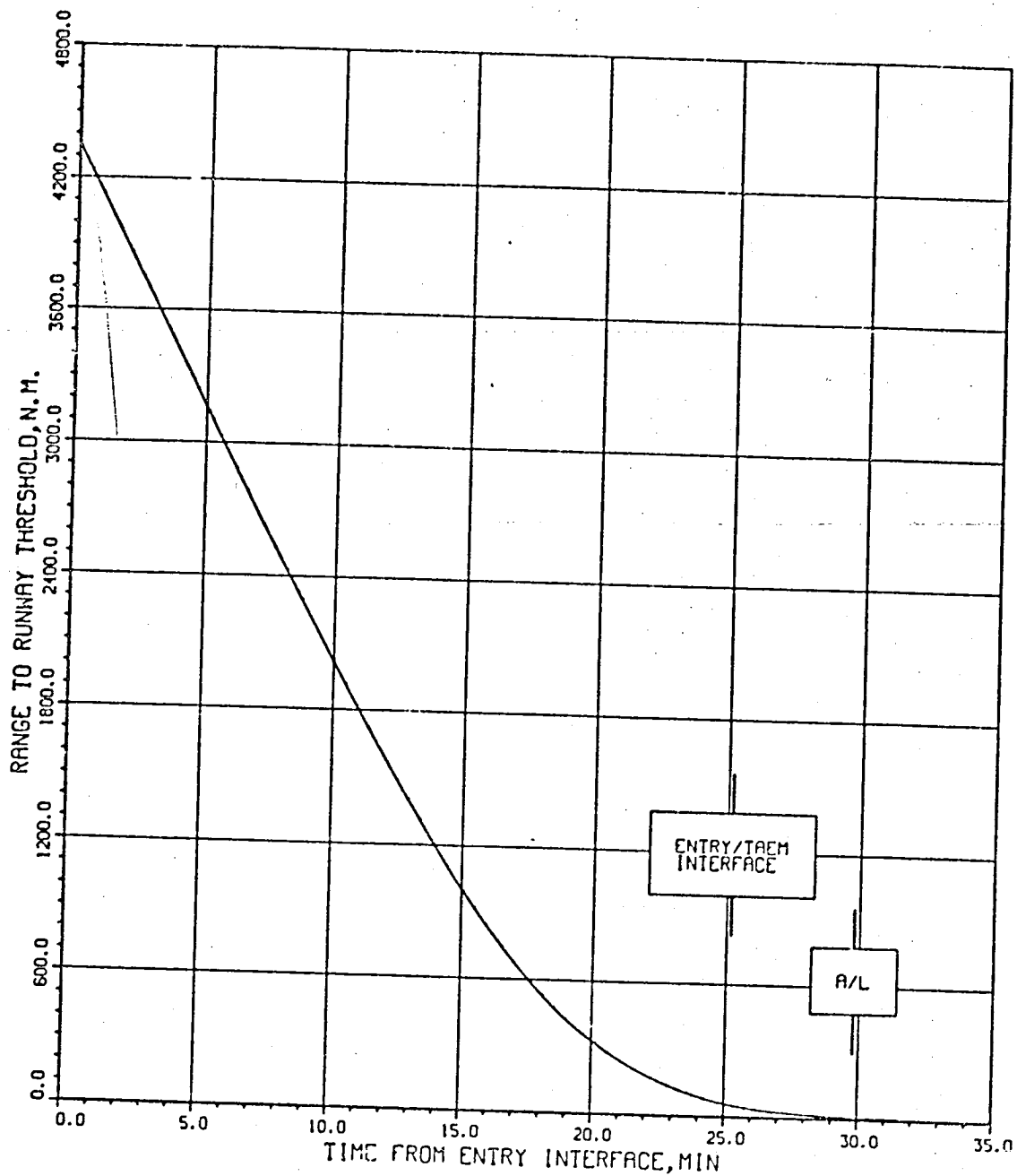
ALTITUDE VS. TIME FROM
ENTRY INTERFACE

Figure 6.2-30



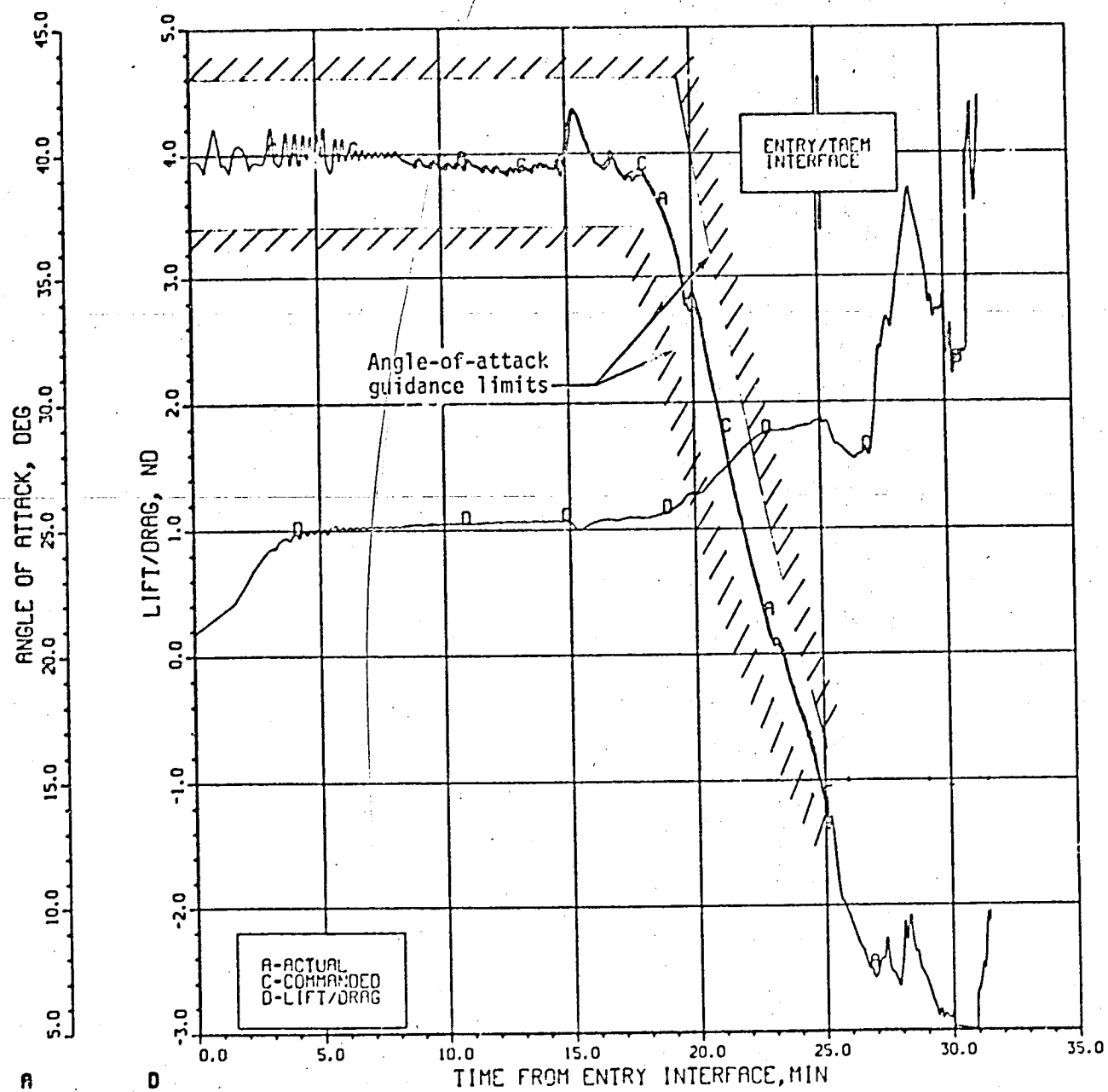
ACTUAL AND REFERENCE ALTITUDE RATE
VS. TIME FROM ENTRY INTERFACE

Figure 6.2-31



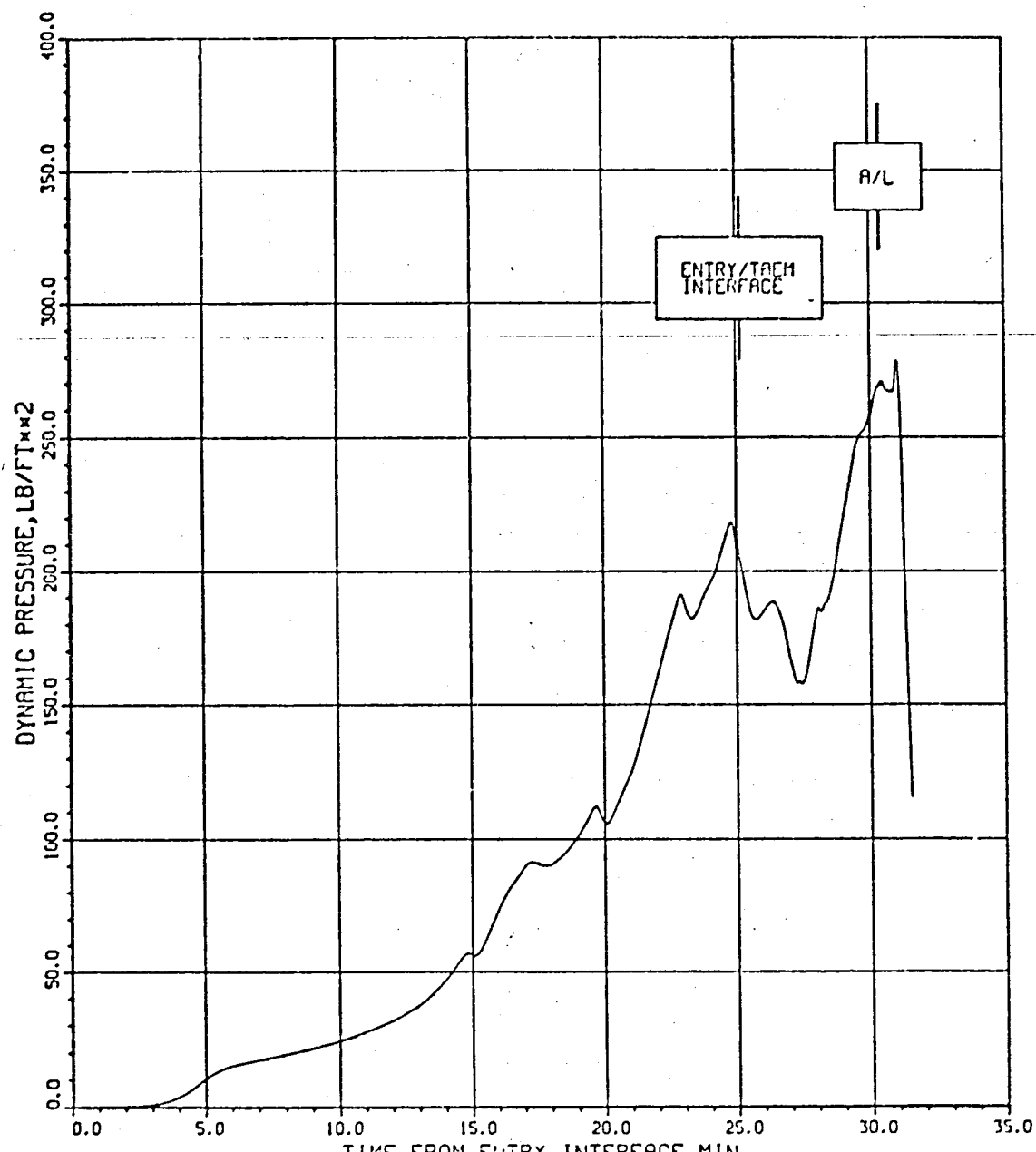
RANGE-TO-RUNWAY THRESHOLD VS.
TIME FROM ENTRY INTERFACE

Figure 6.2-32



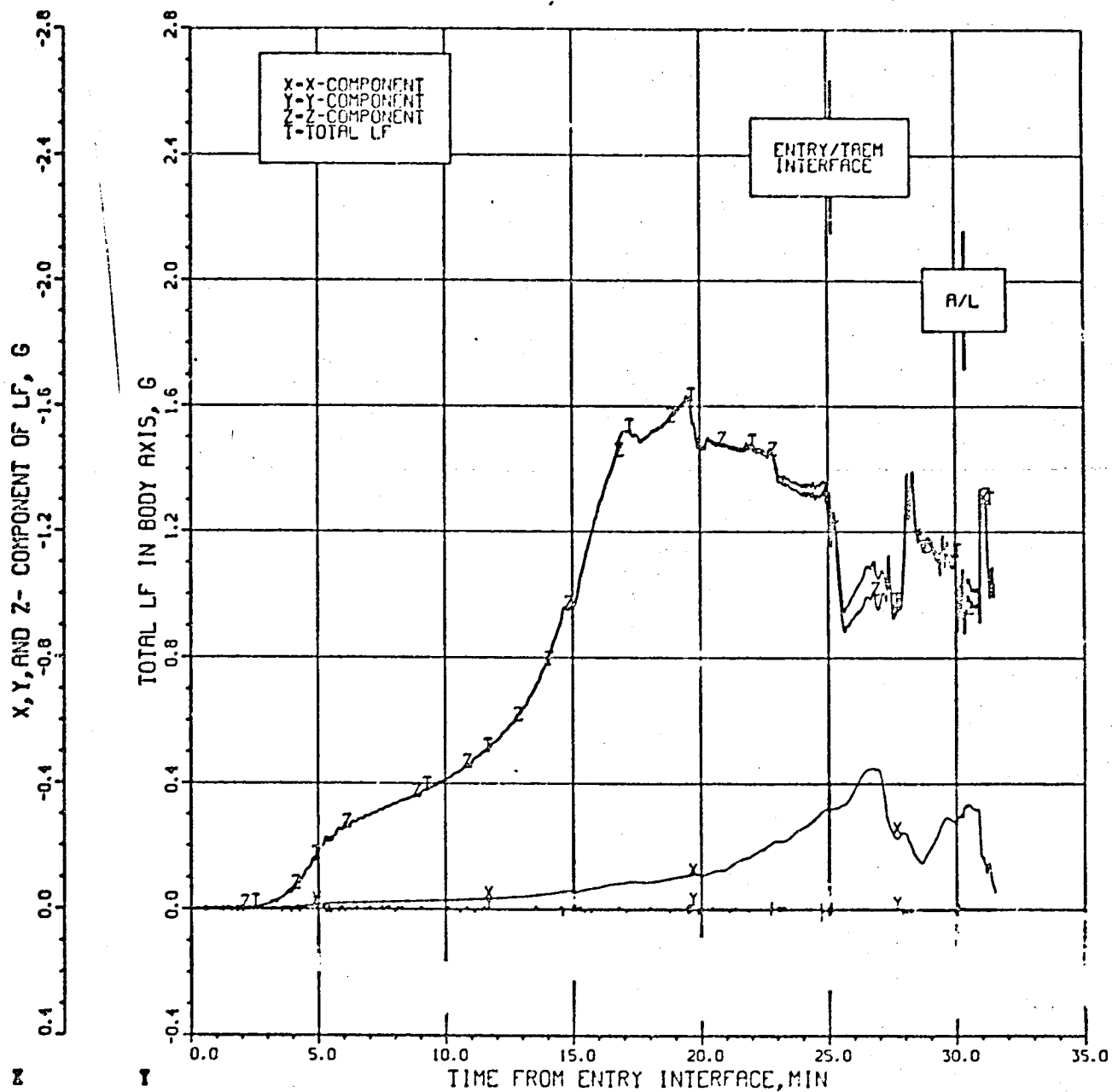
LIFT/DRAG, ACTUAL AND COMMANDED ANGLE OF ATTACK VS. TIME FROM ENTRY INTERFACE

Figure 6.2-33



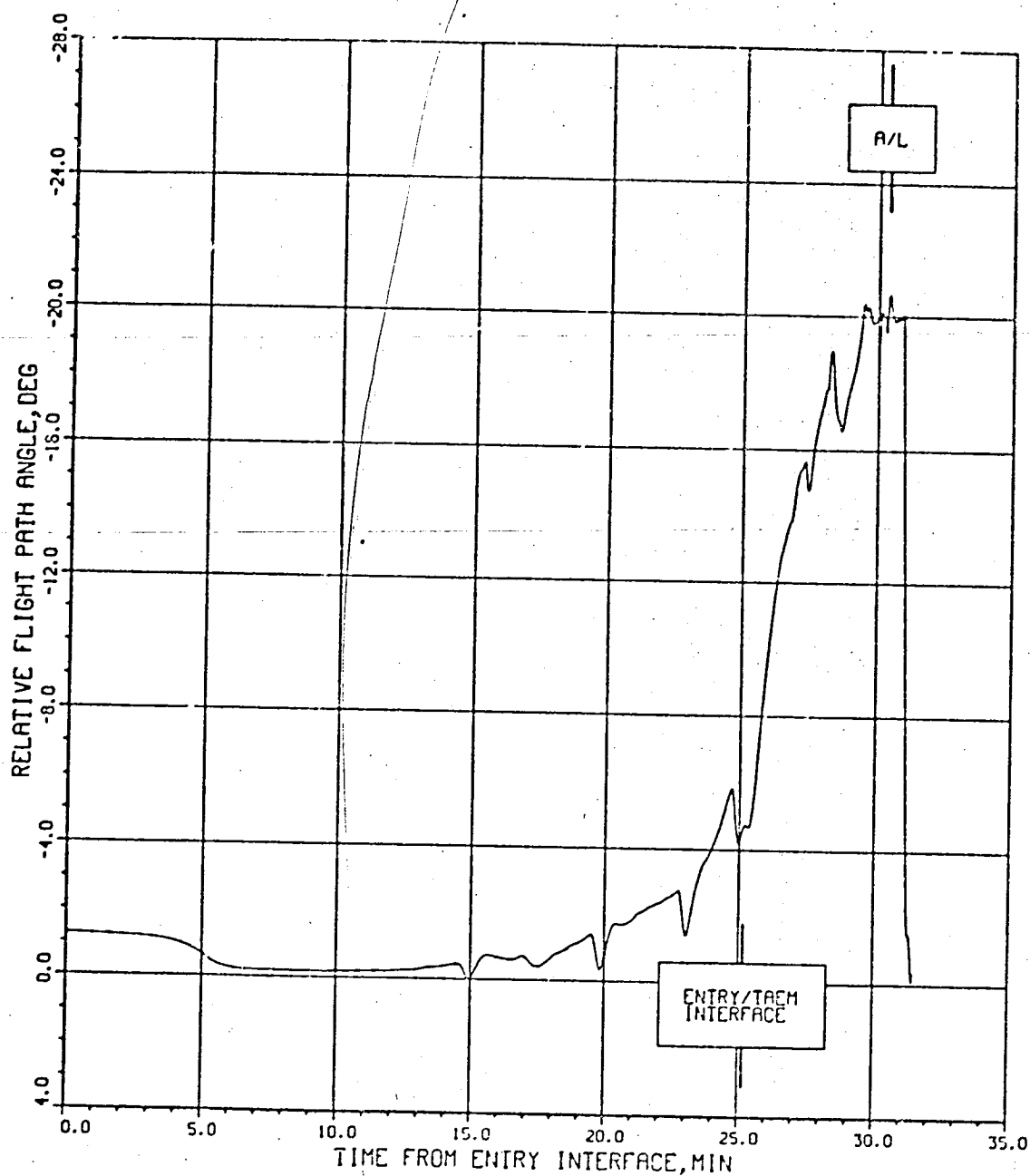
DYNAMIC PRESSURE VS. TIME
FROM ENTRY INTERFACE

Figure 6.2-34



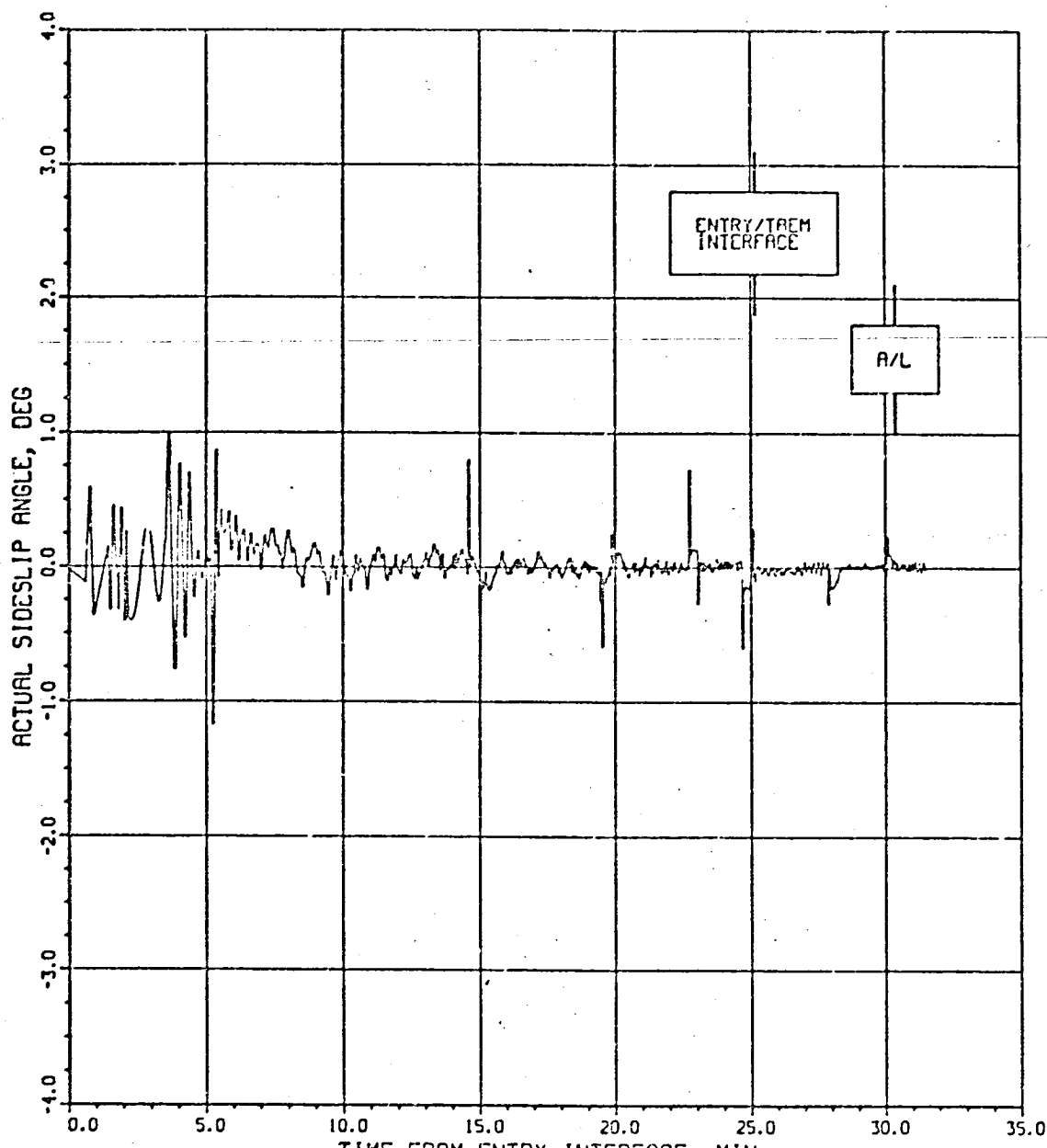
X, Y, AND Z- BODY AXIS COMPONENTS OF LOAD
FACTOR VS. TIME FROM ENTRY INTERFACE

Figure 6.2-35



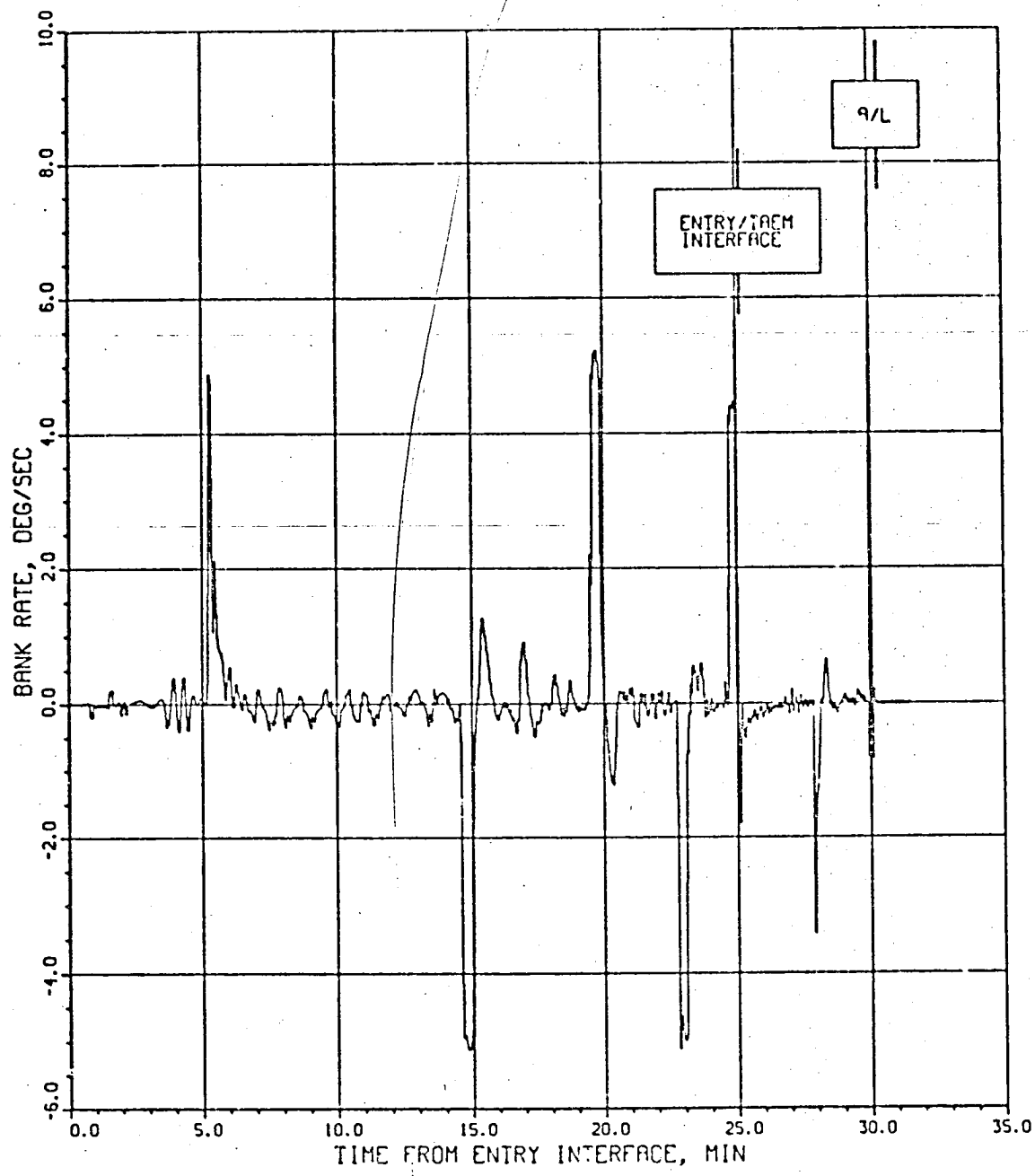
RELATIVE FLIGHTPATH ANGLE VS.
TIME FROM ENTRY INTERFACE

Figure 6.2-36



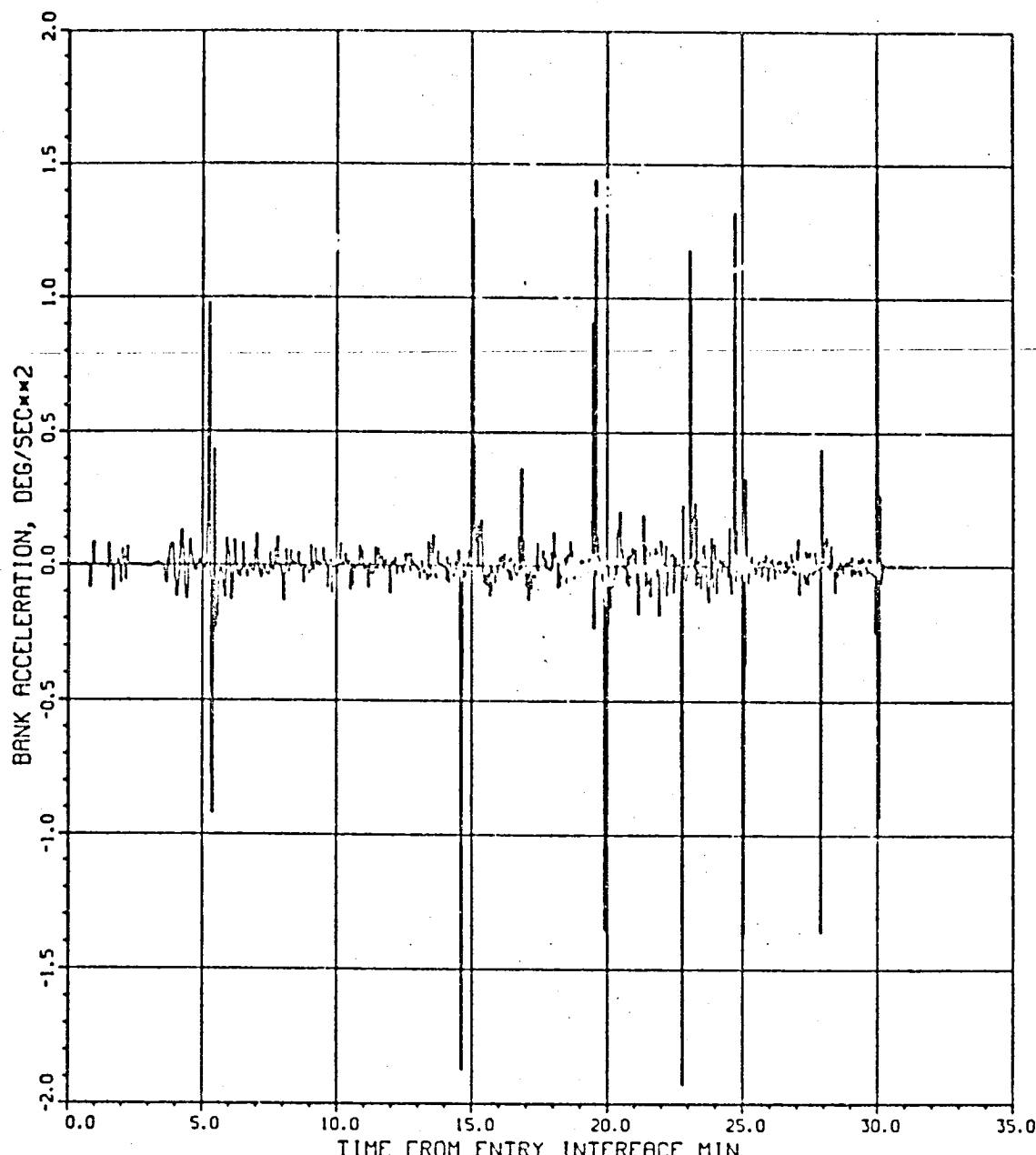
ACTUAL SIDESLIP ANGLE VS.
TIME FROM ENTRY INTERFACE

Figure 6.2-37



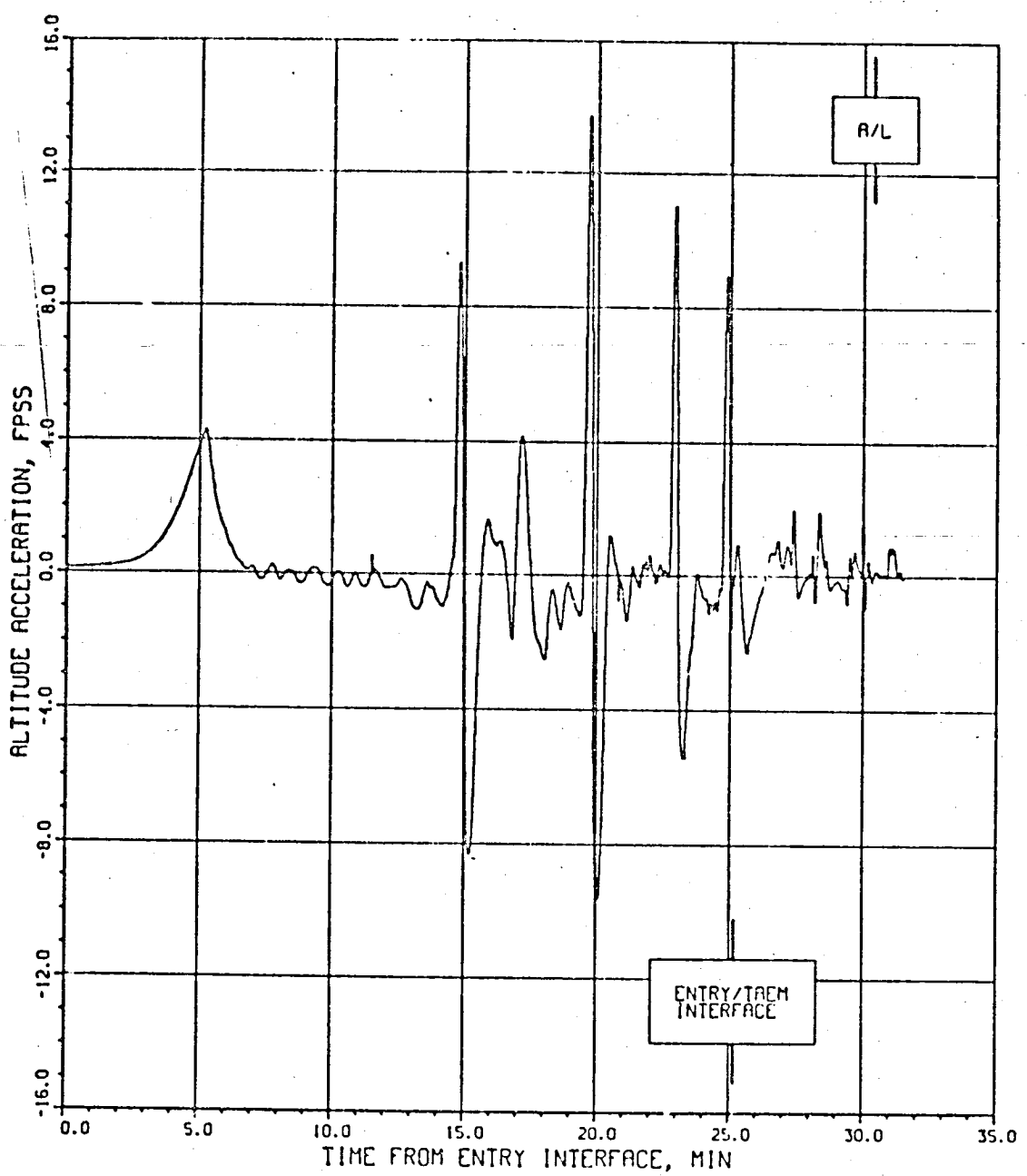
BANK RATE VS. TIME FROM ENTRY INTERFACE

Figure 6.2-38



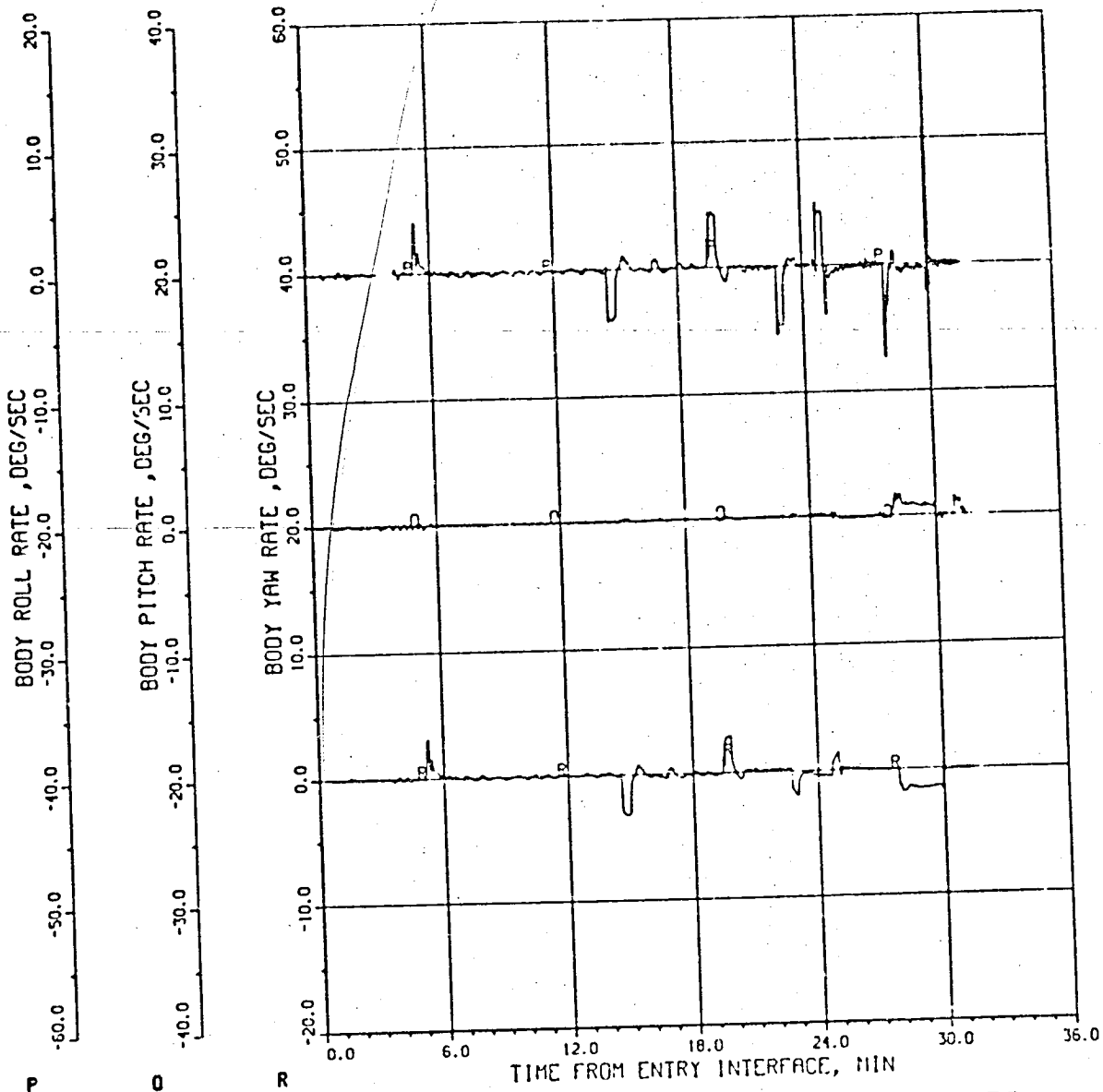
BANK ACCELERATION VS.
TIME FROM ENTRY INTERFACE

Figure 6.2-39



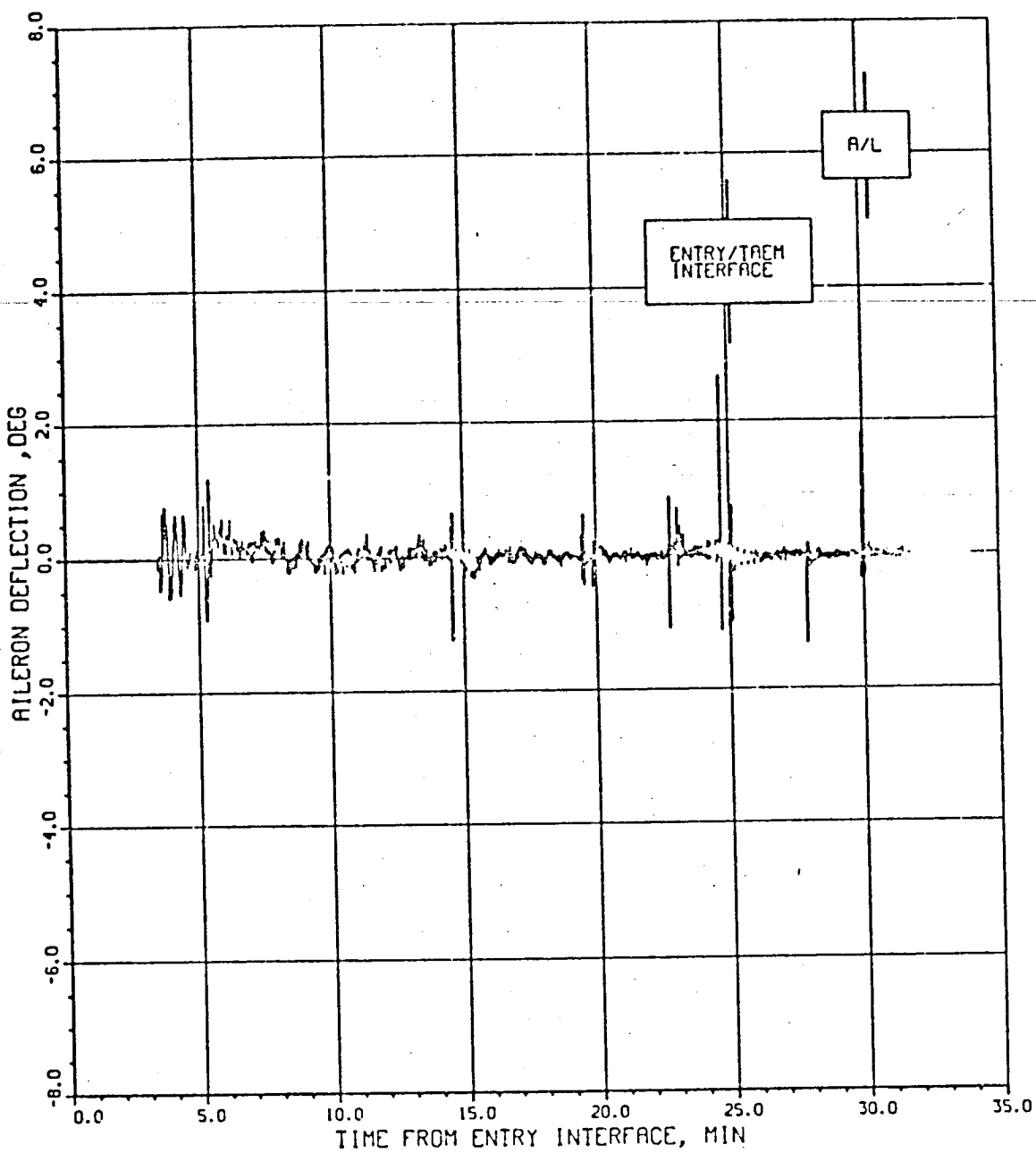
ALTITUDE ACCELERATION VS.
TIME FROM ENTRY INTERFACE

Figure 6.2-40



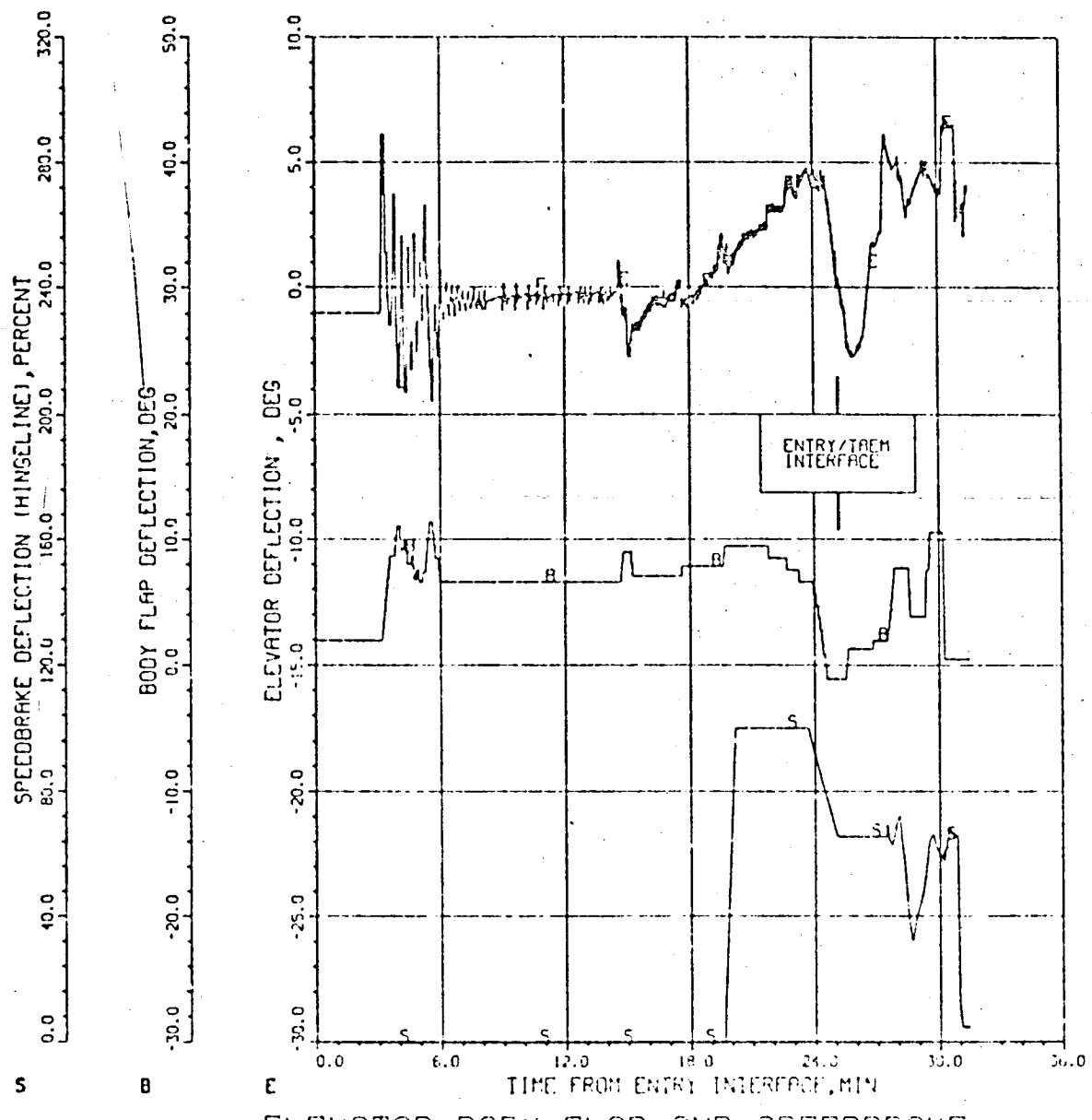
BODY ROLL , PITCH AND YAW RATES
VS. TIME FROM ENTRY INTERFACE

Figure 6.2-41



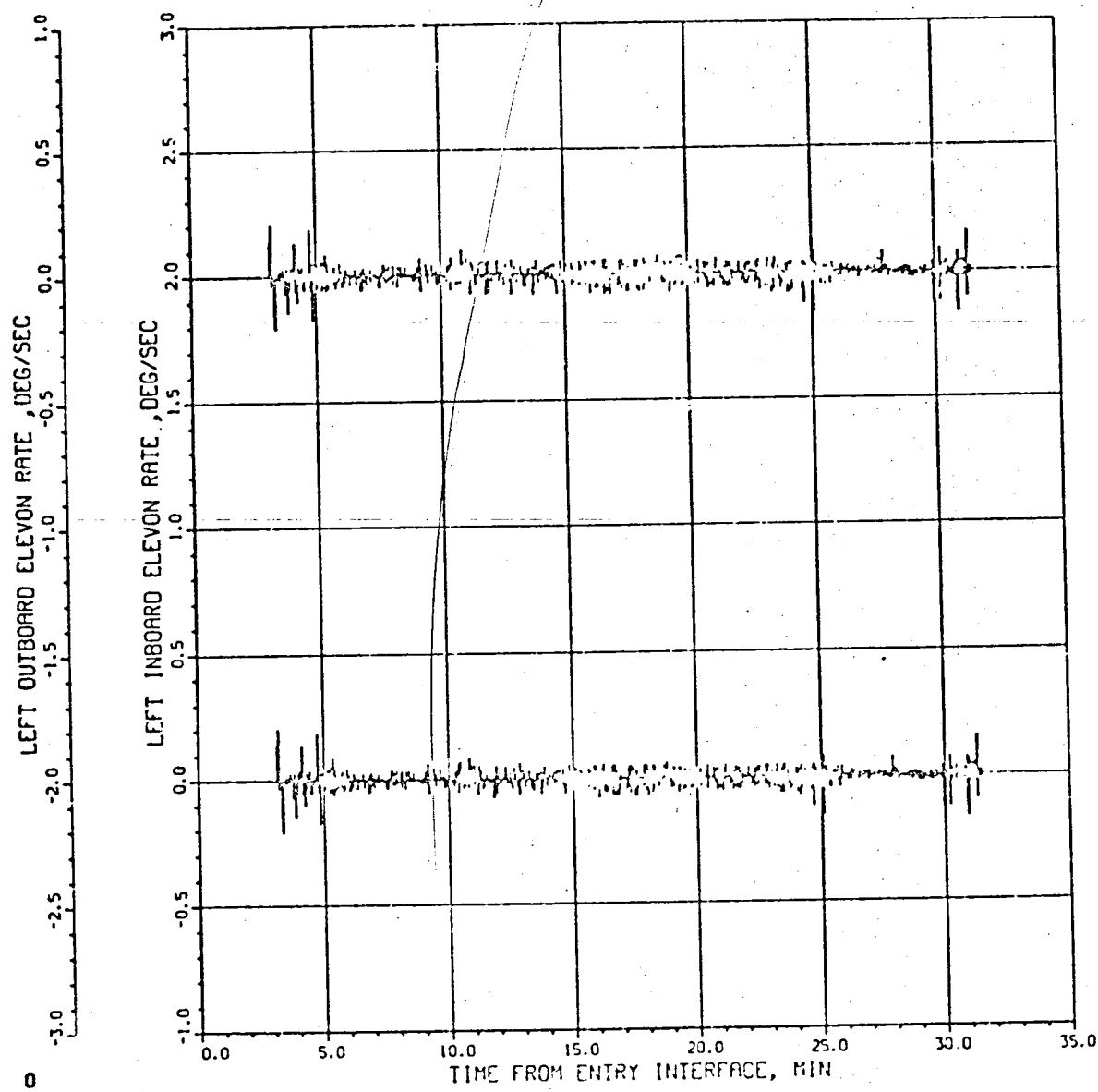
AILERON DEFLECTION VS.
TIME FROM ENTRY INTERFACE

Figure 6.2-42



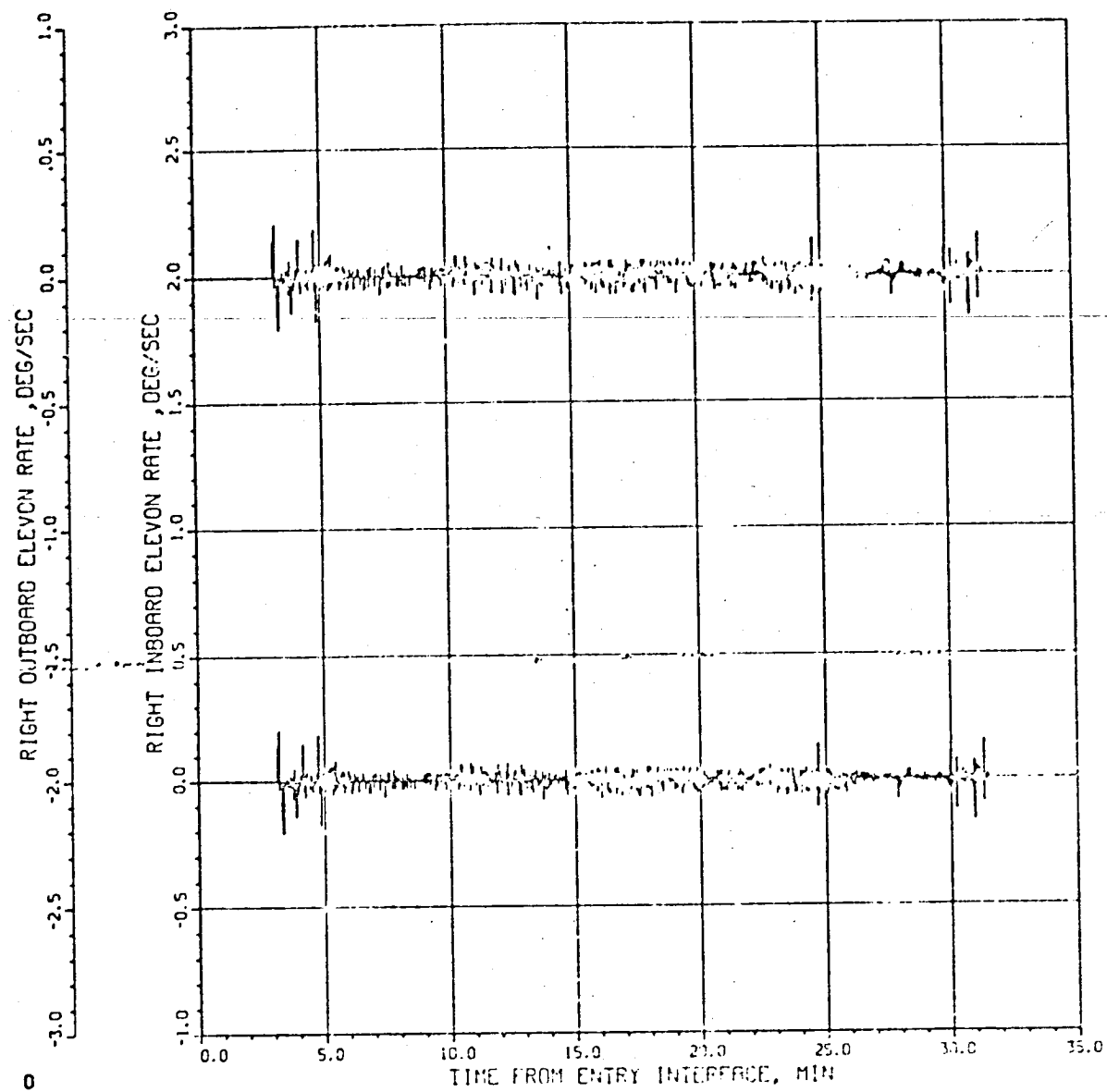
ELEVATOR, BODY FLAP, AND SPEEDBRAKE DEFLECTION VS. TIME FROM ENTRY INTERFACE

Figure 6.2-43



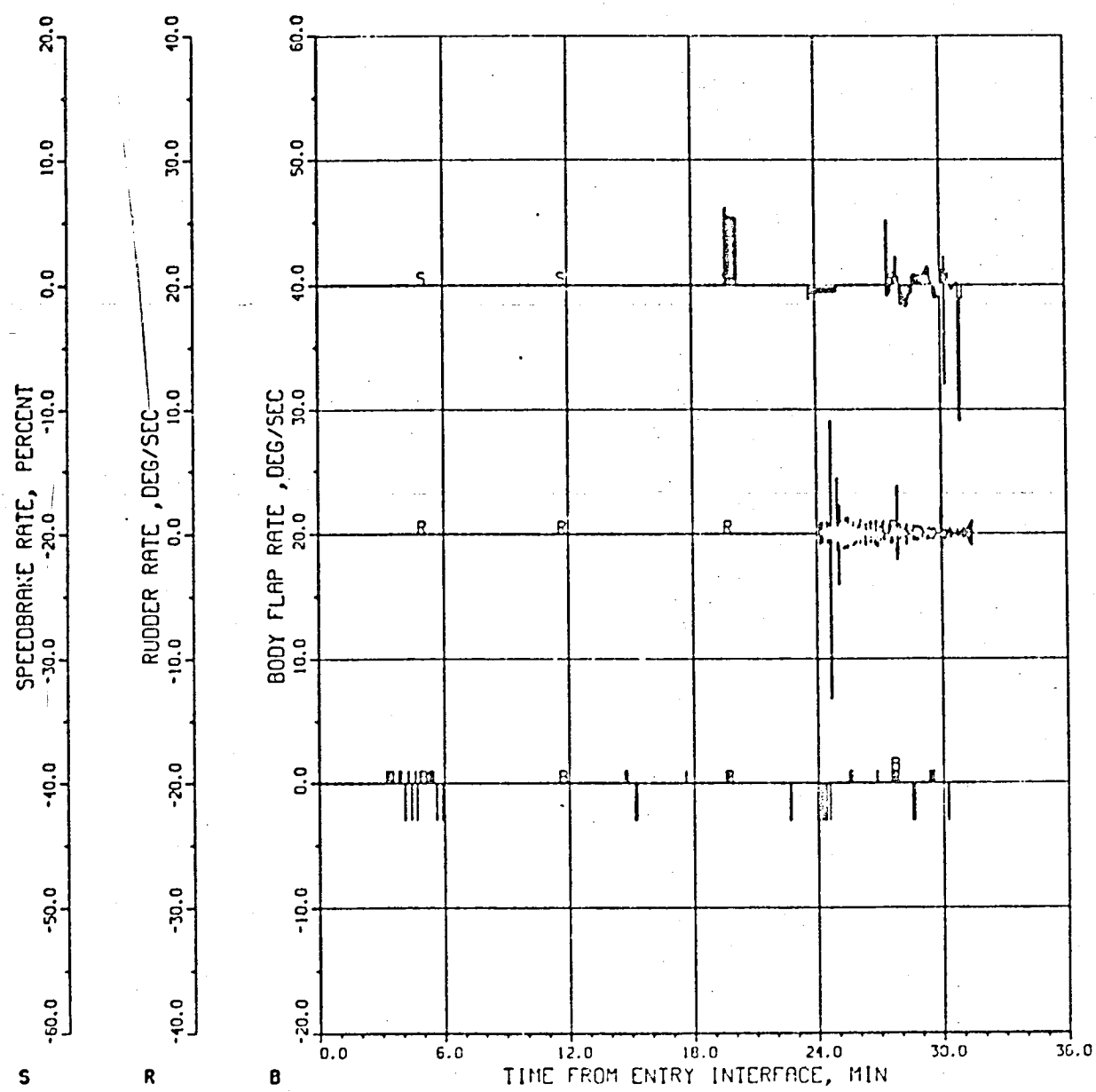
LEFT ELEVON DEFLECTION RATES
VS. TIME FROM ENTRY INTERFACE

Figure 6.2-44



RIGHT ELEVON DEFLECTION RATES
VS. TIME FROM ENTRY INTERFACE

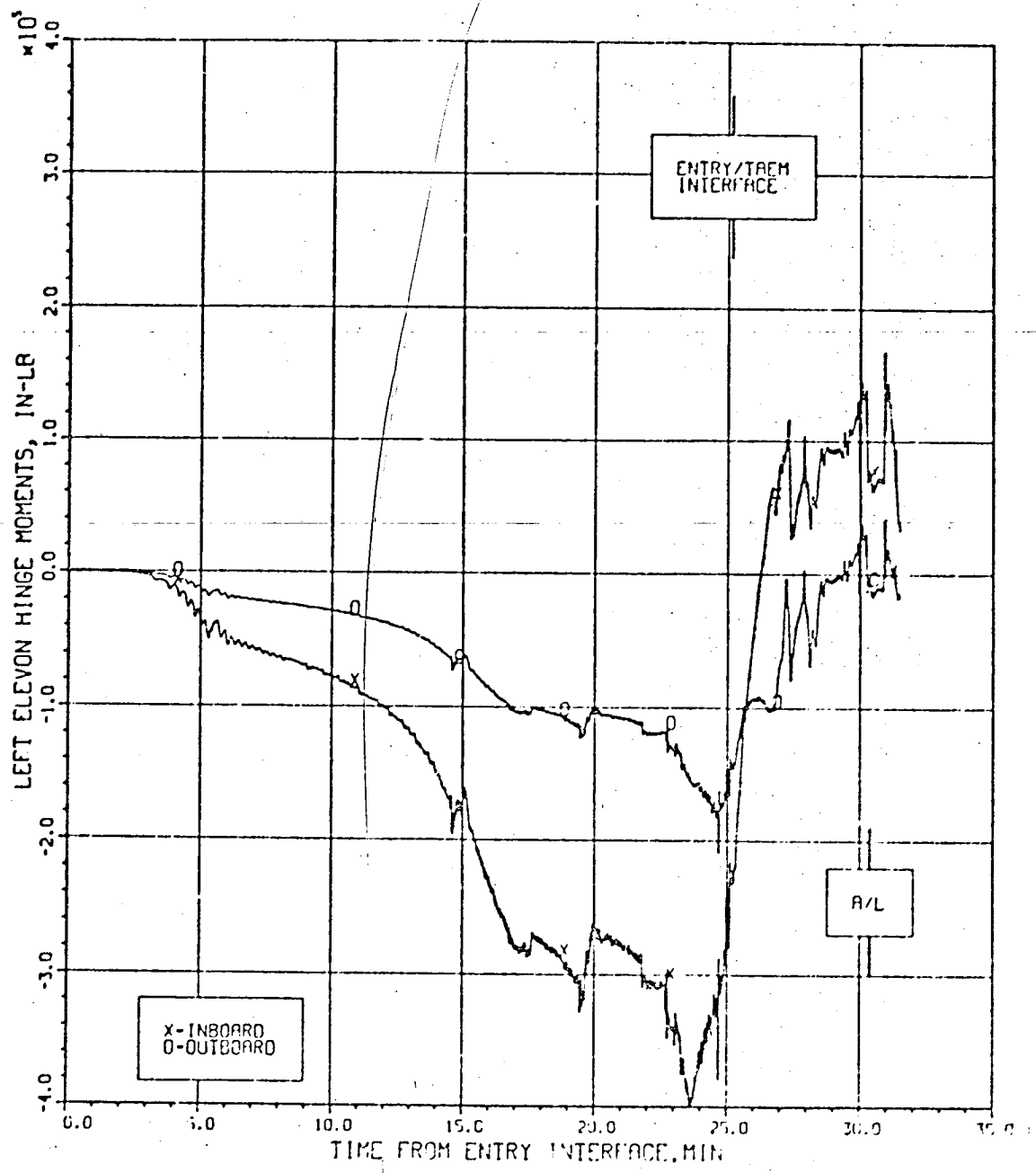
Figure 6.2-45



BODY FLAP, RUDDER AND SPEEDBRAKE RATES
VS. TIME FROM ENTRY INTERFACE.

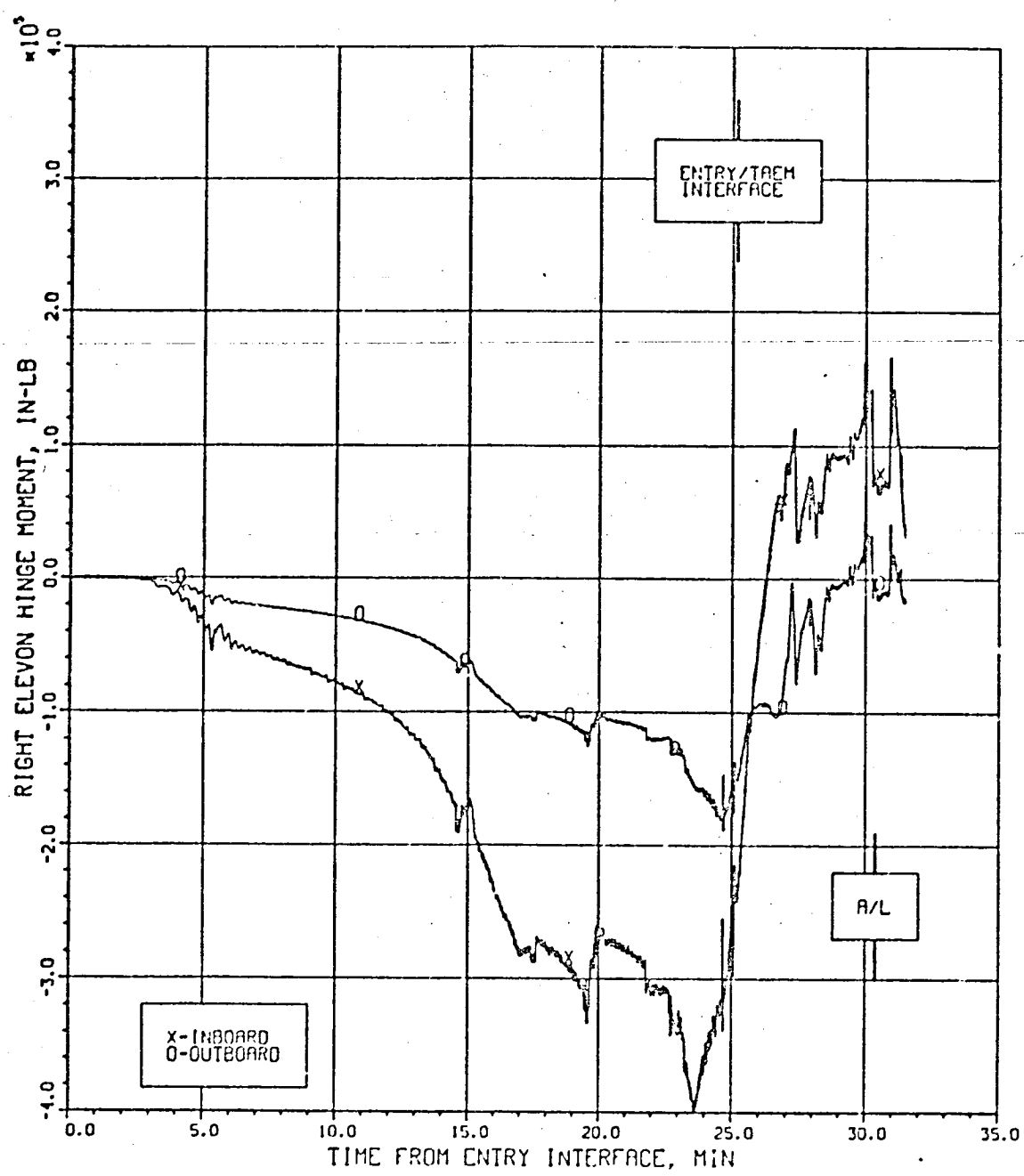
Figure 6.2-46

ORIGINAL PAGE IS
OF POOR QUALITY



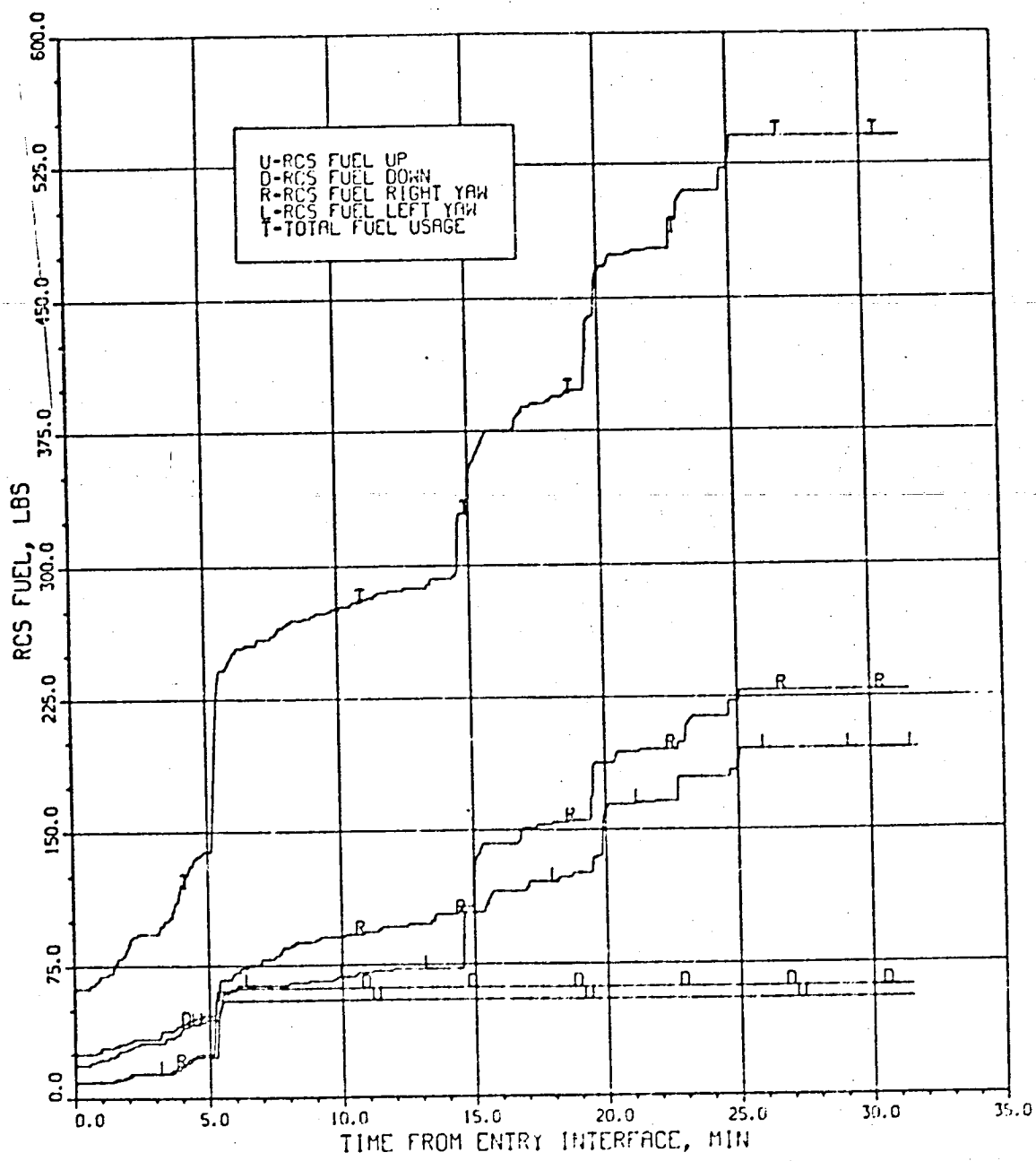
LEFT ELEVON HINGE MOMENTS VS.
TIME FROM ENTRY INTERFACE

Figure 6.2-47



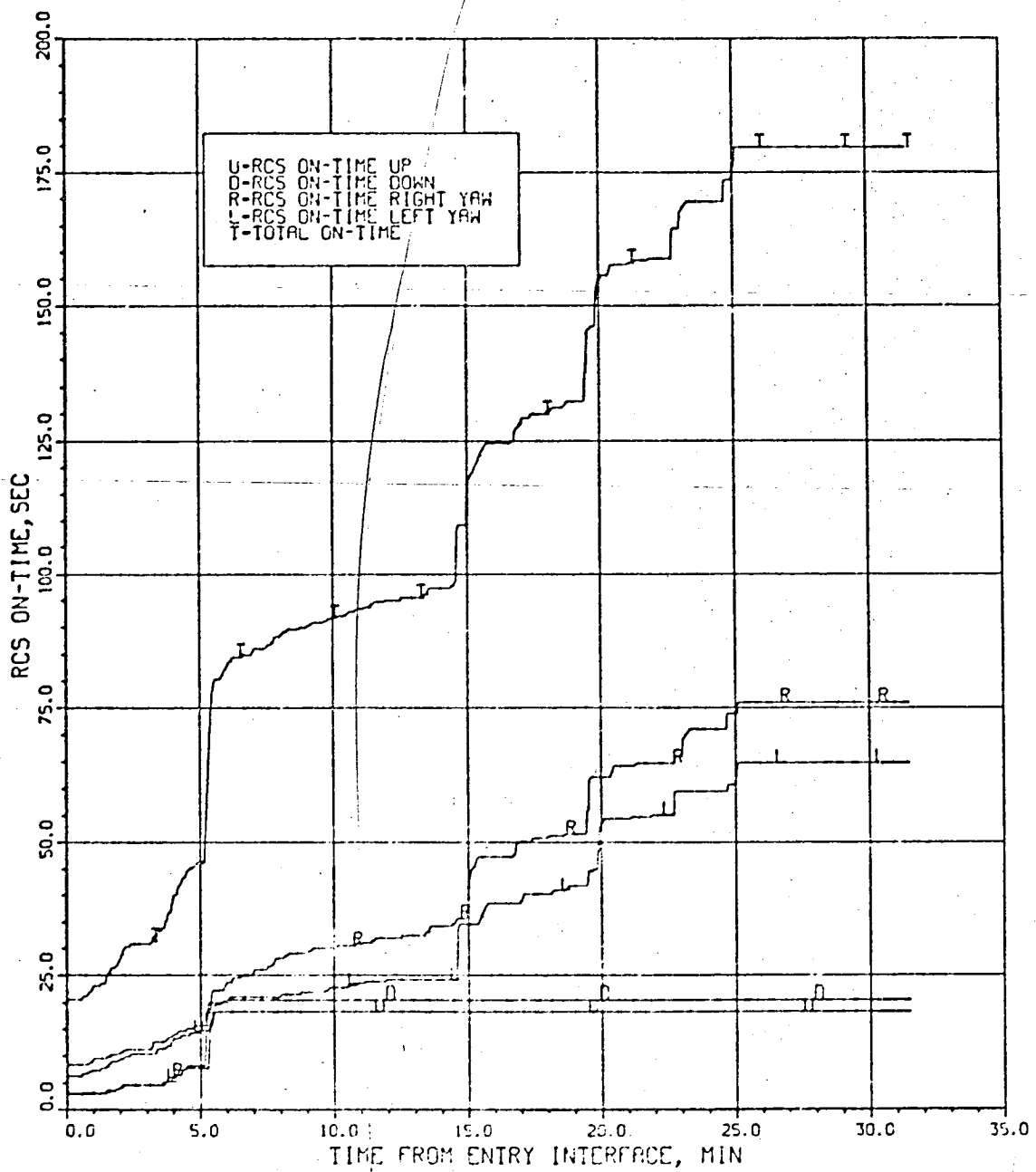
RIGHT ELEVON HINGE MOMENTS VS.
TIME FROM ENTRY INTERFACE

Figure 6.2-48



RCS FUEL USAGE VS. TIME
FROM ENTRY INTERFACE

Figure 6.2-49



RCS ON-TIME VS. TIME
FROM ENTRY INTERFACE

Figure 6.2-50

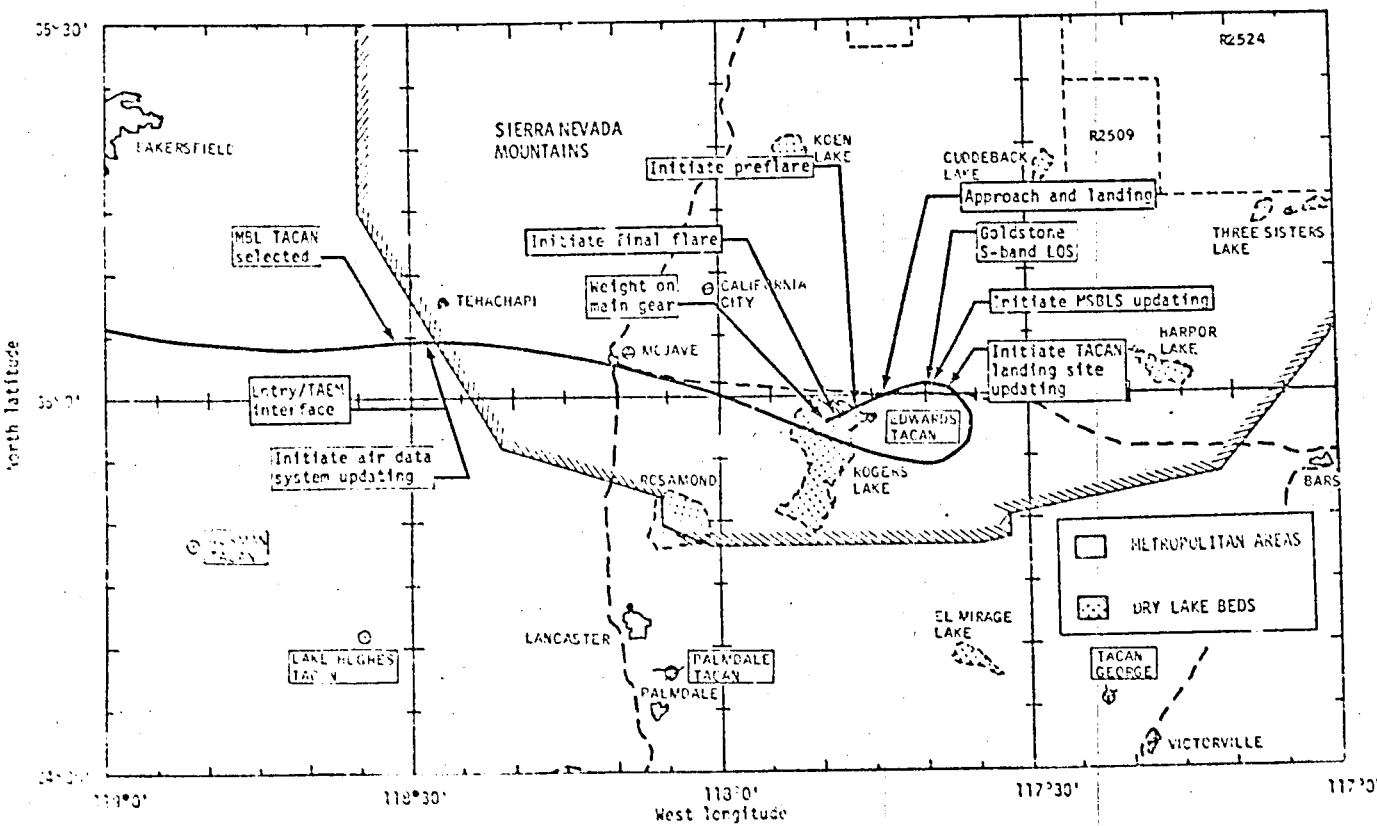
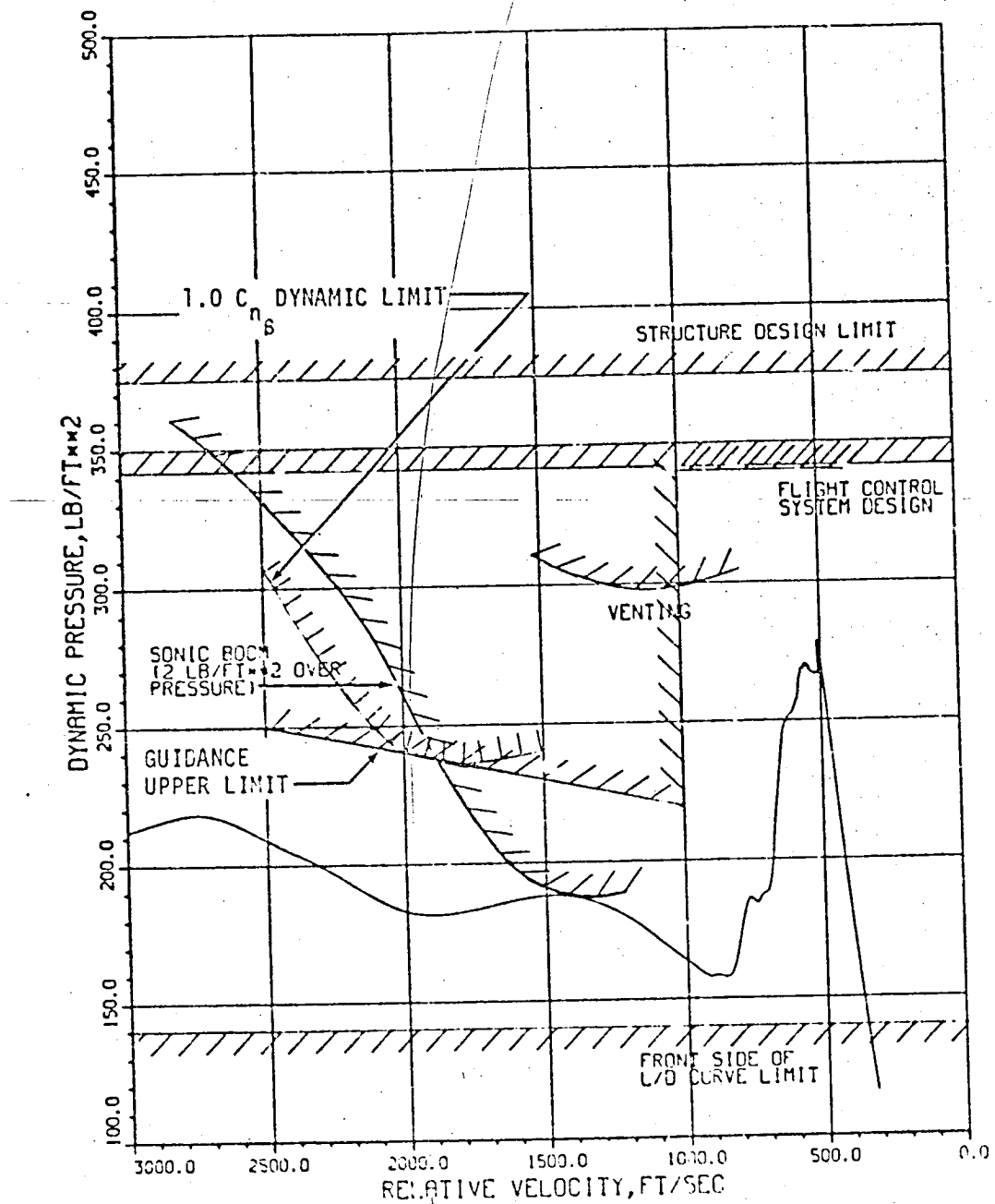
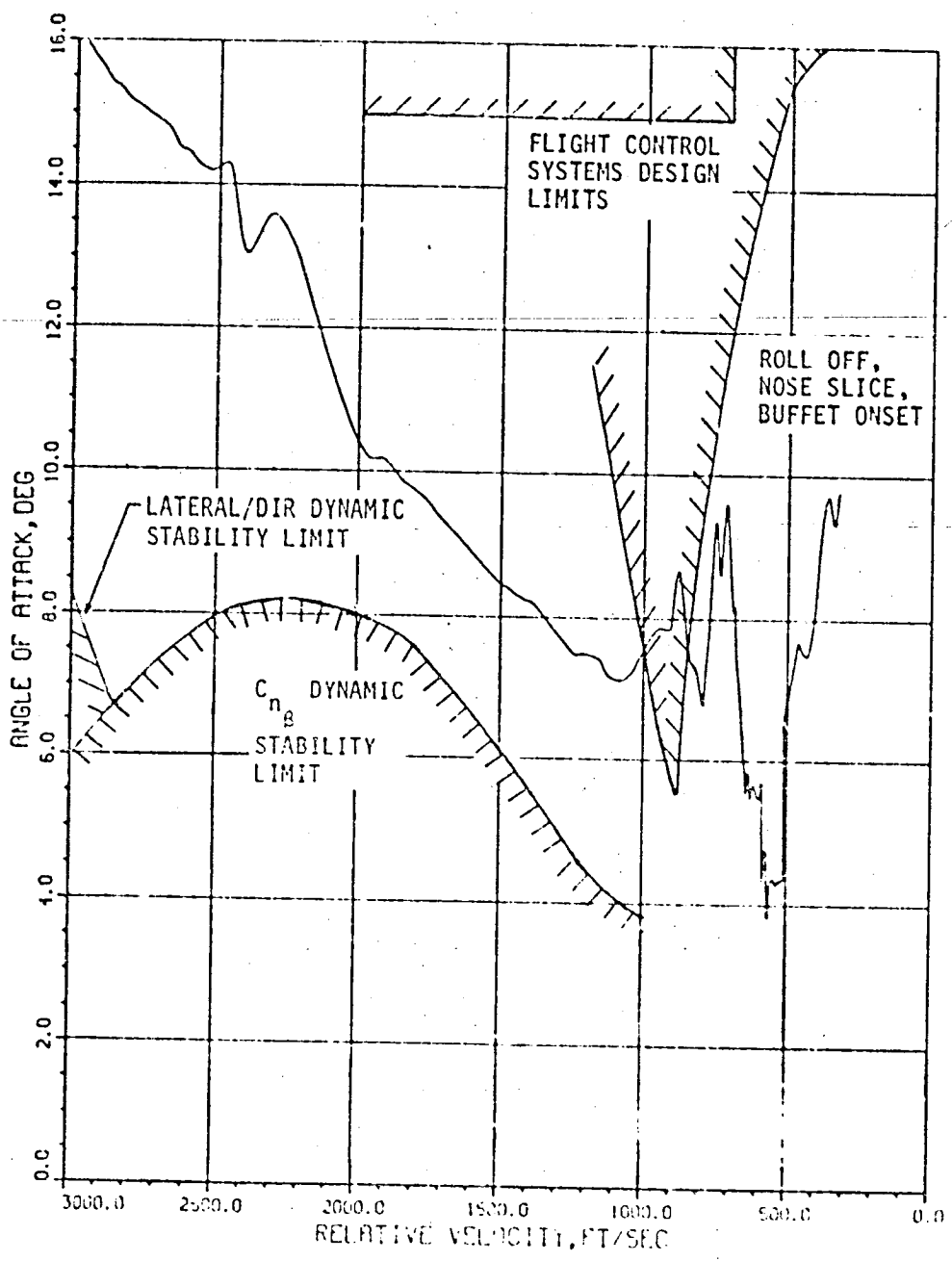


Figure 6.3-1--TACN through landing groundtrack.



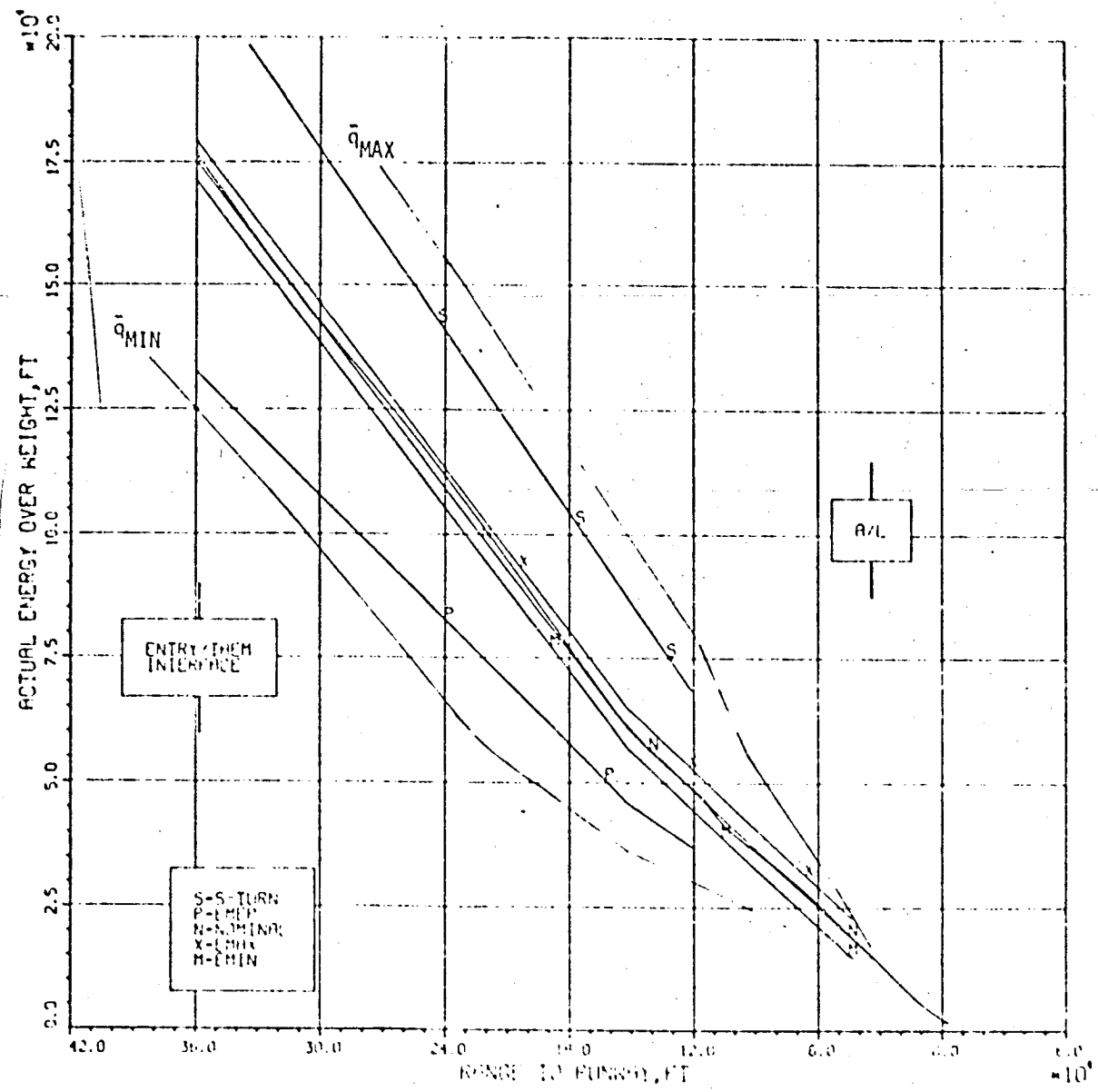
TAEM DYNAMIC PRESSURE CORRIDOR

Figure 6.3-2.



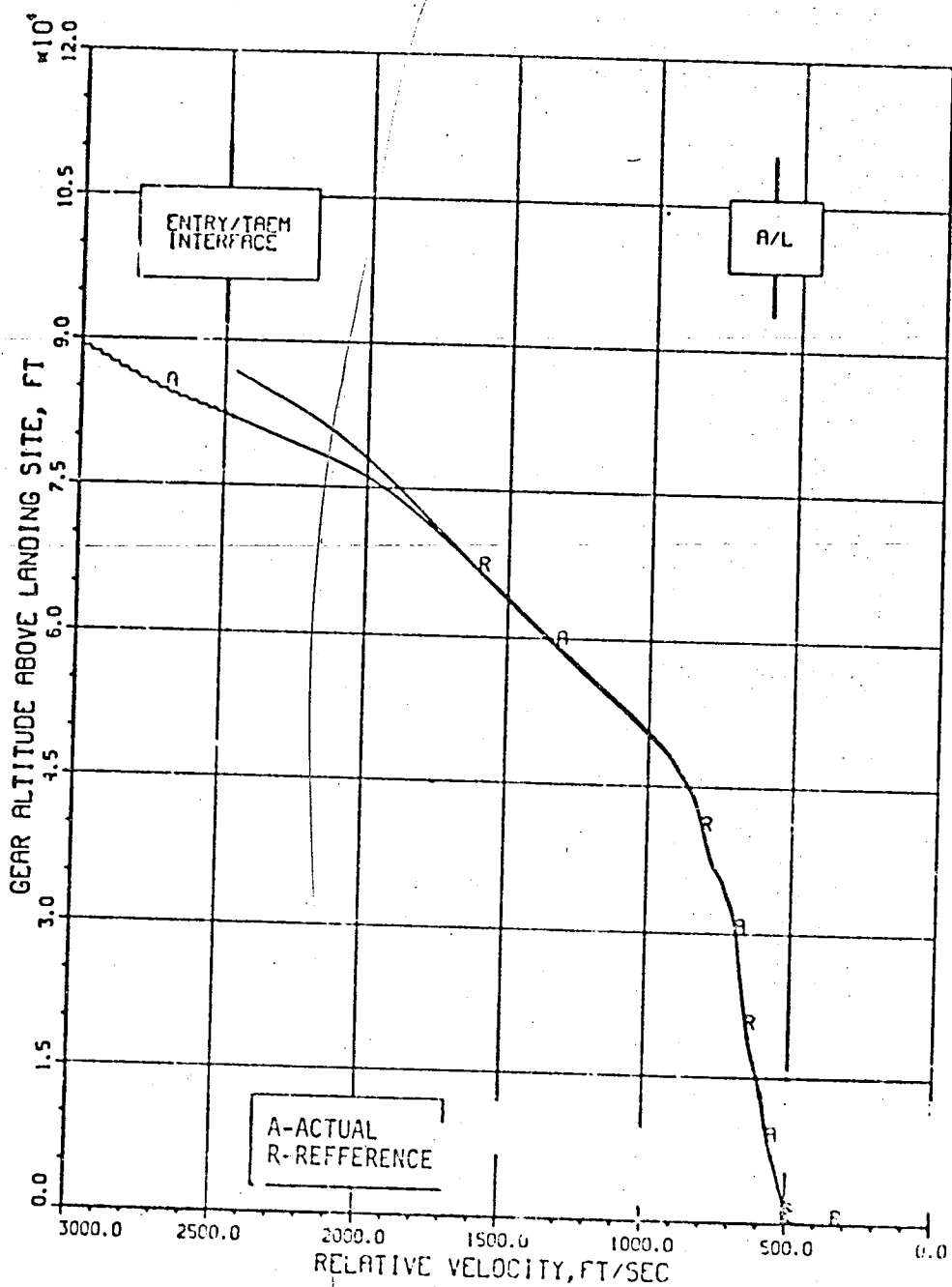
TALM ANGLE-OF-ATTACK CORRIDOR

Figure 6.3-3



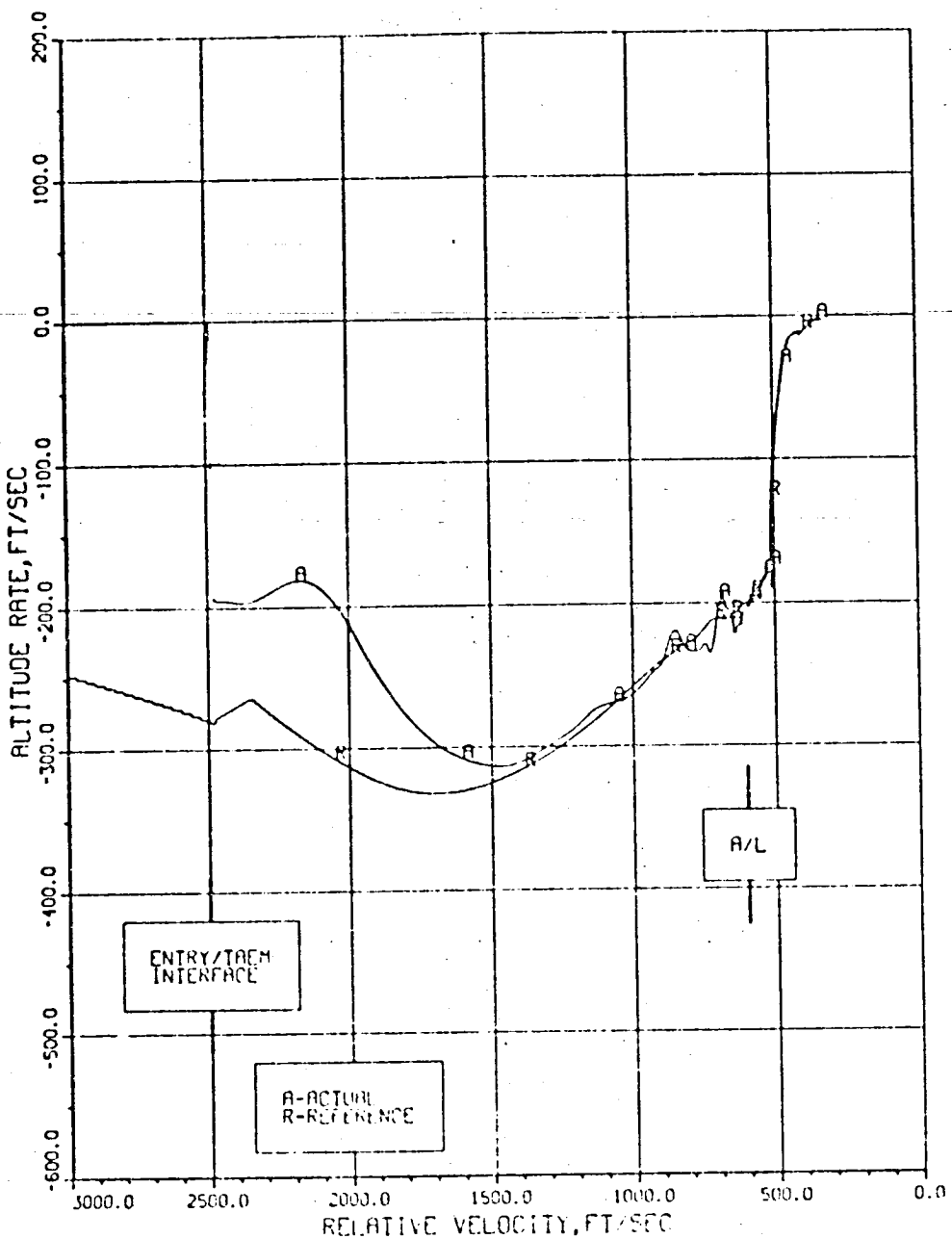
ACTUAL ENERGY OVER HEIGHT DURING TREM

Figure 6.3-4



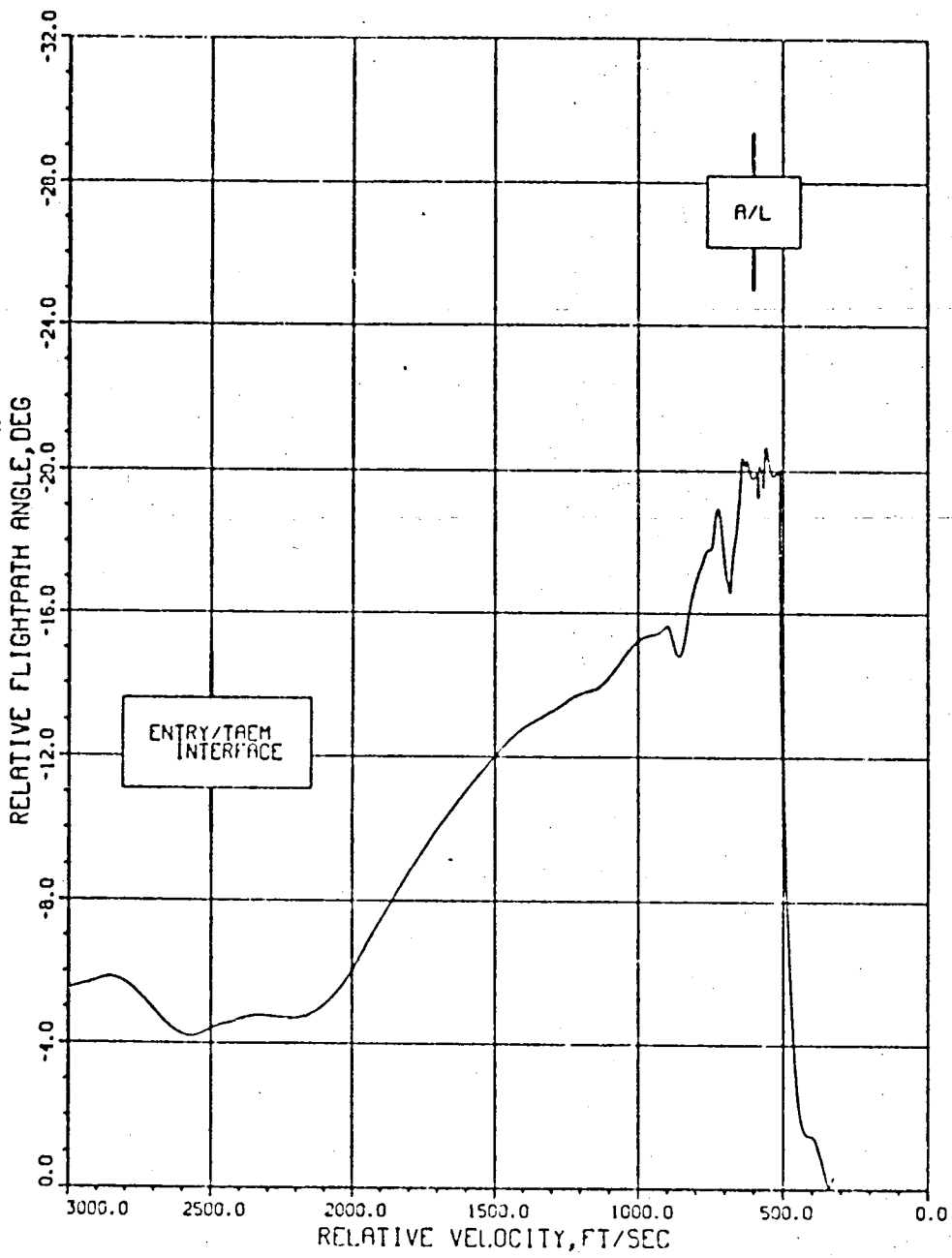
ALTITUDE AND ALTITUDE REFERENCE OF GEAR ABOVE LANDING SITE DURING TAEM

Figure 6.3-5



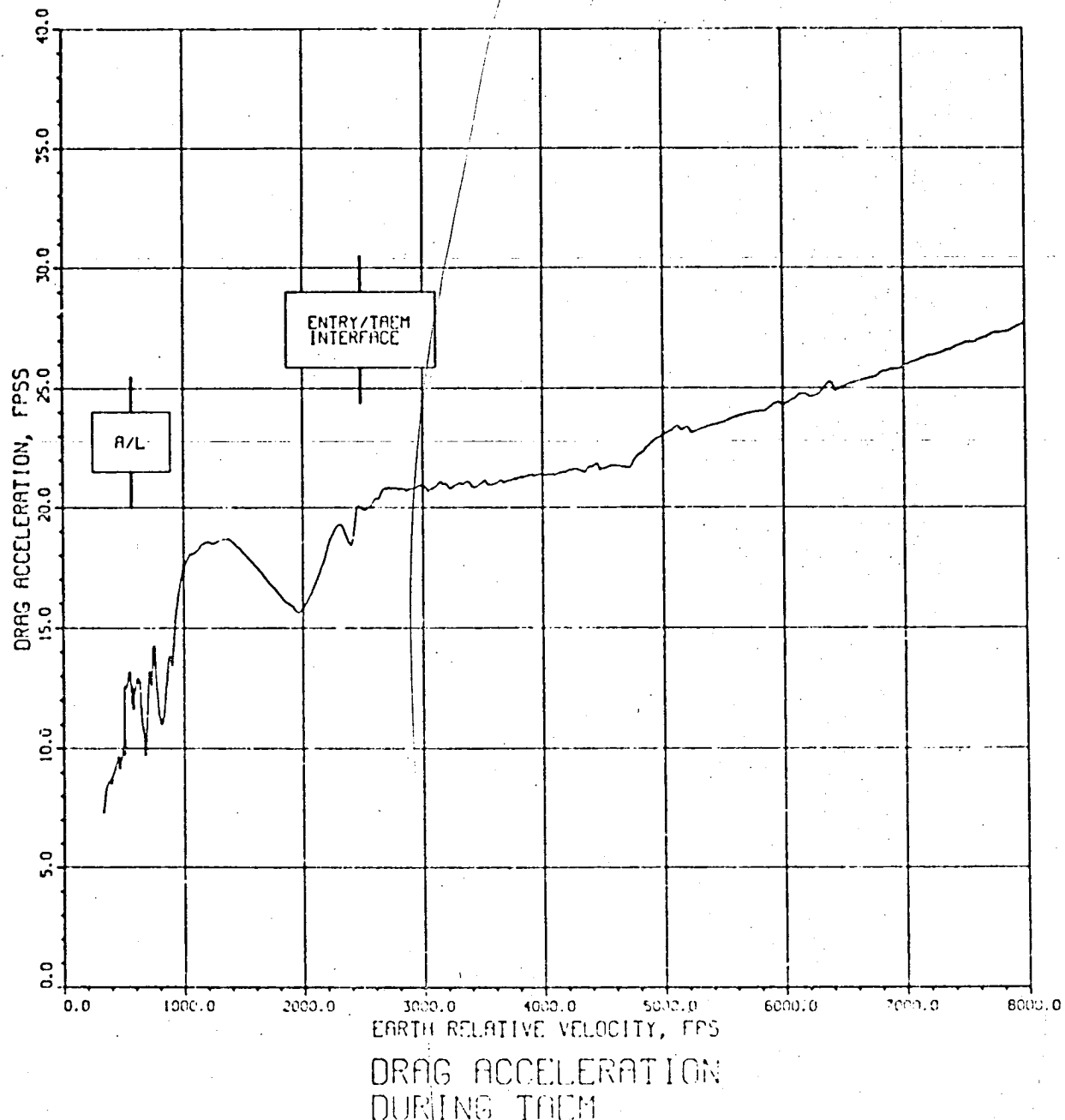
ALTITUDE RATE AND ALTITUDE RATE
REFERENCE DURING TREN

Figure 6.2-6



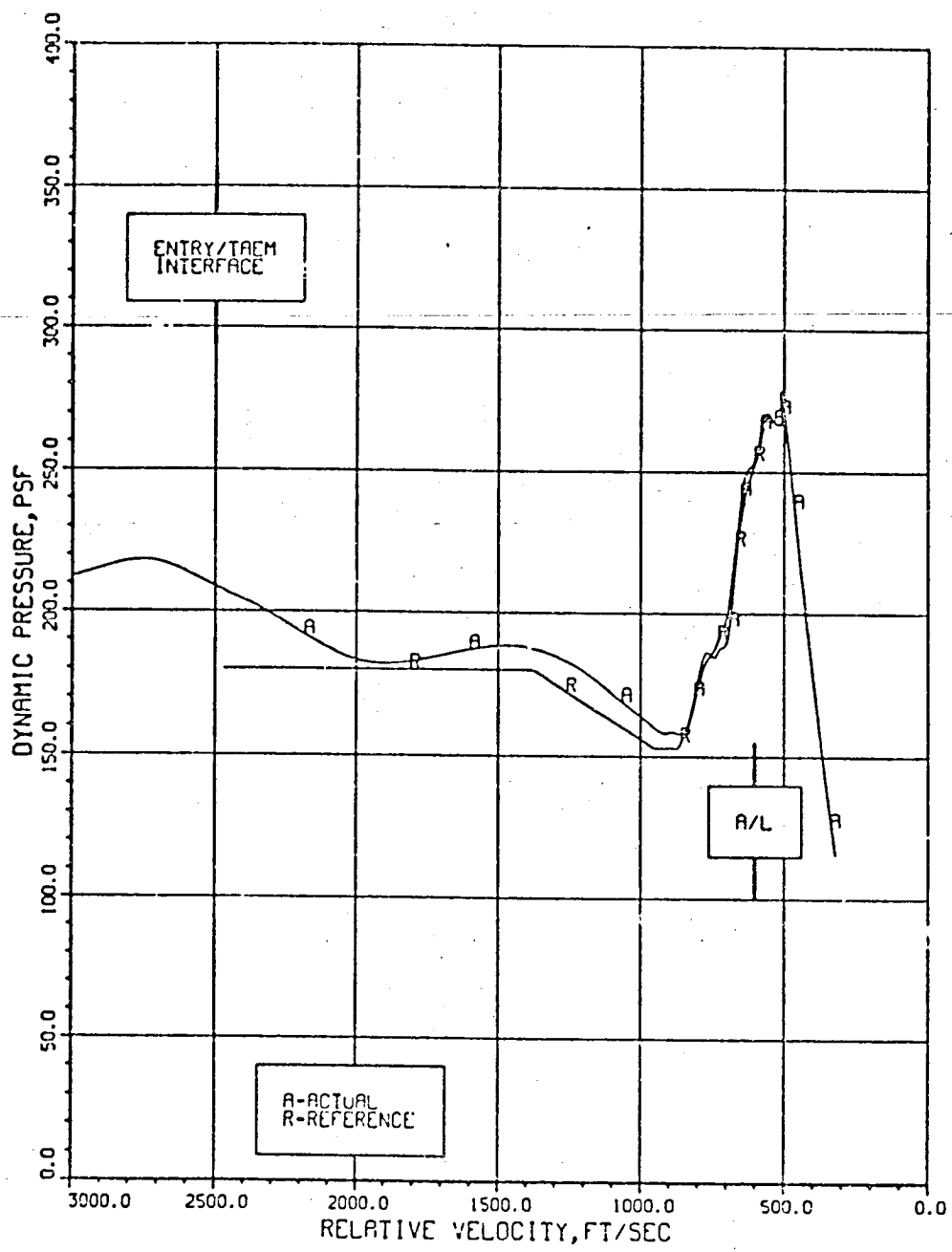
RELATIVE FLIGHTPATH ANGLE
DURING TADM

Figure 6.3-7



DRAG ACCELERATION
DURING TACM

Figure 6.3-8



ACTUAL AND REFERENCE DYNAMIC
PRESSURE DURING TAEM

Figure 6.3-9

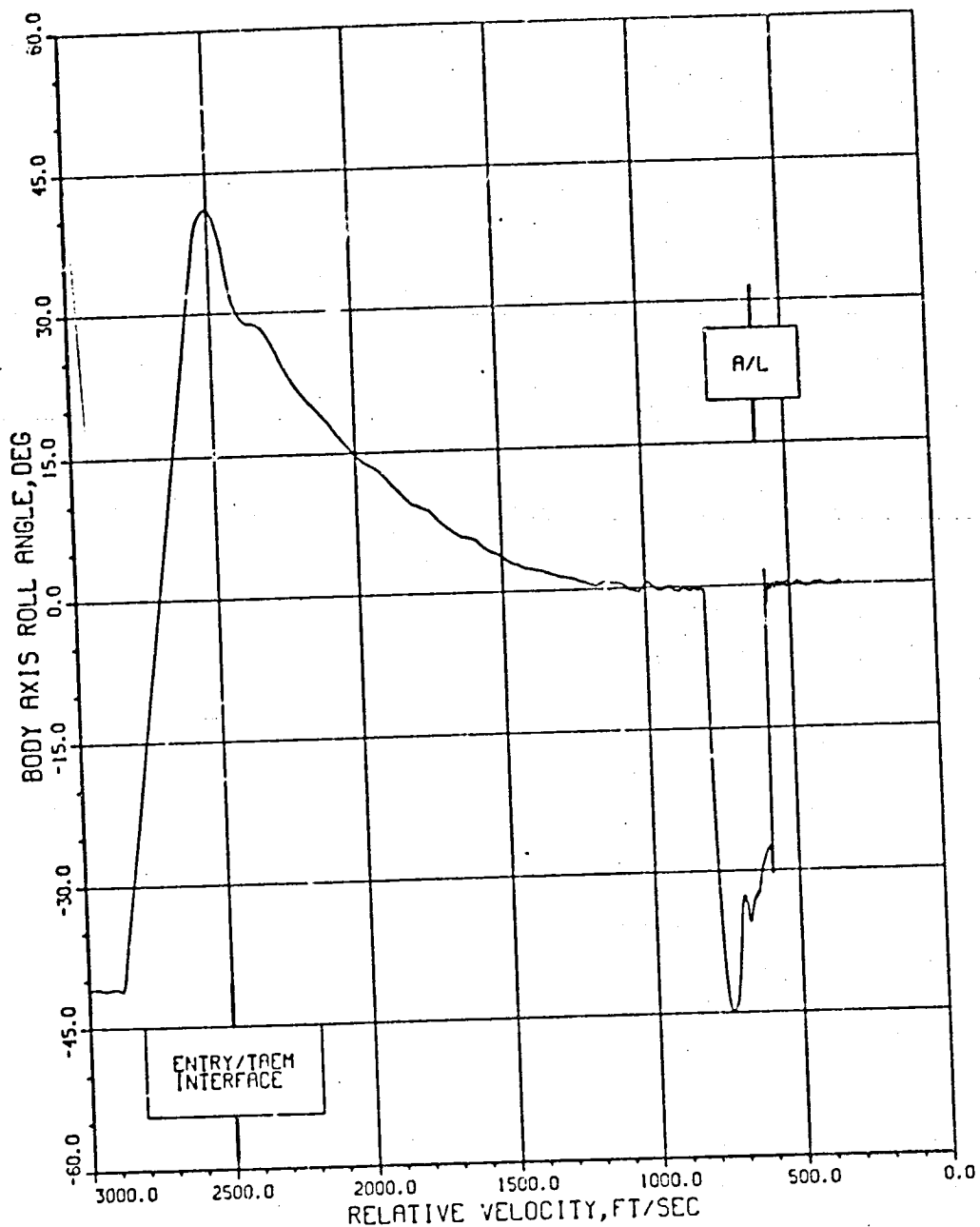
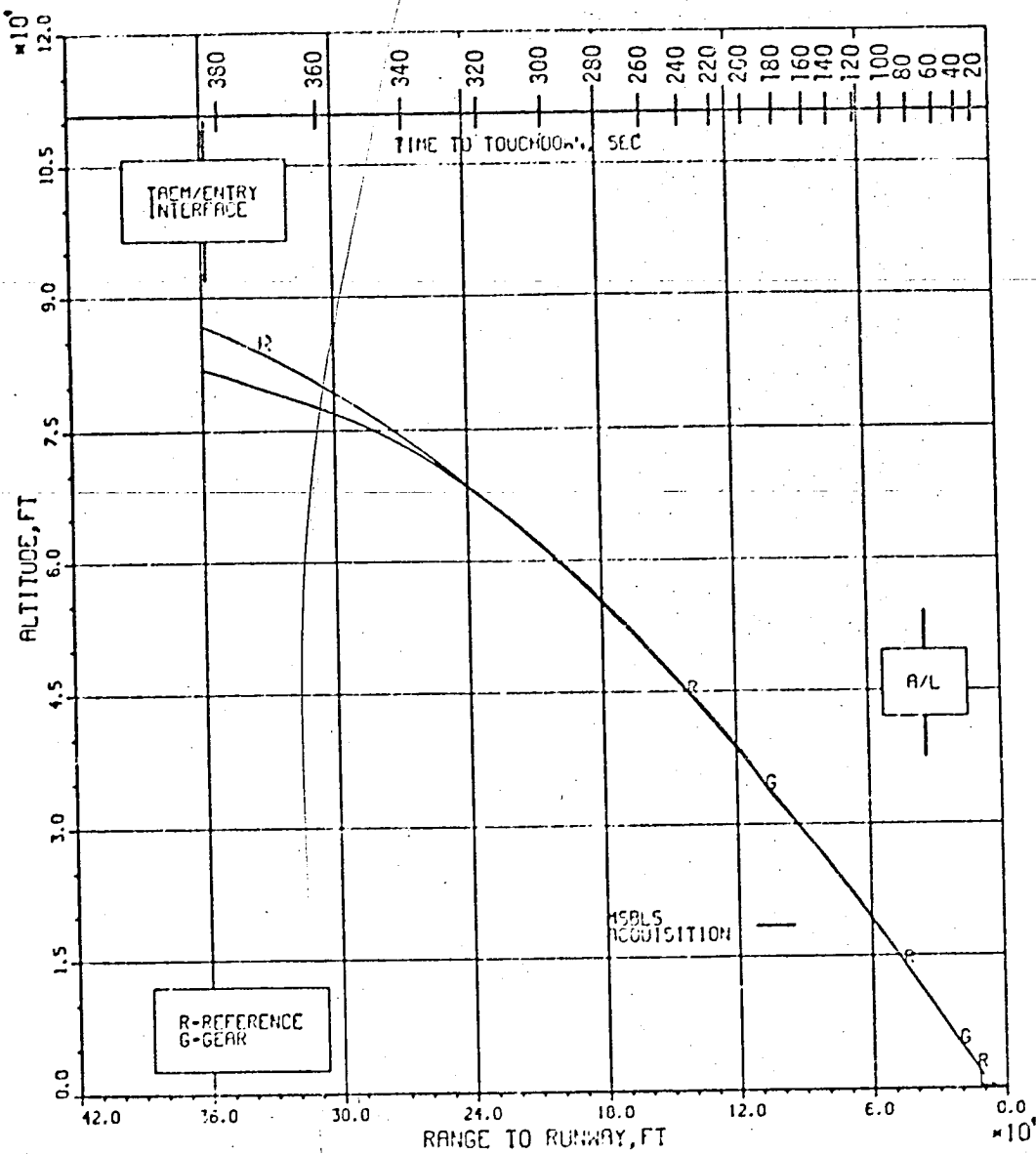
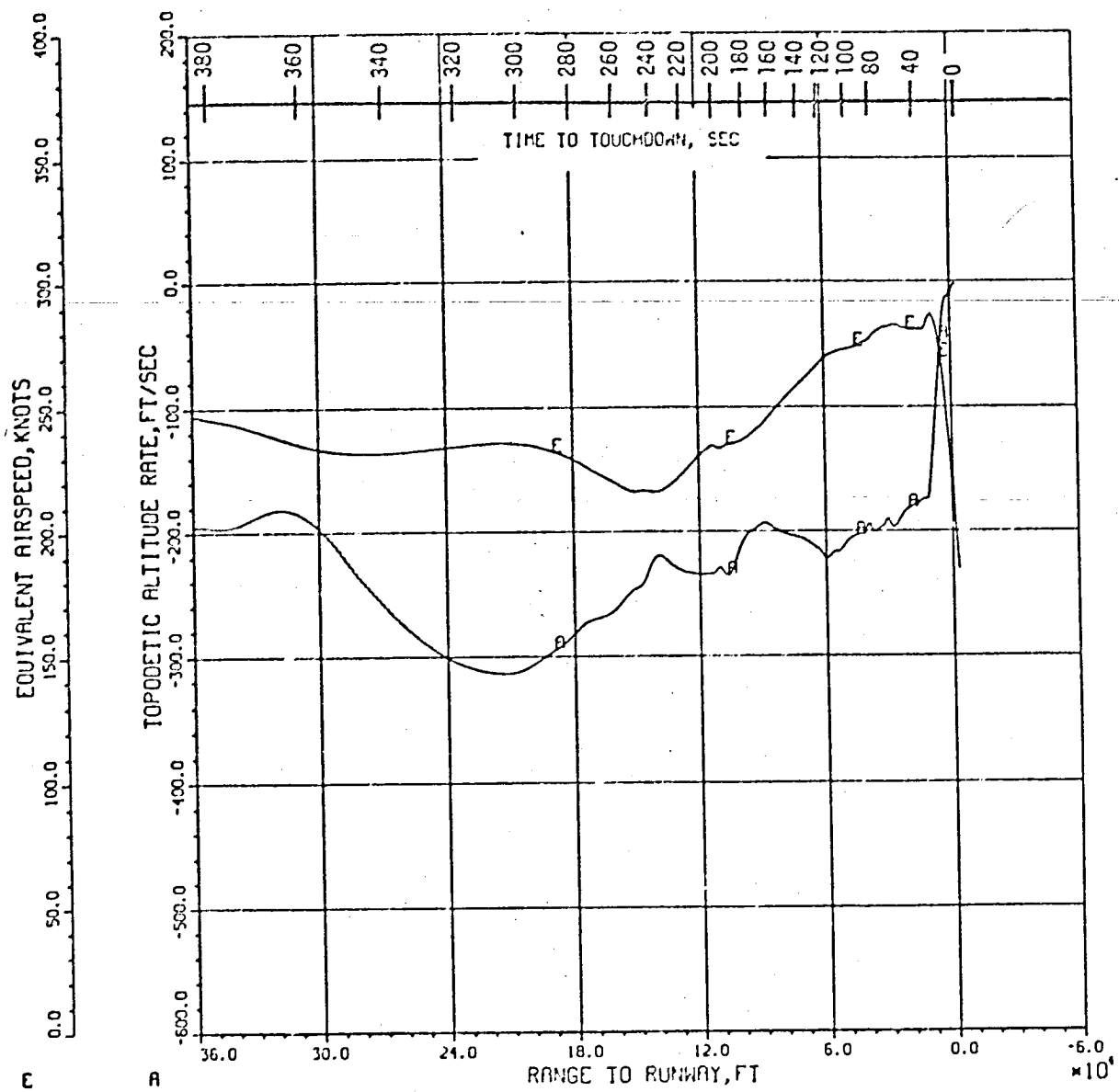


Figure 6.3-10



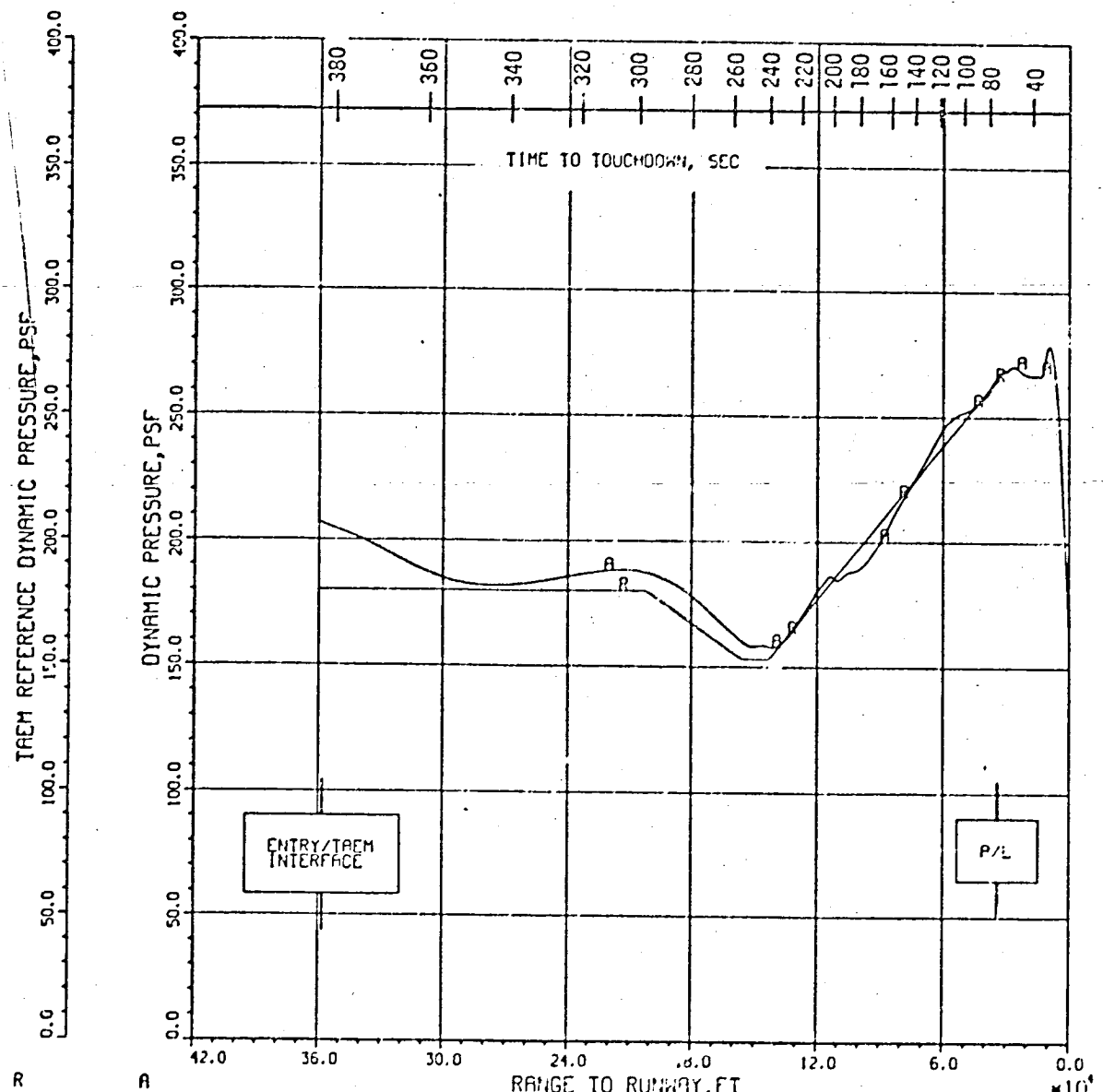
REFERENCE ALTITUDE AND GEAR ALTITUDE DURING TAKEOFF

Figure 6.3-11



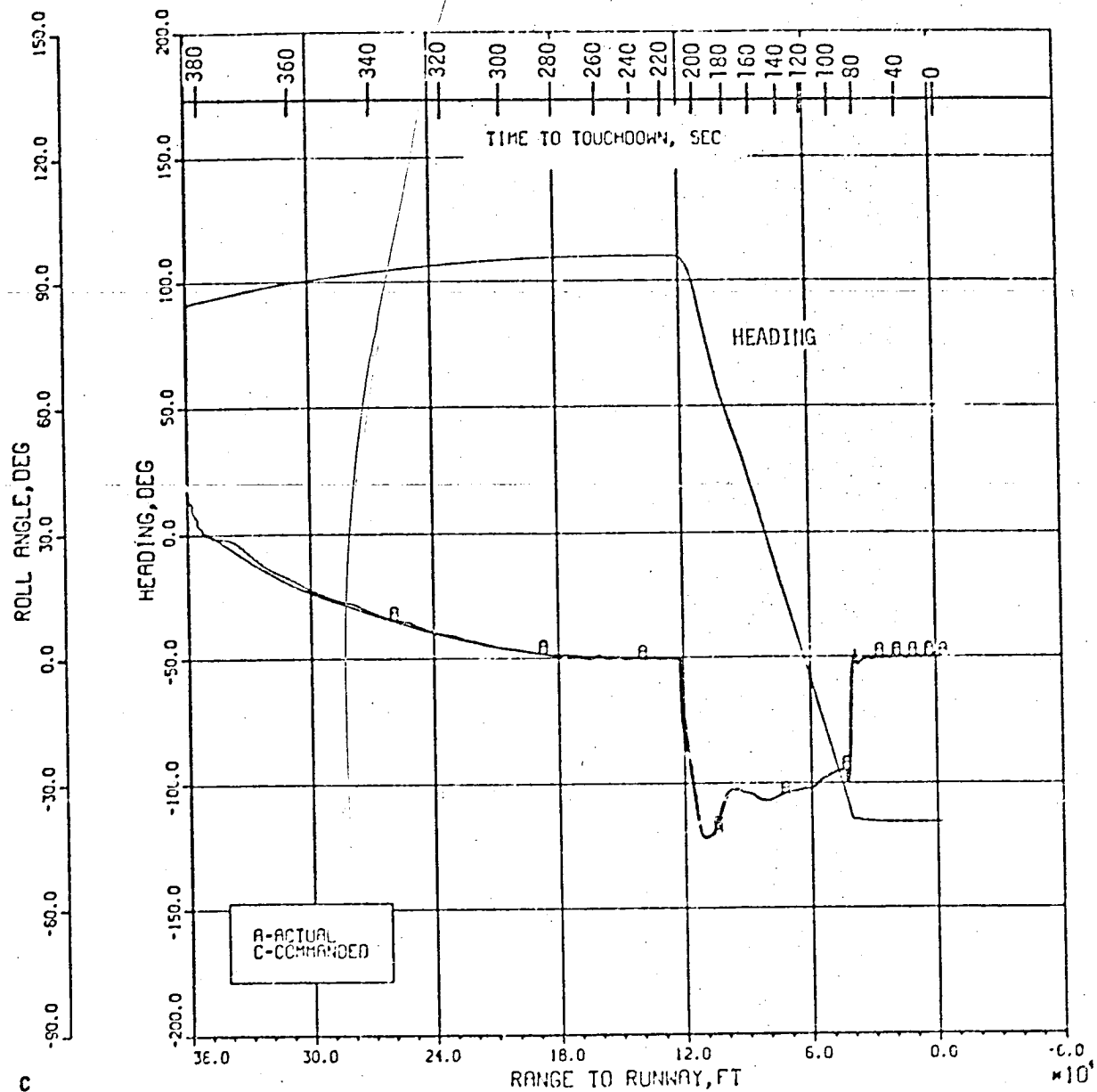
TOPODETIC ALTITUDE RATE AND EQUIVALENT
AIRSPEED DURING TACH

Figure 6.3-12



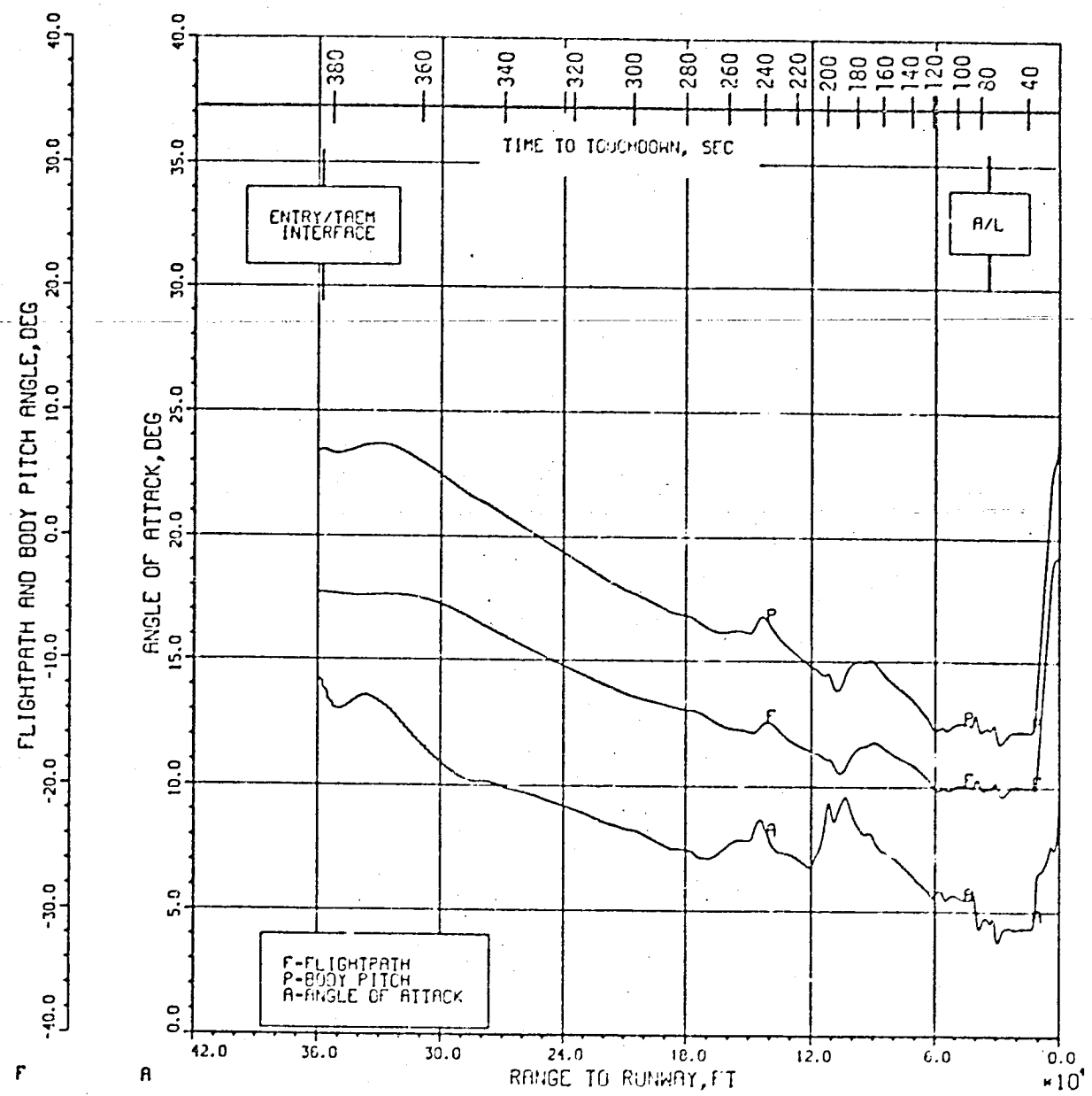
DYNAMIC PRESSURE AND REFERENCE DYNAMIC PRESSURE DURING TACM

Figure 6.3-13



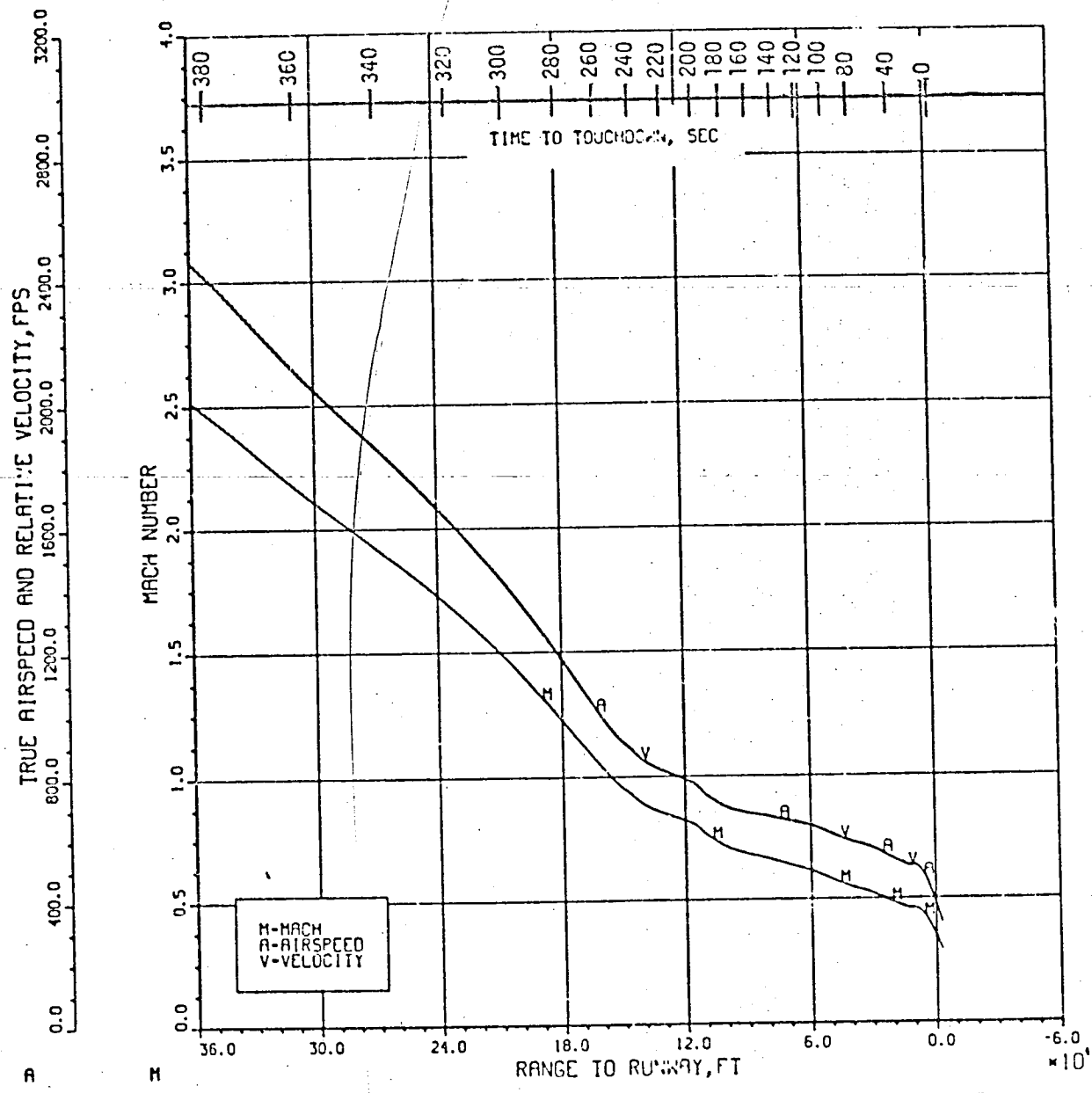
HEADING, ROLL ANGLE, AND COMMANDED
ROLL ANGLE DURING TDIM

Figure 6.3-14



FLIGHTPATH ANGLE, BODY PITCH ANGLE,
AND ANGLE OF ATTACK DURING TADM

Figure 6..15



TRUE AIRSPEED, EARTH RELATIVE VELOCITY,
AND MACH NO. DURING TAFM

Figure 6.3-16

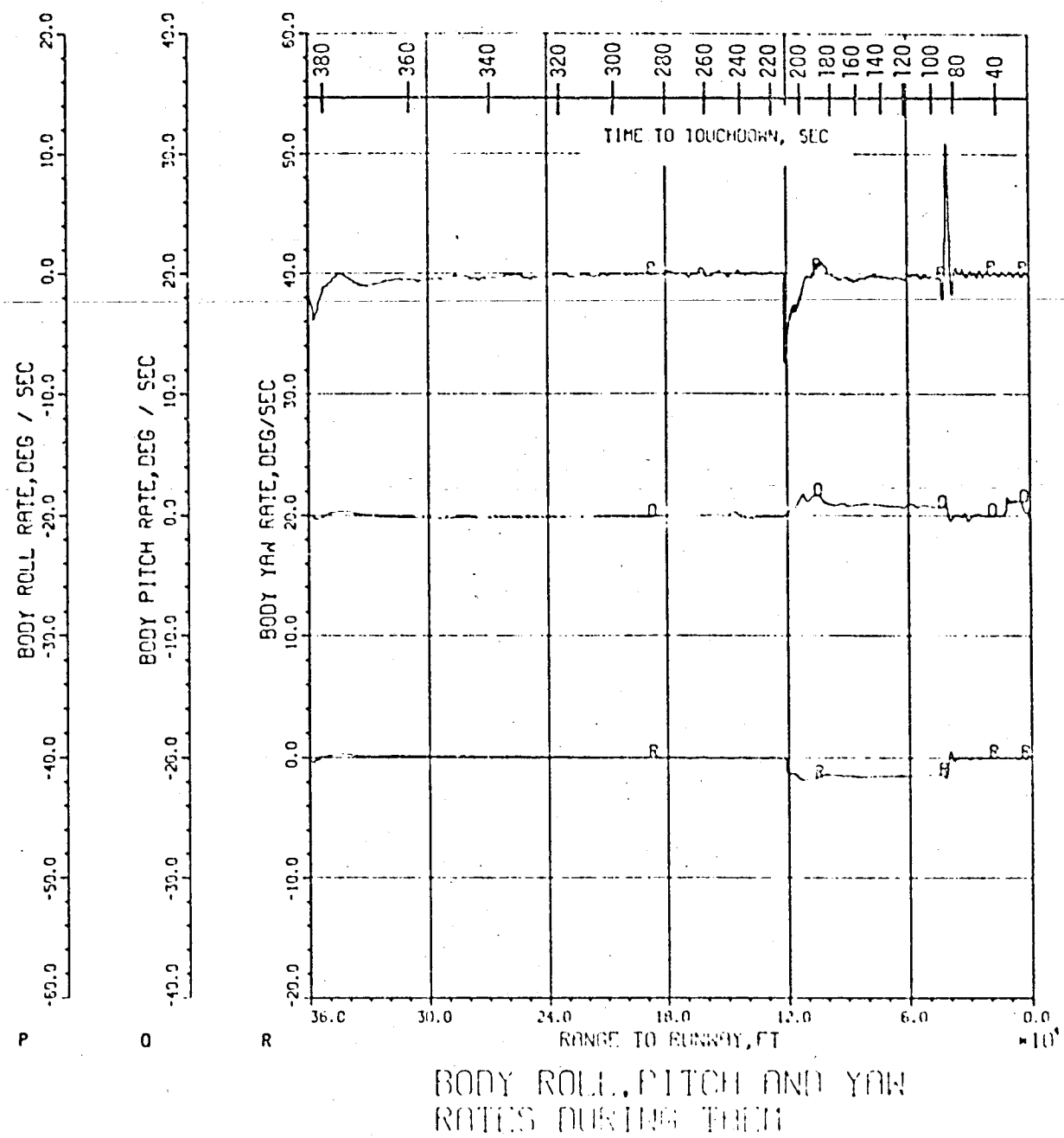
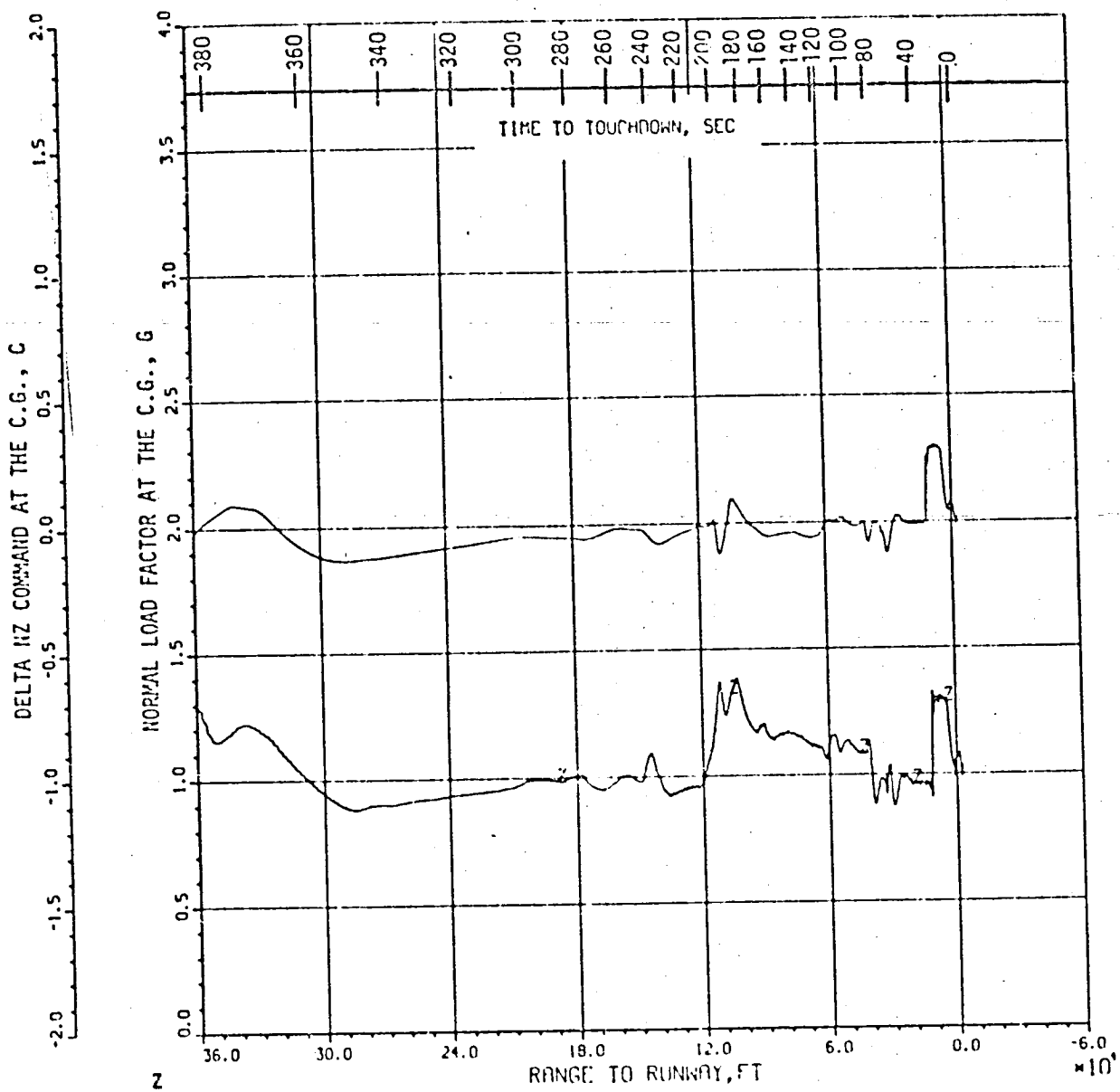


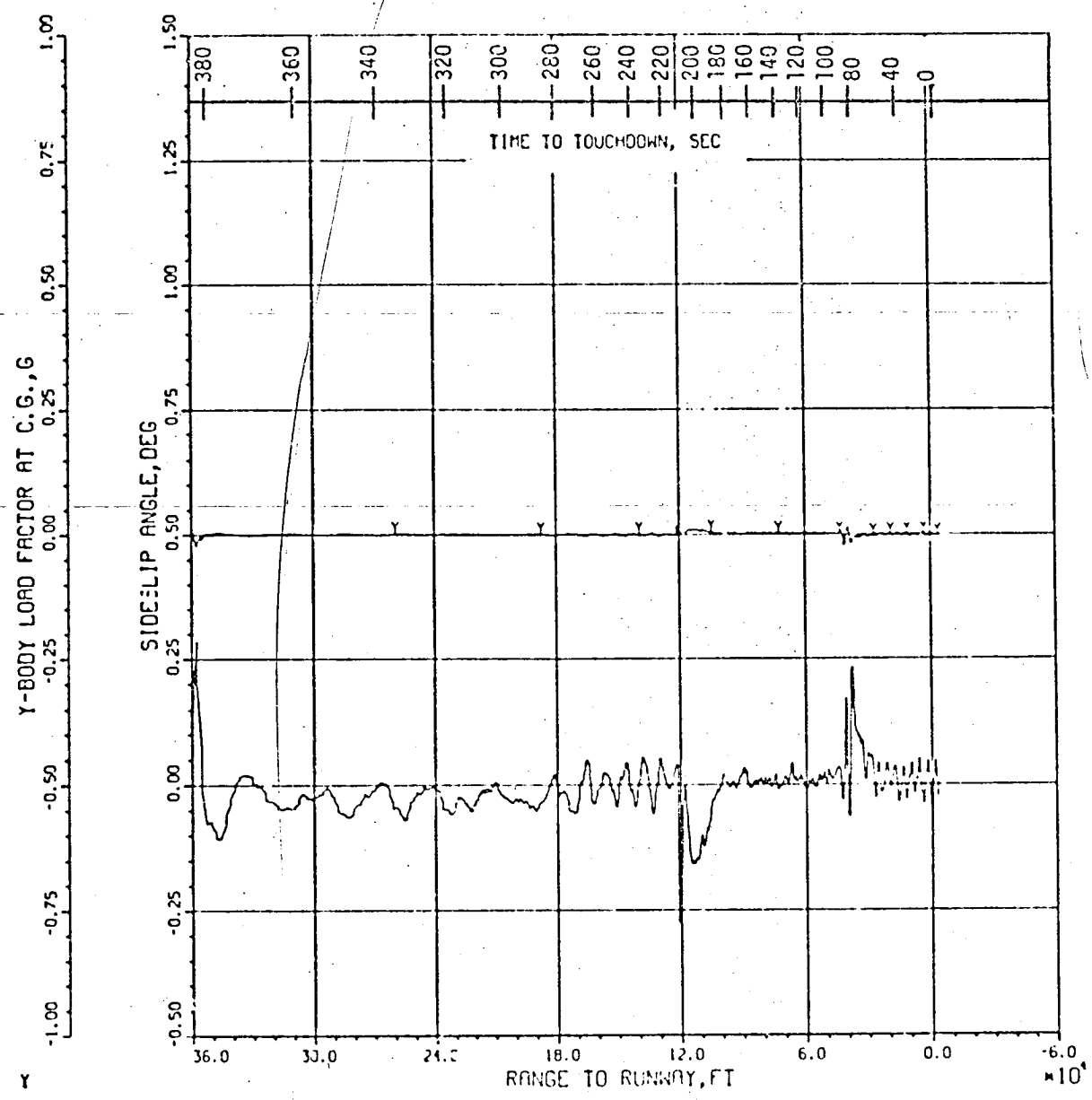
Figure 6.3-17

ORIGINAL PAGE F
1173



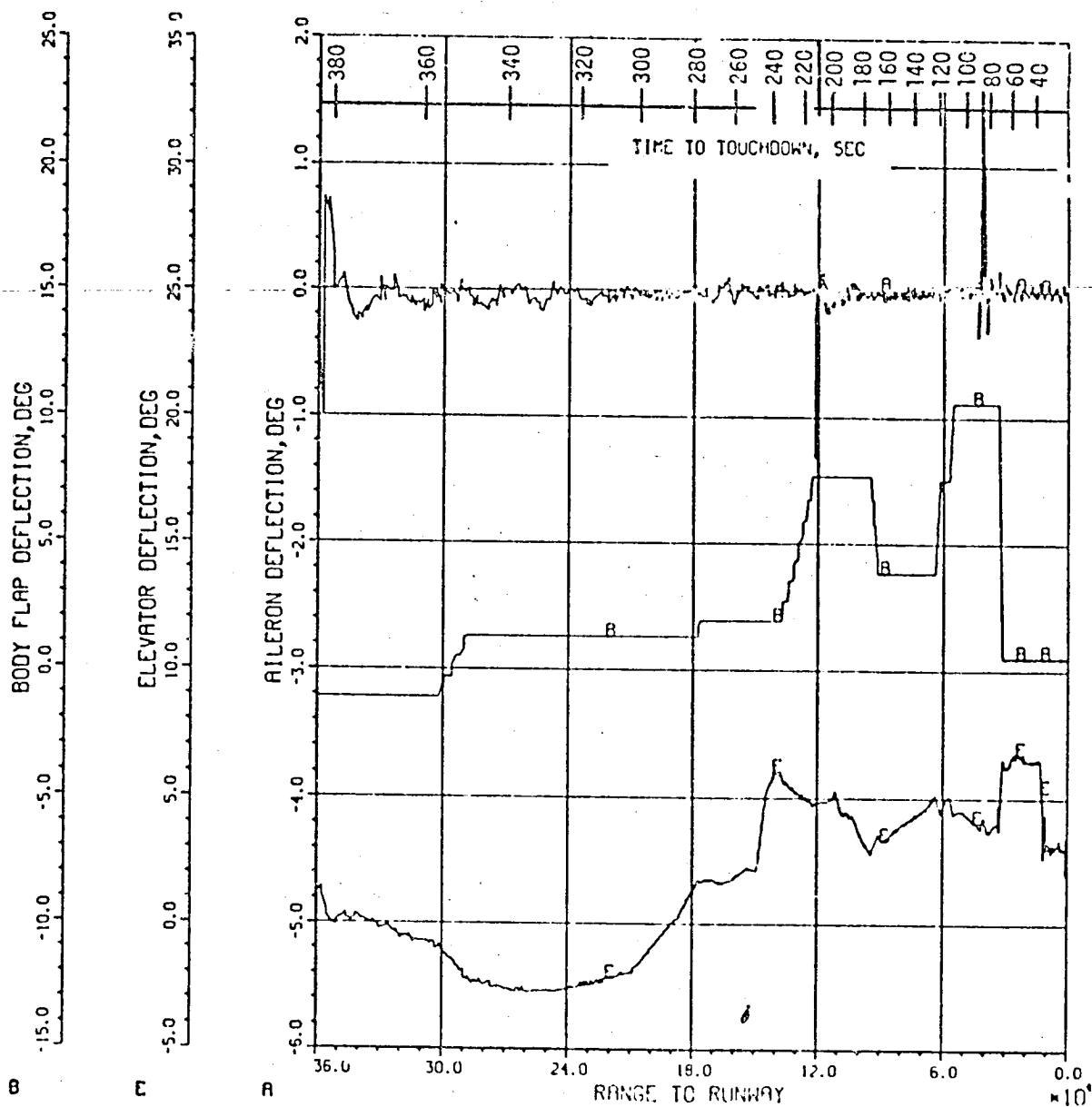
NORMAL LOAD FACTOR AND DELTA NZ
COMMAND AT THE C.G. DURING TACM

Figure 6.3-18



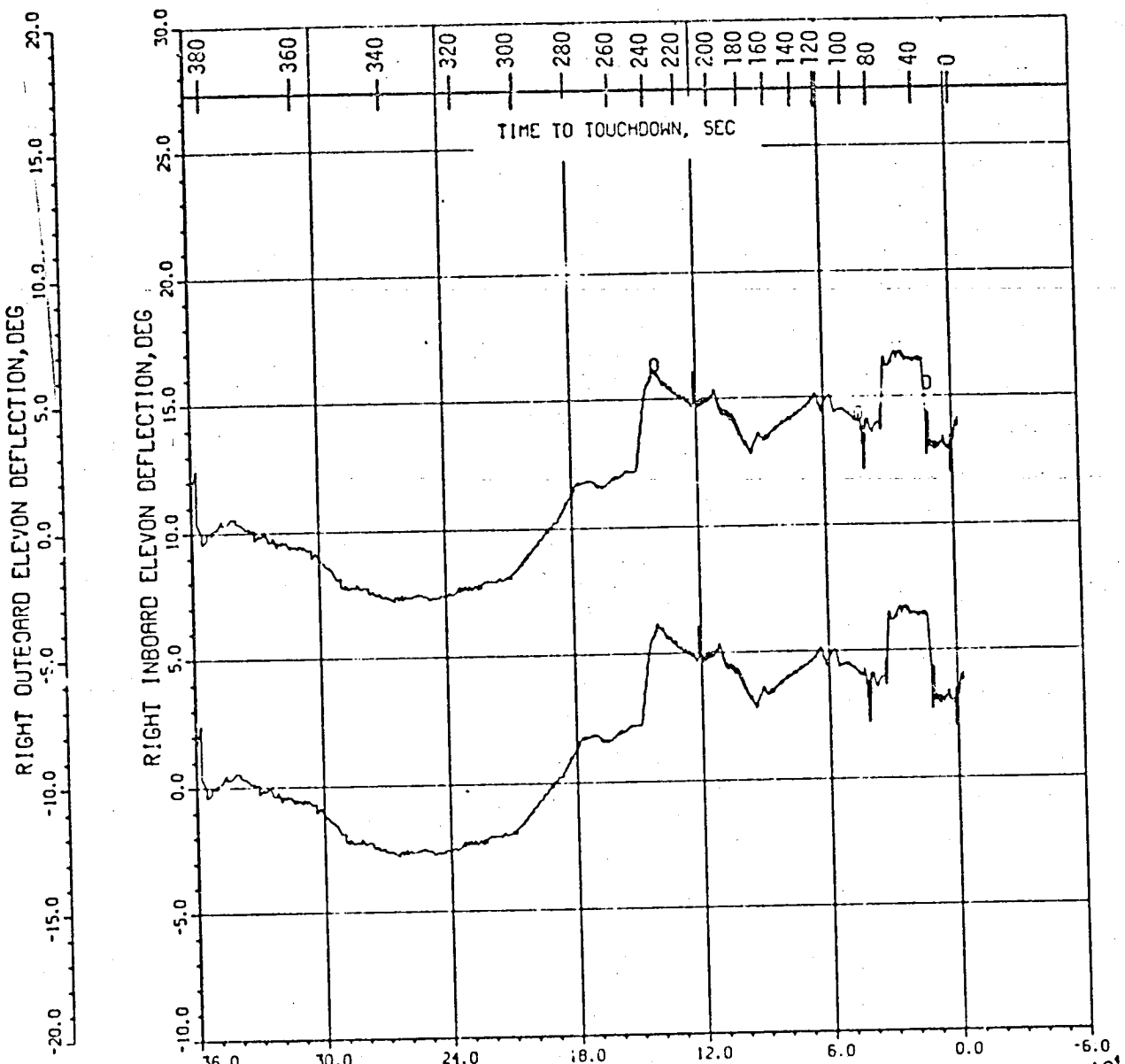
SIDESLIP ANGLE AND Y-BODY LOAD FACTOR
AT THE C.G. DURING TAKEOFF

Figure 6.3-19



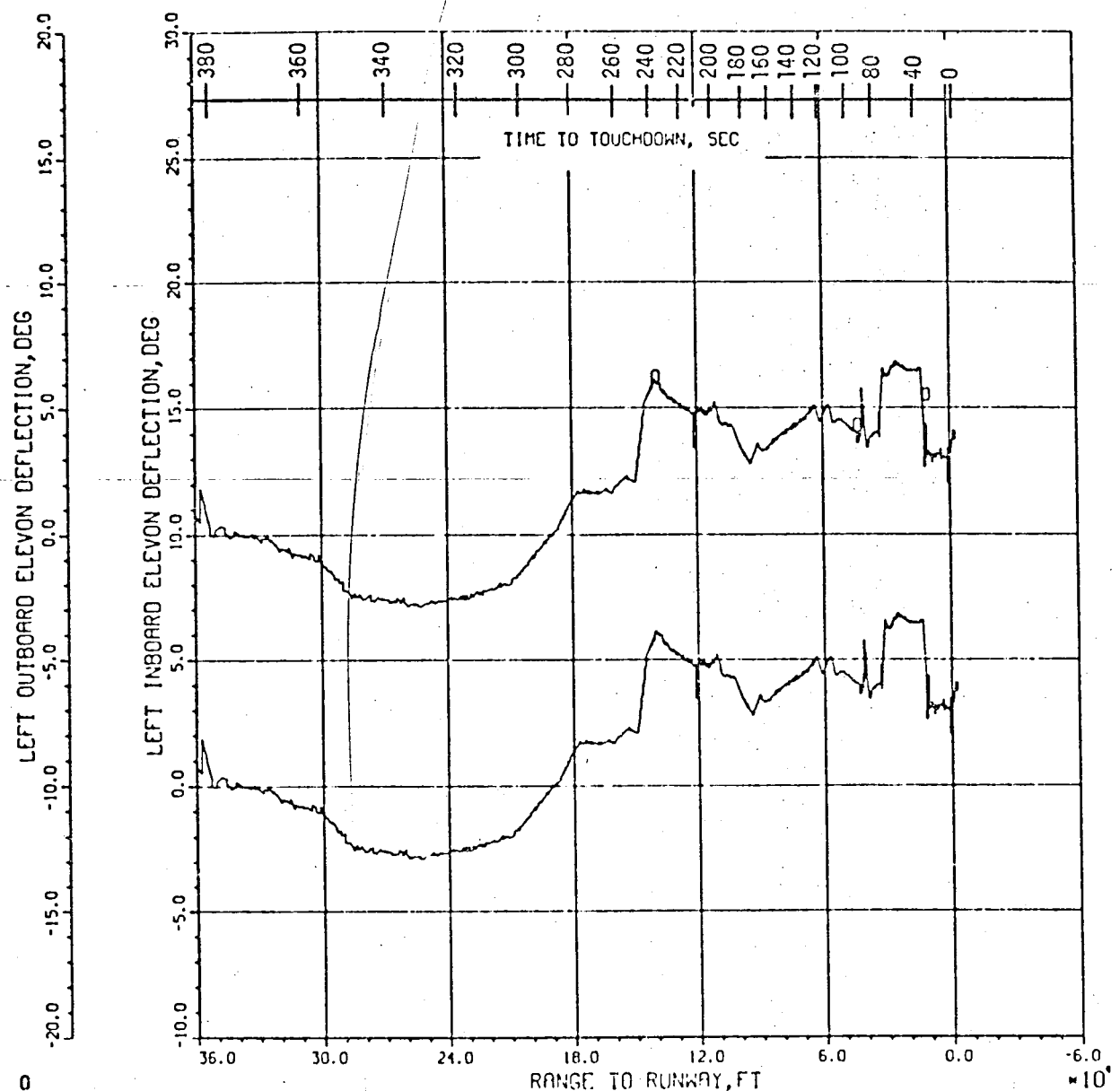
AILERON, ELEVATOR AND BODY FLAP DEFLECTION DURING TEST

Figure 6.3-20



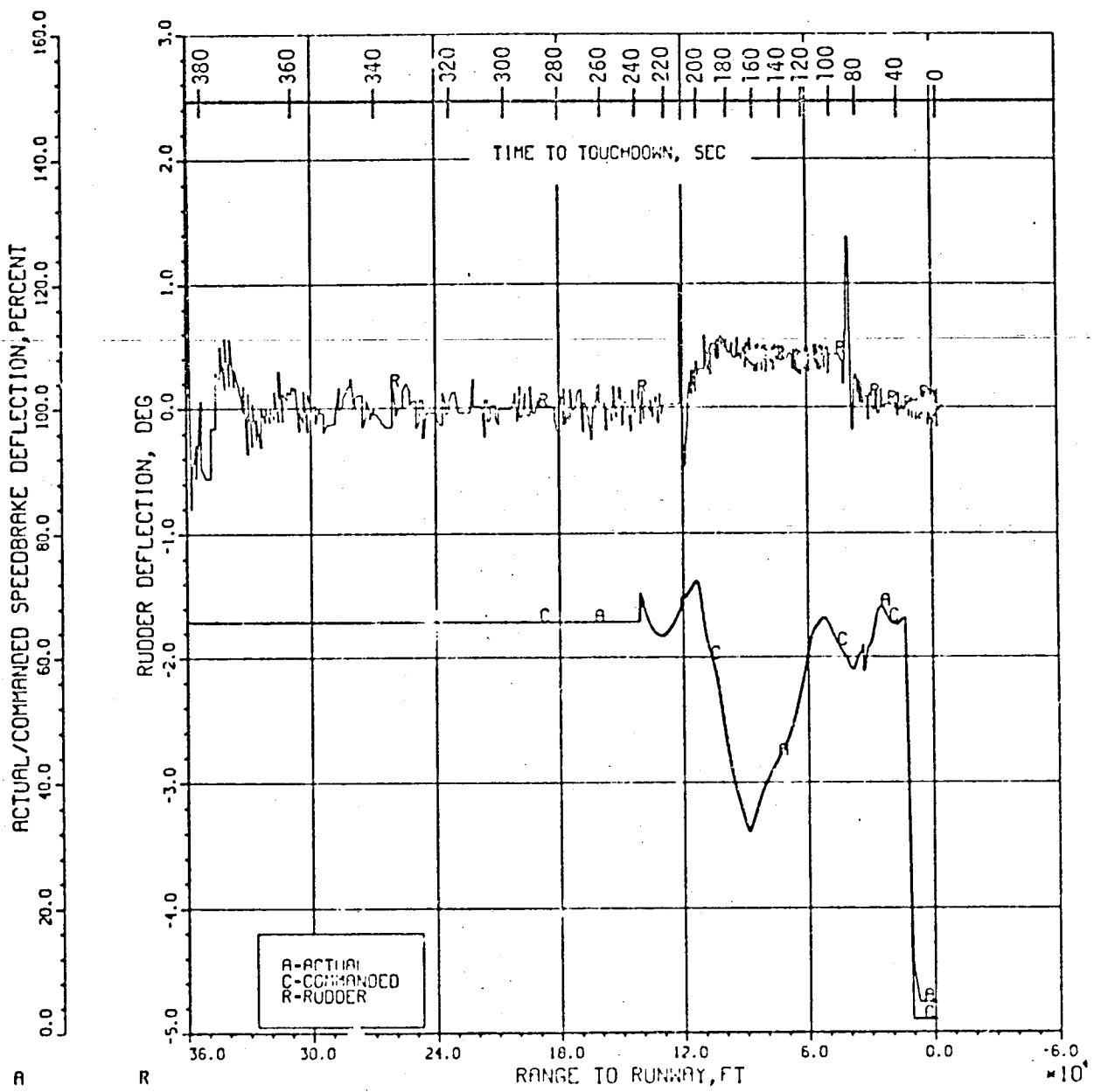
RIGHT ELEVON DEFLECTION DURING TAEM

Figure 6.3-21



LEFT ELEVON DEFLECTION
DURING TDEM

Figure 6.3-22



ACTUAL, COMMANDED SPEEDBRAKE DEFLECTION
AND RUDDER DEFLECTION DURING TAUCH

Figure 6.3-23

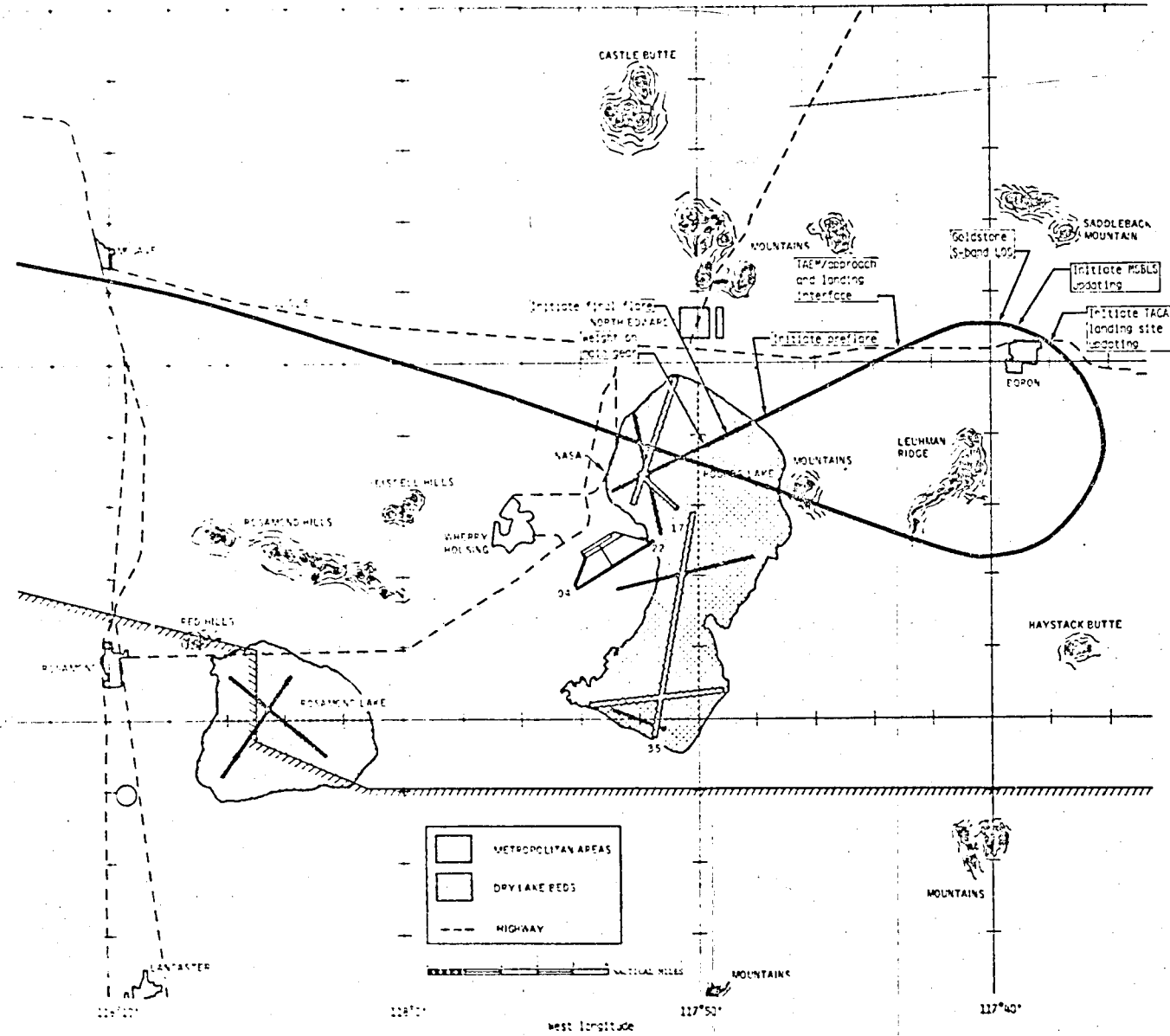
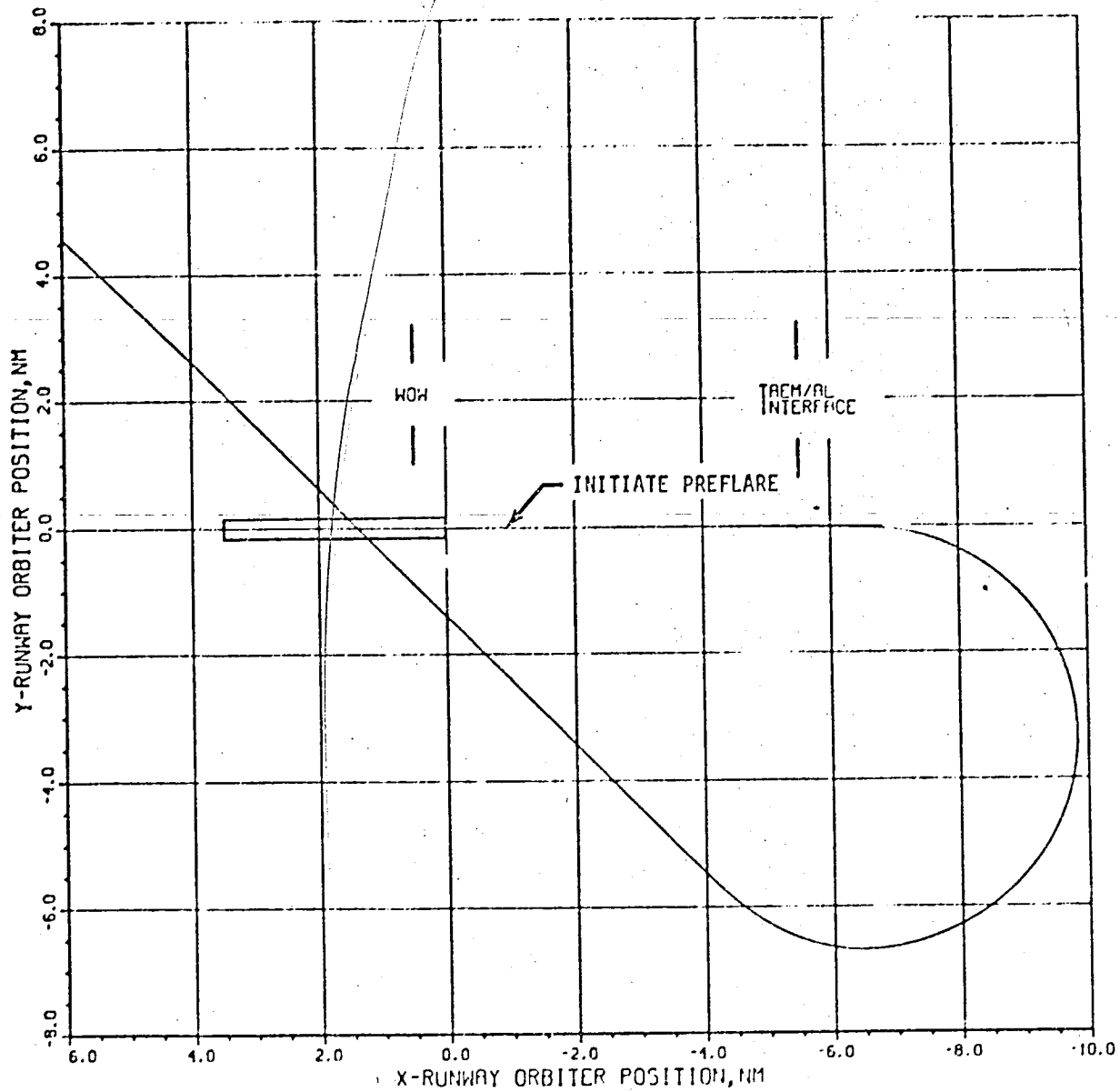


Figure 6.4-1. Approach and landing groundtrack.



ORBITER POSITION WITH RESPECT TO RUNWAY
IN THE VICINITY OF THE END

Figure 6.4-2

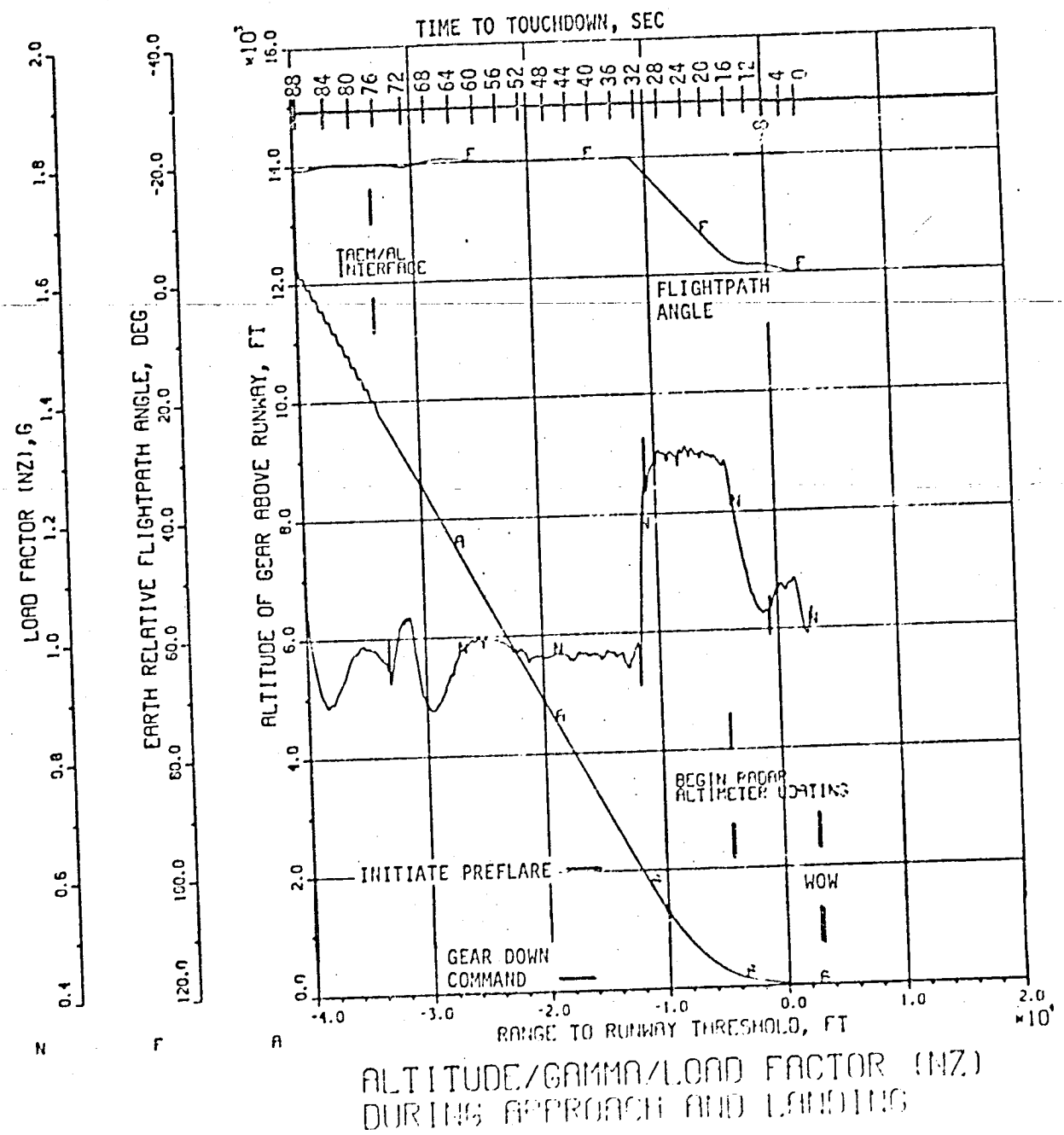
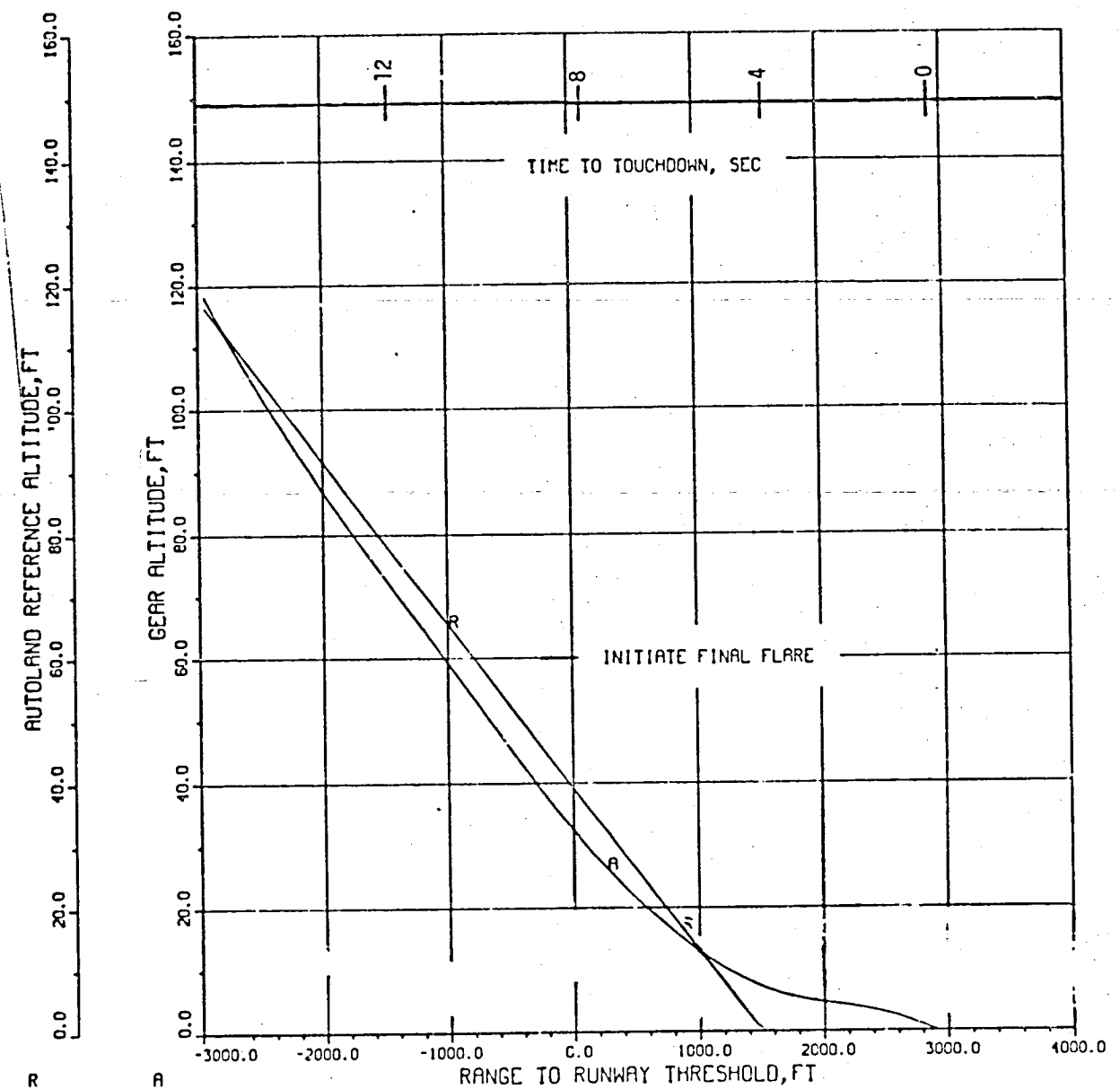
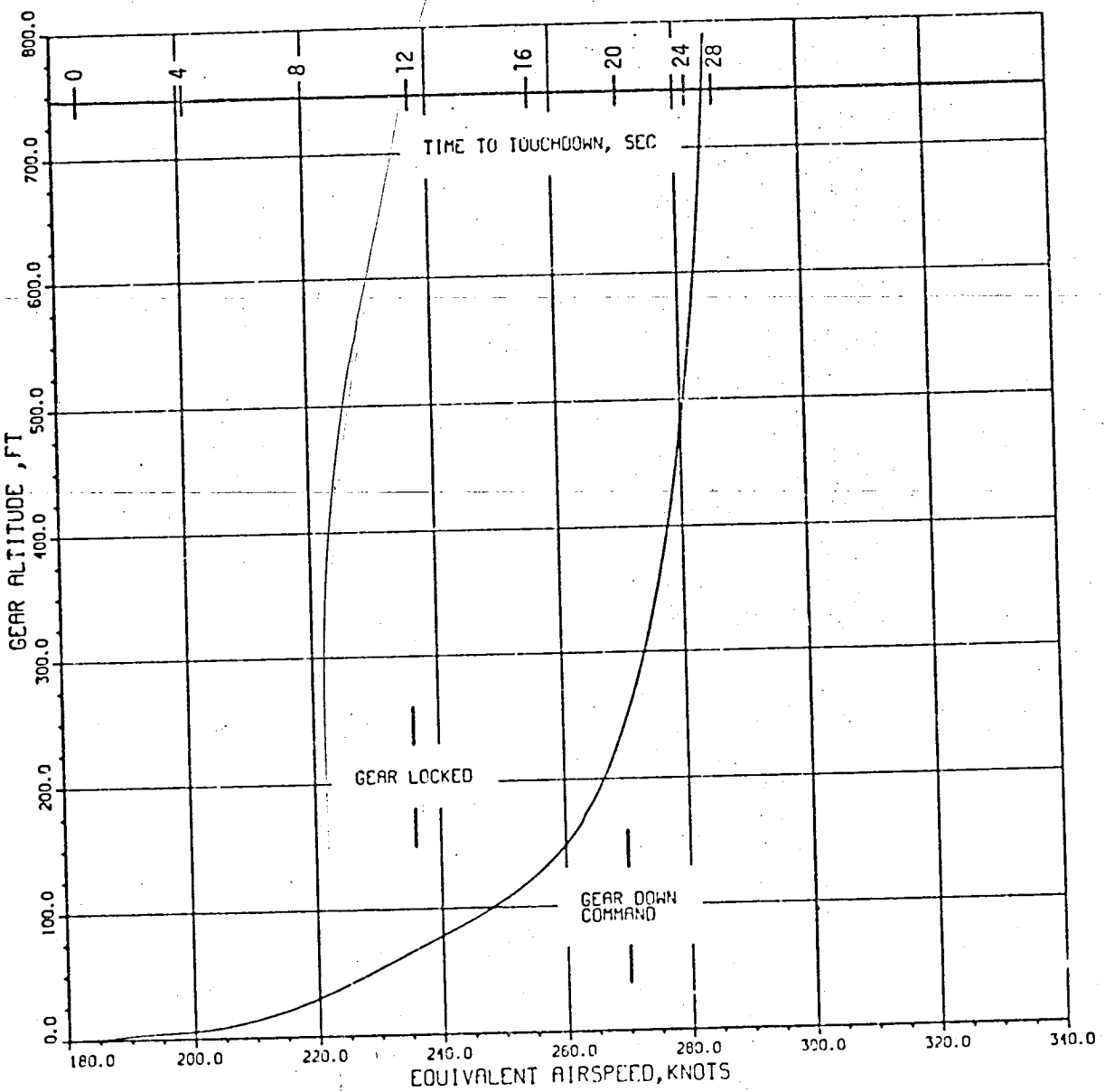


Figure 6.4-3



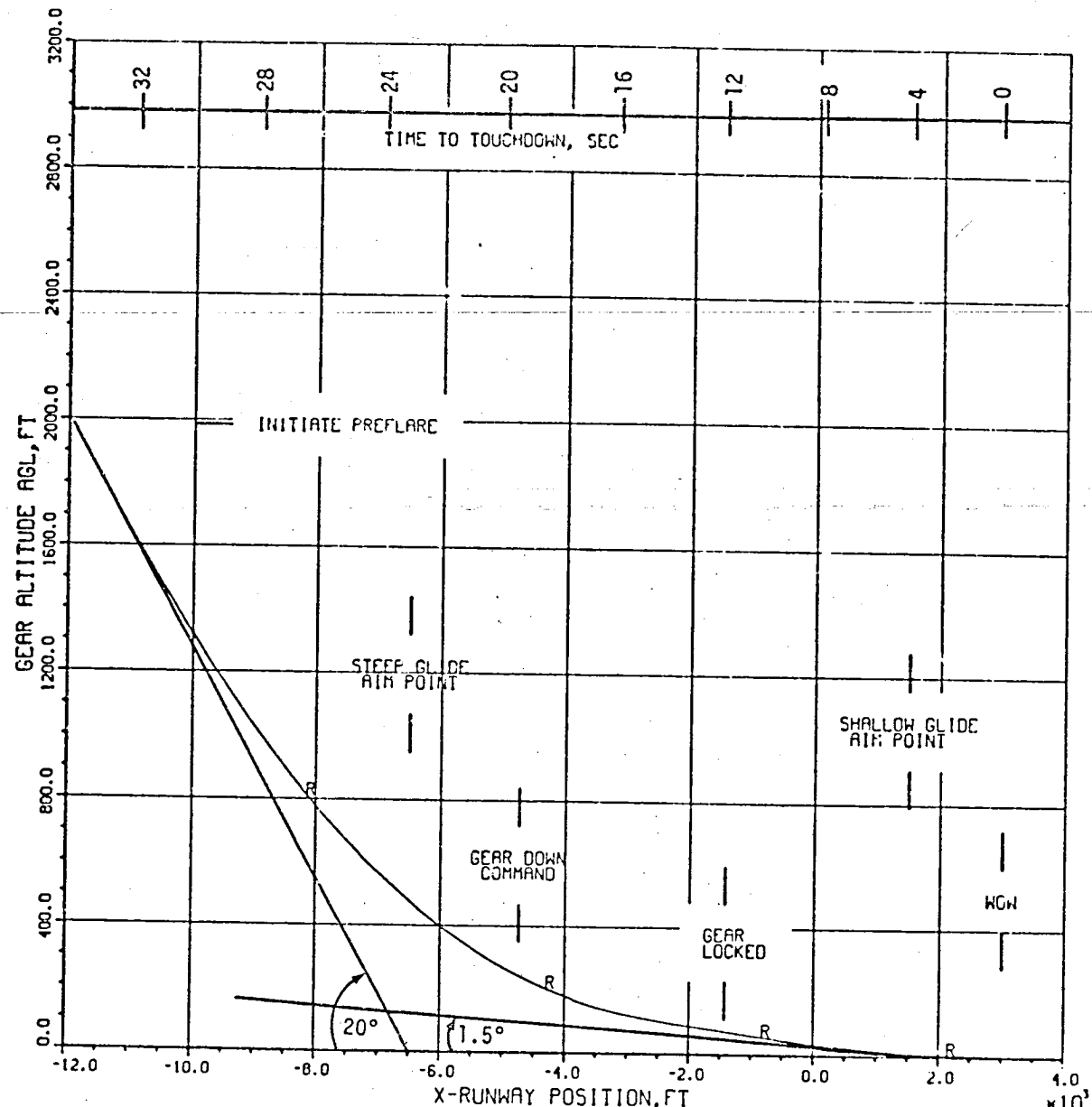
GEAR ALTITUDE FROM FINAL FLARE TO TOUCHDOWN

Figure 6.4-4



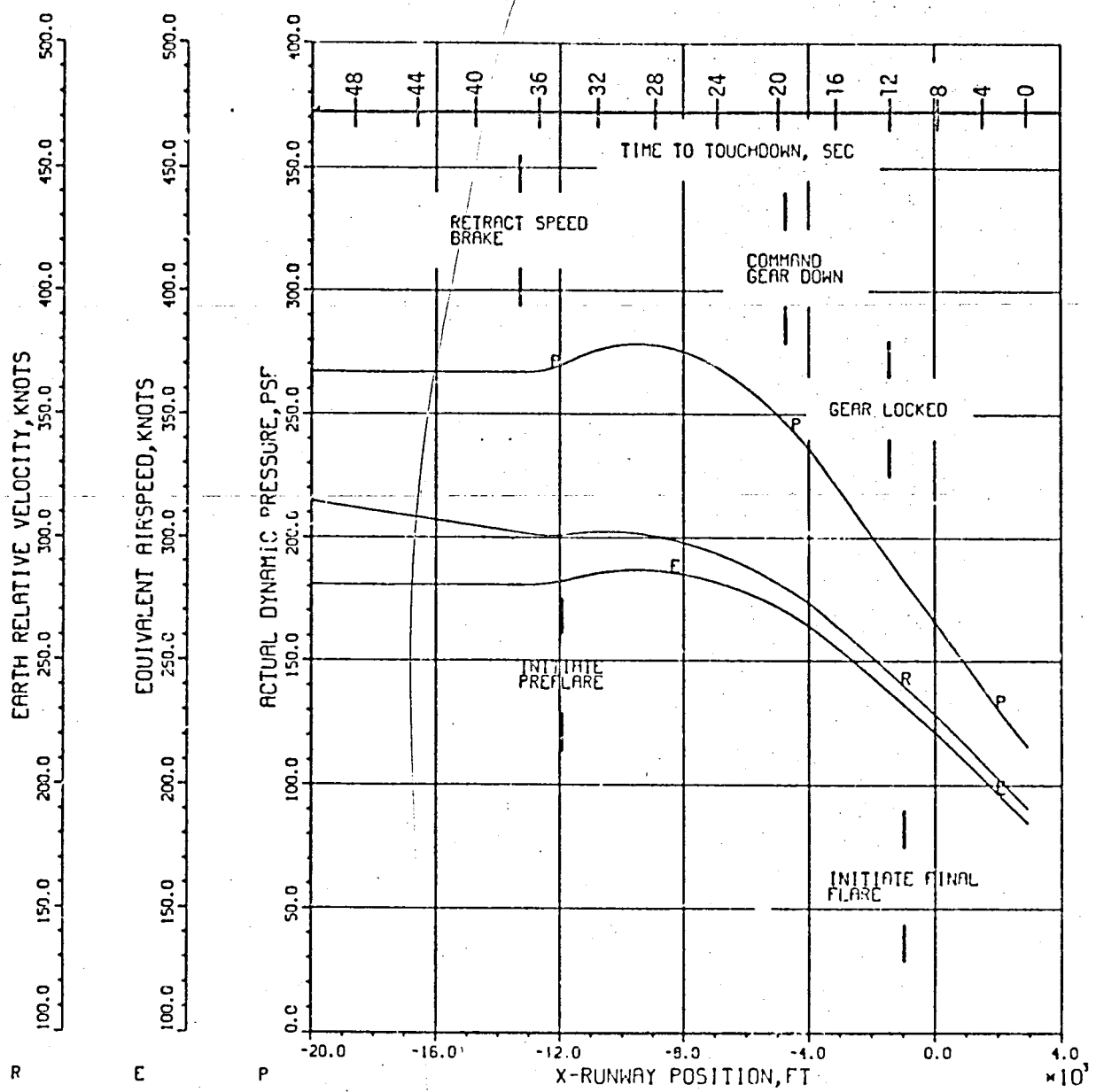
GEAR ALTITUDE DURING LANDING GEAR DEPLOYMENT

Figure 6.4-5



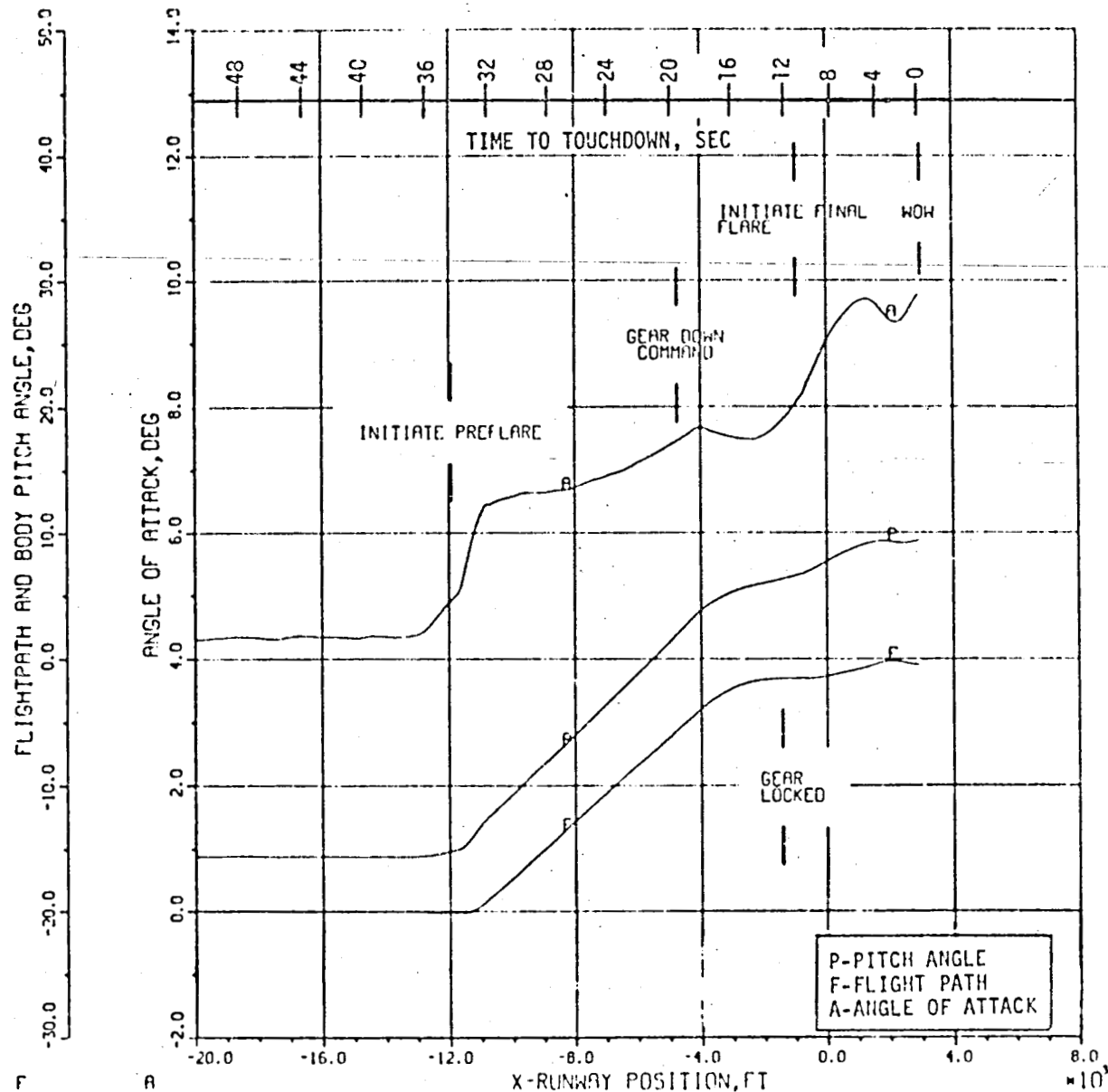
GEAR ALTITUDE AGL FROM PREFLARE TO TOUCHDOWN
X-RUNWAY POSITION

Figure 6.4-6



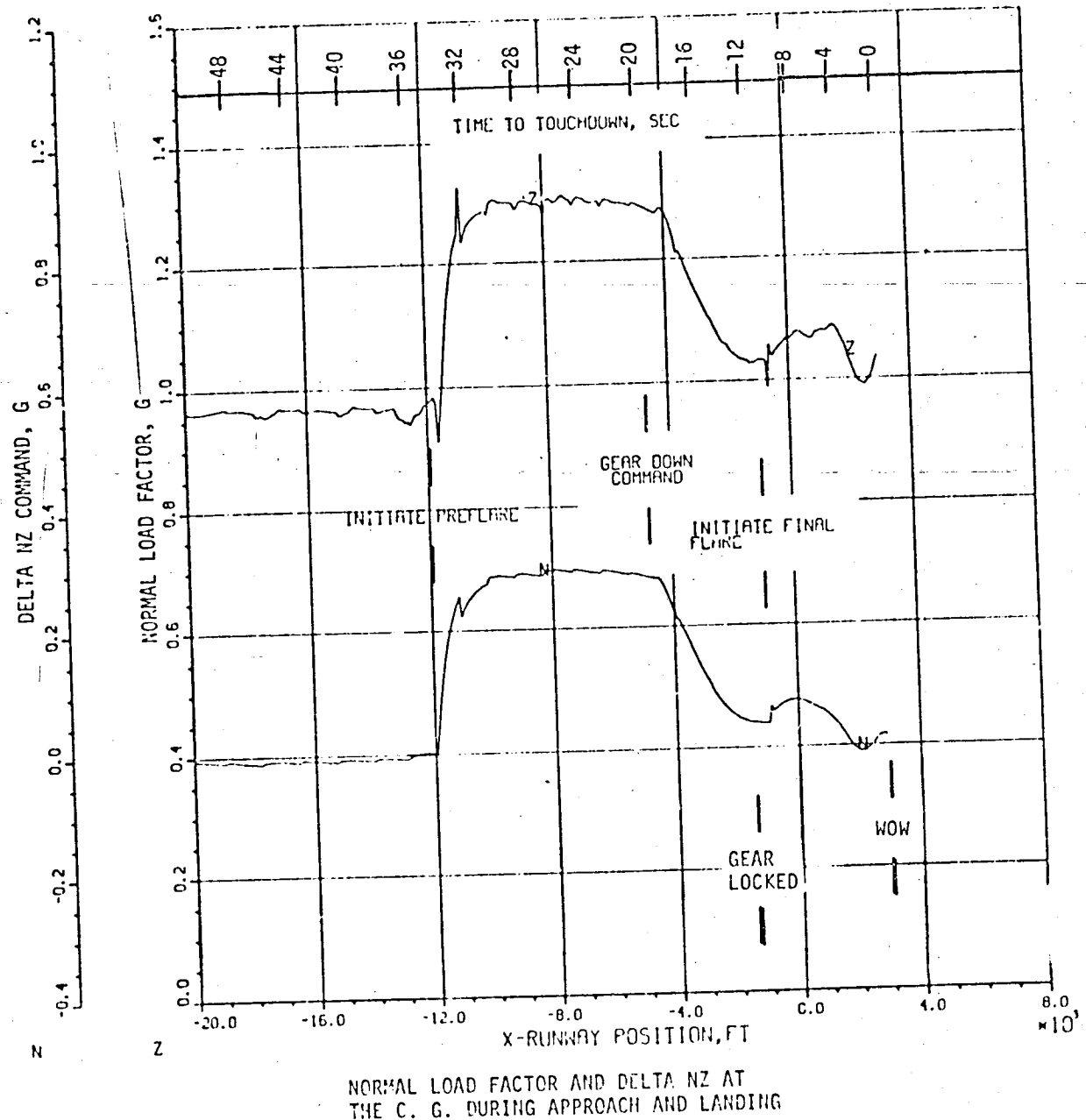
VELOCITY AND DYNAMIC PRESSURE
FROM PREFLARE TO TOUCHDOWN

Figure 6.4-7



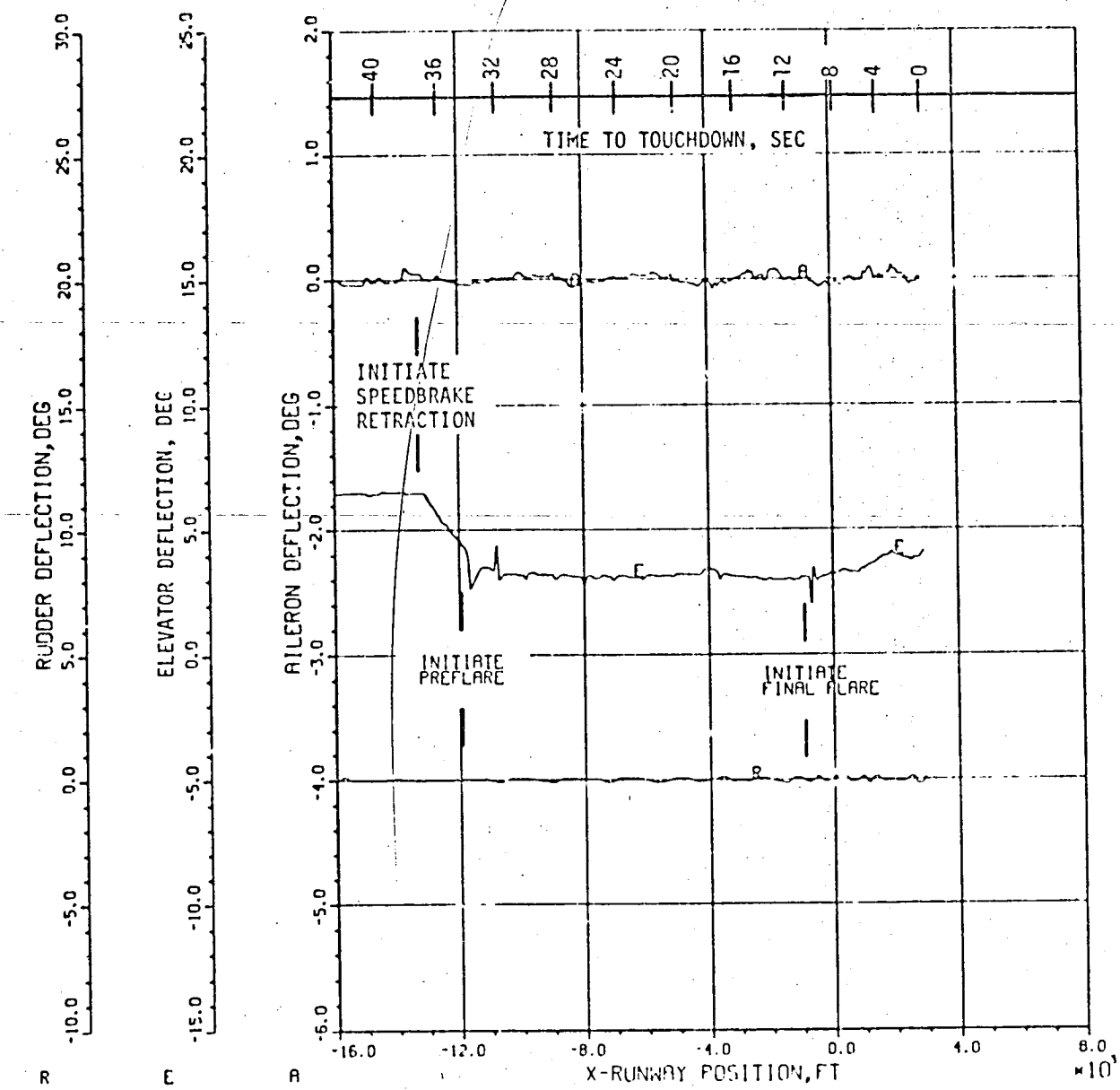
FLIGHTPATH ANGLE, BODY PITCH ANGLE, AND
ANGLE OF ATTACK FROM PREFLARE TO TOUCHDOWN

Figure 6.4-8



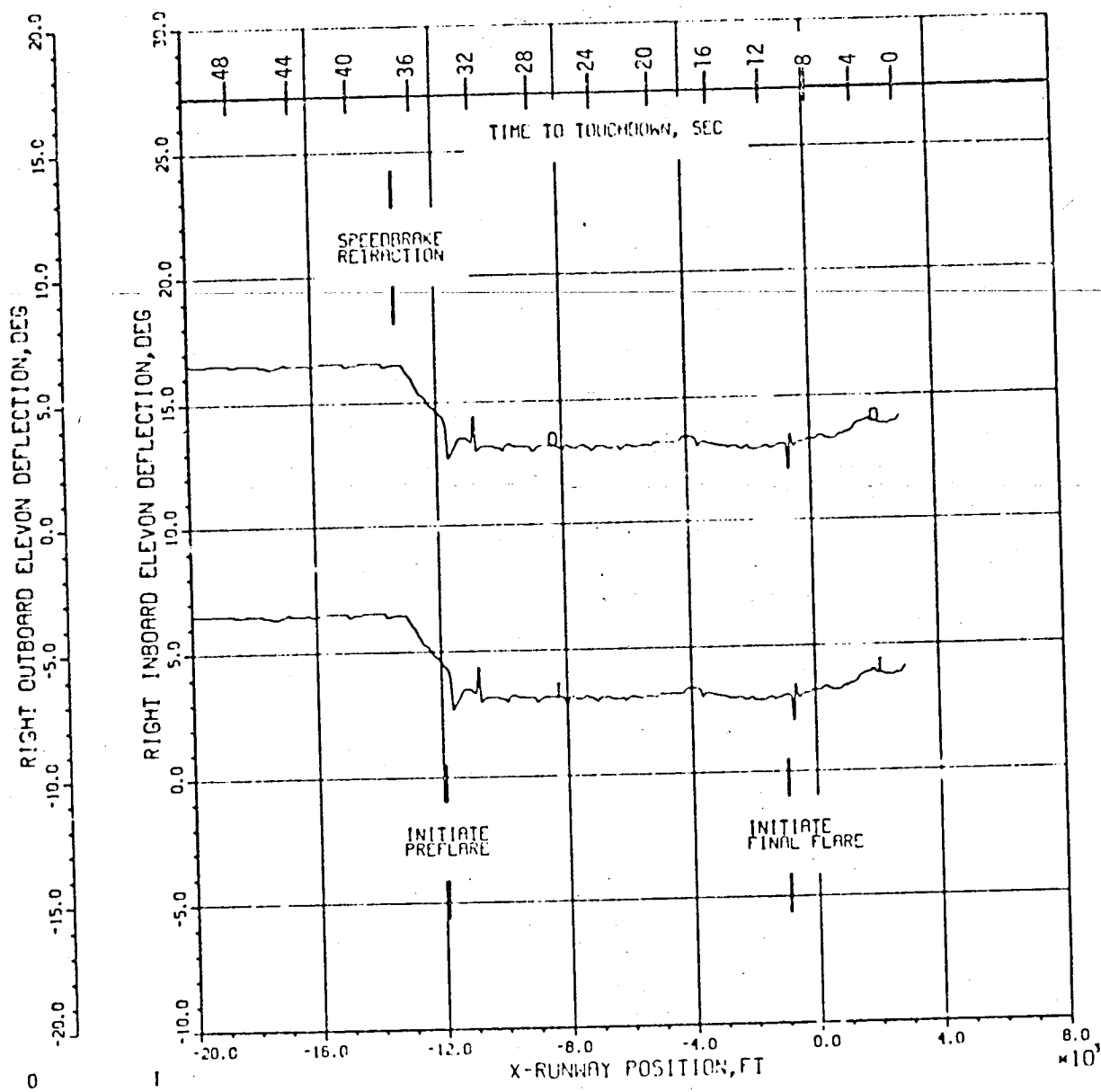
NORMAL LOAD FACTOR AND DELTA NZ AT
THE C. G. DURING APPROACH AND LANDING

Figure 6.4-9



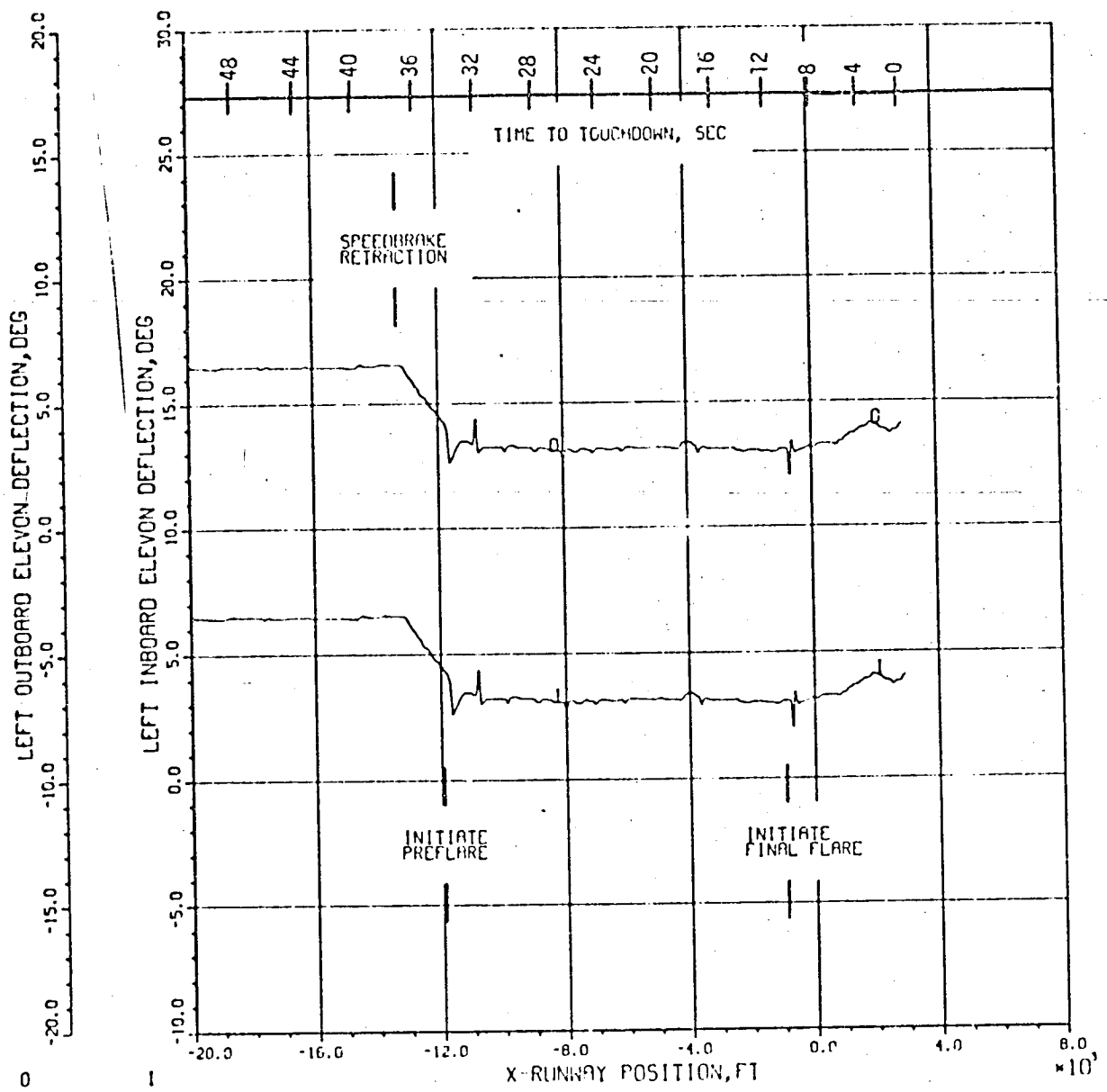
AILERON, ELEVON, AND RUDDER DEFLECTION FROM PREFLARE TO TOUCHDOWN

Figure 6.4-10



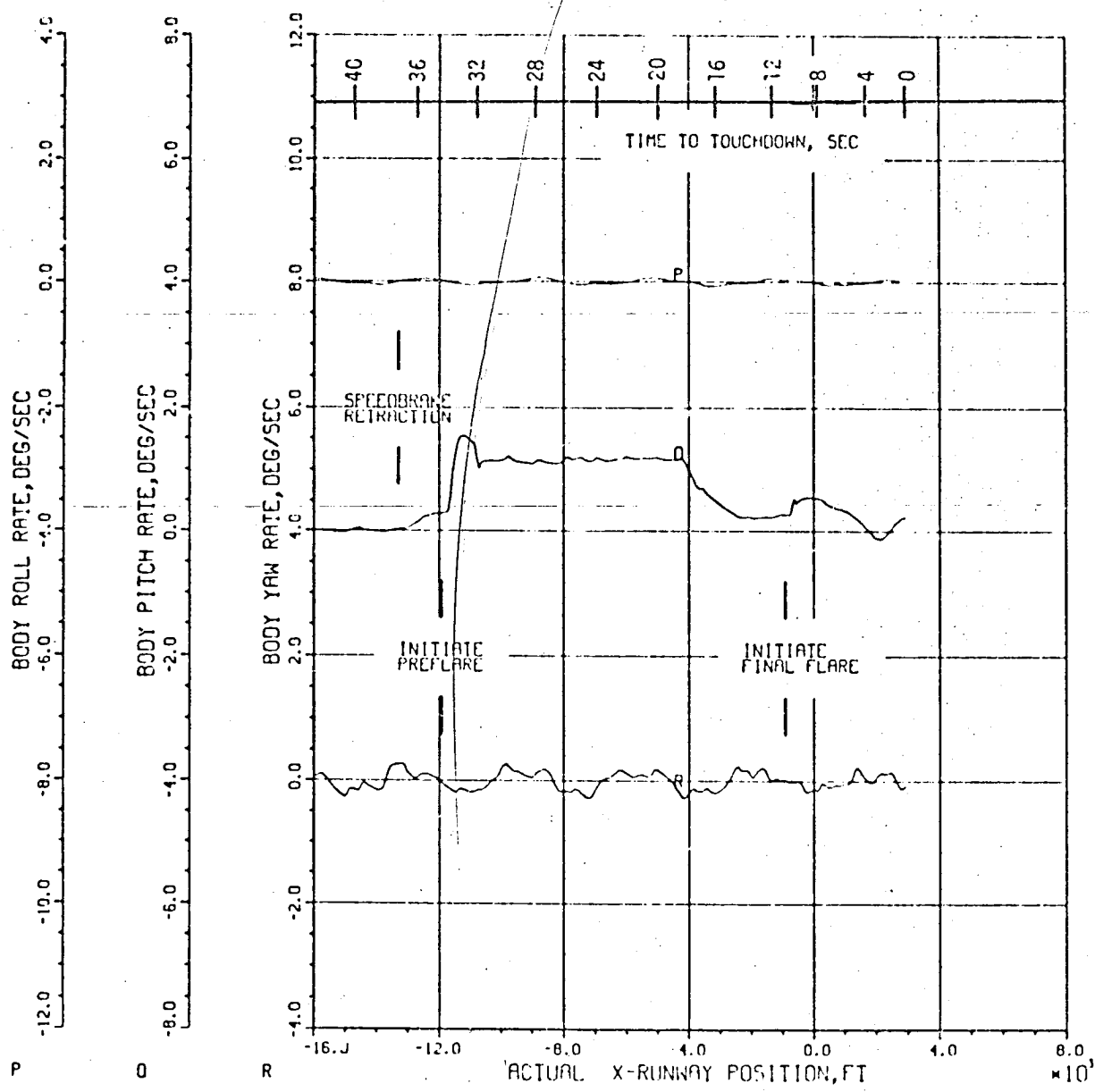
RIGHT INBOARD AND OUTBOARD ELEVON DEFLECTION FROM PREFLARE TO TOUCHDOWN

Figure 6.4-11



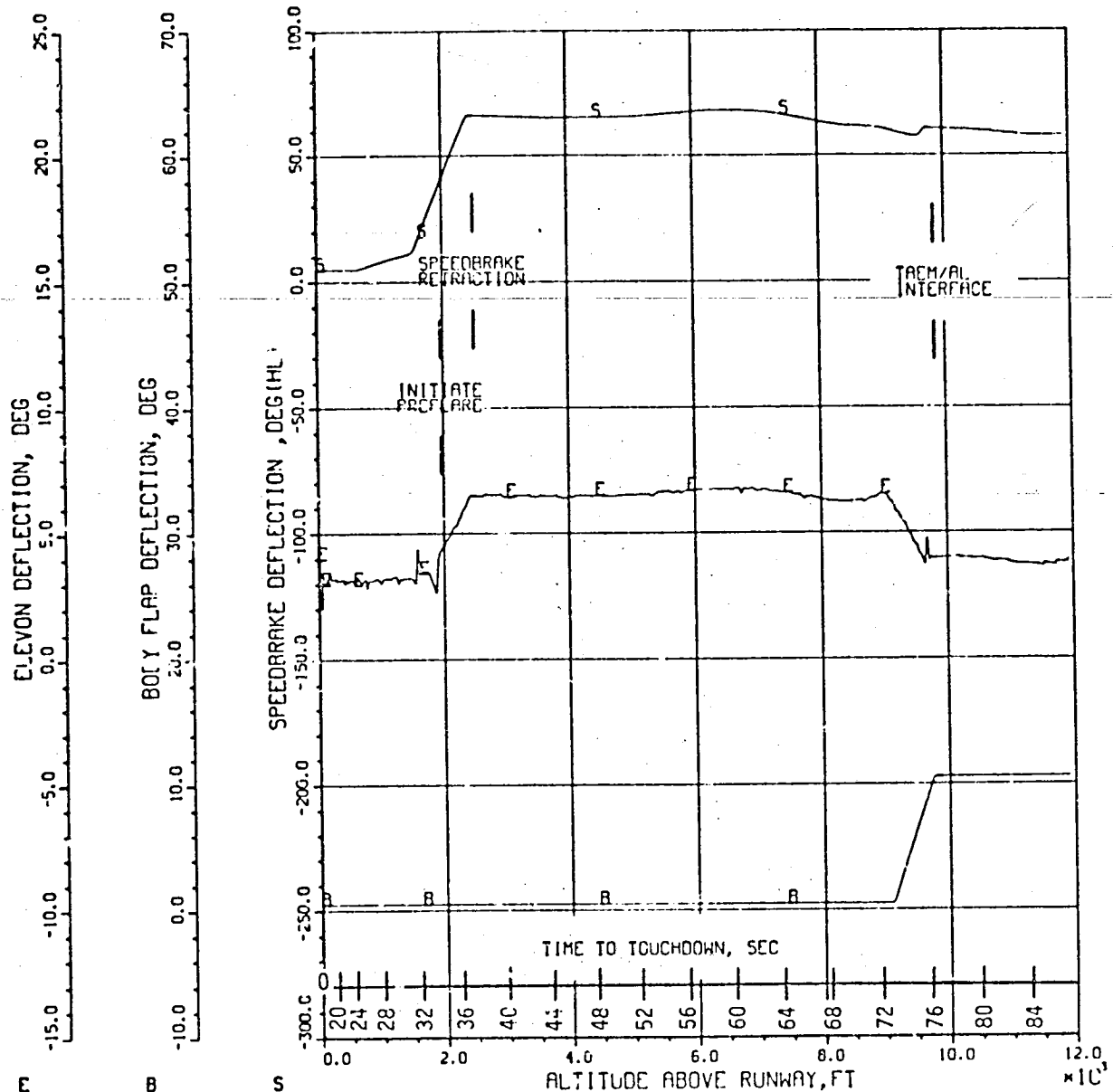
LEFT INBOARD AND OUTBOARD ELEVON DEFLECTION FROM PREFLARE TO TOUCHDOWN

Figure 6.4-12



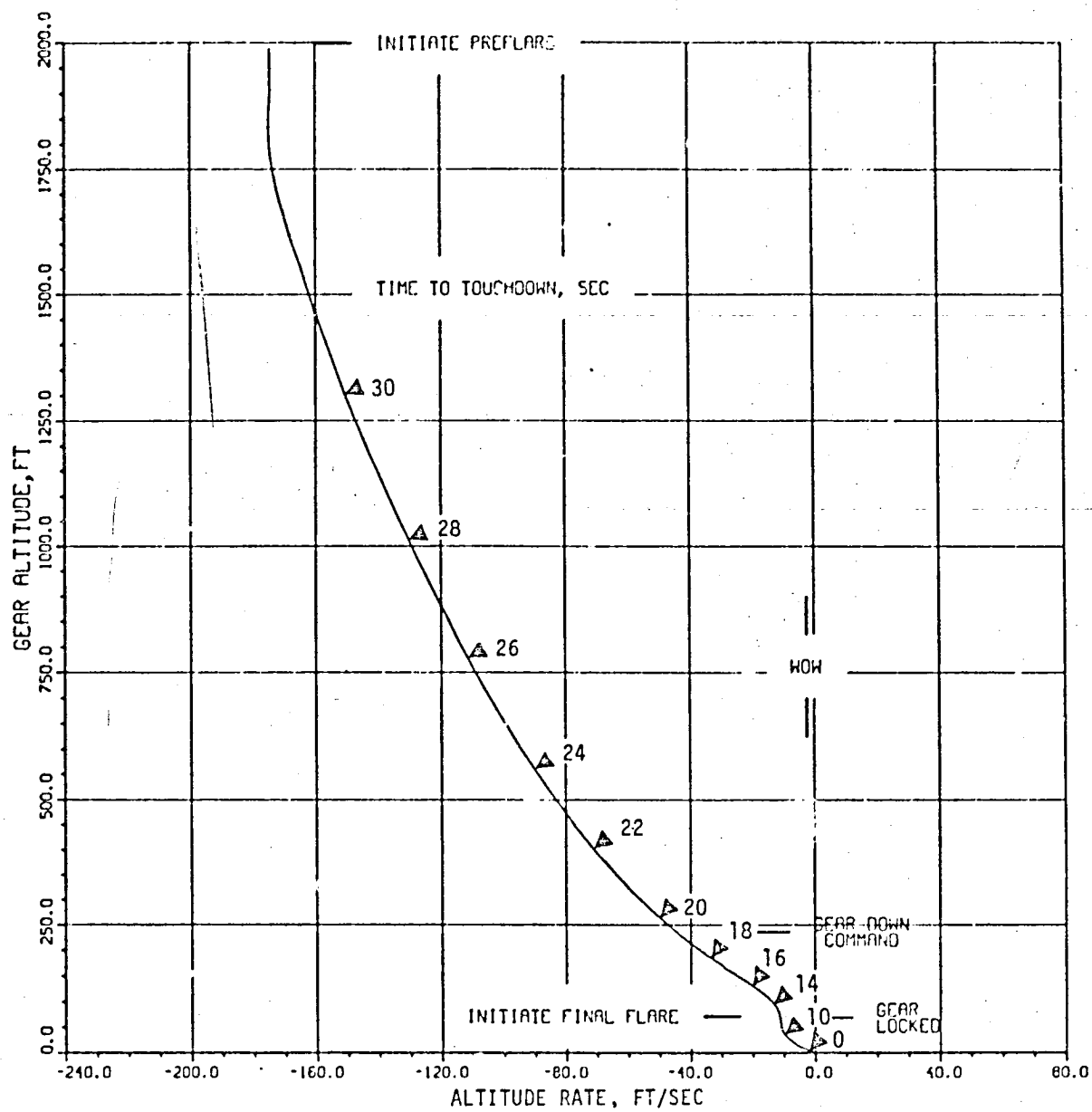
TOPOGRAPHIC BODY ROLL, PITCH AND YAW
RATES FROM PREFLARE TO TOUCHDOWN

Figure 6.4-13



CONTROL SURFACE DEFLECTIONS
DURING APPROACH AND LANDING

Figure 6.4-14



ALTITUDE-ALTITUDE RATE PHASE PLANE
FROM PREFLARE TO TOUCHDOWN

Figure 6.4-15

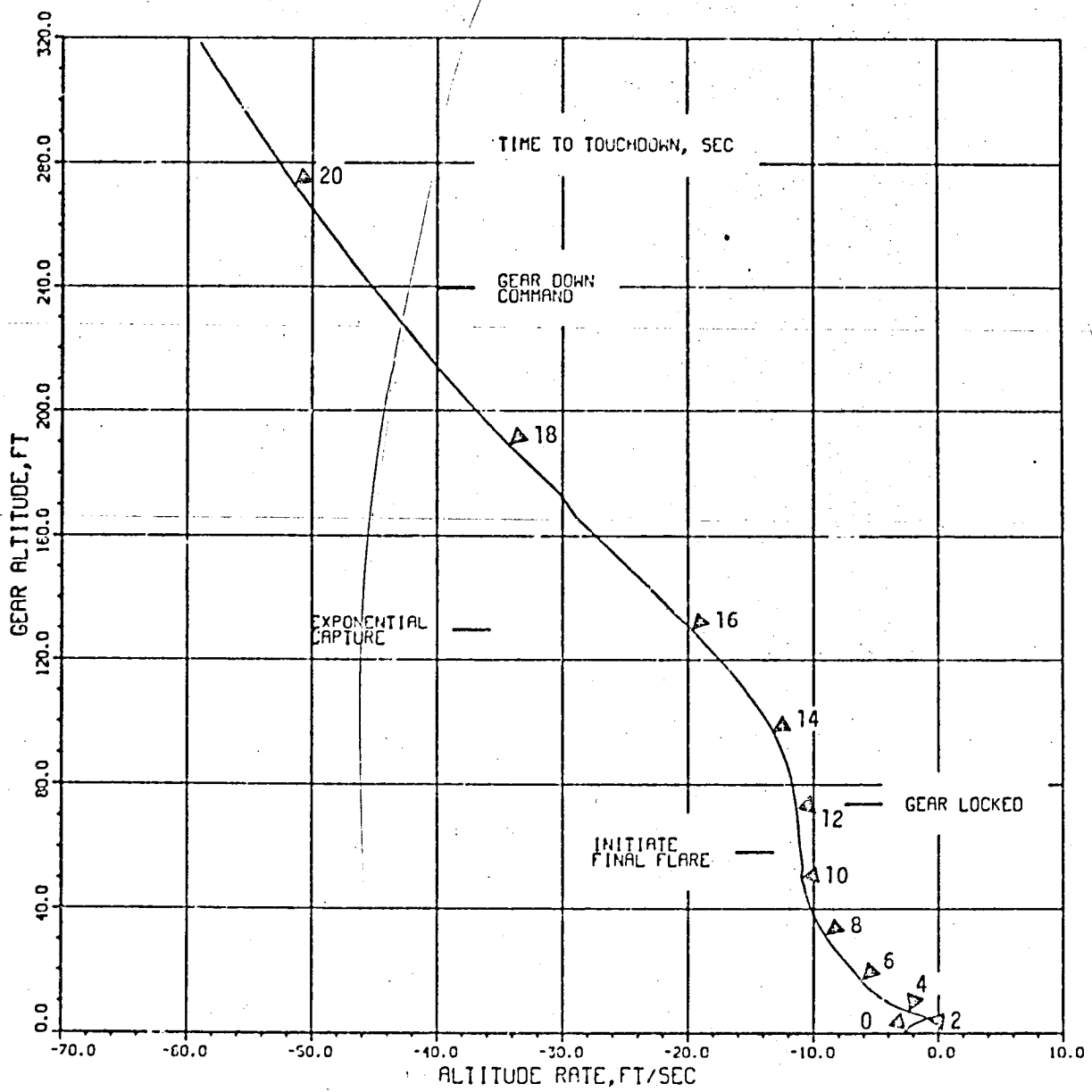
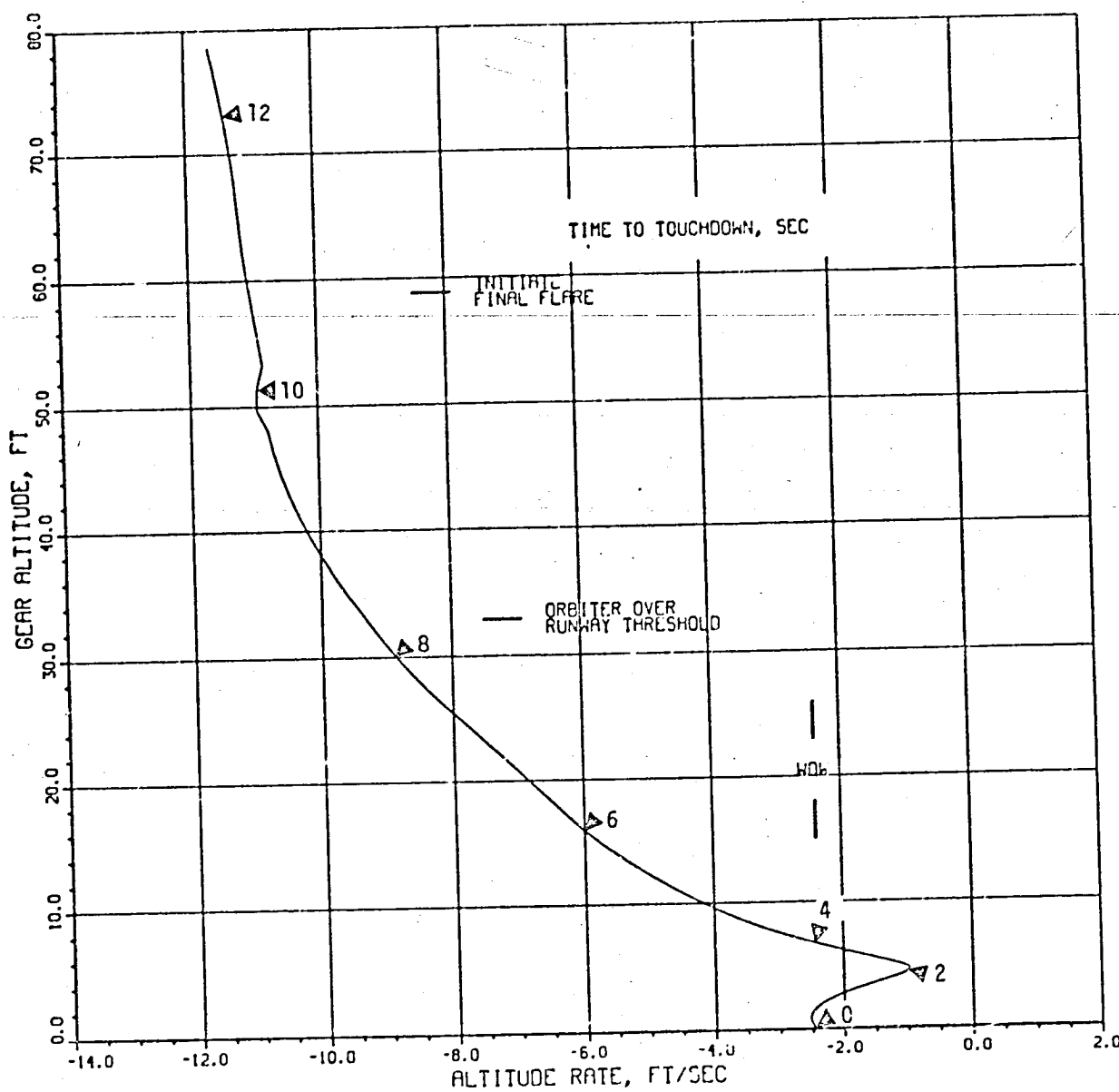


Figure 6.4-16



ALTITUDE-ALTITUDE RATE PHASE PLANE
FROM FINAL FLARE TO TOUCHDOWN

Figure 6.4-17

187

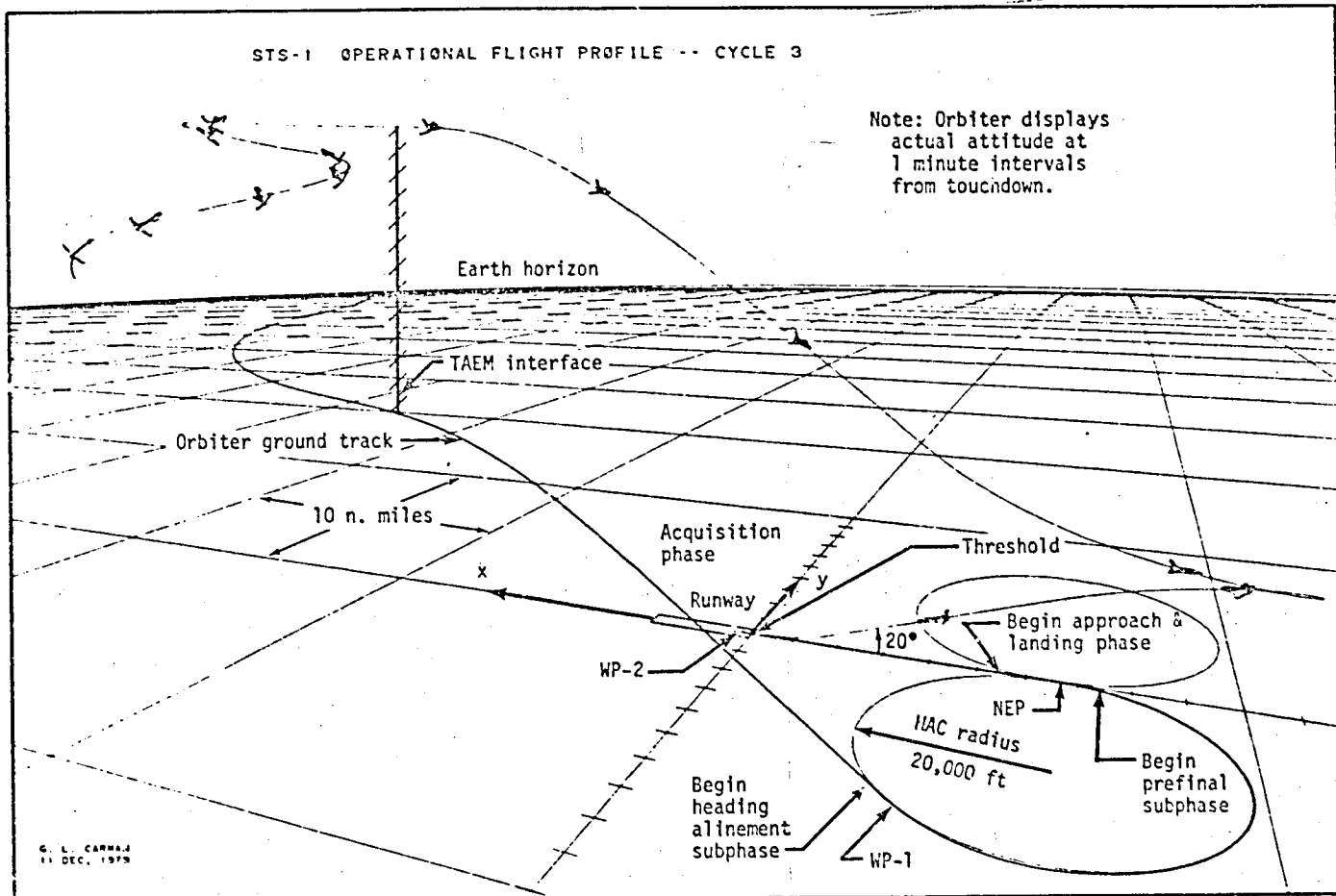
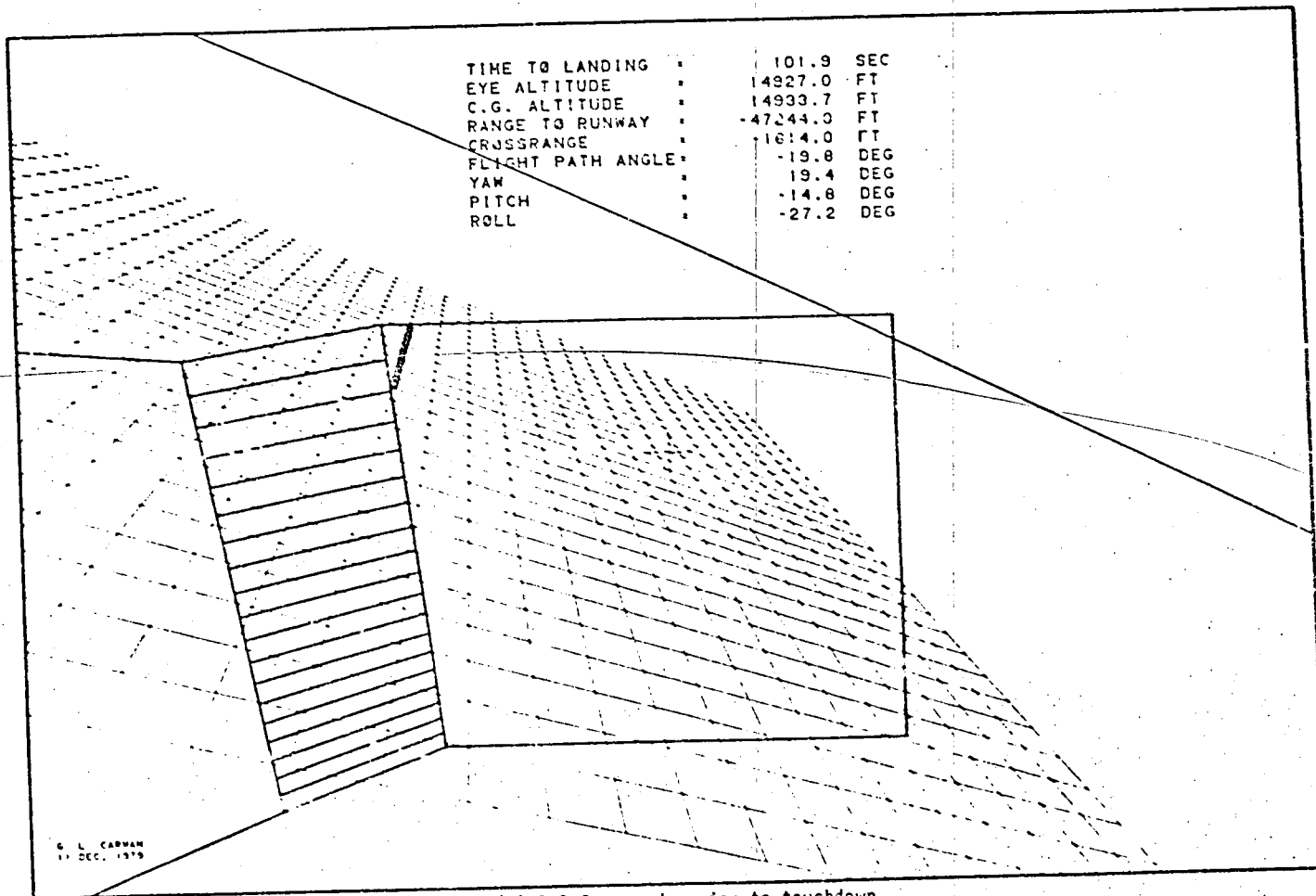


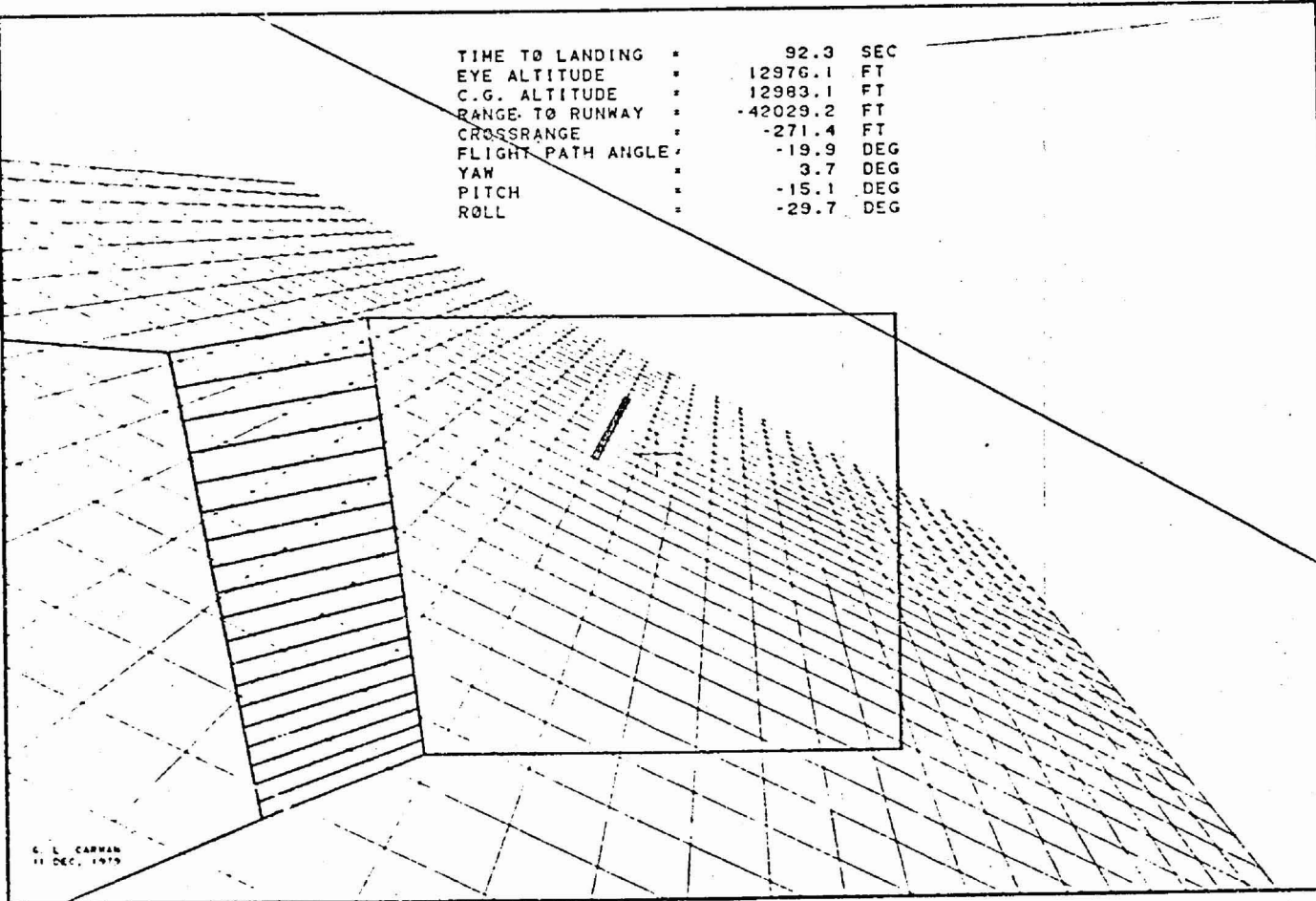
Figure 6.4-18.- STS-1 operational flight profile perspective.

931



(a) 101.9 seconds prior to touchdown.

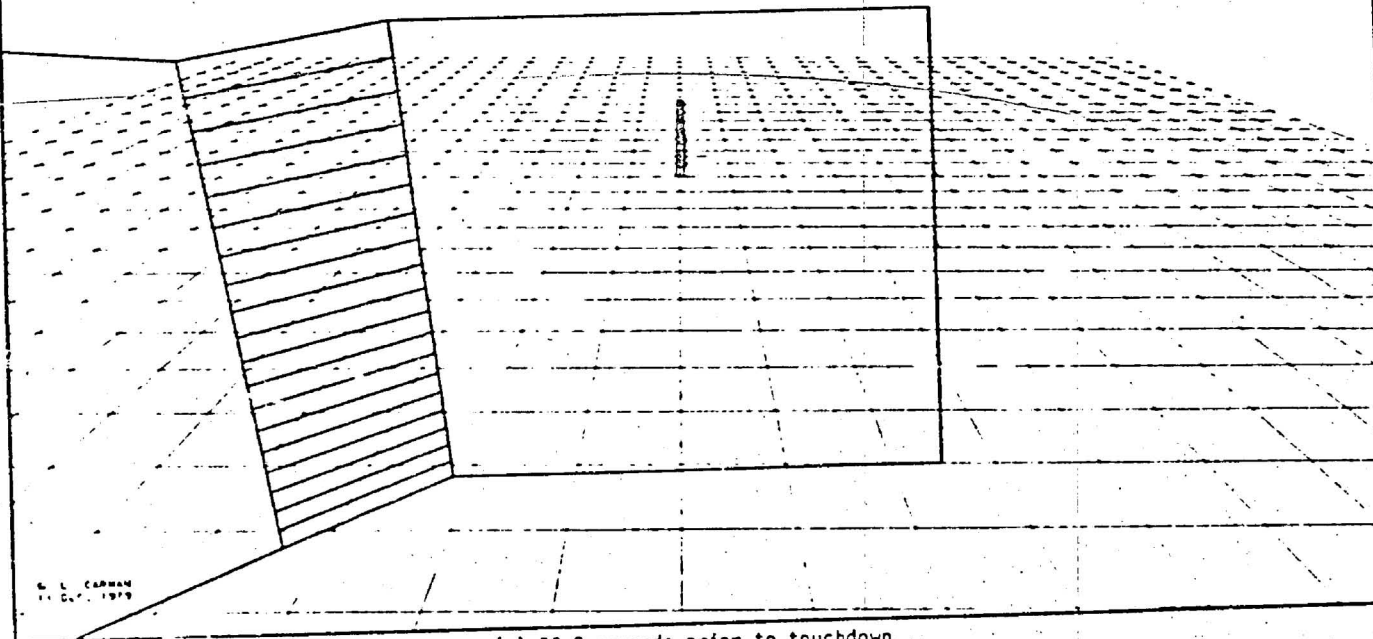
Figure 6.4-19.- View from commander eye position.



(b) 92.3 seconds prior to touchdown.

Figure 6.4-19.- Continued.

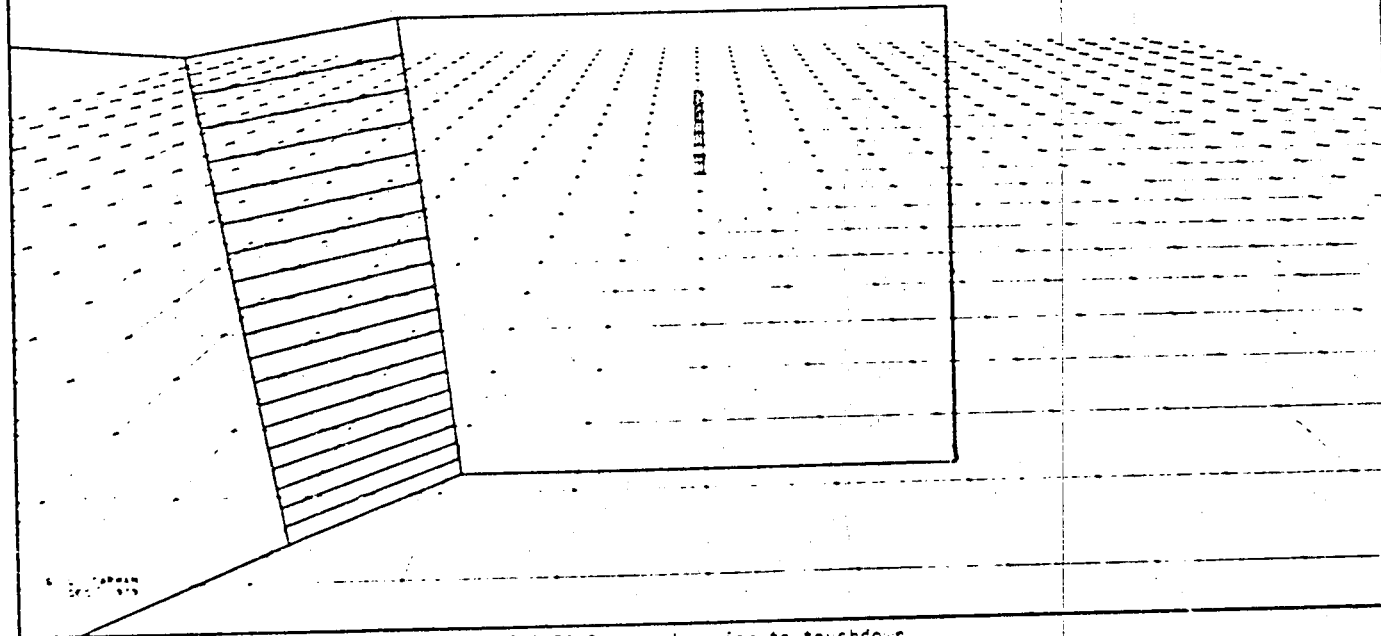
TIME TO LANDING : 82.2 SEC
EYE ALTITUDE : 10981.0 FT
C.G. ALTITUDE : 10986.7 FT
RANGE TO RUNWAY : -36486.9 FT
CROSSRANGE : -82.6 FT
FLIGHT PATH ANGLE : -20.2 DEG
YAW : .5 DEG
PITCH : -15.5 DEG
ROLL : -1.7 DEG



(c) 82.2 seconds prior to touchdown.

Figure 6.4-19.- Continued.

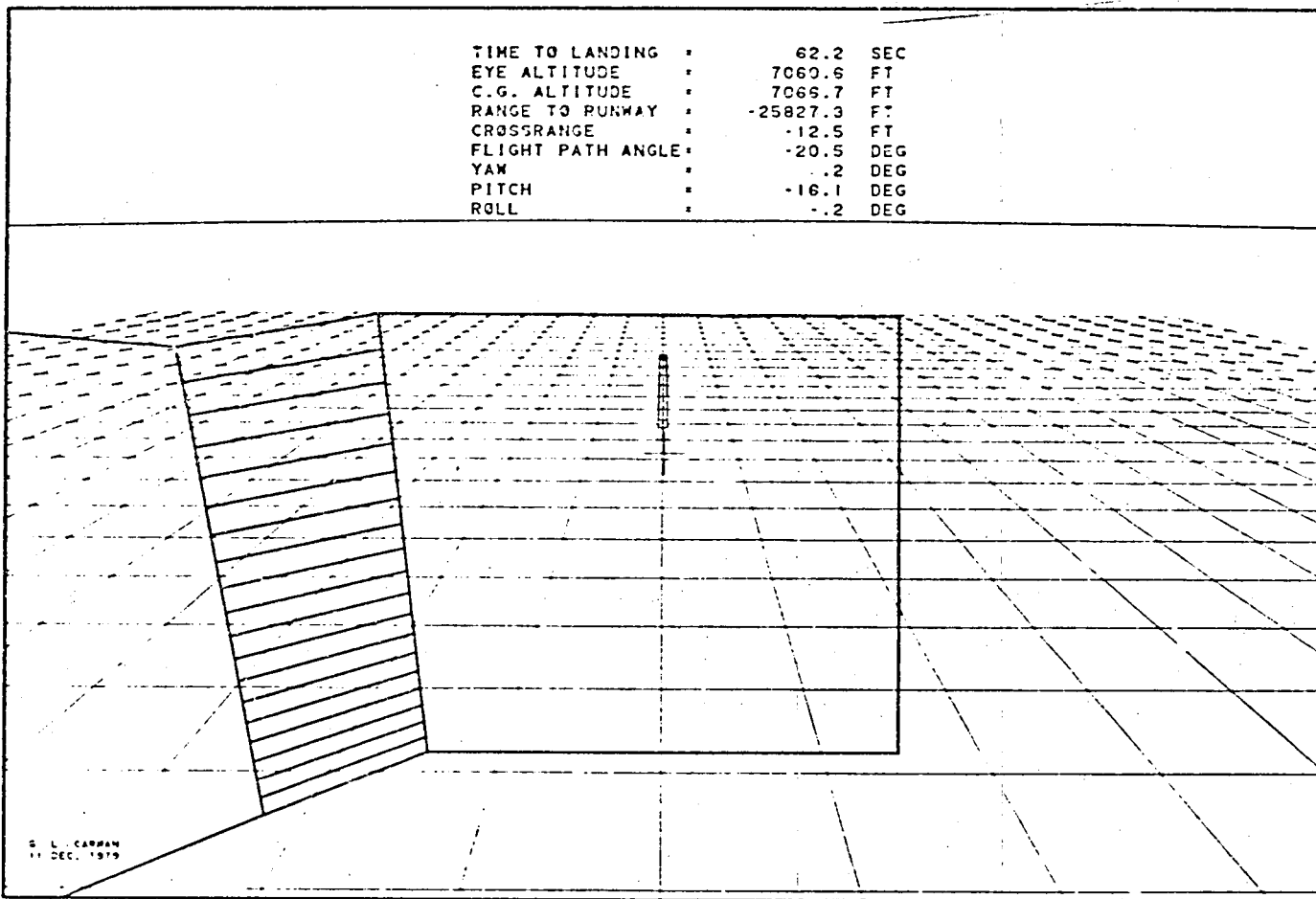
TIME TO LANDING : 72.3 SEC
EYE ALTITUDE : 3029.9 FT
C.G. ALTITUDE : 3029.1 FT
RANGE TO PUNKAH : 01131.4 FT
DISTANCE : 35.0 FT
FLIGHT PATH ANGLE : +13.6 DEG
YAW : .3 DEG
PITCH : +15.0 DEG
ROLL : +.2 DEG



(d) 72.3 seconds prior to touchdown.

Figure E.4-19.- Continued.

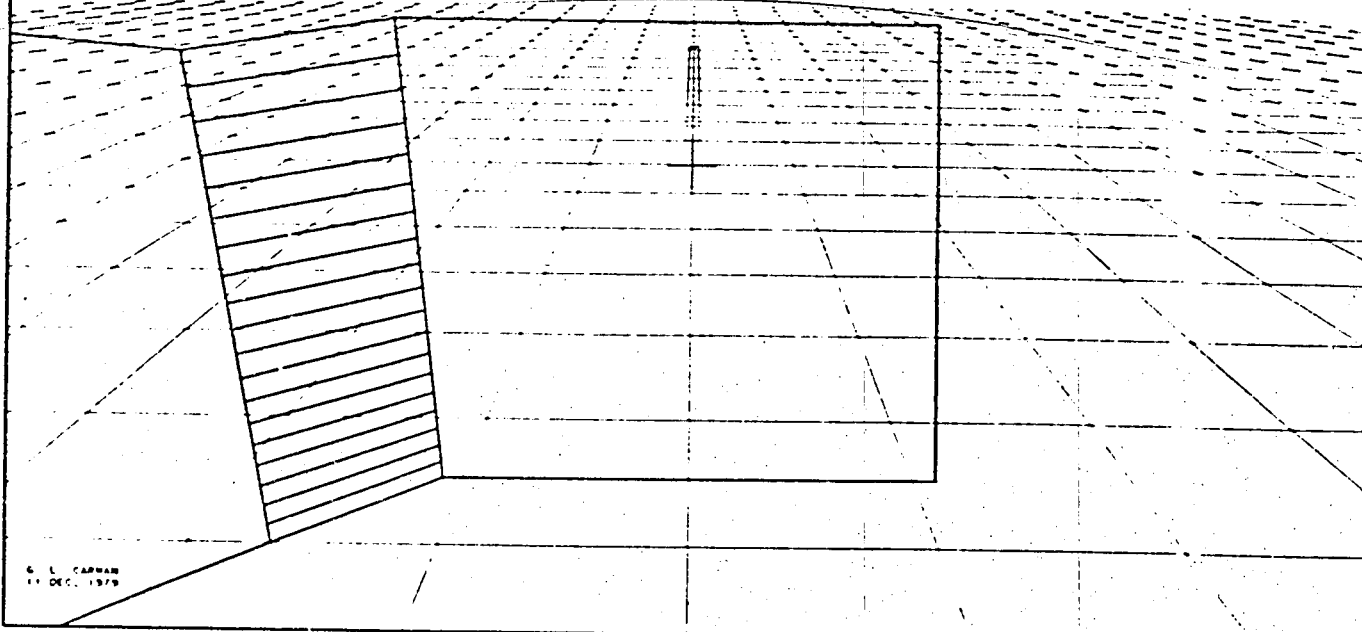
192



(e) 52.2 seconds prior to touchdown.

Figure 6.4-19.- Continued.

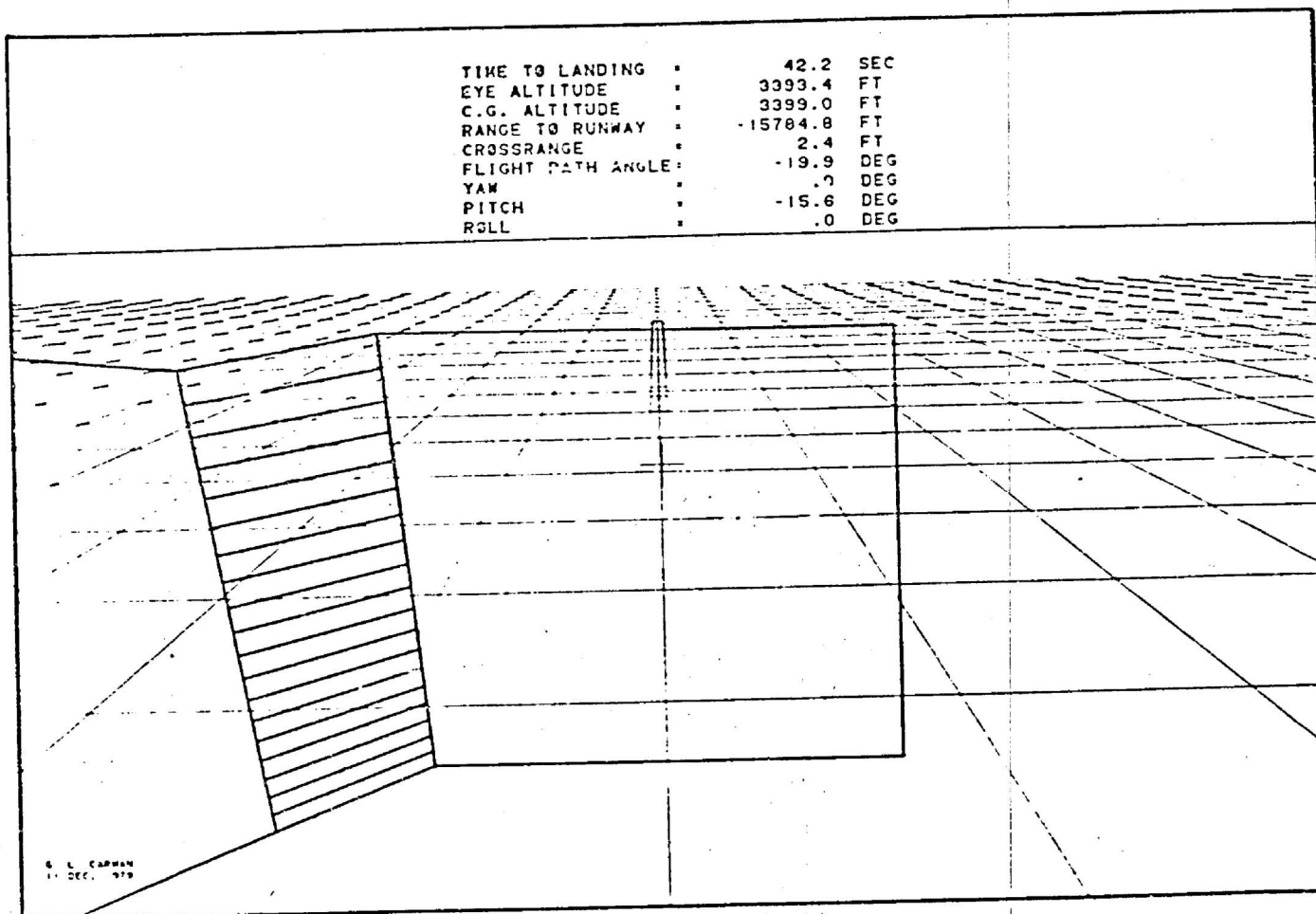
TIME TO LANDING : 52.3 SEC
EYE ALTITUDE : 5204.9 FT
C.G. ALTITUDE : 5210.5 FT
RANGE TO RUNWAY : -20766.1 FT
CROSSRANGE : -212 FT
FLIGHT PATH ANGLE : -19.9 DEG
YAW : .0 DEG
PITCH : -15.6 DEG
ROLL : -41 DEG



(f) 52.3 seconds prior to touchdown.

Figure 6.4-19.- Continued.

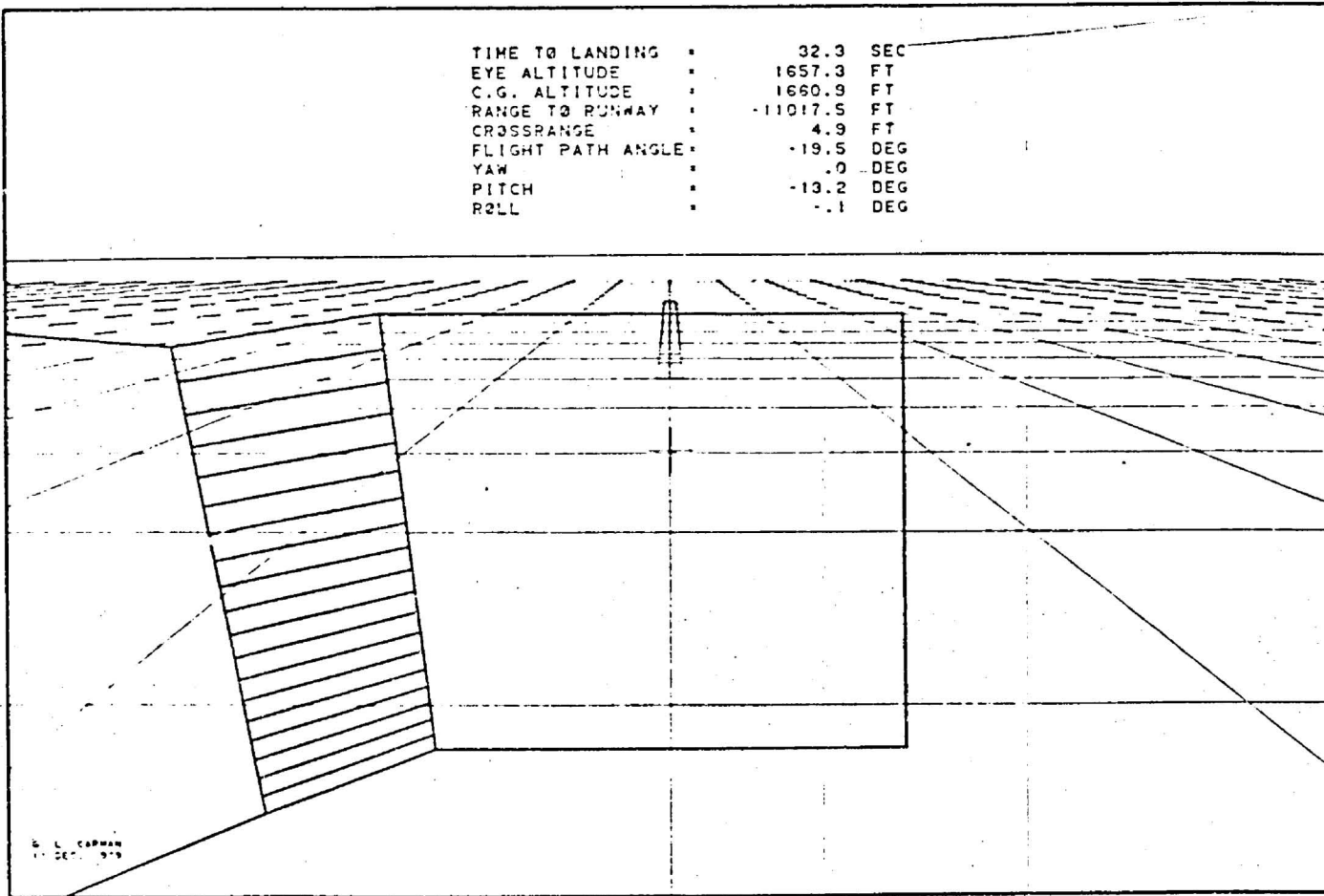
194



(g) 42.2 seconds prior to touchdown.

Figure 6.4-19.- Continued.

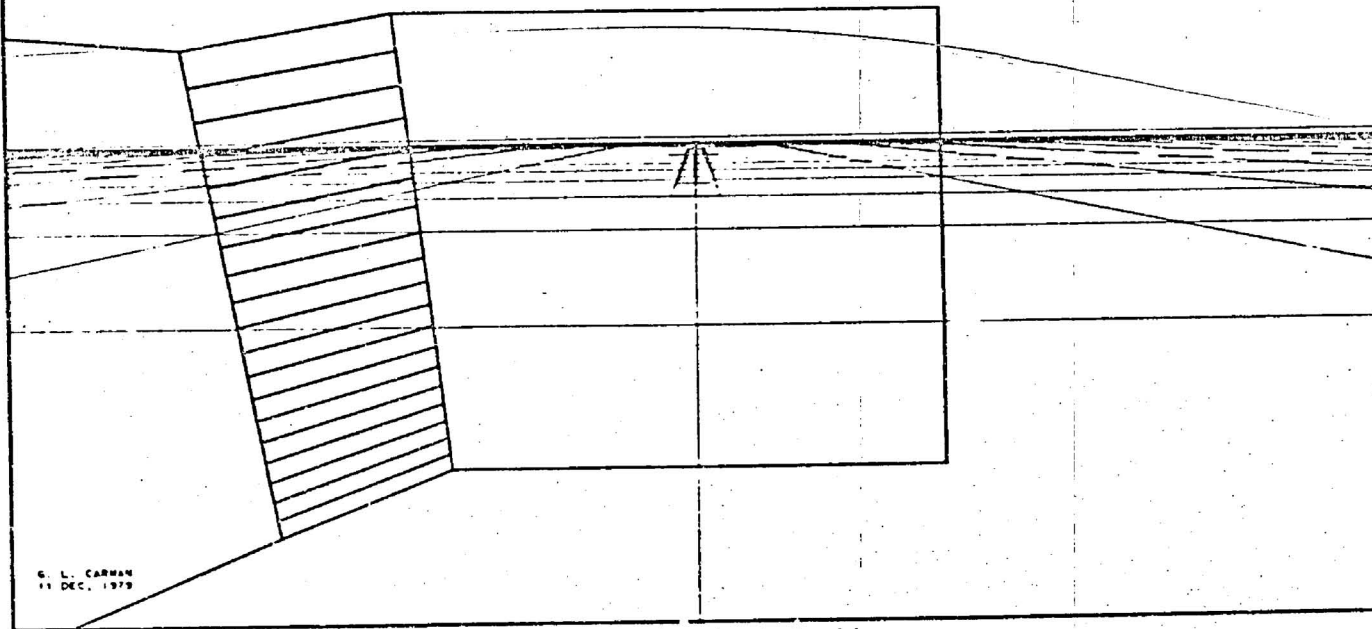
TIME TO LANDING : 32.3 SEC
EYE ALTITUDE : 1657.3 FT
C.G. ALTITUDE : 1660.9 FT
RANGE TO RUNWAY : 11017.5 FT
CROSS RANGE : 4.9 FT
FLIGHT PATH ANGLE : +19.5 DEG
YAW : .0 DEG
PITCH : -13.2 DEG
ROLL : -.1 DEG



(h) 32.3 seconds prior to touchdown.

Figure 6.4-19.- Continued.

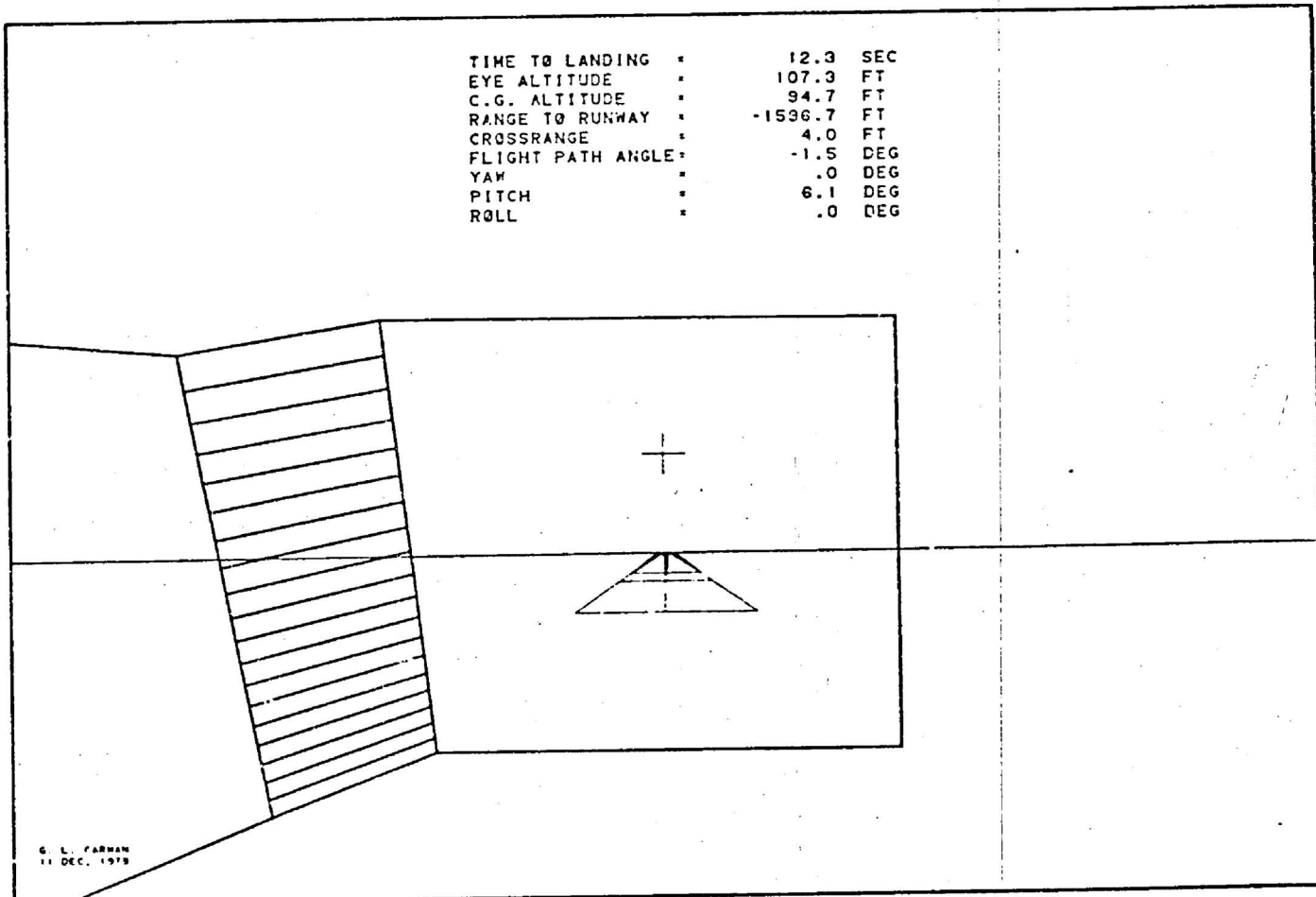
TIME TO LANDING : 22.2 SEC
EYE ALTITUDE : 430.7 FT
C.G. ALTITUDE : 424.4 FT
RANGE TO RUNWAY : -6101.7 FT
CROSSRANGE : 4.6 FT
FLIGHT PATH ANGLE : -0.5 DEG
YAW : .0 DEG
PITCH : -1.5 DEG
ROLL : -.1 DEG



(1) 22.2 seconds prior to touchdown.

Figure 6.4-19.- Continued.

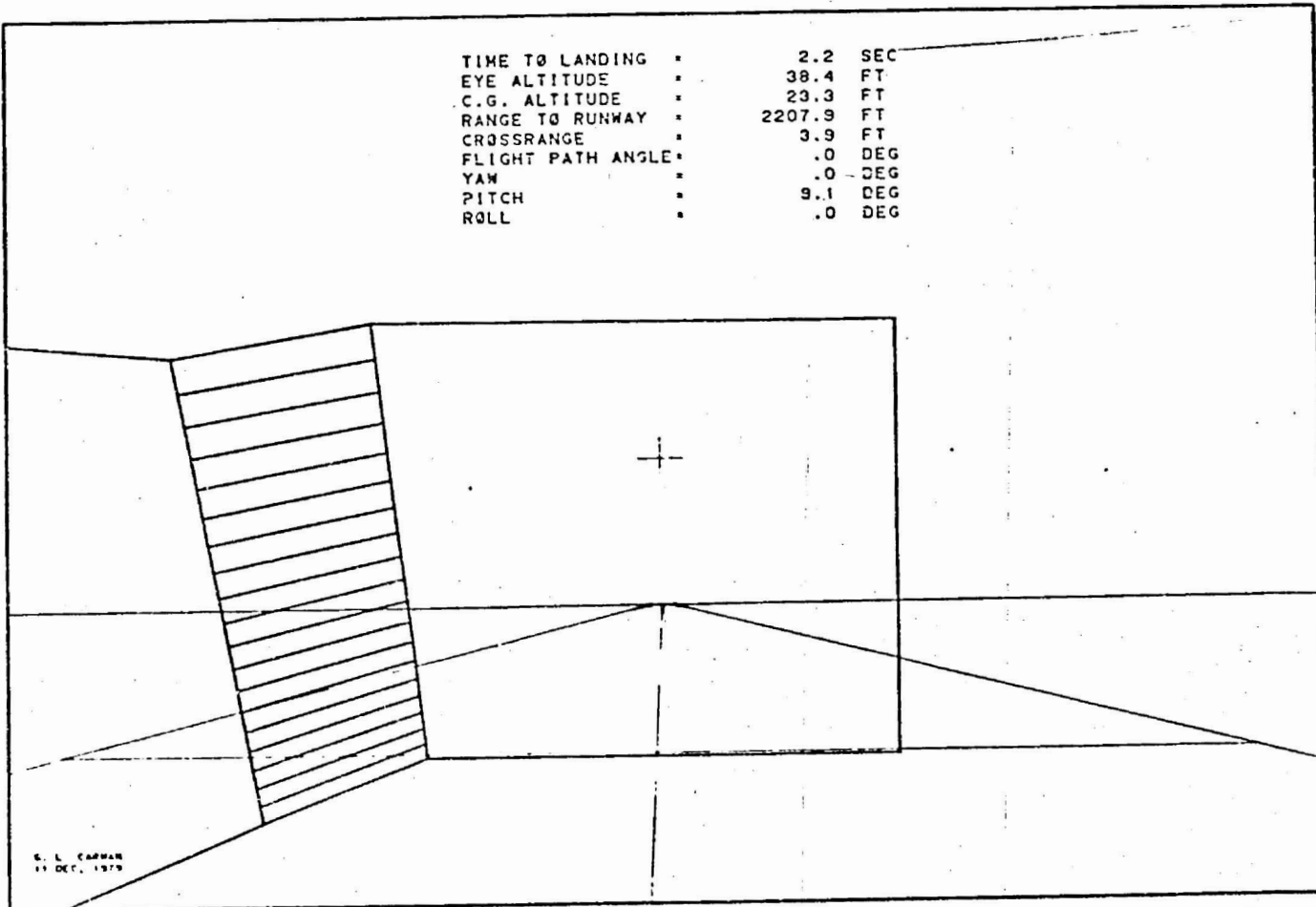
197



(j) 12.3 seconds prior to touchdown.

Figure 6.4-19.- Continued.

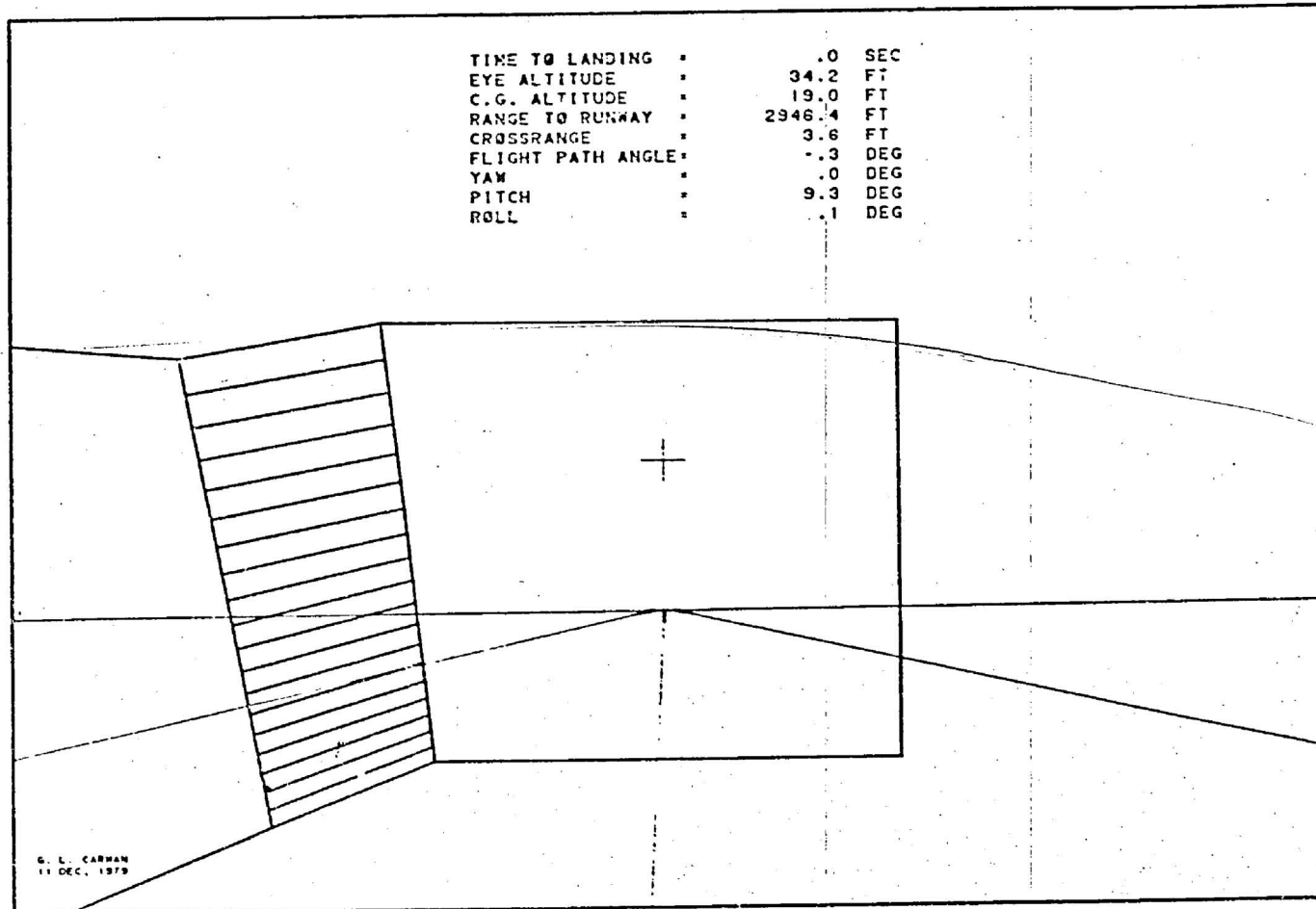
198



(k) 2.2 seconds prior to touchdown.

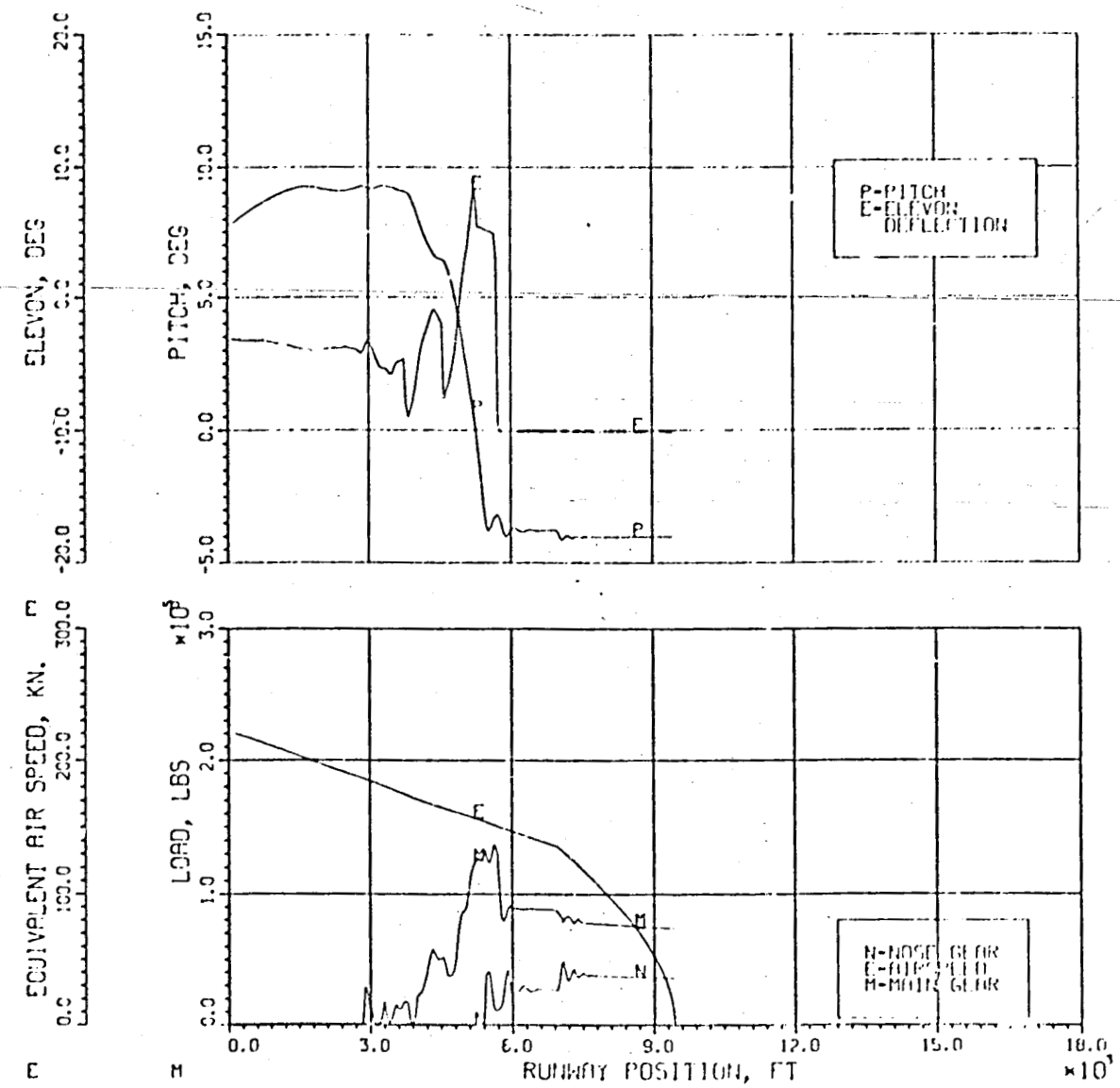
Figure 6.4-19.- Continued.

TIME TO LANDING .0 SEC
EYE ALTITUDE 34.2 FT
C.G. ALTITUDE 19.0 FT
RANGE TO RUNWAY 2946.4 FT
CROSSRANGE 3.6 FT
FLIGHT PATH ANGLE .3 DEG
YAW .0 DEG
PITCH 9.3 DEG
ROLL .1 DEG



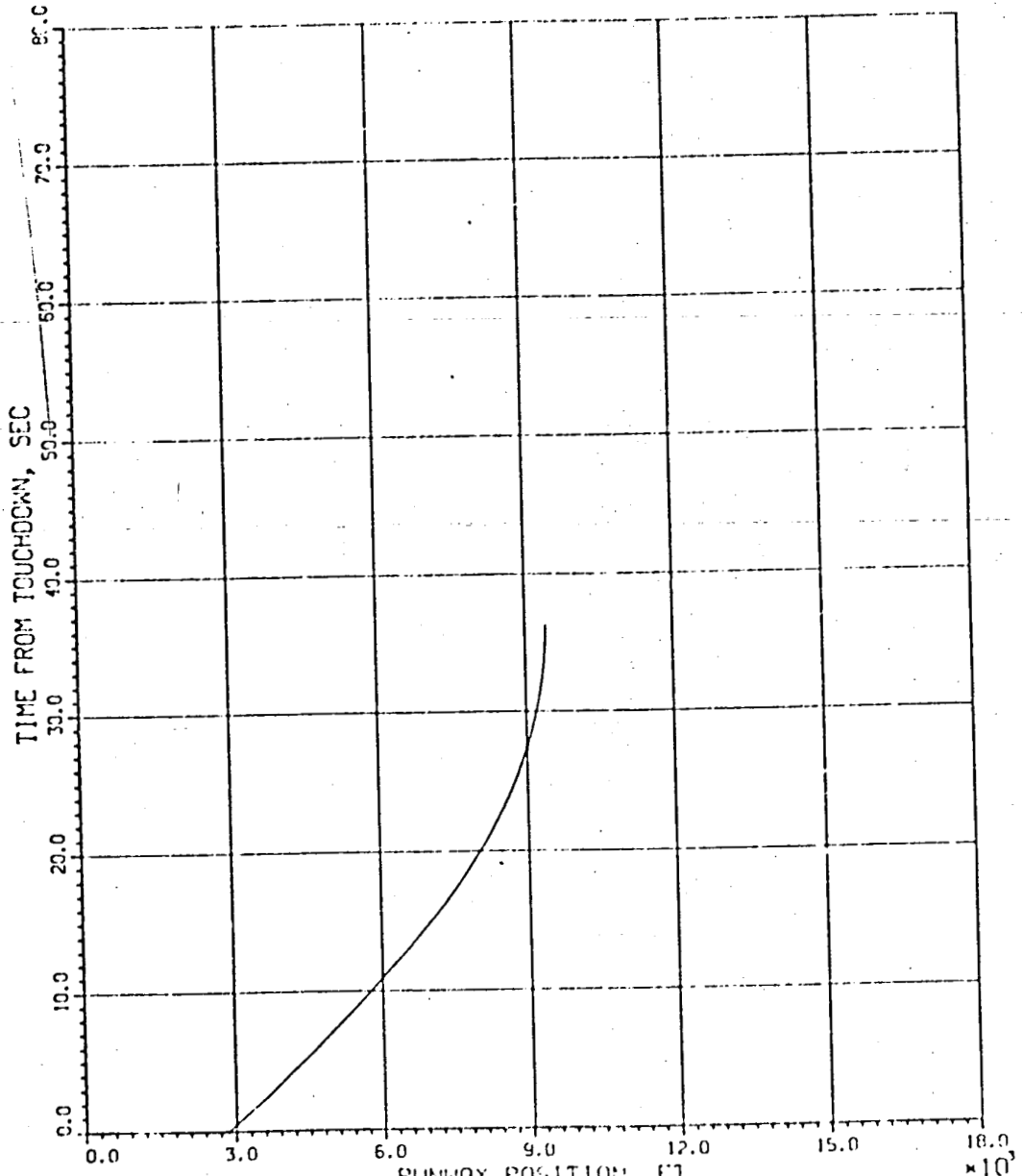
(1) Touchdown.

Figure 6.4-19.- Concluded.



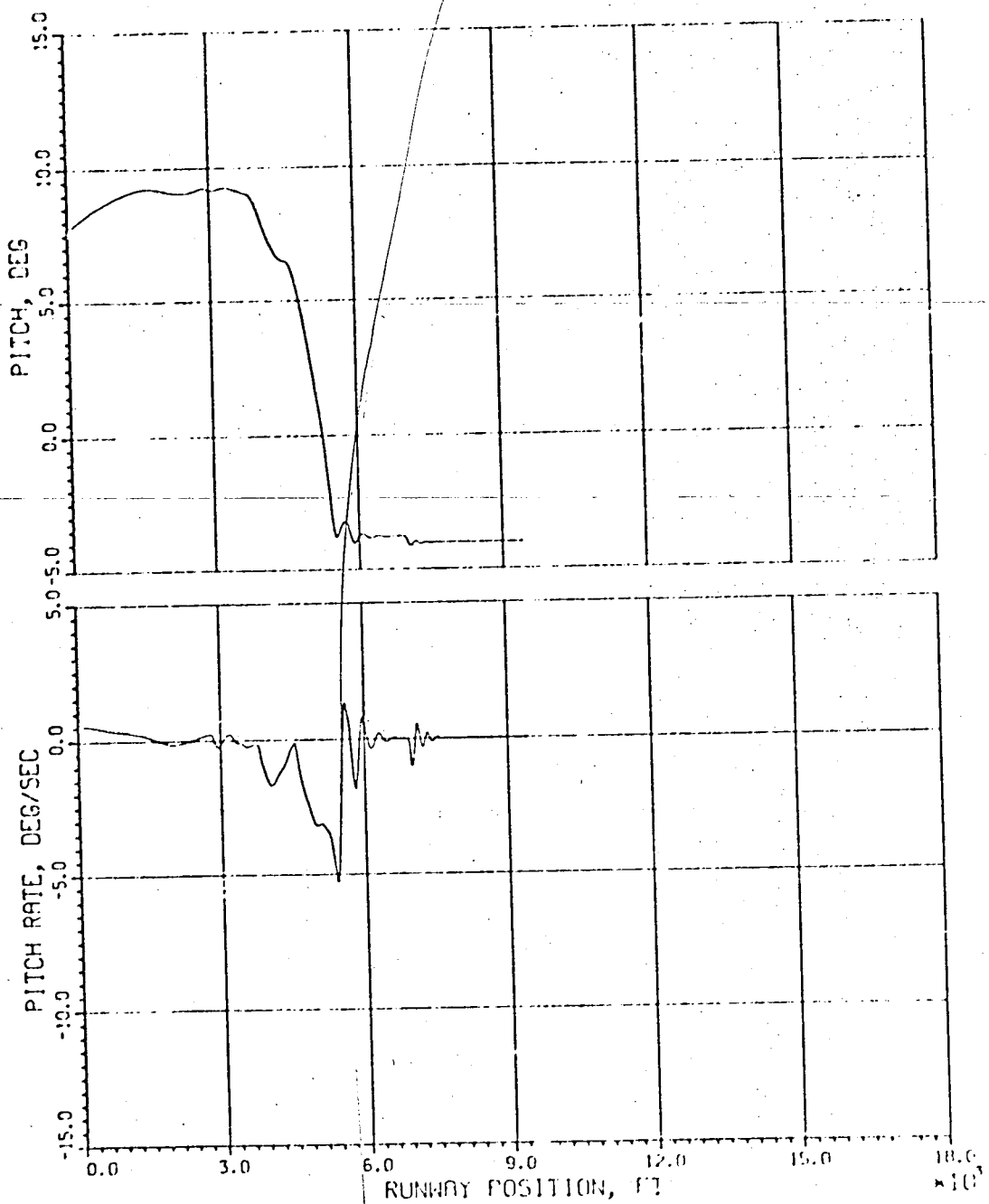
GEAR VERTICAL LOAD, EAS, PITCH AND ELEVON DEFLECTION DURING ROLLOUT

Figure 6.5-1



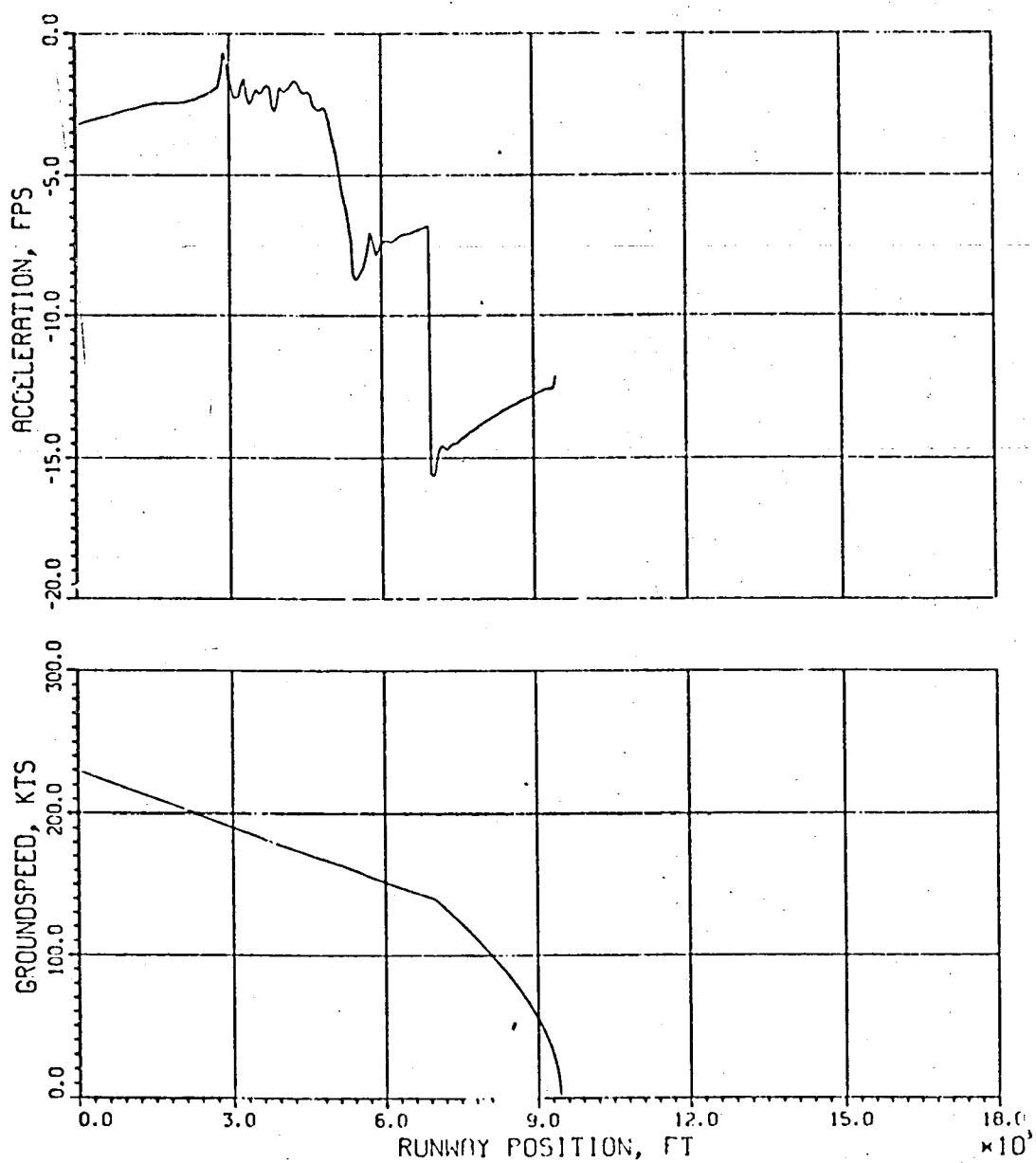
TIME FROM MAINGEAR TOUCHDOWN
DURING ROLLOUT

Figure 6.5-2



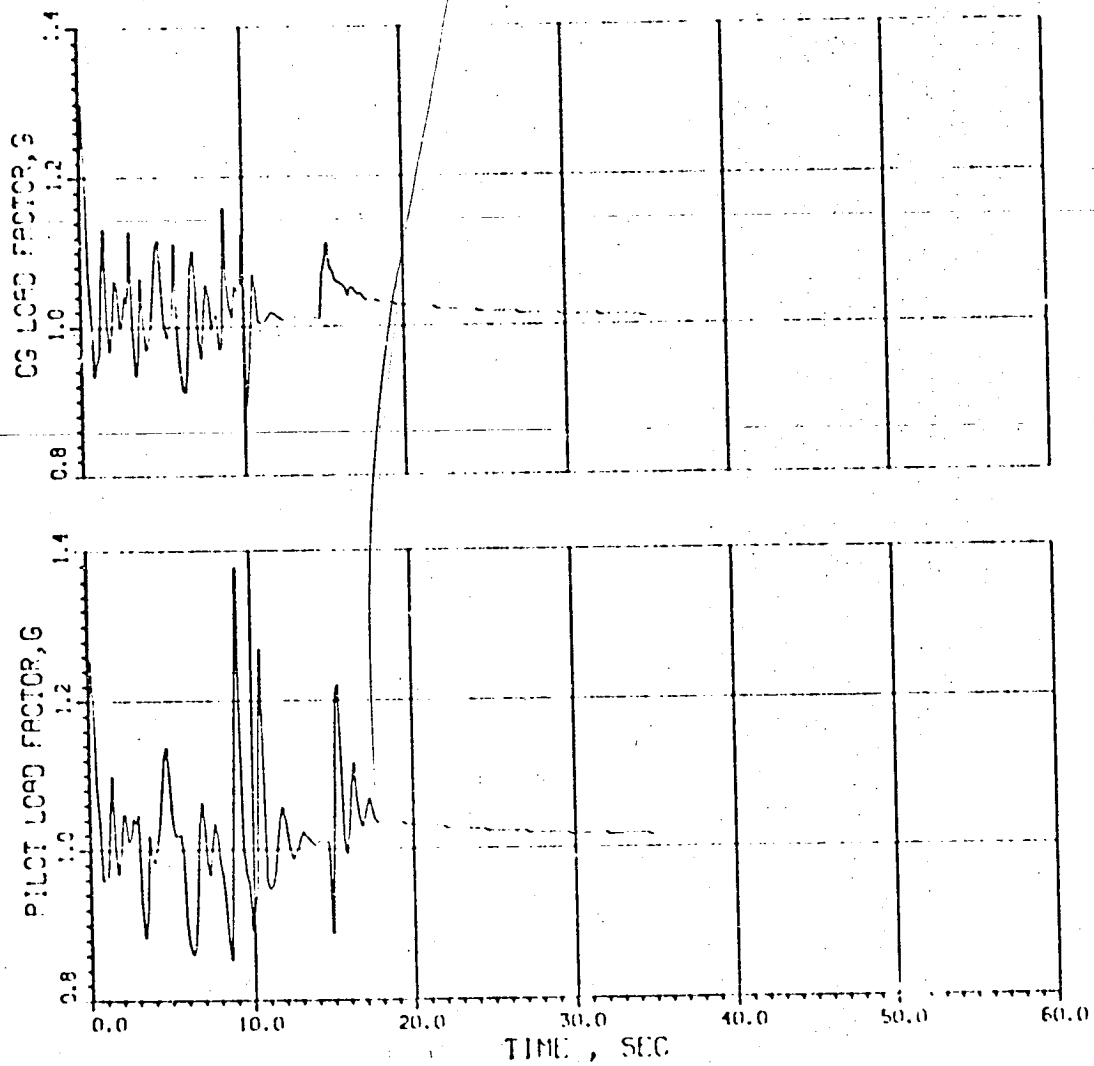
PITCH AND PITCH RATE DURING ROLL OUT

Figure 6.5-3



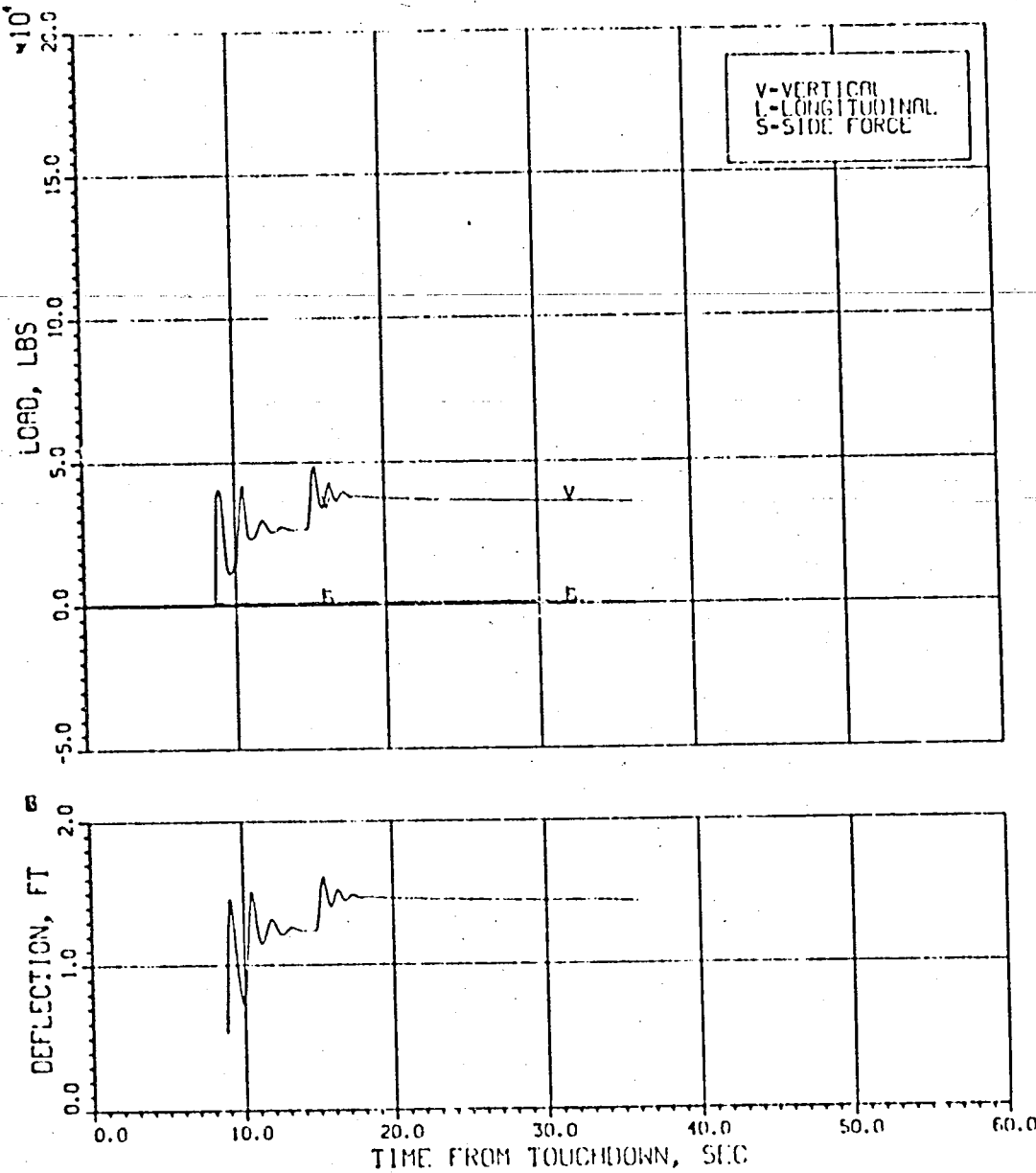
GROUND SPEED AND ACCELERATION
DURING ROLLOUT

Figure 6.5-4



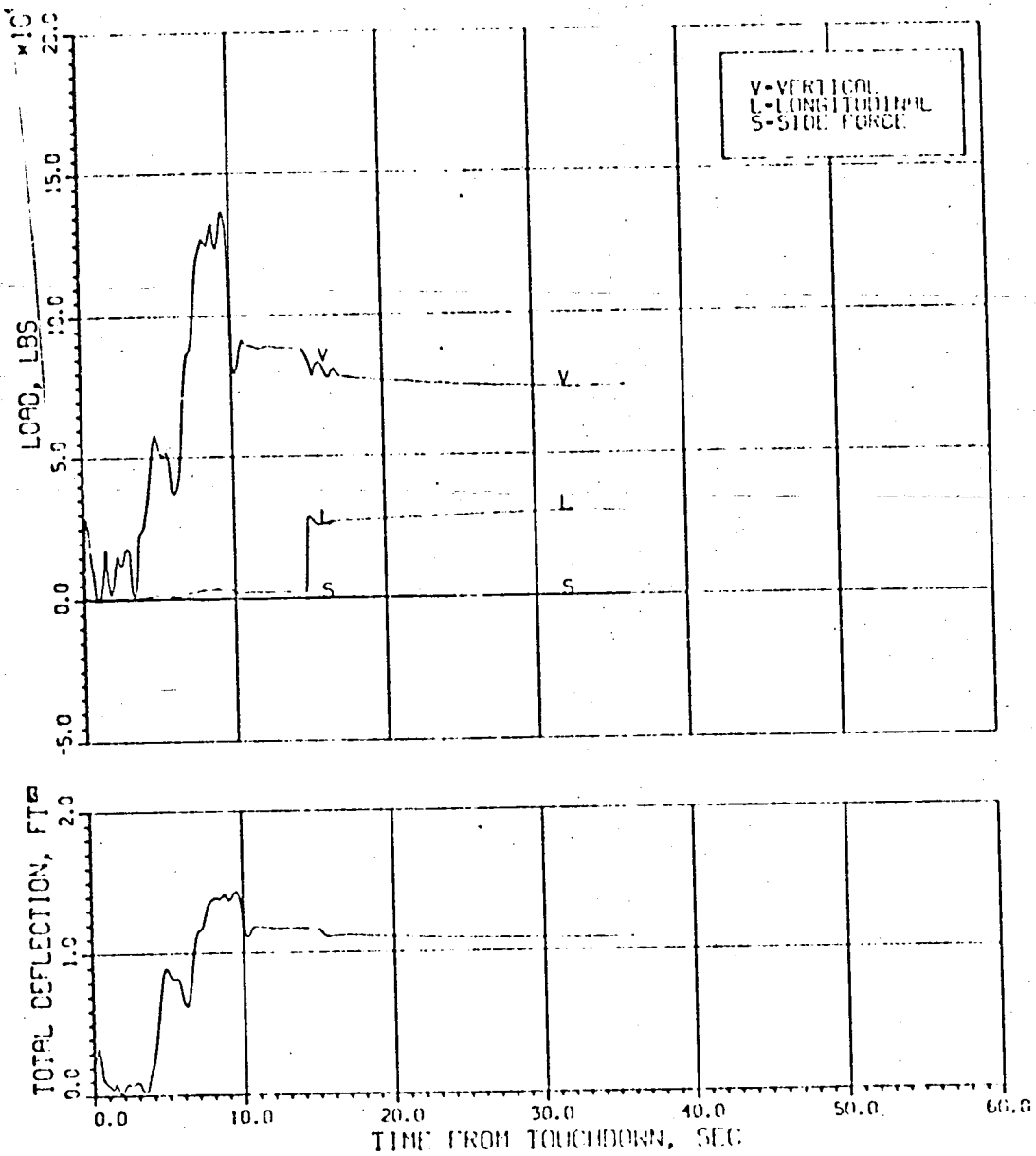
PILOT AND CG LOAD FACTORS
DURING ROLLOUT

Figure 6.5-5



NOSE GEAR STRUT, TIRE DEFLECTION
AND LOADS DURING ROLLOUT

Figure 6.5-6



MAIN GEAR STRUT, TIRE DEFLECTION
AND LOADS DURING ROLLOUT

Figure 6.5-7

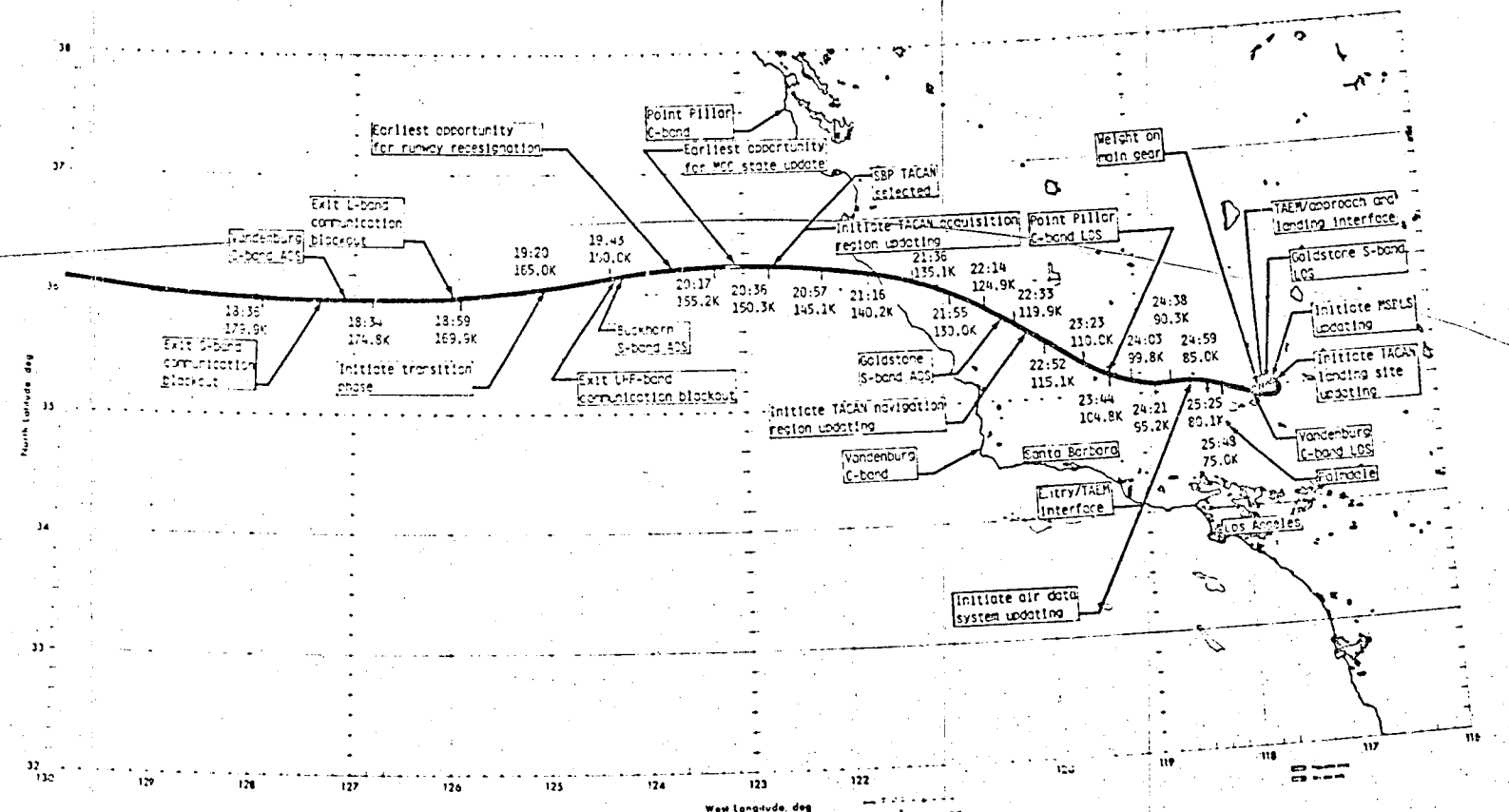


Figure 6.6-1.- Postblockout entry groundtrack for Orbiter STS-1.

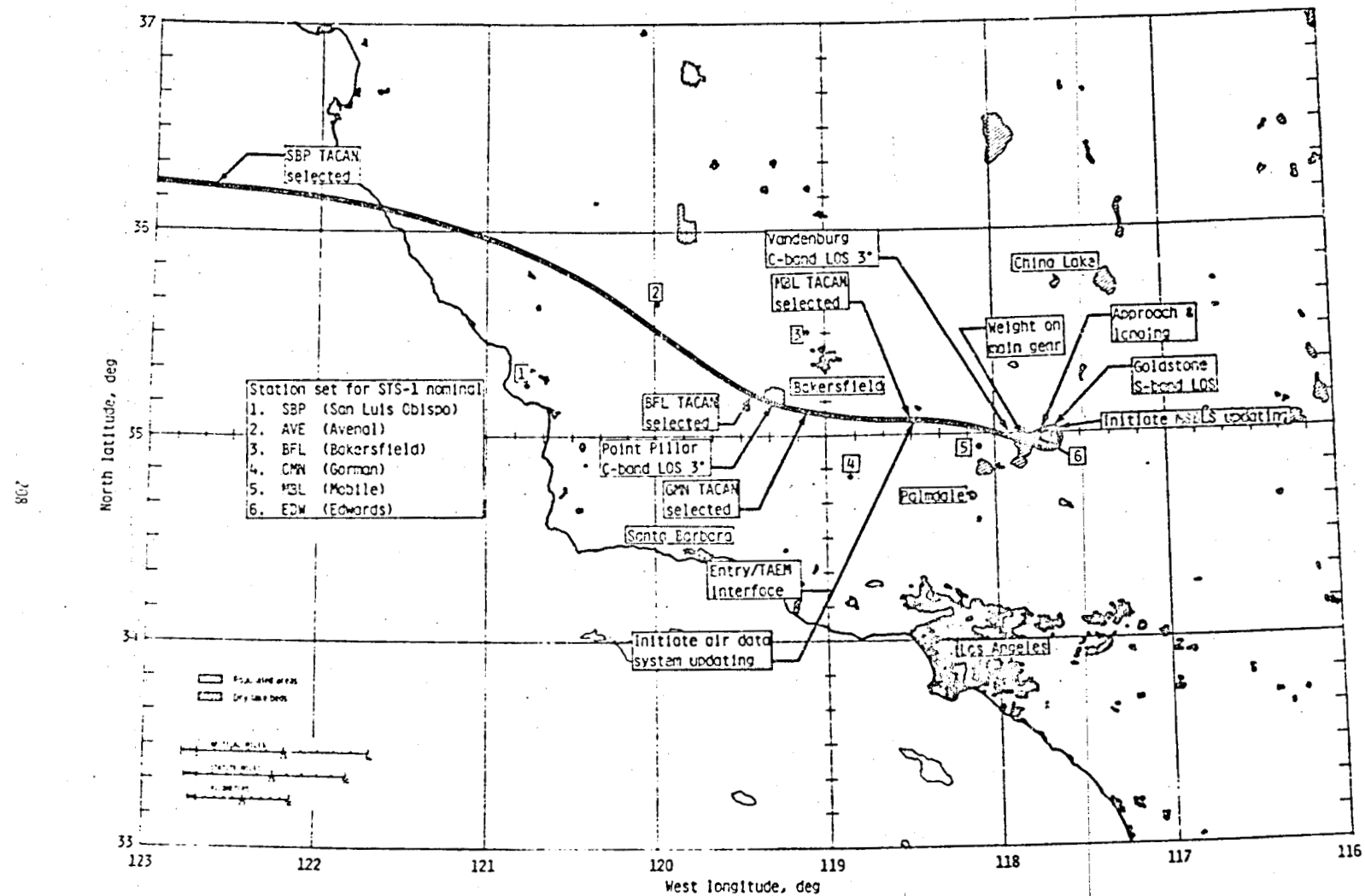
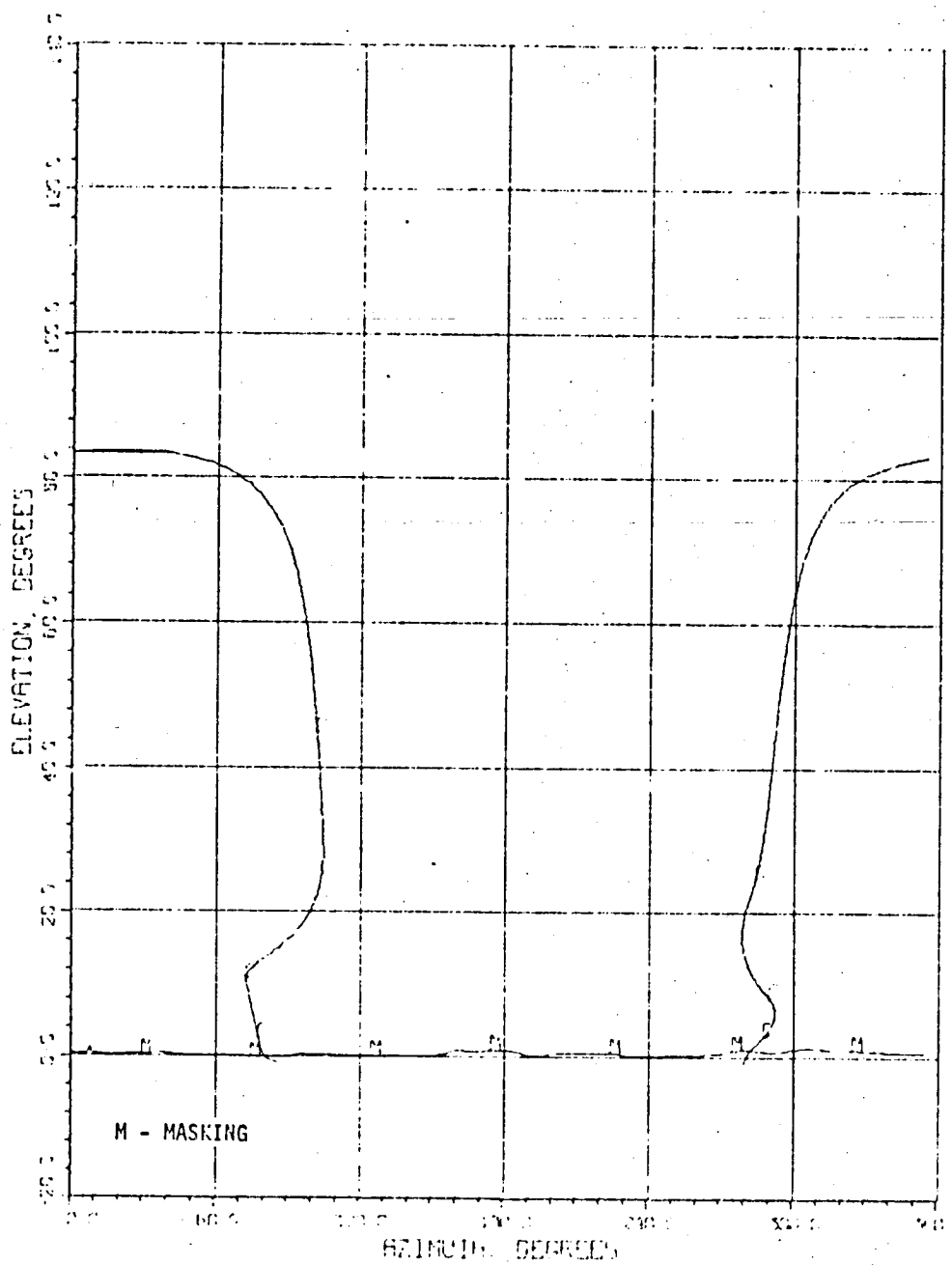
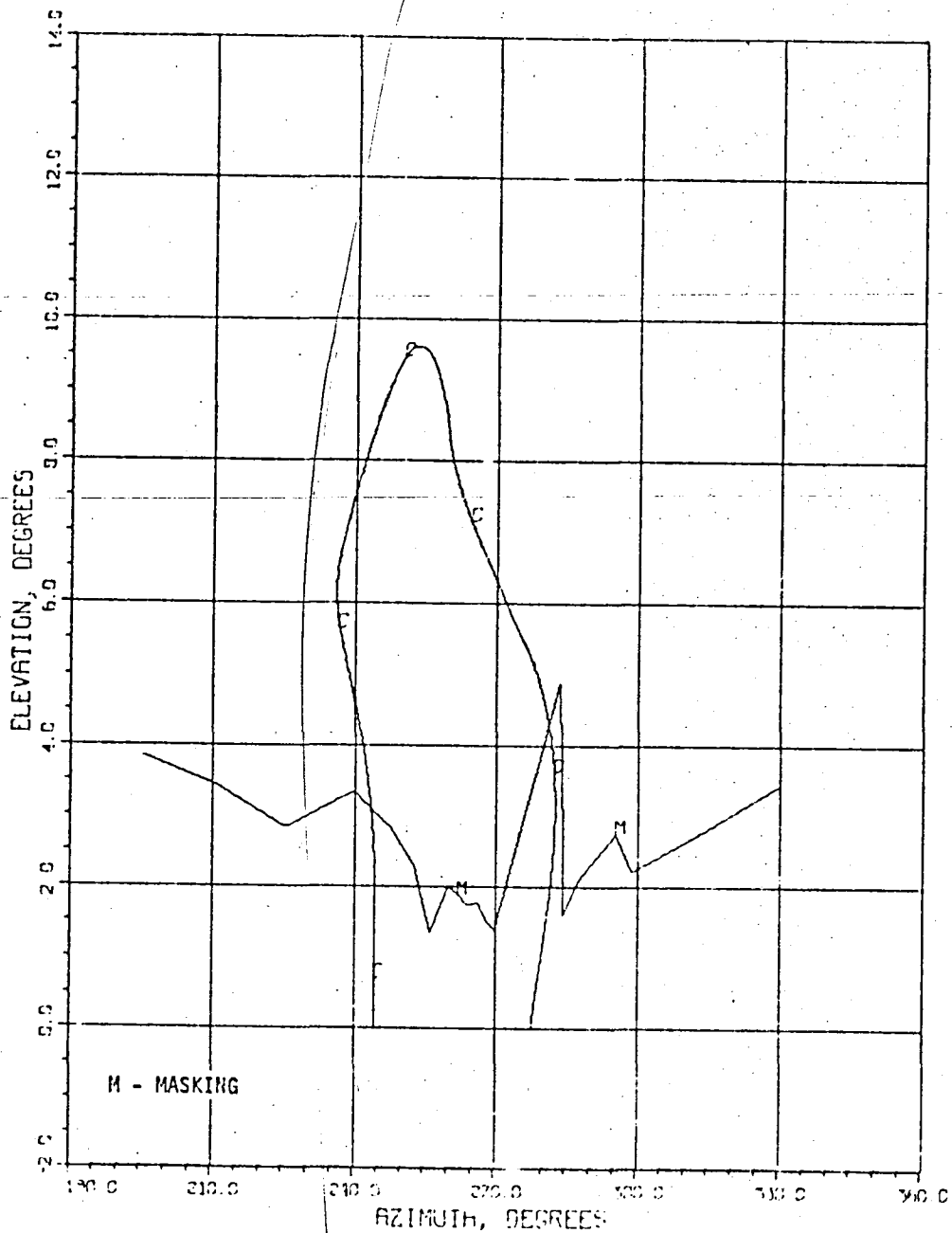


Figure 6.6-2.- STS-1 entry groundtrack and TACAN events.



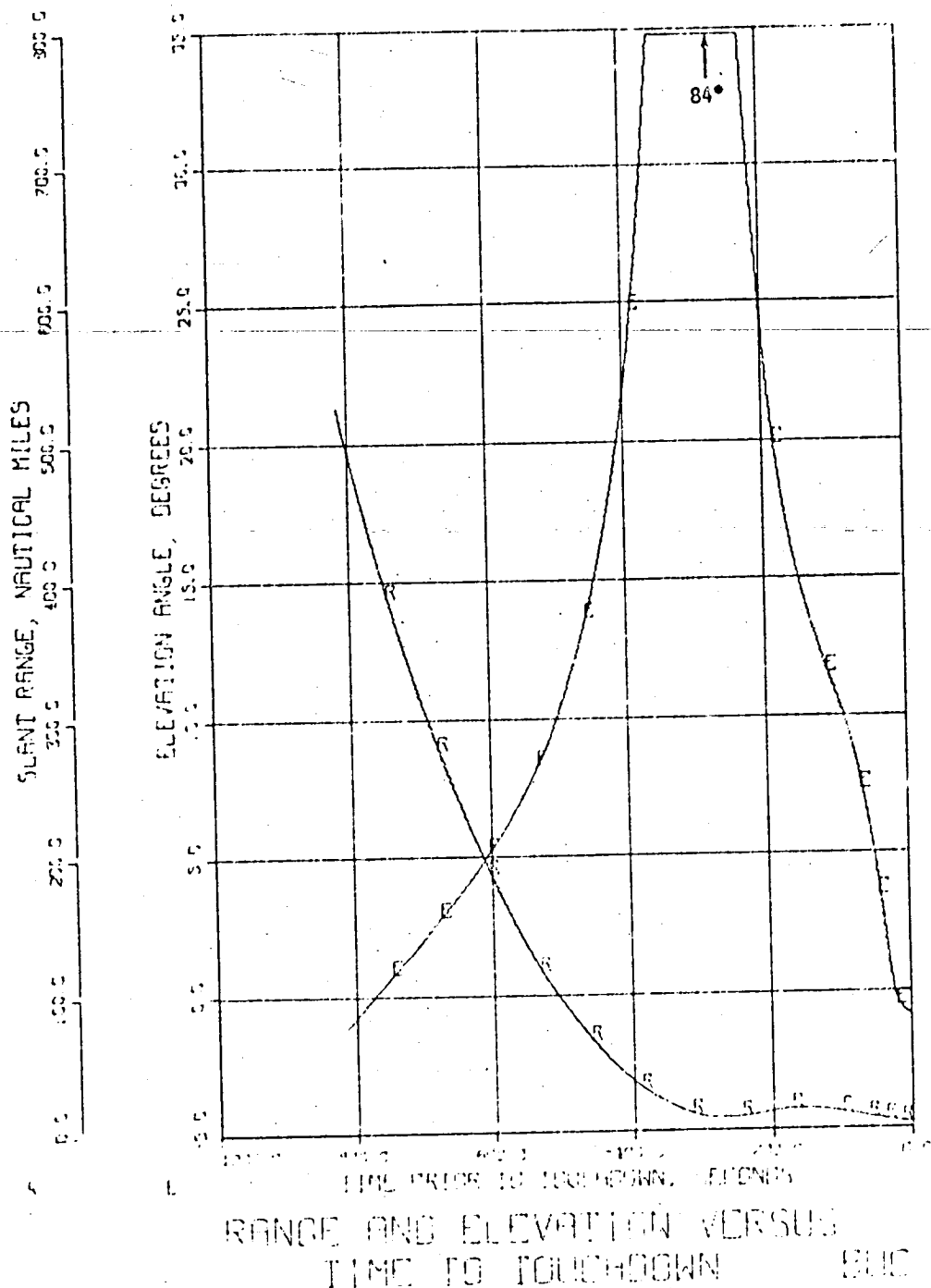
ELLEVATION ANGLE VERSUS AZIMUTH
BUCKHORN, BUD

Figure 6.6-3

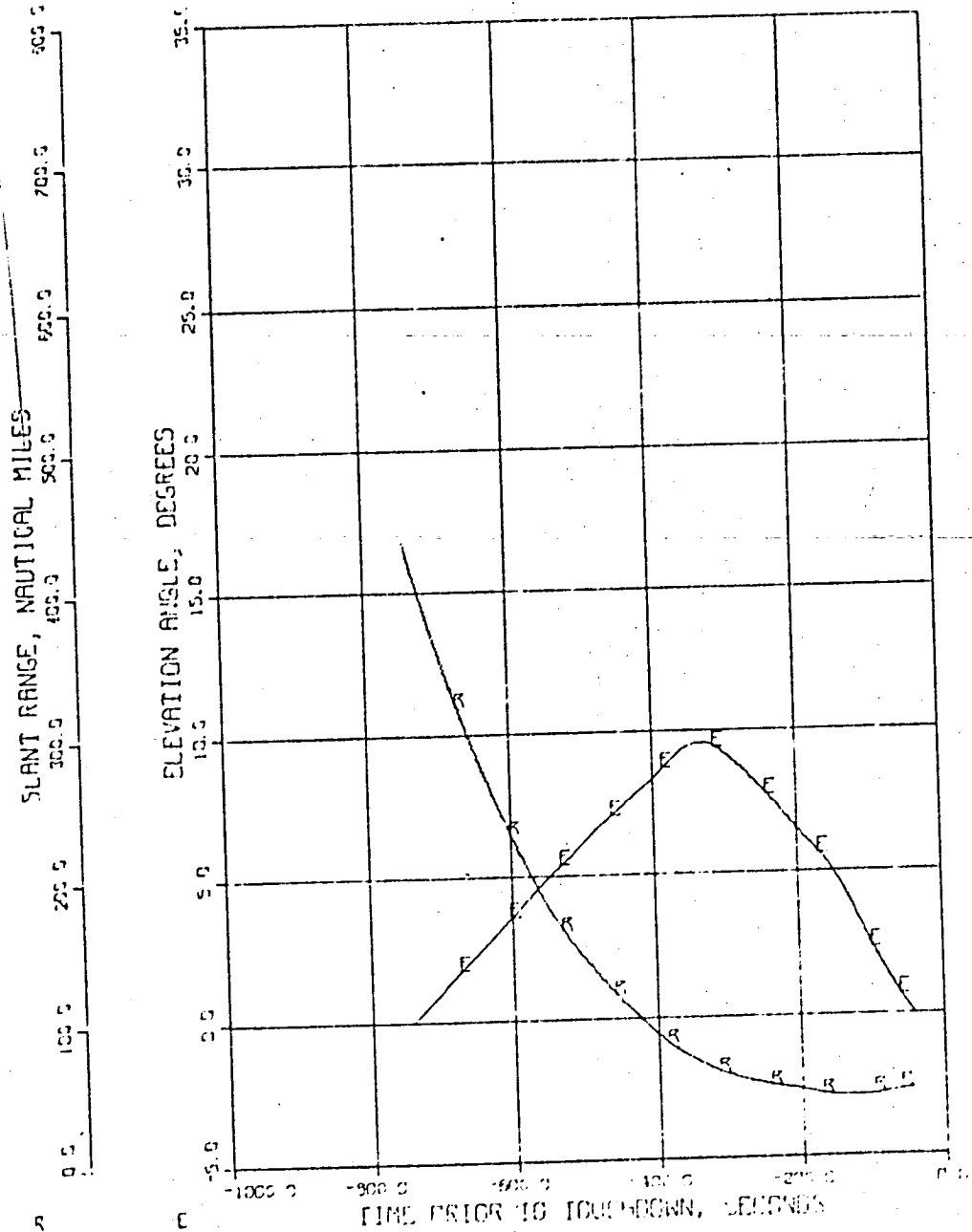


EL E V A T I O N A N G L E V E R S U S A Z I M U T H
G O L D S T O N E , G D S

Figure 6.6-4

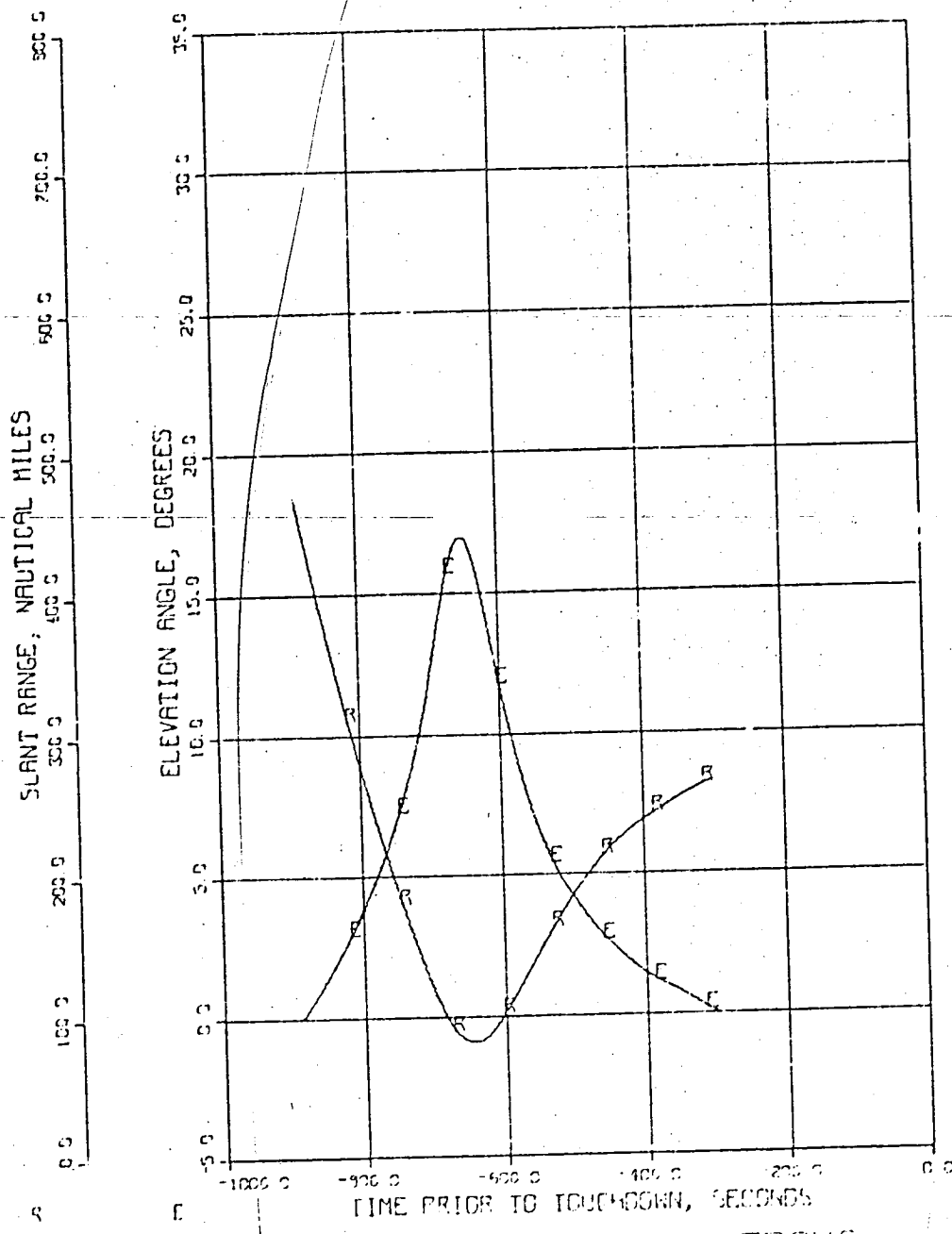


(a)
Figure 6.6-5



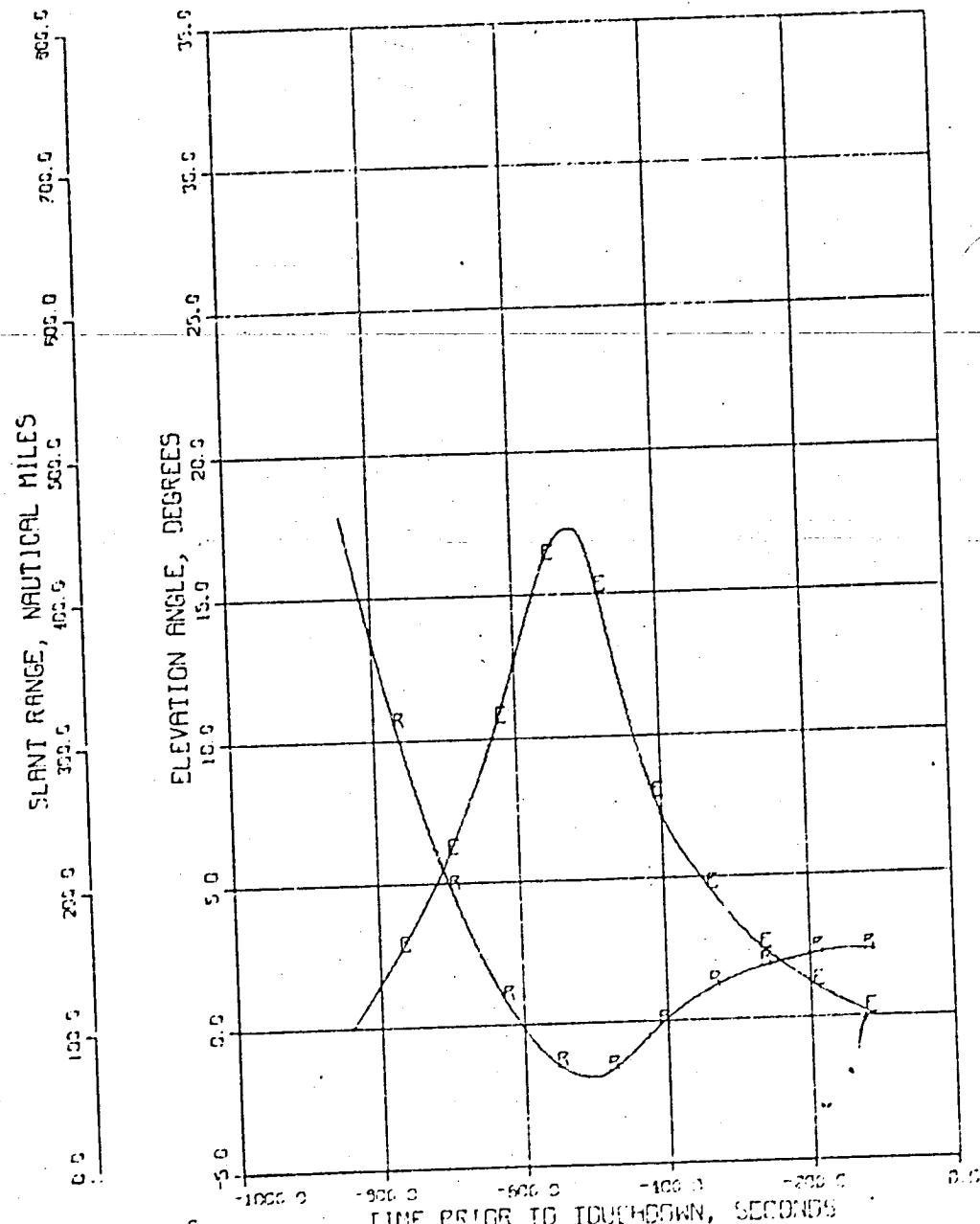
RANGE AND ELEVATION VERSUS
TIME TO TOUCHDOWN 60S

(b)
Figure 6.6-5



RANGE AND ELEVATION VERSUS
TIME TO TOUCHDOWN TTP

(c)
Figure 6.6-5



RANGE AND ELEVATION VERSUS
TIME TO TOUCHDOWN VDB

(d)
Figure 6.6-5

215

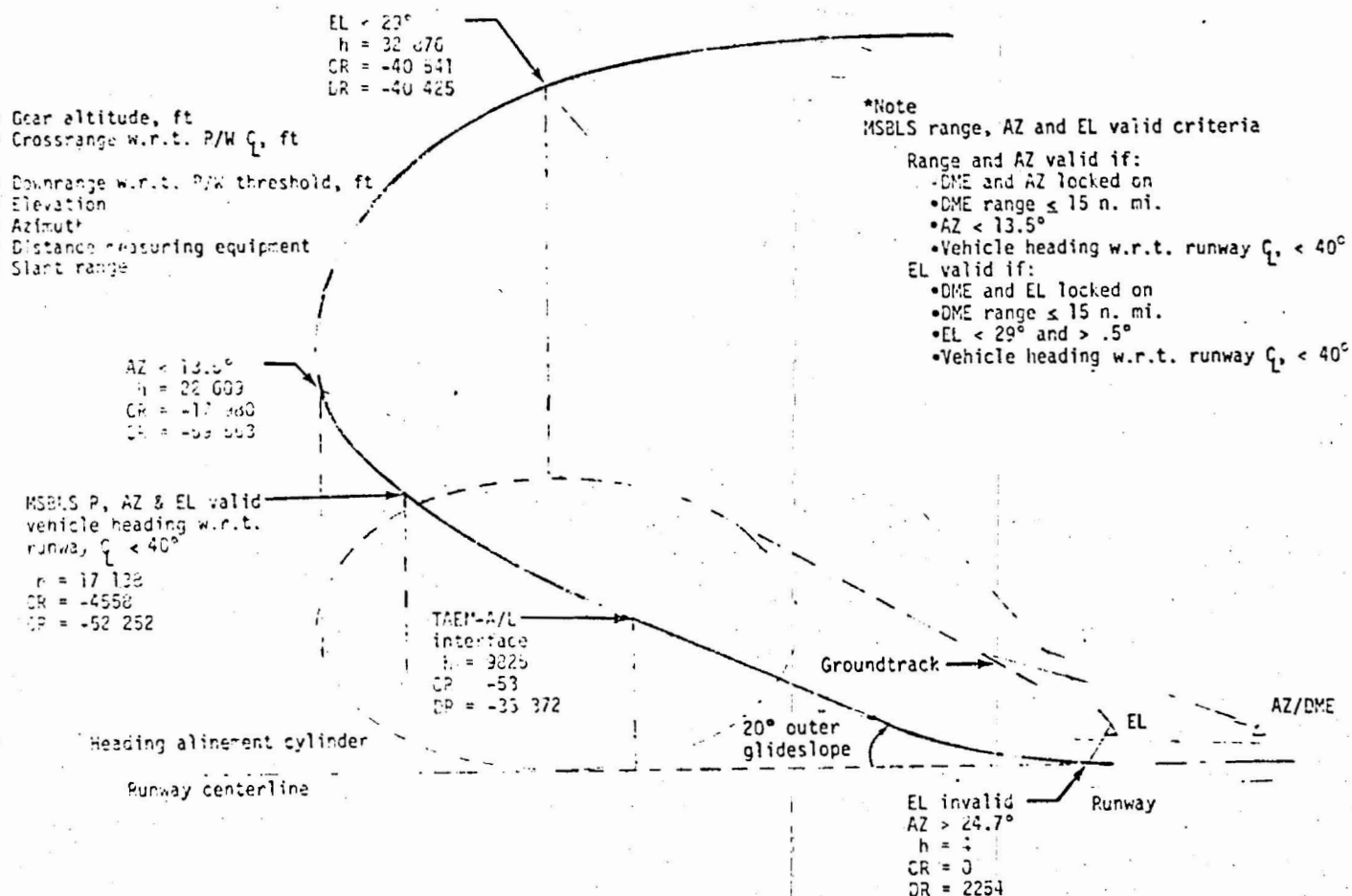


Figure 6. -- MSBLS coverage sequence.

APPENDIX A

ENTRY INITIALIZATION LOAD FOR THE ONBOARD COMPUTER

The guidance constants for the entry, TAEM, and A&L phases are presented in tables A-I(a), A-I(b), and A-I(c), respectively.

TABLE A-I(a).- DEFINITION OF ENTRY GUIDANCE CONSTANTS(G4.8)

MISID # VSTU	SW	SYMBOL	DESCRIPTION	MC	VALUE	UNITS	MISSION DEPENDENT CONSTANT
0495C	C	ACLM1	MAXIMUM ALPHA COMMAND INTERCEPT CONSTANT	03	.75000000+01	DEG	D
0495C	C	ACLM2	MAXIMUM ALPHA COMMAND SLOPE CONSTANT	03	.35000000-02	DEG-S/FT	D
0497C	C	ACLM1	MINIMUM ALPHA COMMAND UPPER LIMIT INTERCEPT	03	.37000000+02	DEG	D
0498C	C	ACLM2	MINIMUM ALPHA COMMAND UPPER LIMIT SLOPE	03	.00000000	DEG-S/FT	D
0499C	C	ACLM3	MINIMUM ALPHA COMMAND LOWER LIMIT INTERCEPT	03	.76666670+01	DEG	D
0500C	C	ACLM4	MINIMUM ALPHA COMMAND LOWER LIMIT SLOPE	03	.22333330-02	DEG-S/FT	D
0006C	C	ACN1	TIME CONSTANT FOR H DOT FEEDBACK	03	.50000000+02	S	D
0007C	C	AK	FACTOR IN DD/DV FOR TEMPERATURE CONTROL GUIDANCE USED TO DEFINE C23	03	-	ND	M
0008C	C	AK1	FACTOR IN DD/DV FOR TEMPERATURE CONTROL GUIDANCE USED TO DEFINE C23	03	-4512770+01	ND	M
0009C	C	ALFM	DESIPED CONSTANT DRAG LEVEL	03	.33000000+02	FT/SEC**2	M
0010C	C	ALIM	MAXIMUM SENSED ACCELERATION IN TRANSITION	03	.70840000+02	FT/SEC**2	D
0011C	C	ALMN1	MAXIMUM L/D COMMAND OUTSIDE OF HEADING ERROR DEADBAND	03	.72863550+00	ND	D
001	C	ALMN2	MAXIMUM L/D COMMAND INSIDE OF HEADING ERROR DEADBAND	03	.96592580+00	ND	D
0013C	C	ALMN3	MAXIMUM L/D COMMAND BELOW VYLMIN	03	.93969000+00	ND	D
0014C	C	ALMN4	MAXIMUM L/D COMMAND ABOVE VYLMAX	03	.10000000+01	ND	D
0042C	C	ASTART	SENSED ACCELERATION TO ENTER PHASE 2	03	.56600000+01	FT/SEC**2	D
0043C	C	CALPO(1)	ALPCMD CONSTANT TERM IN VE	03	.54245050+01	DEG	M
0044C	C	CALPO(2)	ALPCMD CONSTANT TERM IN VE	03	.54245050+01	DEG.	M
0045C	C	CALPO(3)	ALPCMD CONSTANT TERM IN VE	03	-.42778000+01	DEG	M

TABLE A-I(a).- Continued.

MSID # V37U	SW	SYMBOL	DESCRIPTION	MC	VALUE	UNITS	MISSION DEPENDENT CONSTANT
C046C	C	CALPC(4)	ALPCMD CONSTANT TERM IN VE	03	.16398000+02	DEG	M
C047C	C	CALPO(5)	ALPCMD CONSTANT TERM IN VE	03	.44760900+01	DEG	M
C048C	C	CALPO(6)	ALPCMD CONSTANT TERM IN VE	03	-.99339000+01	DEG	M
C049C	C	CALPO(7)	ALPCMD CONSTANT TERM IN VE	03	.40000000+02	DEG	M
C049C	C	CALPO(8)	ALPCMD CONSTANT TERM IN VE	03	.40000000+02	DEG	M
C049C	C	CALPO(9)	ALPCMD CONSTANT TERM IN VE	03	.40000000+02	DEG	M
C049C	C	CALPO(10)	ALPCMD CONSTANT TERM IN VE	03	.40000000+02	DEG	M
C050C	C	CALP1(1)	ALPCMD RATE TERM IN VE	03	.34301980-02	DEG-SEC/FT	M
C051C	C	CALP1(2)	ALPCMD RATE TERM IN VE	03	.34301980-02	DEG-SEC/FT	M
C052C	C	CALP1(3)	ALPCMD RATE TERM IN VE	03	.88750020-02	DEG-SEC/FT	M
C053C	C	CALP1(4)	ALPCMD RATE TERM IN VE	03	-.31431090-03	DEG-SEC/FT	M
C054C	C	CALP1(5)	ALPCMD RATE TERM IN VE	03	.31875030-02	DEG-SEC/FT	M
C055C	C	CALP1(6)	ALPCMD RATE TERM IN VE	03	.60874360-02	DEG-SEC/FT	M
C055C	C	CALP1(7)	ALPCMD RATE TERM IN VE	03	.00000000	DEG-SEC/FT	M
C049C	C	CALP1(8)	ALPCMD RATE TERM IN VE	03	.00000000	DEG-SEC/FT	M
C049C	C	CALP1(9)	ALPCMD RATE TERM IN VE	03	.00000000	DEG-SEC/FT	M
C049C	C	CALP1(10)	ALPCMD RATE TERM IN VE	03	.00000000	DEG-SEC/FT	M
C057C	C	CALP2(1)	ALPCMD QUADRATIC TERM IN VE	03	.00000000	DEG(S/FT)**2	M
C058C	C	CALP2(2)	ALPCMD QUADRATIC TERM IN VE	03	.00000000	DEG(S/FT)**2	M
C059C	C	CALP2(3)	ALPCMD QUADRATIC TERM IN VE	03	-.76388910-C6	DEG(S/FT)**2	M
C060C	C	CALP2(4)	ALPCMD QUADRATIC TERM IN VE	03	.25714550-C6	DEG(S/FT)**2	M
C061C	C	CALP2(5)	ALPCMD QUADRATIC TERM IN VE	03	.00000000	DEG(S/FT)**2	M
C062C	C	CALP2(6)	ALPCMD QUADRATIC TERM IN VE	03	+.23749780-C6	DEG(S/FT)**2	M
C063C	C	CALP2(7)	ALPCMD QUADRATIC TERM IN VE	03	.00000000	DEG(S/FT)**2	M
C065C	C	CALP2(8)	ALPCMD QUADRATIC TERM IN VE	03	.00000000	DEG(S/FT)**2	M

TABLE A-I(a).- Continued.

MSID #	S#	SYMBOL	DESCRIPTION	NC	VALUE	UNITS	MISSION DEPENDENT CONSTANT
		CALP2(9)	ALPCMD QUADRATIC TERM IN VE	03	.0000000	DEG(S/FT)**2	M
		CALP2(10)	ALPCMD QUADRATIC TERM IN VE	03	-.0000000	DEG(S/FT)**2	M
		CDDOT1	CD VELOCITY COEFFICIENT	03	-.5000000+04	FT/S	D
		CDDOT2	CD VELOCITY COEFFICIENT	03	.2000000+04	FT/S	D
		CDDOT3	CD VELOCITY COEFFICIENT	03	.1800000+00	ND	D
		CDDOT4	CD ALPHA COEFFICIENT	03	.7930000-01	ND	D
		CDDOT5	CD ALPHA COEFFICIENT	03	-.8165000-02	1/DEG	D
		CDDOT6	CD ALPHA COEFFICIENT	03	.6833000-03	1/DEG**2	D
		CDDOT7	CD COEFFICIENT	03	.9000000-04	S/FT	D
		CDDOT8	CD COEFFICIENT	03	.13565000-02	1/DEG**2	D
		CDDOT9	CD COEFFICIENT	03	-.8165000-02	1/DEG	D
		CRGEAF	GAIN ON ROLL BIAS	03	.4000000+01	ND	D
		CT16(1)	C16 COEFFICIENT	03	.13540000-00	S**2/FT	D
		CT16(2)	C16 POWER COEFFICIENT	03	-.10000000+00	ND	D
		CT16(3)	GAIN ON C16 ERROR TERM	03	.60000000-02	S**4/FT**2	D
		CT17(1)	C17 COEFFICIENT	03	.15370000-01	S/FT	D
		CT17(2)	C17 POWER COEFFICIENT	03	-.58146000+00	ND	D
		CT17MP	MULTIPLICATION FACTOR ON C17 FOR ALPHA MODULATION	03	.7500000+00	ND	D
		CT16MN	MINIMUM VALUE OF C16	03	.2500000-01	S**2/FT	D
		CT16MX	MAXIMUM VALUE OF C16	03	.35000000+00	S**2/FT	D
		CT17MN	MINIMUM VALUE OF C17	03	.25000000-02	S/FT	D
		CT17MX	MAXIMUM VALUE OF C17	03	.14000000-01	S/FT	D
		CT17M2	VALUE OF CT17MN FOR ALPHA MODULATION	03	.13300000-02	S/FT	D

TABLE A-I(a).- Continued.

MFD # 1970	SW	SYMBOL	DESCRIPTION	AC	VALUE	UNITS	MISSION DEPENDENT CONSTANT
C109C	C	CY0	CONSTANT TERM IN HEADING ERROR DEADBAND	03	.13099000+00	RAD	D
C110C	C	CY1	SLOPE OF HEADING ERROR DEADBAND WRT VE	03	.10908300-03	RAD-S/FT	D
C506C	C	C21	C20 CONSTANT VALUE	03	.60000000-01	1/DEG	M
C507C	C	C22	C20 CONSTANT VALUE LINEAR TERM	03	.10000000-02	1/EEG	M
C508C	C	C23	C20 LINEAR TERM	03	.42500000-05	S/FT-DEG	M
C509C	C	C24	C20 CONSTANT VALUE	03	.10000000-01	1/EFG	M
C510C	C	C25	C20 CONSTANT VALUE IN LINEAR TERM	03	.10000000-01	1/DEG	M
C511C	C	C26	C20 LINEAR VALUE	03	.00000000	S/FT-DEG	M
C512C	C	C27	C20 CONSTANT VALUE	03	.00000000	1/LEG	M
C111C	C	DDLM	MAXIMUM DELTA DRAG FOR HOOT FEEDBACK	03	.20000000+01	FT/S**2	D
C534C	C	DDVIN	MAXIMUM DRAG ERROR	03	.15000000+00	FT/S**2	D
C118C	C	DELV	PHASE TRANSFER VELOCITY BIAS	03	.23000000+04	FT/S	D
C121C	C	DF	FINAL DRAG VALUE IN TRANSITION PHASE	03	.20800310+02	FT/S**2	M
C141C	C	D230	INITIAL VALUE OF D23	03	.19380000+02	FT/S**2	M
C477C	C	DLRDTM	MAXIMUM VALUE OF DLRCOT	03	.15000000+03	FT/S	D
C504C	C	DLALLM	MAXIMUM ALPHA CONSTANT	03	.43000000+02	DEG	D
C505C	C	DALPLM	LIMIT VALUE FOR DLAPIM	03	.20000000+01	DEG	D
C128C	C	DRDOL	MINIMUM VALUE OF DRDD	03	.15000000+01	NM-S**2/FT	D
C140C	C	DT2MIN	MINIMUM VALUE OF T2DOT	03	.80000000-02	FT/S**3	D
C160C	C	EEF4	FINAL REFERENCE ENERGY LEVEL IN TRANSITION PHASE	03	.20000000+07	(FT/S)**2	M
C227C	C	ETRAN	ENERGY LEVEL AT START OF TRANSITION	03	.59984730+08	(FT/S)**2	M
C228C	C	E1	MINIMUM VALUE OF DREFP AND DREFP-DF IN TRANSITION PHASE	03	.10000000-01	FT/S**2	D

TABLE A-I(a).- Continued.

NSID # V97U	SW	SYMBOL	DESCRIPTION	NC	VALUE	UNITS	MISSION DEPENDENT CONSTANT
	0259C	C GS1	FACTOR IN SMOOTHING ROLL COMMAND	03	.0000000	1/S	M
	0260C	C GS2	FACTOR IN SMOOTHING ROLL COMMAND	03	.1000000-03	1/S	M
	0261C	C GS3	FACTOR IN SMOOTHING ROLL COMMAND	03	.0000000	1/S	M
	0262C	C GS4	FACTOR IN SMOOTHING ROLL COMMAND	03	.0000000	1/S	M
	0293C	C HSMIN	MINIMUM VALUE OF SCALE HEIGHT	03	.2050000+05	FT	D
	0294C	C HS01	SCALE HEIGHT CONSTANT TERM	03	.1807500+05	FT	D
	0295C	C HS02	SCALE HEIGHT CONSTANT TERM	03	.2700000+05	FT	D
	0296C	C HS03	SCALE HEIGHT CONSTANT TERM	03	.45503500+05	FT	D
A-6	0297C	C HS11	SCALE HEIGHT SLOPE WRT VE	03	.7250000+00	S	D
	0298C	C HS13	SCALE HEIGHT SLOPE WRT VE	03	.9445000+00	S	D
	0316C	C LDCMIN	MINIMUM L/D RATIO	03	.5000000+03	ND	D
	0321C	C NALP	NUMBER OF ALPCMD VELOCITY SEGMENT BOUNDARIES	03	.9000000+01	ND	D
	0349C	C PREBNK	PREENTRY BANK ANGLE COMMAND	03	.0000000	DEG	M
	0535C	C RDMAX	MAXIMUM ROLL BIAS	03	.1200000+02	DEG	D
	0470C	C RLMC1	MAXIMUM VALUE OF RLM	03	.7000000+02	DEG	D
	0471C	C RLMC2	COEFFICIENT IN FIRST RLM SEGMENT	03	.7000000+02	DEG	D
	0472C	C RLMC3	COEFFICIENT IN FIRST RLM SEGMENT	03	.0000000	DEG-S/FT	D
	0473C	C RLMC4	COEFFICIENT IN SECOND RLM SEGMENT	03	.3700000+03	DEG	D
	0474C	C RLMC5	COEFFICIENT IN SECOND RLM SEGMENT	03	.1600000+00	DEG-S/FT	D
	0475C	C RLMC6	MINIMUM VALUE OF RLM	03	.3000000+02	DEG	D
	0392C	C RPT1	RANGE BIAS TERM	03	.2944000+02	RM	M
	0421C	C VA	INITIAL VELOCITY FOR TEMPER- ATURE QUADRATIC. DD/DV=0	03	.23163700+05	FT/S	M
	0513C	C VALMOD	VELOCITY TO START ALPHA MODULATION FOR NON-CONVERGENCE	03	.2300000+05	FT/S	M

TABLE A-I(a).- Continued.

NSIC # V970	SW	SYMBOL	DESCRIPTION	MC	VALUE	UNITS	MISSION DEPENDENT CONSTANT
0422C	C	VALP(1)	ALPCMD VS VE BOUNDARY	03	.28500000+04	FT/S	M
0423C	C	VALP(2)	ALPCMD VS VE BOUNDARY	03	.35636700+04	FT/S	M
0424C	C	VALP(3)	ALPCMD VS VE BOUNDARY	03	.45000000+04	FT/S	M
0425C	C	VALP(4)	ALPCMD VS VE BOUNDARY	03	.68090000+04	FT/S	M
0426C	C	VALP(5)	ALPCMD VS VE BOUNDARY	03	.77694500+04	FT/S	M
0427C	C	VALP(6)	ALPCMD VS VE BOUNDARY	03	.14500000+05	FT/S	M
0428C	C	VALP(7)	ALPCMD VS VE BOUNDARY	03	.14500000+05	FT/S	M
0429C	C	VALP(8)	ALPCMD VS VE BOUNDARY	03	.14500000+05	FT/S	M
0429C	C	VALP(9)	ALPCMD VS VE BOUNDARY	03	.14500000+05	FT/S	M
0428C	C	V41	BOUNDARY VELOCITY BETWEEN QUADRATIC SEGMENTS IN TEMPERATURE CONTROL PHASE	03	.21000000+05	FT/S	M
0429C	C	V42	INITIAL VELOCITY FOR TEMPERATURE QUADRATIC. DO/DV=0	03	.27197460+05	FT/S	M
0430C	C	V81	HEAT RATE-EQUILIBRIUM GLIDE PHASE BOUNDARY VELOCITY	03	.19000000+05	FT/S	M
0432C	C	VC16	VELOCITY TO START C16 DRAG ERROR TERM	03	.23000000+05	FT/S	D
0514C	C	VC20	C20 VELOCITY BREAKPOINT	03	.25000000+04	FT/S	M
0433C	C	VELMN	MAXIMUM VELOCITY FOR LIMITING LMN BY ALVM3	03	.95000000+04	FT/S	D
0434C	C	VEROLC	MAXIMUM VELOCITY FOR LIMITING BANK ANGLE COMMAND	03	.80000000+04	FT/S	D
0435C	C	VHS1	SCALE HEIGHT VS VE BOUNDARY	03	.12310340+05	FT/S	D
0436C	C	VHS2	SCALE HEIGHT VS VE BOUNDARY	03	.19675500+05	FT/S	D
0515C	C	VNDALP	VELOCITY TO START ALPHA MODULATION	03	.25000000+05	FT/S	M
0437C	C	VO	PREDICTED END VELOCITY FOR CONSTANT DRAG PHASE	03	.50000000+04	FT/S	M

TABLE A-I(a).- Concluded.

MSID # V97U	SW	SYMBOL	DESCRIPTION	MC	VALUE	UNITS	MISSION DEPENDENT CONSTANT	
	0438C	C	VRDT		.23000000+05	FT/S	D	
	0476C	C	VRLMC	VELOCITY IN TRANSITION MAXIMUM ROLL COMMAND DETERMINATION	.03	.27500000+04	FT/S	D
A-8	0439C	C	VSAT	LOCAL CIRCULAR ORBIT VELOCITY	.03	.25766200+05	FT/S	D
	0440C	C	VS1	REFERENCE VELOCITY FOR EQUILIBRIUM GLIDE	.03	.23271870+05	FT/S	M
	0420C	C	V TAEM	REFERENCE VELOCITY AT ENTRY- TAEM INTERFACE	.03	.25000000+04	FT/S	D
	0441C	C	VTRAN	NOVINAL VELOCITY AT START OF TRANSITION PHASE	.03	.10500000+05	FT/S	M
	0442C	C	YLMAX	MINIMUM VELOCITY FOR LIMITING LMN BY ALMN4	.03	.23000000+05	FT/S	D
	0465C	C	YLMIN	YL BIAS USED IN TEST FOR LMN	.03	.30000000-01	RAD	D
	0466C	C	YLMN2	MINIMUM YL BIAS	.03	.70000000-01	RAD	D
	0467C	C	Y1	MAXIMUM HEADING ERROR DEADBAND FOR INITIAL BANK MANEUVER	.03	.16325950+00	RAD	D
	0468C	C	Y2	MINIMUM HEADING ERROR DEADBAND	.03	.17453290+00	RAD	D
	0478C	C	Y3	MAXIMUM HEADING ERROR DEADBAND	.03	.30543260+00	RAD	D
	0469C	C	ZXT	GAIN FOR H DOT FEEDBACK	.03	.60000000+00	S	D

TABLE A-I(b).- DEFINITION OF TAEM GUIDANCE CONSTANTS(G4.9)

MSID # V97U	SW	SYMBOL	DESCRIPTION	MC	VALUE	UNITS	MISSION DEPENDENT CONSTANT
0073C	P	CDEOD	CONSTANT GAIN USED TO COMPUTE OBD (= EXP (-0.4 DTG))	03	.68113130+00	ND	D
0075C	P	COPMIN	MINIMUM VALUE OF COSPHI	03	.70700000+00	ND	D
0076C	P	CODG	CONSTANT GAIN USED TO COMPUTE OBD (= 1 + CDEOD)	03	.31886860+00	ND	D
0077C	P	COG	CONSTANT GAIN USED TO COMPUTE CGARD AND CNZCD (= 1 + EXP (-0.08 DTG))/DTG)	03	.155835580+00	1/S	D
0103C	P	CUBIC C3(1)	COEFFICIENT USED TO COMPUTE HREF AND DHORRF	03	-.36411680-05	1/FT	M
0104C	P	CUBIC C3(2)	HREF AND DHORRF	03	-.36411680-06	1/FT	M
0105C	P	CUBIC C4(1)	COEFFICIENT USED TO COMPUTE HREF AND DHORRF	03	-.94810260-13	FT**-2	M
0106C	P	CUBIC C4(2)	HREF AND DHORRF	03	-.94810260-13	FT**-2	M
0113C	P	DEL H1	ALTITUDE ERROR COEFFICIENT	03	.19000000+00	ND	D
0114C	P	DEL H2	ALTITUDE ERROR COEFFICIENT	03	.90000000+03	FT	D
0115C	P	DEL R EMAX(1)	DELTA RANGE USED TO COMPUTE EMAX	03	.54000000+05	FT	M
0116C	P	DEL R EMAX(2)	EMAX	03	.54000000+05	FT	M
0123C	P	DNZCG	GAIN USED TO COMPUTE DNZC	03	.10L00000-01	G-S/FT	D
0124C	P	DNZLC1	PHASES 0,1, AND 2 LOWER NZC LIMIT	03	-.50000000+00	G	D
0125C	P	DNZLC2	PHASE 3 LOWER NZC LIMIT	03	-.75L00000+00	G	D
0126C	P	DNZUC1	PHASES 0,1, AND 2 UPPER NZC LIMIT	03	.50000000+00	G	D
0127C	P	DNZUC2	PHASE 3 UPPER NZC LIMIT	03	.15000000+01	G	D
0131C	P	DSBCM	MACH VALUE TO INITIATE SPEEDBRAKE MODULATION	03	.90000000+00	ND	D
0132C	P	DSBIL	LIMIT ON INTEGRAL COMPONENT OF SPEEDBRAKE COMMAND	03	.20000000+02	DEG	D
0133C	P	DSBLIM	MAXIMUM VALUE FOR SPEEDBRAKE COMMAND	03	.98600000+02	DEG	D

TABLE A-I(b).- Continued.

MSID # V97U	SW	SYMBOL	DESCRIPTION	MC	VALUE	UNITS	MISSION DEPENDENT CONSTANT
	P	DSBNOM	NOMINAL SPEEDBRAKE COMMAND VALUE	03	.65000000+02	DEG	D
	P	DSBSUP	MACH DSBCM SPEEDBRAKE COMMAND	03	.65000000+02	DEG	D
	P	DSHPLY	DELTA RANGE VALUE USED TO COMPUTE SHPLYK	03	.40000000+04	FT	D
	P	EDEL01	CONSTANT USED IN DETERMINATION OF EMAX	03	.10000000+01	ND	M
	P	EDEL02	CONSTANT USED IN DETERMINATION OF EMAX	03	.10000000+01	ND	M
	P	EDELNZ(1)	DELTA ENERGY OVER WEIGHT USED TO COMPUTE EMAX AND EMIN	03	.40000000+04	FT	M
	P	EDELNZ(2)	SLOPE OF ES WITH RANGE	03	.40000000+04	FT	M
	P	EDRS(1)	SLOPE OF ES WITH RANGE	03	.60894920+00	ND	M
	P	EDRS(2)	SLOPE OF ES WITH RANGE	03	.60894920+00	ND	M
	P	EMEP C1 (1,1)	CONSTANT ENERGY OVER WEIGHT	03	-.37137970+03	FT	M
	P	EMEP C1 (1,2)	USED TO COMPUTE EMEP	03	.14604870+05	FT	M
	P	EMEP C1 (2,1)		03	-.37137970+03	FT	M
	P	EMEP C1 (2,2)		03	.14604870+05	FT	M
	P	EMEP C2 (1,1)	SLOPE OF EMEP WITH RANGE	03	.41682740+00	ND	M
	P	EMEP C2 (1,2)	SLOPE OF EMEP WITH RANGE	03	.28211870+00	ND	M
	P	EMEP C2 (2,1)	SLOPE OF EMEP WITH RANGE	03	.41682740+00	ND	M
	P	EMEP C2 (2,2)	SLOPE OF EMEP WITH RANGE	03	.28211870+00	ND	M
	P	EN C1 (1,1)	CONSTANT ENERGY OVER WEIGHT	03	-.25423950+03	FT	M
	P	EN C1 (1,2)	USED TO COMPUTE EN	03	.17645340+05	FT	M
	P	EN C1 (2,1)		03	-.25423950+03	FT	M
	P	EN C1 (2,2)		03	.17645340+05	FT	M
	P	EN C2 (1,1)	SLOPE OF EN WITH RANGE	03	.55002750+00	ND	M
	P	EN C2 (1,2)	SLOPE OF EN WITH RANGE	03	.38902400+00	ND	M

OL-A

TABLE A-I(b).- Continued.

MSID # V97U	SW	SYMBOL	DESCRIPTION	MC	VALUE	UNITS	MISSION DEPENDENT CONSTANT
	P	EN C2 (2.1)	SLOPE OF EN WITH RANGE	03	.55002750+00	ND	M
	P	EN C2 (2.2)	SLOPE OF EN WITH RANGE	03	.38902400+00	ND	M
	P	EOW SPT(1)	RANGE USED FOR IEL SELECTION	03	.11771800+06	FT	M
	P	EOW SPT(2)	RANGE USED FOR IEL SELECTION	03	.11771800+06	FT	M
	P	ES1(1)	CONSTANT ENERGY OVER WEIGHT	03	.90000000+05	FT	M
	P	ES1(2)	USED TO COMPUTE ES	03	.90000000+05	FT	M
	P	GAMMA-COEF1	FLIGHTPATH ERROR COEFFICIENT	03	.70000000-03	DEG/FT	D
	P	GAMMA-COEF2	FLIGHTPATH ERROR COEFFICIENT	03	.30000000+01	DEG	D
	P	GAMMA ERR TRAN	FLIGHTPATH ERROR BAND	03	.40000000+01	DEG	D
	P	GAMSGS(1)	STEEP GLIDESLOPE ANGLE	03	.20000000+02	DEG	M
	P	GAMSGS(2)	STEEP GLIDESLOPE ANGLE	03	.20000000+02	DEG	M
	P	GDHC	CONSTANT USED TO COMPUTE GDH	03	.20000000+01	ND	D
	P	GDHLL	LOWER LIMIT ON GDH	03	.30000000+00	ND	D
	P	GDHS	SLOPE OF GDH WITH ALTITUDE	03	.70000000-04	1/FT	D
	P	GDHUL	UPPER LIMIT ON GDH	03	.10000000+01	ND	D
	P	GEHOLL	GAIN USED TO COMPUTE EOW-ZLL	03	.10000000-01	G-S/FT	D
	P	GEHOLUL	GAIN USED TO COMPUTE EOW-ZUL	03	.10000000-01	G-S/FT	D
	P	GEELL	GAIN USED TO COMPUTE EOW-ZLL	03	.10000000+00	1/S	D
	P	GEUL	GAIN USED TO COMPUTE EOW-ZUL	03	.10000000+00	1/S	D
	P	GPHI	GAIN ON HEADING ERROR FOR PHASE 1 ROLL COMMAND	03	.25000000+01	ND	D
	P	GR	GAIN ON RADIAL ERROR FOR PHASE 2 ROLL COMMAND	03	.20000000-01	DEG/FT	D
	P	GRDOT	GAIN ON RADIAL RATE ERROR FOR PHASE 2 ROLL COMMAND	03	.20000000+00	DEG-S/FT	D
	P	GSBE	SPEEDBRAKE PROPORTIONAL GAIN ON GSERR	03	.15000000+01	DEG/PSF	D

TABLE A-I(b).- Continued.

MSIO #	SW	SYMBOL	DESCRIPTION	NC	VALUE	UNITS	MISSION DEPENDENT CONSTANT
V97U							
0256C	P	GSBI	SPEEDBRAKE INTEGRAL GAIN ON OBERR	03	.10000000+00	DEC/S-PSF	D
0263C	P	GY	PHASE 3 LATERAL ERROR GAIN	03	.50000000-01	DEG/FT	D
0264C	P	GYDOT	PHASE 3 LATERAL RATE ERROR GAIN	03	.60000000+00	DEG-S/FT	D
0267C	P	H ERR TRAN	ALTITUDE ERROR BOUND FOR TRANSITION TO AUTOLAND	03	.10000000+04	FT	D
0279C	P	H REF1	ALTITUDE REFERENCE FOR TRANSITION TO AUTOLAND	03	.10000000+05	FT	D
0280C	P	H REF2	ALTITUDE REFERENCE FOR TRANSITION TO AUTOLAND	03	.50000000+04	FT	D
0287C	P	HALI(1)	ALTITUDE USED TO COMPUTE XALI	03	.10018000+05	FT	M
0288C	P	HALI(2)	AND HREF	03	.10018000+05	FT	M
0290C	P	HDREQG	GAIN ON HERROR TO COMPUTE DNZC	03	.10000000+00	1/S	D
0291C	P	HFTC(1)	ALTITUDE USED TO COMPUTE XFTC	03	.12018000+05	FT	M
0292C	P	HFTC(2)	ALTITUDE USED TO COMPUTE XFTC	03	.12018000+05	FT	M
0319C	P	MXQBT	CONSTANT USED TO COMPUTE QBTLL = (140./190000 PSF/LB M)	03	.23707160-01	PSF/SLUGS	M
0327C	P	PBGC(1)	LOWER LIMIT ON DMRRF =	03	.11259530+00	ND	M
0328C	P	PBGC(2)	(TAN (6.2 DTR), TAN (6.2DTR))	03	.11259530+00	ND	M
0330C	P	PBRCQ(1)	RANGE BREAKPOINT FOR QBREF	03	.12200000+06	FT	M
0334C	P	PBRCQ(2)	RANGE BREAKPOINT FOR QBREF	03	.12200000+06	FT	M
0329C	P	PBHC(1)	ALTITUDE REFERENCE FOR	03	.84821290-05	FT	M
0330C	P	PBHC(2)	RPRFD = PBRC	03	.84821290+05	FT	M
0331C	P	PBRC(1)	MAXIMUM RANGE FOR CUBIC	03	.20810950+06	FT	M
0332C	P	PBRC(2)	ALTITUDE REFERENCE	03	.30810950+06	FT	M
0335C	P	PHAVGC	CONSTANT USED TO COMPUTE PHAVG	03	.63330000+02	DEG	D
0336C	P	PHAVGLL	LOWER LIMIT ON PHAVG	03	.30000000+02	DEG	D
0337C	P	PHAVGS	SLOPE OF PHAVG WITH MACH	03	.13330000+02	DEG	D

A-12

TABLE A-I(b).- Continued.

MSID #	SW	SYMBOL	DESCRIPTION	NC	VALUE	UNITS	MISSION DEPENDENT CONSTANT
V97U							
0338C	P	PHAVGUL	UPPER LIMIT ON PHAVG	03	.50000000+02	DEG	D
0342C	P	PHILMSUP	SUPERSONIC ROLL COMMAND LIMIT	03	.30000000+02	DEG	D
0343C	P	PHILMO	S TURN ROLL COMMAND LIMIT	03	.50000000+02	DEG	D
0344C	P	PHILM1	ACQUISITION ROLL COMMAND LIMIT	03	.50000000+02	DEG	D
0345C	P	PHILM2	HEADING ALIGNMENT ROLL COMMAND LIMIT	03	.60000000+02	DEG	D
0346C	P	PHILM3	PREFINAL ROLL COMMAND LIMIT	02	.30000000+02	DEG	D
0347C	P	PHIM	MACH VALUE FOR PHILIMIT TEST	03	.10000000+01	ND	D
0348C	P	PHIP2C	NOMINAL ROLL COMMAND DURING PHASE 2	03	.30000000+02	DEG	D
0351C	P	P2TRNC1	CONSTANT USED IN PHASE 2 INITIATION TEST	03	.11000000+01	ND	D
0352C	P	P2TRNC2	CONSTANT USED IN PHASE 2 INITIATION TEST	03	.13100000+01	ND	D
0353C	P	QB ERROR1	DYNAMIC PRESSURE ERROR BOUND FOR TRANSITION TO AUTOLAND	03	-.10000000+01	PSF	D
0354C	P	QB ERRCR2	DYNAMIC PRESSURE ERROR BOUND FOR TRANSITION TO AUTOLAND	03	.24000000+02	PSF	D
0355C	P	QBCRD1	LIMIT ON QBCRD	03	.20000000+02	PSF/S	D
0356C	P	QBC1(1)	SLOPE OF QBCREF WITH DRPRED	03	.58695650-03	PSF/FT	M
0357C	P	QBC1(2)	PBRCO	03	.58695650-03	PSF/FT	M
0358C	P	QBC2(1)	SLOPE OF QBCREF WITH DRPRED	03	-.10316950-02	PSF/FT	M
0359C	P	QBC2(2)	PBRCO	03	-.10316950-02	PSF/FT	M
0360C	P	QBG1	GAIN USED TO COMPUTE QBNZLL AND QBNZUL	03	.10000000+00	1/S	D
0361C	P	QBG2	GAIN USED TO COMPUTE QSNZLL AND QSNZUL	03	.12500000+00	S-G/PSF	D
0366C	P	QBMXN2	SLOPE OF QBMXN2 WITH MACH QBY2	03	.20000000+02	PSF	D

A-13

TABLE A-I(b).- Continued.

MSID # V97U	SW	SYMBOL	DESCRIPTION	NC	VALUE	UNITS	MISSION DEPENDENT CONSTANT
	0367C	QBMX1	CONSTANT USED TO COMPUTE QBMNZ	03	.34000000+03	PSF	D
	0368C	QBMX2	CONSTANT USED TO COMPUTE QBMNZ	03	.22000000+03	PSF	D
	0369C	QBMX3	CONSTANT USED TO COMPUTE QBMNZ	03	.25000000+03	PSF	D
	0371C	QBM1	MACH BREAKPOINT FOR COMPUTING QBMNZ	03	.10000000+01	ND	D
	0372C	QBM2	MACH BREAKPOINT FOR COMPUTING QBMXYZ	03	.10000000+01	ND	D
A-14	0373C	QBRLL(1)	OBREF LOWER LIMIT	03	.15300000+03	PSF	M
	0374C	QBRLL(2)	OBREF LOWER LIMIT	03	.15300000+03	PSF	M
	0375C	QBRML(1)	OBREF MIDDLE LIMIT	03	.18000000+03	PSF	M
	0376C	QBRML(2)	OBREF MIDDLE LIMIT	03	.18000000+03	PSF	M
	0377C	QBRUL(1)	OBREF UPPER LIMIT	03	.26543000+03	PSF	M
	0378C	QBRUL(2)	OBREF UPPER LIMIT	03	.26543000+03	PSF	M
	0384C	RERRLM	LIMIT ON RERRC	03	.50000000+02	DEG	D
	0385C	RFTC	ROLL FADER TIME CONSTANT	03	.50000000+01	S	D
	0387C	RMINST(1)	MINIMUM RANGE TO INITIATE	03	.12220450+06	FT	M
	0388C	RMINST(2)	S TURN PHASE	03	.12220460+06	FT	M
	0389C	RN1(1)	CONSTANT RANGE USED IN COM-	03	.65428860+04	FT	M
	0390C	RN1(2)	PUTING EN, EMEP, AND EMAX	03	.65428860+04	FT	M
	0393C	RTBIAS	CONSTANT USED IN PHASE2 INITIATION TEST	03	.30000000+04	FT	D
	0394C	RTURN	HAC RADIUS	03	.20000000+05	FT	D
	0414C	TGGS(1)	TANGENT OF A/L STEEP GLIDESLOPE	03	.36397000+00	ND	M
	0415C	TGGS(2)	TANGENT OF A/L STEEP GLIDESLOPE	03	.36397000+00	ND	M

TABLE A-I(b).- Concluded.

MSID #	SW	SYMBOL	DESCRIPTION	MC	VALUE	UNITS	MISSION DEPENDENT CONSTANT
V97U							
0431C	P	VCO	CONSTANT USED TO COMPUTE GCONT (=RTD G/GON, WHERE GON = GON (IGCS))	03	.10000000+21	FT/SEC	D
0536C	P	V DEF	NAVDAD/DEFAULT QBAR SWITCH ON VELOCITY	03	.00000000	FT/SEC	M
0444C	P	WT GS1	WEIGHT USED FOR IGS SELECTION	03	.65270000+04	SLUGS	M
0456C	P	X _A (1)	STEEP GLIDESLOPE GROUND INTERCEPT	03	.65000000+04	FT	M
0457C	P	X _A (2)		03	-.55000000+04	FT	M
0459C	P	Y ERROR	CROSSRANGE ERROR BOUND FOR AUTOLAND INITIATION WHEN H > H REF 1	03		FT	D
0462C	P	Y RANGE1	COEFFICIENT ON H USED TO COMPUTE CROSSRANGE ERROR BOUND WHEN H < H REF 1	03	.10000000+04	ND	D
0463C	P	Y RANGE2	CONSTANT USED TO COMPUTE CROSSRANGE ERROR BOUND WHEN H < H REF 1	03	.18000000+00	FT	D
0464C	P	YERRLM	LIMIT ON YERRC	03	.80000000+03		
				03	.12000000+05	DEG	D

A-15

TABLE A-I(c).- DEFINITION OF AUTOLAND GUIDANCE CONSTANTS(G4.10)

MSID # V37U	SW	SYMBOL	DESCRIPTION	MC	VALUE	UNITS	MISSION DEPENDENT CONSTANT
0004C	P	A 3	FINAL FLARE FILTER CONSTANT	03	.10000000+02	1/S	D
0000C	P	A INT	CROSSRANGE ERROR INTEGRATOR GAIN	03	.00000000	DEG-S/FT	D
0001C	P	A SBF	SPEEDBRAKE COMMAND FILTER CONSTANT	03	.50000000+00	1/S	D
0002C	P	A 13	AIRSPEED FILTER CONSTANT	03	.10000000+01	1/S	D
0003C	P	A 14	SPEED CONTROL FILTER CONSTANT	03	.10000000+01	1/S	D
0005C	P	A 40	OPEN LOOP FILTER CONSTANT	03	.13330000+01	1/S	D
C117C	P	DELTA SB	SPEEDBRAKE THRESHOLD ANGLE FACTOR	03	.28000000+01	DEG	D
C129C	P	DSBC TD(1)	SPEEDBRAKE ANGLE AT TD	03	.00000000	DEG	D
C130C	P	DSBC TD(2)	SPEEDBRAKE ANGLE AT TD	03	.00000000	DEG	D
C229C	P	GAMMA CAPTURE	MAXIMUM GAMMA ERROR TO ENGAGE STEEP GLIDESLOPE	03	.20000000+01	DEG	D
C233C	P	GAMMA REF 1(1)	STEEP GLIDESLOPE FLIGHTPATH	03	-.20000000+02	DEG	M
C234C	P	GAMMA REF 1(2)	REFERENCE	03	-.20000000+02	DEG	M
C235C	P	GAMMA REF 2	SHALLOW GLIDESLOPE FLIGHTPATH REFERENCE	03	-.15000000+01	DEG	M
C265C	P	H CLOOP	ALTITUDE AT WHICH START CLOSED LOOP PULLUP	03	.17000000+04	FT	M
C266C	P	H DECAY	EXPONENTIAL CAPTURE ALTITUDE REFERENCE	03	.29000000+02	FT	M
C268C	P	H ERROR CAPTURE	MAXIMUM ALTITUDE ERROR TO ENGAGE STEEP GLIDESLOPE	03	.50000000+02	FT	D
C269C	P	H ERROR MAX	MAXIMUM ALTITUDE ERROR	03	.30000000+03	FT	D
C270C	P	H FF	ALTITUDE TO START CHECKING FINAL FLARE ALTITUDE	03	.80000000+02	FT	D
C271C	P	H FLARE	FLARE ALTITUDE	03	.20000000+04	FT	M
C272C	P	H INTMX	ALTITUDE ERROR INTEGRATOR MAXIMUM	03	.50000000+02	FT	D

TABLE A-I(c).- Continued.

MSID #	SW	SYMBOL	DESCRIPTION	MC	VALUE	UNITS	MISSION DEPENDENT CONSTANT
V97U							
0273C	P	H K (1,1)	CONSTANT G CIRCLE CENTER	03	.26320000+05	FT	M
0274C	P	H K (1,2)	ALTITUDE	03	.26796000+05	FT	N
0275C	P	H K (2,1)		03	.26320000+05	FT	M
0276C	P	H K (2,2)		03	.26796000+05	FT	M
0277C	P	H MIN	MINIMUM ALTITUDE FOR FINAL FLARE	03	.30000000+02	FT	D
0278C	P	H NO ACC	ALTITUDE FOR ZERO ACCELERATION	03	-20000000+01	FT	D
0281C	I	H SBR TABLE(1)	TABLE OF SPEEDBRAKE RETRACT	03	.25000000+04	FT	M
0282C	P	H SBR TABLE(2)	ALTITUDES	03	.25000000+04	FT	M
0283C	P	H SBR TABLE(3)		03	.10000000+04	FT	M
0284C	P	H TD1 DOT	TOUCHDOWN ALTITUDE RATE	03	.90000000+01	FT/S	D
0285C	P	H TD2 DOT	CLOSED-LOOP TOUCHDOWN ALTITUDE RATE	03	-.30000000+01	FT/S	D
0286C	P	H WL	ALTITUDE REFERENCE FOR LIMITER	03	.75000000+04	FT	D
0492C	P	INT RET BF	INITIAL RETRACT BODY FLAP FLAG	03	.10000000+01	NO	M
0301C	P	K H SGS	ALTITUDE ERROR GAIN, SGS	03	.24000000-02	G/FT	D
0299C	P	K FLR	FEED-FORWARD GAIN, F-F	03	.25000000-01	G-S**2/FT	D
0300C	P	K H FSGS	ALTITUDE ERROR GAIN, FSGS	03	.24000000-02	G/FT	D
0302C	P	K H TC	ALTITUDE ERROR GAIN, TC, SGS	03	.24000000-02	G/FT	D
0303C	P	K HOOT FF	VERTICAL VELOCITY GAIN, FF	03	.12000000-01	G-S/FT	D
0304C	P	K HOOT FSGS	VERTICAL VELOCITY GAIN, FSGS	03	.12000000-01	G-S/FT	D
0305C	P	K HOOT SGS	VERTICAL VELOCITY GAIN, SGS	03	.12000000-01	G-S/FT	D
0306C	P	K HOOT TC	VERTICAL VELOCITY GAIN, TC	03	.12000000-01	G-S/FT	D
0307C	P	K HINTI	INTEGRATOR GAIN, SGS	03	.12000000-03	G/FT-S	D
0308C	P	K IFLR	INTEGRATOR GAIN, FF	03	.00000000	1/S	D
0309C	P	K INT FSGS	INTEGRAL GAIN, FSGS	03	.50000000-01	1/S	D

TABLE A-I(c).- Continued.

VSID # V970	SW	SYMBOL	DESCRIPTION	MC	VALUE	UNITS	MISSION DEPENDENT CONSTANT
03100	P	K R1	YAW RATE COMMAND GAIN, FLAT TURN	03	.25000000+00	1/S	D
03110	P	K R2	YAW RATE COMMAND GAIN, TOUCHDOWN	03	.50000000+00	1/S	D
03120	P	K SB	SPEEDBRAKE GAIN	03	.20000000+01	DEG-S/FT	D
03130	P	K SB1	SPEEDBRAKE INTEGRAL GAIN	03	.10000000+00	DEG/FT	D
03150	P	K Y1	CROSSRANGE ERROR INTEGRATOR GAIN	03	.70000000-01	DEG/FT	D
03140	P	K YDOT	CROSSRANGE RATE GAIN	03	.10000000+02	S	D
03200	P	N FADER	ROLL FADER CONSTANT	03	.00000000	ND	D
03220	P	NSB	MAXIMUM VALUE OF ISB	03	.30000000+01	ND	D
03230	P	NZC LIM	MAX-G LIMIT FOR NZC	03	.10000000+01	G	D
03390	P	PHI M1	MAXIMUM ROLL ATTITUDE COMMAND	03	.45000000+02	DEG	D
03400	P	PHI M2	MAXIMUM ROLL ATTITUDE COMMAND	03	.20000000+02	DEG	D
03410	P	PHI M3	MAXIMUM ROLL ATTITUDE COMMAND	03	.45000000+02	DEG	D
03260	P	P MODE INITIAL	INITIAL PITCH SUBPHASE, INDICATOR	03	.10000000+01	ND	D
03500	P	PSI CAP	MAXIMUM HEADING ERROR (RC)	03	.20000000+01	DEG	D
03790	P	R (1,1)	CONSTANT G CIRCLE RADIUS	03	.26200000+05	FT	M
03800	P	R (1,2)	CONSTANT G CIRCLE RADIUS	03	.26707000+05	FT	M
03810	P	R (2,1)	CONSTANT G CIRCLE RADIUS	03	.26200000+05	FT	M
03820	P	R (2,2)	CONSTANT G CIRCLE RADIUS	03	.26707000+05	FT	M
03960	P	SB RATE	SPEEDBRAKE RETRACT RATE	03	.11000000+02	DEG/S	D
03970	P	SB REF	SPEEDBRAKE REFERENCE	03	.55000000+02	DEG	D
03980	P	SBF TABLE(1)	TABLE OF REFERENCE SPEEDBRAKE	03	.25000000+02	DEG	M
03990	P	SBF TABLE(2)	POSITIONS FOR RETRACTION ALTITUDE	03	.75000000+02	DEG	M

TABLE A-I(c).~ Continued

MSID #	SW	SYMBOL	DESCRIPTION	MC	VALUE	UNITS	MISSION DEPENDENT CONSTANT
V97U							
0400C	P	SOF TABLE(3)	POSITIONS FOR RETRACTION ALTITUDE	03	.90600000+02	DEG	M
0402C	P	SIGMA(1)	EXPONENTIAL DISTANCE	03	.85000000+03	FT	M
0403C	P	SIGMA(2)	EXPONENTIAL DISTANCE	03	.85000000+03	FT	M
0409C	P	T Q	MINIMUM TIME WITH BOUNDED ERRORS FOR TRANSITION TO STEEP GLIDESLOPE PHASE	03		S	D
0410C	P	TAU GAMMA	TIME CONSTANT, FSGS	03	.20000000+01	S	D
0411C	P	TAU TD	TIME CONSTANT, FSGS	03	.60000000+01	S	D
0412C	P	TAU TD1	TIME CONSTANT, FF	03	.50000000+01	S	D
0413C	P	TAU TD2	TIME CONSTANT, FF	03	.50000000+01	S	D
0416C	P	TQ LAT	MINIMUM TIME WITH BOUNDED ERROR TO ENGAGE LATERAL TRACK	03		S	D
0417C	P	V LIMIT	MAXIMUM ERROR VELOCITY LIMIT	03	.10000000+02	FT/S	D
0418C	P	V REF(1)	REFERENCE AIRSPEED	03	.47300000+03	FT/S	M
0419C	P	V REF(2)	REFERENCE AIRSPEED	03	.47300000+03	FT/S	M
0444C	P	WT GS1	WEIGHT FOR GLIDESLOPE SELECTION	03	.65270000+04	SLUGS	M
0445C	P	X AIM PT	AIM POINT X-DISTANCE	03	.15000000+04	FT	M
0446C	P	X EXP (1.1)	EXPONENTIAL CAPTURE X DISTANCE	03	.37840000+04	FT	M
0447C	P	X EXP (1.2)	EXPONENTIAL CAPTURE X DISTANCE	03	.26460000+04	FT	M
0448C	P	X EXP (2.1)	EXPONENTIAL CAPTURE X DISTANCE	03	.37840000+04	FT	M
0449C	P	X EXP (2.2)	EXPONENTIAL CAPTURE X DISTANCE	03	.26460000+04	FT	M
0450C	P	X K (1.1)	CONSTANT G CIRCLE CENTER RANGE	03	.22090000+04	FT	M
0451C	P	X K (1.2)	CONSTANT G CIRCLE CENTER RANGE	03	.10360000+04	FT	M
0452C	P	X K (2.1)	CONSTANT G CIRCLE CENTER RANGE	03	.22090000+04	FT	M
0453C	P	X K (2.2)	CONSTANT G CIRCLE CENTER RANGE	03	.10360000+04	FT	M

A-19

TABLE A-I(c).- Concluded.

MSIO #	SW	SYMBOL	DESCRIPTION	MC	VALUE	UNITS	MISSION DEPENDENT CONSTANT
197U							
0454C	P	X ZERO(1)	STEEP GLIDESLOPE INTERCEPT	03	.6500000+04	FT	M
0455C	P	X ZERO(2)	STEEP GLIDESLOPE INTERCEPT	03	.5500000+04	FT	M
0460C	P	Y INLIM	CROSSRANGE ERROR INTEGRATION LIMIT	03	.5000000+02	FT	D
0458C	P	Y CAP	LATERAL CAPTURE-DISTANCE (TRC)	03	.5000000+02	FT	D
0461C	P	Y LIMIT	CROSSRANGE ERROR LIMIT	03	.1000000+04	FT	D

END

DATE

FILMED

AUG 8 1980